Biopanning, Identification and Application of Peptides Targeting the Vasculature of Orthotopic Colorectal Cancer Based on *in vivo* Phage Display Technology

LI, Zhijie

A Thesis Submitted in Partial Fulfillment of the Requirements for the Degree of Doctor of Philosophy in Pharmacology

The Chinese University of Hong Kong

May 2010

Thesis/Assessment Committee

Professor LAU Hang Yung Alaster *(Chair)*

Professor CHO Chi Hin (Thesis Supervisor)

Professor NG Tzi Bun (Committee Member)

Professor KOO Marcel Wing-Leung (External Examiner)

論文評審委員會

劉行榕 教授 (*主席*)

曹之憲 教授(論文導師)

吳子斌 教授 (委員)

古永亮 教授(校外委員)

ABSTRACT

Abstract of the thesis entitled

Biopanning, identification and application of peptides targeting the vasculature of orthotopic colorectal cancer based on *in vivo* phage display technology

Submitted by

LI, Zhijie

For the degree of Doctor of Philosophy at the Chinese University of Hong Kong

in February 2010

Colorectal cancer (CRC) is one of the most common malignancies worldwide. However, adjuvant chemotherapeutic agents exhibit poor accumulation in the tumor mass and frequently result in serious side effects due to nonspecific damage to normal organs. Therefore, the development of more selective anticancer drugs with targeted delivery to tumor sites is the current trend in cancer therapies. Among these sites, tumor neovasculature is an attractive target for anticancer agents. It is because tumor growth is largely limited by blood supply which is dependent on the extent of angiogenesis in the tumor.

To identify specific ligands targeting the tumor neovasculature, *in vivo* phage display technology has been extensively used. Several dozens of peptides homing to normal or diseased vasculature have been identified through this technology. However, these peptides target mainly the tumors growing at distant sites but not at the primary organ, thus limiting their clinical application. To obtain specific peptides targeting the neovasculature of colorectal cancer growing *in situ*, we established an orthotopic colorectal cancer model in normal BALB/c mice by using syngeneic colon cancer

cells (colon 26). Subsequently, *in vivo* phage display technology was utilized to isolate peptides which specifically recognized the vasculature of the cancer. Four peptides (termed TCP-1, 2, 3, 4) were enriched more than once after four-round selections. Further investigation disclosed that TCP-1 and TCP-2 phages had relatively stronger binding abilities to cancer tissues among the four phage clones. They were chosen for further study.

Experimental analysis suggested that TCP-1 phage and synthetic TCP-1 peptide specifically homed to colorectal cancer tissues and co-localized with the tumor vasculature. Moreover, TCP-1 peptide also recognized the vasculature of human colorectal cancer specimens. Subsequently, the homing abilities of TCP-1 phage were extensively tested in other cancer models. Results showed that TCP-1 peptide could also target the vasculature of orthotopic gastric cancer induced by human colon cancer cell line (MKN45) in BALB/c nude mice. Meanwhile, TCP-1 phage exhibited binding activity to colorectal cancer cells such as colon 26 and SW1116. TCP-1 peptide could carry a pro-apoptotic peptide into these cells and markedly enhanced its pro-apoptotic action.

We further demonstrated that TCP-1 could serve as a carrier for image detection and drug delivery. FITC-labeled TCP-1 could specifically produce a strong fluorescence signal in the tumors after intravenous injection into the orthotopic tumor-bearing mice. Moreover TCP-1, when conjugated with a pro-apoptotic peptide, could also specifically induce apoptosis of tumor vasculature *in vivo.*

Similarly, TCP-2 phage or its peptide also targeted specifically the orthotopic colorectal cancer, and co-localized with the tumor vasculature in mice. Meanwhile, TCP-2 peptide recognized the vasculature of human colorectal cancer specimens. FITC-labeled TCP-2 peptide could also be used to detect cancer tissues in

tumor-bearing mice.

In summary, we have used the phage display technology to isolate two unique peptides TCP-1 and TCP-2, which targeted the vasculature of orthotopic colorectal cancer and also recognized the vasculature of human colorectal cancer. Moreover, they could deliver fluorescein or pro-apoptotic peptide only to the tumor vasculature but not to other normal tissues, for imaging detection and targeted therapy. In conclusion, both TCP-1 and TCP-2 may have significant clinical applications as carriers in diagnostic imaging and ligand-mediated targeted therapy for human colorectal cancer.

中文摘要

基于体内噬菌体展示技术、靶向结肠直肠癌血管的多肽的筛选、鉴定及应运

结肠直肠癌是世界范围内较常见和多发的恶性肿瘤；研发选择性抗肿瘤药物一定程度上能够增强辅助性化疗的抗肿瘤功效；而肿瘤的生长与新生血管的扩展紧密相关。因此，肿瘤新生血管成为选择性抗癌药物研发的热门靶点之一。体内噬菌体展示技术已被广泛应用于鉴定靶向肿瘤新生血管多肽的研究中。

我们的研究目的就是期望分离出特异性靶向结肠直肠癌血管的多肽，并将其应运于结肠直肠癌的配体介导的靶向诊断和治疗中。首先，我们应运鼠源性的结肠直肠癌细胞株 colon 26 在正常的 BALB/c 小鼠上建立一个原位的结肠直肠癌模型。随后，体内噬菌体展示筛选技术被使用来分离特异性结合于该模型肿瘤血管的多肽。四轮筛选后，发现四条多肽（依次命名为 TCP-1，2，3，4）被富集超过一次。进一步的研究发现 TCP-1 和 TCP-2 两条多肽显示出相对较高的靶向能力被选择进一步阐述。

进一步的分析揭示TCP-1和TCP-2 多肽均能特异性地靶向原位结肠直肠癌组织，并且定位于肿瘤组织的血管；也均能够识别人结肠直肠癌组织的血管。

随后， TCP-1 多肽在各种不同的结肠直肠癌相关模型中的靶向能力被广泛检测。我们发现 TCP-1 多肽也能靶向由胃癌细胞株 MKN45 诱导的原位胃癌组织的血管。此外 TCP-1 多肽能够与结肠直肠癌细胞株 Colon 26 和 SW1116 结合，而且能够携带促凋亡肽进入这两个细胞中并极大地增强它的促凋亡效应。

进而，我们尝试将 TCP-1 和 TCP-2 多肽作为一个靶向载体应运于结肠直肠癌的图像检测和靶向治疗上。结果显示，FITC 标记的 TCP-1 或 TCP-2 多肽静

脉注射到小鼠模型后，可以在肿瘤组织产生较强的荧光信号；此外，TCP-1 多肽偶联促凋亡多肽能够显著增加原位结肠直肠癌组织血管的凋亡数量。

总之，在我们的研究中，我们通过体内噬菌体展示筛选技术分离获得两条多肽序列 TCP-1 和 TCP-2。他们均能特异性地靶向原位结肠直肠癌组织的血管，并且也识别来源于人结肠直肠癌组织的血管。应运实验发现他们能够输送荧光探针或者促凋亡多肽到达肿瘤部位，增强图像检测肿瘤的特异性和治疗的靶向性。因此，这两条多肽显示出较好的临床应运潜力，在人的结肠直肠癌的特异性诊断和靶向治疗中的应运值得进一步探讨和研究。

Declaration

I declare that this thesis represents my own work, except where due acknowledgement is made, and it has not been previously included in a thesis, dissertation or report submitted to this University or any other institution for a degree, diploma or other qualification.

Signed Li Zhijie

Li Zhijie

Acknowledgements

Looking back on the last three years in my life, time flied like an arrow. However, I am fully satisfied and feel deeply indebted.

Here I should first extend my heartfelt thanks to my supervisor Professor Cho Chi Hin. Grateful to him for accepting my doctoral application, which gave me an opportunity to be engaged in research in Hong Kong; grateful to him for his guidance, encouragement and help to me within these three years, so as to make my experiments and study completed successfully. Through countless communications with him during the last three years, his profound knowledge, meticulous thinking ability, keen insight, rigorous attitude to academic research, excelsior work style and great enthusiasm to scientific research, have impressed and benefited me deeply and abundantly. In scientific research, he respects analysis and opinions of every student, which gives us a more relaxed and free environment of scientific research, and also fosters our habit of thinking independently. In the daily life, his optimistic, positive and amiable character as well as his broad-minded bosom are also the good model that I should follow. At the time of completion of my thesis, I thank Prof. Cho again for his revisions and improvements of the thesis.

At the same time, I appreciate help and assistance from our technician Mr. Chan Kam Ming. His excellent skills in animal experiments ensured that my study went smoothly. During the last three years, good cooperation with him has benefited me a lot, and is also a memory of my lifetime. I also give special thanks to Dr. Sun Xuegang of the Southern Medical University; he provided great assistance to me in the imaging detection part of my study. I also express heartfelt thanks to my

colleagues: Dr. William Ka Kei Wu, Dr. Yu Le, Dr. Li Haitao, Ms. Winnie Lai Ting Kan, Ms. Clover Ching Man Wong, Mr. Ye Caiguo, Ms. Wu Yachun, Ms. ZhangLin, Ms. Ren Shunxiang, etc. The days we made our endeavors shoulder to shoulder, made me feel the strength of the whole team, and also became the most beautiful scenery in my memory.

When I arrived in Hong Kong three years ago, the unknown strange environment made me feel very lonely. I am grateful to the following friends: Mr. Yu Tian, Mr. Zheng Zebin, Mr. Chen Feng, Mr. Lu Qiang, Ms. Li Mi, Mr. Zhao Chunzhong, Dr. Tang Jing, Dr. Wang Xin, Dr. Liu Yawei， Dr. Liu Jinghua. Your encouragement and company, just like the bright sunshine, warm me at all times.

Finally, I give truehearted thanks to my beloved family. Your support is always the strongest backing. Your safety and health are also my best wishes.

The time has passed in a hurry. A new journey is going to be started. Thank this beautiful university, which preserves my three years' wonderful memories and gives me many harvests and hopes. With these harvests and hopes, I feel fully confident to start a new journey.

Publications

Publications, Patent and Abstracts based on the work described in this thesis

Full papers

1 **Zhi Jie Li,** Chi Hin Cho Development of peptide as a potential drug of cancer therapy (2010). Curr. Pharm. Des. In press.

2 **Zhi Jie Li,** William Ka Kei Wu, Le Yu, Simon Siu Man Ng , Hai Tao Li, Clover Ching Man Wong, Ya Chun Wu, Lin Zhang, Shun Xiang Ren, Kam Ming Chan, Chi Hin Cho A peptide specifically targeting the vasculature of orthotopic colorectal cancer for imaging detection and drug delivery (2010). The Journal of Controlled Release. (Under review).

Patent

- ✓ Filing receipt of a peptide TCP-1(CTPSPFSHC), specifically targeting the vasculature of colorectal cancer for image detection and drug delivery, is acknowledged by Unite States Patent and Trademark Office.
- ✓ Patent application No.: 61/229,606

Abstracts

1 **Zhi Jie Li**, Chi Hin Cho. Biopanning the peptides targeting the orthotopic colorectal cancer. Annual Taiwan, Hong Kong and Singapore Pharmacological Academic Meeting. November 21-23, 2008, Taiwan, China.

2 **Zhi Jie Li**, Chi Hin Cho. A peptide specifically targeting the vasculature of orthotopic colorectal cancer for image detection and drug delivery. Postgraduate Oral Presentation Symposium-Annual Scientific Meeting of the Hong Kong Pharmacology Society and Annual Hong Kong, Taiwan and Singapore Pharmacological Academic Meeting. June 6-8, 2009, Hong Kong, China.

3 **Zhi Jie Li**, Chi Hin Cho. A peptide derived from phage library biopanning for image detection and drug delivery of orthotopic colorectal cancer. 13th ICUR (International Conference on Ulcer Research)/ICGR (International Conference on Gastrointestinal Research), September 10-16, 2009, Split, Croatia.

Publications related to the work in this thesis

Full papers

1. Wu WK, Cho CH, Lee CW, Wu YC, Yu L, **Li ZJ**, Wong CC, Li HT, Zhang L, Ren SX, Che CT, Wu K, Fan D, Yu J, Sung JJ. Macroautophagy and ERK phosphorylation counteract the antiproliferative effect of proteasome inhibitor in gastric cancer cells. Autophagy. 2010,24;6(2):1-11.
2. Wong HP, **Li ZJ**, Shin VY, Tai EK, Wu WK, Yu L, Cho CH. Effects of cigarette smoking and restraint stress on human colon tumor growth in mice. Digestion. 2009;80(4):209-214.
3. Yu L, Wu WK, **Li ZJ**, Li HT, Wu YC, Cho CH. Prostaglandin E(2) promotes cell proliferation via protein kinase C/extracellular signal regulated kinase pathway-dependent induction of c-Myc expression in human esophageal squamous cell carcinoma cells. Int J Cancer. 2009;125(11):2540-6.
4. Li H, Wu WK, Zheng Z, Che CT, Yu L, **Li ZJ**, Wu YC, Cheng KW, Yu J, Cho CH, Wang M. 2,3',4,4',5'-Pentamethoxy-trans-stilbene, a resveratrol derivative, is a potent inducer of apoptosis in colon cancer cells via targeting microtubules. Biochem Pharmacol. 2009;78(9):1224-32.
5. Wu WK, Volta V, Cho CH, Wu YC, Li HT, Yu L, **Li ZJ**, Sung JJ. Repression of protein translation and mTOR signaling by proteasome inhibitor in colon cancer cells. Biochem Biophys Res Commun. 2009; 386(4):598-601.
6. Wu WK, Tse TT, Sung JJ, **Li ZJ**, Yu L, Cho CH. Expression of ErbB receptors and their cognate ligands in gastric and colon cancer cell lines. Anticancer Res. 2009;29(1):229-34.
7. Wu YC, Wu WK, Li Y, Yu L, **Li ZJ**, Wong CC, Li HT, Sung JJ, Cho CH.

Inhibition of macroautophagy by bafilomycin A1 lowers proliferation and induces apoptosis in colon cancer cells. Biochem Biophys Res Commun. 2009; 382(2):451-6.

8. Yu L, Wu WK, **Li ZJ**, Liu QC, Li HT, Wu YC, Cho CH. Enhancement of doxorubicin cytotoxicity on human esophageal squamous cell carcinoma cells by indomethacin and SC236 via inhibiting P-glycoprotein activity. Mol Pharmacol. 2009;75(6):1364-73.
9. Wu WK, Sung JJ, Wu YC, Li HT, Yu L, **Li ZJ**, Cho CH. Inhibition of cyclooxygenase-1 lowers proliferation and induces macroautophagy in colon cancer cells. Biochem Biophys Res Commun. 2009; 382(1):79-84.
10. Wu WK, Wu YC, Yu L, **Li ZJ**, Sung JJ, Cho CH. Induction of autophagy by proteasome inhibitor is associated with proliferative arrest in colon cancer cells. Biochem Biophys Res Commun. 2008; 374(2):258-63.
11. Yu L, Wu WK, **Li ZJ**, Wong HP, Tai EK, Li HT, Wu YC, Cho CH. E series of prostaglandin receptor 2-mediated activation of extracellular signal-regulated kinase/activator protein-1 signaling is required for the mitogenic action of prostaglandin E2 in esophageal squamous-cell carcinoma. J Pharmacol Exp Ther. 2008; 327(1):258-67.
12. Wu WK, Sung JJ, Yu L, **Li ZJ**, Chu KM, Cho CH. Constitutive hypophosphorylation of extracellular signal-regulated kinases-1/2 and down-regulation of c-Jun in human gastric adenocarcinoma. Biochem Biophys Res Commun. 2008; 373(2):330-4.
13. Wu WK, Sung JJ, Wu YC, **Li ZJ**, Yu L, Cho CH. Bone morphogenetic protein signalling is required for the anti-mitogenic effect of the proteasome inhibitor MG-132 on colon cancer cells. Br J Pharmacol. 2008; 154(3):632-8.

14. Liu X, Wu WK, Yu L, **Li ZJ**, Sung JJ, Zhang ST, Cho CH. Epidermal growth factor-induced esophageal cancer cell proliferation requires transactivation of beta-adrenoceptors. J Pharmacol Exp Ther. 2008; 326(1):69-75.

Table of Contents

List of illustrations

Figures

Tables

Abbreviations

APC	=	Adenomatous polyposis coli
CAC	=	Colitis-associated CRC
CD	=	Crohn's disease
CEA	=	Carcinoembryonic antigen
CEPs	=	Circulating endothelial precursor cells
CIN	=	Chromosomal instability
CRC	=	Colorectal cancer
CS	=	Cigarette smoking
DSS	=	Dextran sulphate sodium
ECM	=	Extracellular matrix
EGF	=	Epidermal growth factor
EGFR	=	Epidermal growth factor receptor
FAP	=	Familial adenomatous polyposis
FDA	=	US Food and Drug Administration
Ff	=	filamentous bacteriophage
FGF	=	Fibroblast growth factor
FITC	=	Fluorescein isothiocyanate
FU	=	Fluorouracil
HBV	=	Hepatitis B virus
HGF	=	Hepatocyte growth factor
HNPCC	=	Hereditary non-polyposis colorectal cancer
HRCC	=	Human renal carcinoma cells
IBD	=	Inflammatory bowel disease

IL	=	Interleukin
KDR	=	Kinase domain receptor
LV	=	Leucovorin
MMP	=	Metalloproteinase
MSI	=	Microsatellite instability
NRP	=	Neuropilin
PD-ECGF	=	Platelet-derived endothelial cell growth factor
PDGF	=	Platelet-derived growth factor
RGD	=	ArgGlyAsp integrin binding peptide
SCC	=	Sporadic colorectal cancer
TGF	=	Transforming growth factor
UC	=	Ulcerative colitis
VEGF	=	Vascular endothelial growth factor

Chapter 1

Introduction

1.1 Current status of colorectal cancer

1.1.1 Epidemiology

According to the 2001 through 2003 Surveillance, Epidemiology and End Results (SEER) database, the possibility of developing cancer during one's lifetime is approximately one in two for men and one in three for women (Hayat *et al.*, 2007). Colorectal cancer (CRC) is the third most common malignancy and the fourth most frequent cause of cancer deaths worldwide (500,000 deaths worldwide each year) (Jemal *et al.*, 2009; Pearson *et al.*, 2009). Overall, CRC makes up approximately 10% of all cancer deaths. The incidence and mortality from CRC is about equal in men and women. The mean age at diagnosis is between 60 and 65 year group, with 90% of all cases definitely diagnosed in people over the age of 50 (Ahmed, 2004). CRC is infrequent among those younger than age 40. However, the incidence of CRC is not equally distributed in terms of geographic area. Countries in Asia, Africa, and Latin American have a lower incidence of CRC than those in North America and Western Europe. But incidence rate in these regions which are undergoing rapid industrialization is increasing (e.g. China) (Huxley, 2007). Despite advances in surgical techniques, improved adjuvant chemotherapy and early detection, CRC is still correlated with a relatively poor prognosis. At least 40% of patients undergoing radical resection of the primary tumor die within 5 years either because of local recurrence or metastatic disease (Mancuso *et al.*, 2005). Therefore, CRC is still an important health problem, urgently demanding the elucidation of the mechanism that induces initiation and progression of this neoplasm.

1.1.2 Etiology and risk factors

The entire etiology of CRC is not fully understood. It is generally accepted that CRC is a multistep and complicated process involving in a transition from normal mucosa to the development of cancer. It is the endpoint result of a series of genetic alteration, environmental insults and host responses over time (Huxley, 2007; Sandler, 1996).

Several risk factors have been identified for the development of CRC. They might make an individual at increased risk of CRC. Life style, genetic factors and chronic colitis are thought to be the three typical risk factors.

Results from international correlation and migrant studies suggest that environmental factors, most possible western lifestyle, are likely to explain most cases of CRCs (Armstrong *et al.*, 1975). When individuals emigrate from areas of low to high incidence areas, their risk of disease increases rapidly, often within a couple of generations (Sandler, 1996). These life style risk factors include diet, physical activity, smoking and obesity, etc.

In terms of diet, there has been a long debate as to the role of fat and fiber in one's daily intake and risk of CRC. Evidence from epidemiological studies appears to show countries that get used to a low-fat, high-fiber diet have a much lower incidence of CRC as compared to countries that get into the habit of a high-fat, low-fiber diet around the world (Boyle *et al.*, 2000). Human studies have generally suggested that individuals who habitually consume a diet high in fat have an increased risk of colon cancer (Willett, 1989). Moreover saturated fat might be a more vital risk factor than unsaturated fat (Willett *et al.*, 1990). The mechanism for increased risk from dietary fat might involve changes in the gut microflora and increase the concentration of fecal bile acids. Studies have elucidated that bile salts exert well-defined detergent and obvious tissue-damaging effects that are related to increased cell proliferation (Sandler, 1996). However, dietary fiber can prevent the

development of CRC through multiple mechanisms. Fiber can increase stool bulk and dilute colonic contents, including carcinogenic agents, thereby decreasing transit time and contact time for intraluminal carcinogens. Fiber can absorb bile salts and other potential carcinogens and lower anaerobic fecal flora levels. Fermentation of fiber by bacteria can generate short-chain fatty acids that lower the pH, thereby inactivating bile acids and inhibit bacterial degradation of food constituents into potential carcinogens, which is beneficial to create an environment that contribute less to cancer development (Cummings *et al.*, 1998; Reddy, 1999; Sandler, 1996). Meanwhile, the short-chain fatty acids butyrate that is produced by fermentation of fiber, may protect against CRC through the ability to inhibit cell growth, induce differentiation, and promote apoptosis in the cells with damaged DNA (Reddy, 1999).

It is always thought that routine and energetic physical exercise could provide strong preventative medicine against cancer with the potential to reduce incidence (Newton *et al.*, 2008). The effect is strongest for breast and CRC (Newton *et al.*, 2008). Physical inactivity may be associated with 13-14% of colon cancer, an attributable risk greater than family history (Harriss *et al.*, 2007). But a systematic review and meta-analysis of prospective observational studies showed that increased physical activity is responsible for a modest reduction in colon but not rectal cancer risk; a risk reduction, which previously might have been overestimated (Harriss *et al.*, 2009).

Obesity (Excess body weight, defined as body mass index (BMI) $\geqslant$30 kg/m^2) is increasing dramatically in most regions of the world, and can lead to a number of obesity-related diseases. Two similar meta-analysis of cohort studies (Dai *et al.*, 2007; Larsson *et al.*, 2007) showed that obesity is a statistically significant risk factor

for CRC and the relationship is verified more significant correlation in men than in women among different cancer subsites. Indexes of abdominal obesity seem to be more sensitive than those of overall obesity. Other epidemiological evidence suggested that individuals with a BMI $\geq$30 kg/m^2 had a 40% greater risk of CRC as compared to individuals with a BMI $\leq$ 25 kg/m^2, and the correlation between obesity and colon cancer was not obviously higher than that of the association between obesity and rectal cancer (Huxley *et al.*, 2009; Moghaddam *et al.*, 2007).

Cigarette smoking (CS) is estimated to involve eight different types of cancers (lung, mouth, pharynx, larynx, esophagus, pancreas, kidney, and bladder), and cigarette smoking has been estimated to result in approximately 5 million deaths per year worldwide (Chao *et al.*, 2000; Limsui *et al.*, 2008). CRC is not presently included among the smoking-associated cancers, even more the correlation between cigarette smoking and CRC is controversial. But more and more epidemiological and experimental evidences implicated that an increased risk of CRC is highly associated with long-term cigarette smoking (Hannan *et al.*, 2009). Two studies about the association between cigarette smoking and CRC incidence and mortality disclosed similar results (Chao *et al.*, 2000; Liang *et al.*, 2009). Compared with nonsmokers, current and former smokers had an obviously increased risk of CRC incidence and mortality in both men and women, respectively. Risk among current and former smokers is positively correlated with duration of smoking and average number of cigarettes smoked per day. Obvious reduction in risk is observed with early smoking cessation. Some studies revealed that smokers often lead a life with unhealthy dietary habits, such as higher intakes of energy, total fat, saturated fat, alcohol and cholesterol etc. Unhealthy dietary habits and lifestyle contribute to the increased CRC risk in smokers (van Duijnhoven *et al.*, 2009). A series of studies from our lab

also suggested that nicotine (a major alkaloid in cigarette smoke), 4-(methylni-trosamino)-1- (3-pyridyl)-1-butanone (NNK, a tobacco-specific nitrosamine) could promote colorectal cancer cell proliferation *in vitro* and stimulate colorectal cancer growth in mice through several receptors and signal pathways, which further implies the direct relationship between cigarette smoking and CRC (Wong *et al.*, 2009; Wong *et al.*, 2007a; Wong *et al.*, 2007b; Wu *et al.*, 2005).

In addition, the risk of CRC was significantly associated with alcohol: individuals with the heaviest and most frequent drinking had 60% greater risk of CRC as compared to non- or light-drinkers; the risk of CRC in individuals with diabetes was 20% higher when compared with unaffected individuals (Huxley *et al.*, 2009). Public-health strategies that contribute to modest alcohol uptake, smoking cessation, weight loss, increased physical activity and moderate consumption of a low-fat, high-fiber diet are possibly beneficial to reduce significantly the incidence of CRC at the population level (Huxley *et al.*, 2009).

Although environmental factors play a pivotal role in the etiology of CRC, a number of hereditary factors have been identified to increase further the feasibility of the development of CRC under the catalysis of environmental factors. Genetic factors often are divided into two groups: familial adenomatous polyposis (FAP) and hereditary non-polyposis colorectal cancer (HNPCC).

First, FAP is an autosomal dominant disease with almost 100% penetrance and affects both sexes equally (Strate *et al.*, 2005). It is characterized by the emergence of more than 100 colorectal polyps during puberty (Merg *et al.*, 2005a). Patients with FAP have a strong predisposition for early CRC, as well as for other malignancies (Strate *et al.*, 2005). Only a small percentage (<1%) of all CRCs are due to FAP and the risk of developing cancer is approximately 100% by the fourth or fifth decade if

prophylactic colectomy is not performed (Al-Sukhni *et al.*, 2008). Mutations in the adenomatous polyposis coli (APC) gene are directly related to the syndrome. The APC gene is a tumor suppressor gene located on chromosome 5q21-q22 (Al-Sukhni *et al.*, 2008). The APC gene normally blocks DNA transcription that would otherwise result in uncontrolled cellular growth, helps control cell adhesion, and regulates migration of enterocytes (Desai *et al.*, 2008; Grady *et al.*, 2002). A number of patients with FAP have now been found to have mutations in this gene. The majority of these mutations (>90%) are nonsense mutations or frameshift mutations that lead to premature stop codons (Strate *et al.*, 2005). The resulting protein is truncated and presumably nonfunctional. The loss of both functioning copies of the APC gene induces uncontrolled cell growth. Mutations in the APC gene can also be detected in the development of sporadic CRCs. Somatic mutations of the APC gene are found in as many as 80% of sporadic tumors, and seem to be involved in initiating tumorigenesis (Powell *et al.*, 1992). In addition, nearly 30% of patients who have FAP have no family history of the syndrome, suggesting the presence of a *de novo* germline APC mutations (Hernegger *et al.*, 2002). Biallelic germline mutations of the base-excision-repair gene MYH resulting in the polyposis phenotype serves as a recessive trait in these FAP patients with 'APC-negative' mutations (Varesco, 2004).

Second, HNPCC (termed also Lynch syndrome) is the most common cause of hereditary CRC and is inherited by an autosomal dominant fashion with incomplete penetrance (Al-Sukhni *et al.*, 2008). Lynch syndrome accounts for about 1% to 6% of all colorectal malignancies. It is marked by the development of colorectal or several extracolonic cancers at an earlier age than the general population; unlike FAP, the presence of multiple polyps is not a crucial feature of Lynch syndrome (Vasen,

2007). Patients with HNPCC also have a predisposition associated with extracolonic tumors including endometrial, ovarian, stomach, small bowel, hepatobiliary, pancreatic, upper uroepithelial tract, and brain (Merg *et al.*, 2005b). Lynch syndrome is caused by six mismatch repair (MMR) genes, primarily MLH1, MSH2, MSH6, MLH3, PMS1 and PMS2, which recognize and correct errors that occur during DNA replication (Bapat *et al.*, 1999; Desai *et al.*, 2008). Lynch syndrome now refers to patients who have mutations in one of four DNA mismatch repair (MMR) genes—MLH1, MSH2, MSH6 and PMS2 (Desai *et al.*, 2008; Lindor *et al.*, 2006). Mutations in MMR genes are currently elucidated in the pathogenesis of this disorder. 80% to 90% of patients with the clinical diagnosis of Lynch syndrome are found to have mutations in MSH2 and MLH1 genes; mutations in MSH6 and PMS2 are inclined to result in a less severe phenotype (Al-Sukhni *et al.*, 2008; Boland *et al.*, 2008). Mutations in MMR genes responsible for a loss of DNA mismatch repair during replication result in insertion or deletion of repeats in microsatellites; More than 90% of patients who have Lynch syndrome exhibit high microsatellite instability (MSI) in their tumors (Hampel *et al.*, 2005).

Patients with longstanding ulcerative colitis (UC) and Crohn's disease (CD) have also an increased risk of development of CRC. This is further discussed below.

1.2 Colitis and colorectal cancer

Ulcerative colitis (UC) and Crohn's disease (CD) are characterized by chronic relapsing inflammatory disorders of unknown origin, collectively known as idiopathic inflammatory bowel disease (IBD), which share many common features. Indeed, IBD, taken together FAP and HNPCC, ranks among the top three high-risk conditions for CRC. Compared with FAP and HNPCC, CRC in the setting of IBD

seems to be related more to chronic inflammation of gastrointestinal mucosa than to a well-characterized genetic etiology (Itzkowitz *et al.*, 2004).

UC is a condition in which part or all of lining of the rectum and colon is damaged by inflammation and ulcers, but the cause in UC is poorly understood. CD is now recognized to cover a wide variety of presentations and patterns of gut inflammation. It can cause problems in any part of gut from ulcers in the mouth to abscesses around the anus. When CD only affects the large bowel (Crohn's colitis), it is difficult to be distinguished from UC to some extent. CD may affect only the internal lining (mucosa) of the gut but the inflammation can also invade deeper into the bowel wall causing a perforation or fistula to form.

IBD-related CRC is estimated to be responsible for less than 2% of all cases of CRC. But CRC accounts for around 15% of all deaths in IBD patients. The risk of CRC for people with IBD increases by 0.5-1% yearly, 8-10 years after diagnosis. Eaden *et al.* reported through a large meta-analysis that the cumulative risk of CRC in UC is 2% at 10 year, 8% at 20 years, and 18% after 30 years of disease (Ahmadi *et al.*, 2009; Eaden *et al.*, 2001). The risk of CRC development in patients with colonic CD is nearly similar to that of UC, and thus the guidelines for UC should be equally suitable to analyze such patients with CD (Carter *et al.*, 2004; Herszenyi *et al.*, 2007).

Several risk factors have been identified which can contribute to the development of CRC in the setting of IBD. The most important factor is the duration of colitis. CRC is rarely detected before 7 years of colitis; the risk increases at a rate of ~0.5-1.0% per year (Itzkowitz *et al.*, 2004). Anatomic extent of colitis is another independent and important factor. The more colonic surface that is invaded with colitis, the greater the CRC risk. Patients with proctitis having more severe inflammation burden

had a 70% higher risk than expected in the general population (Triantafillidis *et al.*, 2009). The furthest extent of microscopical and macroscopical inflammation is used to define the extent of IBD. Study from Rutter, *et al.* demonstrated that the severe degree of colonic inflammation correlates positively with an increased risk of dysplasia and CRC (Rutter *et al.*, 2004). Therefore, histological examination of extent of colitis is the most important factor that must be considered when the risk of CRC development is estimated. Other important factors that might increase the risk of CRC in IBD patients include family history of CRC, the presence of pseudopolyps, primary sclerosing cholangitis and backwash ileitis (Herszenyi *et al.*, 2007; Xie *et al.*, 2008).

The molecular pathway leading to the colitis-associated CRC (CAC) is thought to be similar to the adenoma-carcinoma sequence in sporadic CRC (SCC). However, unlike SCC, where dysplastic lesions emerge in one or two focal areas of the colon, it is not unusual for dysplasia or cancer to be multifocal in colitic mucosa, reflecting a broader "field effect". CAC is thought to occur by a progression from absence of dysplasia, to indefinite dysplasia, to low-grade dysplasia, to high-grade dysplasia, and ultimately to invasive CRC (Herszenyi *et al.*, 2007; Thomas *et al.*, 2005). The major molecular pathways causing SCC also are altered in CAC. The emerging evidence suggests that chromosomal instability (CIN) and microsatellite instability (MSI), two major molecular alterations in SCC, appear with roughly the same frequency (85% CIN, 15% MSI) in CAC (Schulmann *et al.*, 2005; Triantafillidis *et al.*, 2009; van Dieren *et al.*, 2006). However, the differences of CAC that distinguished it from SCC are the timing and frequency of these alterations. For example, the loss of *APC* function in CAC, is much less frequent and usually is detected relatively late in the colitis-associated dysplasia-carcinoma sequence than in

SCC (Aust *et al.*, 2002; Itzkowitz *et al.*, 2004; Tarmin *et al.*, 1995). Conversely, *p53* mutations appear early and are often found in mucosa that is non-dysplastic or indefinite for dysplasia in patients with colitis, but *p53* mutations in SCC usually are detected late in the adenoma-carcinoma sequence (Triantafillidis *et al.*, 2009). Methylation is another important factor as a mechanism responsible for the genetic alterations in CAC. Methylation of CpG islands in several genes appears to occur prior to dysplasia and is extensively spread throughout the mucosa of UC patients (Maeda *et al.*, 2006).

1.3 Metastasis of colorectal cancer

Metastasis is the primary cause of death for most cancer patients. Approximately 90% of cancer deaths are due to the metastatic spread of the primary solid tumors (Uneda *et al.*, 2009). Distant metastatic disease from CRC represents a major cause of death of patients in spite of advances in operative technique and adjuvant chemotherapy. The liver and the lung are the most frequent sites of metastases of CRC. Depending on the stage of the primary cancer, liver metastases occur in 20% to 70% of CRC patients and lung metastases in 10% to 20% (Penna *et al.*, 2002). Unlike many other types of cancer, the presence of distant metastases from CRC does not preclude curative treatment. Radical resection of metastatic tumors remains the only treatment that can ensure long-term survival and cure in some patients.

Invasion and metastasis of CRC is a complex multistage process, including proteolysis of the local extracellular matrix (ECM), the motility, migration and adhesion of cells, proliferation, angiogenesis, dissemination, and cell growth (Takayama *et al.*, 2006; Widel *et al.*, 2006). Many gene alterations are complexly involved in the whole process.

First, the cells released from the primary tumor mass have to break through tissue barriers, such as the blood vessels and lymphatic vessels (Weber, 2008). Invasiveness process represents the earliest features of metastasis, which is the spread of cancer cells throughout the circulation system and colonization of distinct, often distant organs (Weber, 2008; Widel *et al.*, 2006). The secretion of proteinases by tumor cells is necessary to cause invasiveness. Proteinases are capable of degrading extracellular matrix (ECM) components and cause cancer cells to detach from the primary site. Matrix metalloproteinases (MMPs), composed of more than 25 enzymes, are believed to play a crucial role in the proteolysis step (Zucker *et al.*, 2004). Circulating cells can then migrate through the blood or lymphatic vessels to adjacent or distant organs where they reside, proliferate, and induce angiogenesis, forming resultant secondary cancer. Simultaneously, many adhesion molecules are secreted or expressed to enable tumor cell adhesion in secondary sites such as integrins, cadherins, selectins, CD44, ICAM-1, VCAM-1, and carcinoembryonic antigen (CEA), etc (Takayama *et al.*, 2006). Cancer cells expressing these adhesion molecules are easier to adhere to the ECM, leading to subsequent invasion and metastasis. Angiogenesis is one of the fundamental hallmarks of tumor growth and metastasis. Several potential angiogenic factors have been identified in the promotion of tumor angiogenesis (Prat *et al.*, 2007). These growth factors include vascular endothelial growth factor (VEGF), endoglin (CD105), transforming growth factor β (TGFβ), neuropilin (NRP), angiogenin, platelet-derived endothelial cell growth factor (PD-ECGF), etc (Takayama *et al.*, 2006; Woodhouse *et al.*, 1997). The production of these growth factors promotes tumor growth and causes a concomitant increase in vascularization.

1.4 Chemotherapy of colorectal cancer

Successful prevention and treatment of CRC depends on the detection of colonic polyps and tumors at the early stage. Surgery remains the primary treatment and the only successful manner of cure for both primary and metastasis CRC (Mocellin *et al.*, 2005). The primary surgical resection can cure 50%-60% with average-risk stage III disease (Allegra *et al.*, 2005). Adjuvant chemotherapy after complete surgical resection has had an incontrovertible and substantial benefit, with the 4-year rate of overall survival reaching approximately 80% (Andre *et al.*, 2004). The backbone of CRC chemotherapy for the past 40 years has expanded from the single agent 5-fluorouracil (5-FU) to three active cytotoxic agents (5-FU and oral derivation of fluorouracil, oxaliplatin and irinotecan) as well as the novel targeted therapies (discussed separately). Recently, two reports suggested that the combination of 5FU, capecitabine, and oxaliplatin has improved the relapse rate, reduced the relative risk of recurrence by more than 50% (Andre *et al.*, 2004; Kuebler *et al.*, 2007). Metastatic CRC is commonly treated by combining several chemotherapy agents with 5-FU.

5-Fluorouracil (5-FU): 5-FU is an inhibitor of the thymidylate synthase, the rate-limiting enzyme in pyrimidine nucleotide synthesis. The action mechanism of 5-FU is thought to be able to incorporate in RNA as fluorouridine triphosphate and inhibition of thymidylate synthetase by fluorodeoxyuridine monophosphate. It is usually administered in combination with leucovorin (LV), a reduced folate that stabilizes the binding of 5-FU to thymidylate synthase, thereby enhancing the inhibition of DNA synthesis (Goyle *et al.*, 2005). 5-FU was the only effective chemotherapeutic agent for CRC until recently. In patients with advanced CRC, 5-FU/LV reduces tumor volume by 50% or more in about 20% of patients and prolongs median survival from approximately 6 to 11 months (Thirion *et al.*, 2004).

The major adverse side effects related with 5-FU depend on the method of administration. When the drug is administered for five consecutive days every four to five weeks, neutropenia and stomatitis are the most usual toxic effects (de Gramont *et al.*, 1997; Meyerhardt *et al.*, 2005). In contrast, diarrhea is more frequent with weekly bolus doses. Regimens involving intravenous infusions of fluorouracil given as a continuous infusion with a portable infusion pump are responsible for less hematologic and gastrointestinal toxicity, but palmar–plantar erythrodysesthesia ("hand–foot syndrome") is more frequent (de Gramont *et al.*, 1997; Meyerhardt *et al.*, 2005).

Oral fluoropyrimidines mimic protracted venous infusional 5-FU. Potential benefits include convenience, elimination of risks of indwelling central venous catheters and different toxicity profile. 5-FU is unsuitable for oral administration because of the unstable intestinal absorption of oral 5-FU, which might in turn have been a result of the variable mucosal concentrations of dihydropyrimidine dehydrogenase, a rate-limiting catabolic enzyme of the drug (Meyerhardt *et al.*, 2005).

Capecitabine: Capecitabine is a novel oral fluoropyrimidine carbamate that mimics continuous infusion 5-FU which can be metabolised to 5-FU through a three-step enzymatic reaction (Pentheroudakis *et al.*, 2002). Capecitabine is converted to 5-FU and generates tumour-selective 5-FU through exploitation of the higher concentrations of thymidine phosphorylase in tumour tissue as compared to healthy organs (Goyle *et al.*, 2005). The side-effect profile of capecitabine is similar to that observed protracted infusions of 5-FU. The hand–foot syndrome and elevated bilirubin are two major toxic effects; other adverse reactions include diarrhea, nausea, vomiting, and bone marrow suppression. Neutropenia, alopecia and stomatitis are less frequent. (Cassidy *et al.*, 2002; Meyerhardt *et al.*, 2005)

Tegafur and Uracil (UFT): Tegafur, a prodrug of 5-FU, is conjugated with uracil, a competitive blocker of dihydropyrimidine dehydrogenase, to improve the absorption and bioavailability of Tegafur (Sulkes *et al.*, 1998). The drug is usually given together with oral leucovorin. In two randomized studies, this therapy resulted in a response rate and median overall survival similar to those obtained with parenteral 5-FU and leucovorin (Carmichael *et al.*, 2002; Douillard *et al.*, 2002; Meyerhardt *et al.*, 2005).

The prominent side effects for UFT are diarrhoea, nausea, vomiting, mucositis, neutropenia, thrombocytopenia, and increased in bilirubin levels (Douillard *et al.*, 2002).

Oxaliplatin: Oxaliplatin is a platinum derivative which forms bulky DNA adducts and promotes cellular apoptosis (Raymond *et al.*, 1998). Studies found that oxilaplatin and 5-FU can interact synergistically, not only in preclinical models but also in subsequent clinical trials, possibly due to the down-regulation of thymidylate synthase by oxaliplatin, which thereby enhances the efficacy of 5-FU (Raymond *et al.*, 1997; Raymond *et al.*, 2002). Therefore, combination with 5-FU has been developed in the clinical application of the drug rather than single agent therapy.

As a platinum derivative, oxaliplatin unlike cisplatin and carboplatin, seldom produces renal dysfunction, alopecia, and ototoxic effects (Meyerhardt *et al.*, 2005). Most patients experience transient dysesthesias, which are worsened by exposure to low temperatures. After months of therapy, patients may suffer from a cumulative, dose dependent sensory neuropathy in which peripheral dysesthesias and paresthesias persist between cycles of therapy; these effects usually diminish after the cessation of treatment (de Gramont *et al.*, 2000).

Irinotecan: Irinotecan is a semi-synthetic derivative of the natural alkaloid

camptothecin. Its active metabolite SN38 exerts a cytotoxic effect through its interaction with the enzyme topoisomerase I (Goyle *et al.*, 2005). Irinotecan as a prodrug is hydrolyzed to its active metabolite, SN-38, by hepatic carboxylesterases. SN-38 is detoxified to an inactive, glucuronidated form by uridine diphosphate glucuronosyltransferase isoform 1A1 (UGT1A1) and is excreted in the urine and bile (Klein *et al.*, 2002).

The obvious toxic effects of irinotecan include diarrhea, bone marrow suppression, nausea, vomiting, and alopecia. Polymorphisms of UGT1A1 seem to be responsible for the severity of the gastrointestinal effects and bone marrow suppression (Iyer *et al.*, 2002).

Oxaliplatin and irinotecan are often combined with 5-FU which produces two regimens, FOLFOX and FOLFIRI respectively. Reports from two groups indicated that the overall survival of patients with advanced CRC is associated positively with the availability of three active cytotoxic agents-5FU (or capecitabine), oxaliplatin and irinotecan in the course of treatment (Grothey *et al.*, 2005; Grothey *et al.*, 2004).

1.5 Targeted therapy of colorectal cancer

In the last decade, advances in chemotherapeutic agents have resulted in improved overall survival for patients with metastatic or advanced CRC. Especially, irinotecan and oxaliplatin combined with 5-FU/leucovorin(LV) regimens improves not only overall response rate, but also overall survival over 5-FU/LV alone, prolonging the survival for patients with unresectable advanced CRC at around 20 months (Prat *et al.*, 2007). Despite these great developments, the five-year survival rate for all stages ranges from 40% to 60%, because more than half of the patients with CRC relapse in the local region and/or ultimatley develop distant metastasis and die as an end of

their disease (Mocellin *et al.*, 2005). On the other hand, these cytotoxic chemotherapeutic agents, such as 5-FU, oxaliplatin and irinotecan, etc, mainly target tumor cells, they exhibit poor accumulation in the tumor mass owing to poor blood perfusion, irregular vasculature and high interstitial pressure in the tumor environment (Ahlskog *et al.*, 2006). Moreover, cytotoxic drugs not only kill tumor cells but do damage to other proliferating cells in the body, such as blood and hair cells and cells lining the intestine which may lead to commonly induced side effects including myelosuppression, diarrhea or alopecia, etc. (see 1.4 Chemotherapy of Colorectal Cancer). At the same time, long period of drug treatment requiring multiple dosages allows tumor cells to acquire multidrug resistance. Therefore, it is essential to find more effective and well-tolerated therapeutic strategies to treat the patients with advanced CRC. Recently, molecular-targeted strategies are absorbing enormous public interest because the targeted therapeutics exhibit prominent specificity of tumor therapy with acceptable adverse side effects.

Up to now, the most promising molecules for targeted therapy are epidermal growth factor receptor (EGFR) and vascular endothelial growth factor (VEGF). Two agents had been approved by the US Food and Drug Administration (FDA) including cetuximab, which binds to EGFR, and bevacizumab, which interacts with free VEGF.

EGFR, a transmembrane glycoprotein, consists of an extracellular ligand-binding domain, a transmembrane region, and an intracellular tyrosine kinase domain. The main ligands responsible for EGFR activation are EGF and transforming growth factor α (TGFα) (Cunningham *et al.*, 2004). Binding of EGF or TGFα to EGFR induces receptor dimerization, which results in activation of the receptor's intrinsic tyrosine kinase activity and autophosphorylation, initiating downstream signaling

through various pathways (Chung *et al.*, 2005). This signaling transduction cascade regulates gene transcription and protein translation, stimulating tumor cell proliferation, migration, adhesion, angiogenesis and inhibition of apoptosis (Chung *et al.*, 2005; Rajpal *et al.*, 2006). All of these support the conclusion that EGFR might play a pivotal role in tumorigenesis.

EGFR gene expression or upregulation occurs in several epithelial tumors, including 60–80% of CRCs (Cunningham *et al.*, 2004). EGFR overexpression seems to be related to poor survival, an increased risk of metastasis, and reduced sensitivity to chemotherapy (Mendelsohn *et al.*, 2000). Moreover, EGFR antibody has been verified that could block the proliferation of tumor cells both *in vitro* and in xenograft models of several epithelial carcinomas leading in significant increases in mouse survival, and also could inhibit tumor-induced angiogenesis, presumably by down-regulating tumor expression of TGFα, VEGF, interleukin-8 (IL-8), and basic fibroblast growth factor (bFGF) (Ciardiello *et al.*, 2001; Rajpal *et al.*, 2006; Tabernero *et al.*, 2004).

Cetuximab is a recombinant DNA-derived, chimeric monoclonal antibody against the EGFR consisting of the murine Fv region attached a human IgG1 constant region segment (Mancuso *et al.*, 2005). It could specifically bind to EGFR with a higher affinity than EGF or TGFα, resulting in inhibition of cell growth and proliferation, neoangiogenesis, and stimulation of apoptosis (Perrotte *et al.*, 1999). Cetuximab had been approved by the FDA for treatment of EGFR-positive, irinotecan-refractory, metastatic CRC. Clinical benefit has been shown not only that therapeutic synergy occurs between cetuximab and other chemotherapeutic agents, but also that resistance to irinotecan in some tumor cells can also be reversed (Meyerhardt *et al.*, 2005). A study by Saltz et al. suggested that 57 patients with EGFR-positive

colorectal cancer resistant to both fluorouracil and irinotecan, achieved an 8.8% partial response to cetuximab monotherapy, and 36.8% had stable disease (Mancuso *et al.*, 2005; Saltz *et al.*, 2004). Other study found that first-line treatment with FOLFOX plus cetuximab achieved 79% response rate in 43 patients.

The most common adverse effects of cetuximab are dermatological, including an acne-like skin rash, xerosis and fissures of the skin (Cunningham *et al.*, 2004). The acne-like skin rash seems to correlate with survival. This implicates that skin rash may be used as a marker for therapeutic response or, in a quantitative manner, as a tool to determine the optimal dose in individual patients (Perez-Soler *et al.*, 2005).

1.5.1 Anti-angiogenesis therapy

Tumors cannot grow without blood supply. Angiogenesis, the formation of new blood vessels, is essential for tumor growth and metastasis. The complex network of tumor vasculature system provides adequate nutrients and oxygen to tumor cells and allows efficient drainage of metabolites (Eichhorn *et al.*, 2007). The transition from normal to neoplastic vasculature during tumorigenesis has been termed the "angiogenic switch" (Hanahan *et al.*, 2000). Tumor angiogenesis is a complicated multi-step process regulated by the balance between endogenous proagiogenic factors and anti-angiogenic factors (Carmeliet, 2003). During tumor progression, environmental and genetic changes turn on the "angiogenic switch" with either upregulation of angiogenic factors or downregulation of angiogenesis inhibitors (Hanahan *et al.*, 1996; Poon *et al.*, 2003). The tumor obtains an angiogenic phenotype that promotes the formation of neovasculature. Angiogenesis can be activated by a series of environmental signals including metabolic stress, change in pH, hypoxia and cytokines from inflammatory response (Eichhorn *et al.*, 2007). The

development of new blood vessels in a tumor initially is involved in the release of angiogenic factors from tumor cells, which bind to specific receptors of endothelial cells of pre-existing blood vessels and hematopoietic and circulating endothelial precursor cells (CEPs) from the bone marrow, to trigger the process of angiogenesis (Pang *et al.*, 2006). Besides angiogenic factors, additional proteinases such as matrix metalloproteinases (MMPs) and plasminogen activators are secreted by activated endothelial cells to break down the extracellular matrix in front of the sprouting vessels. During the process of angiogenesis, endothelial cell adhesion molecules such as integrin αvβ3 and E-cadherin are required to connect new blood vessels with the preexisting ones to produce the intratumoral vascular network (Whisenant *et al.*, 2005). Most anti-angiogenic agents are designed to target the factors involved in the process.

Up to now, more than 40 known endogenous activators and inhibitors of angiogenesis are identified. Anti-angiogenic agents are created to mainly target the process of angiogenesis in the following aspects (Ferrara, 2002; Whisenant *et al.*, 2005): 1) inhibit/block pro-angiogenic factors or receptors, such as bFGF, VEGF , platelet-derived growth factor (PDGF) and EGFR, etc; 2) prevent degradation of the surrounding matrix; 3) increase the levels of endogenous anti-angiogenic factors; and 4) inhibit cellular adhesion molecules. Among them, bevacizumab, an anti-angiogenic agent targeting VEGF had been approved by FDA in 2004 for use in patients with previously untreated metastatic CRC in conjugation with 5-FU-based chemotherapy.

VEGF is the most potent and best defined inducer of angiogenesis through activation of its receptors Flt-1 and KDR expressed on endothelial cells (Pang *et al.*, 2006). VEGF secreted by almost all solid cancers is a heparin-binding peptide with a

specific mitogenic effect on endothelial cells; it also increases vascular permeability to plasma protein. The VEGF pathway can be upregulated by hypoxia and growth factors such as EGF and PDGF (Reinacher-Schick *et al.*, 2008).

Studies have shown that increased circulating levels of VEGF relate with advanced disease in patients with CRC and VEGF is expressed in about 50% of CRCs, with low to no expression in normal colonic mucosa or adenomas (Galizia *et al.*, 2004; Lee *et al.*, 2000). For some types of cancer, prediction of prognosis and relapse risk are estimated through increased VEGF expression levels in tumors more sensitively as compared to traditional staging methods; survival is significantly worse among patients with highest level of VEGF expression than in patients with negative or lower levels of VEGF expression (Fernando *et al.*, 2004; Galizia *et al.*, 2004). Increased expression of VEGF in patients with CRC has been correlated with tumor neovascularization, metastasis and proliferation of cancer cells (Boocock *et al.*, 1995; Reinacher-Schick *et al.*, 2008).

Bevacizumab is a recombinant anti-VEGF humanized monoclonal antibody that can neutralize free VEGF in the body (Mocellin *et al.*, 2005). It consists of 93% human IgG frameworks and 7% murine-derived antigen-binding regions, the humanization increasing the half-life and less immunogenicity (Fernando *et al.*, 2004). Studies have found that bevacizumab can block the biological properties of VEGF, including endothelial cell mitogenic activity, vascular-permeability-enhancing activity, and angiogenic properties *in vitro* and inhibit the growth of human tumor xenografts, and dramatically reduce the size and number of liver tumors in a mouse xenograft model of human colon cancer metastasis (Kim *et al.*, 1992; Warren *et al.*, 1995). In first-line treatment, the addition of bevacizumab to irinotecan plus bolus 5-FU/leucovorin improved the median overall survival with approximately 5 months (Hurwitz *et al.*,

2004). A phase III study on bevacizumab in advanced CRC including a total of 1,401 patients was recently presented. The patients received FOLFOX4 (continuous plus bolus 5-FU, leucovorin, and oxaliplatin) or CAPOX (capecitabine and oxaliplatin) plus either bevacizumab or placebo. The median progression-free survival (PFS) approached 9.3 vs 8.0 months, respectively, and the difference was significantly obvious (Mayer, 2009). Bevacizumab combined with 5-FU-based chemotherapy is currently considered as the standard first-line treatment of patients with advanced CRC.

Bevacizumab is relatively well tolerated (Fernando *et al.*, 2004). Two frequent but reversible adverse side effects (hypertension and proteinuria) result from bevacizumab, but increase in bleeding or thrombotic events rarely occur. Approximately 50% of patients reported transient minor epistaxis (Fernando *et al.*, 2004).

1.5.2 Phage display and targeted therapy

Currently, human antibodies have been developed as important drug candidates for therapeutics because they are thought to have the advantages of high affinity and specificity, large-scale producibility, favorable pharmacokinetics, acceptable toxicity, low antigenicity and predictable, though with high cost (Ladner *et al.*, 2004; Schaedel *et al.*, 2006) Both cetuximab and bevacizumab, as two novel drugs against CRC approved by FDA recently, belong to recombinant chimeric monoclonal antibody in nature. But uptake and distribution of antibodies in solid tumors remains a substantial challenge. It is difficult for antibodies to penetrate the physical barriers (elevated interstitial pressure, heterogeneous and reduced functional vasculature and lymphatics and the large distances for antibody to travel in the tumor interstitium)

related to large solid tumor volume, to reach tumor tissues due to large molecules weight, which reduces the efficacy of antibody to a great extent (Reilly *et al.*, 1995; Trail *et al.*, 2003). Liver/bone marrow toxicity by nonspecific uptake of antibodies also limits their applications (Goldenberg, 2003; Reilly *et al.*, 1995).

Currently, more and more attention is being paid to other small molecular candidate drugs—peptides. Several dozen peptides have been isolated which can target specific intracellular proteins or receptors of cell surface required by cancer cells for proliferation, apoptosis, migration, invasion and angiogenesis. All of those peptides are isolated through high-affinity selections against predefined target molecules are emerging as important drug candidates, which could extend conventional druggability. It should be feasible that individual peptides or peptides conjugated to cytotoxic agents can be applied to inhibit the cancer in a targeted fashion.

Actually, peptides (are much smaller, usually classified as containing less than 50 amino acids, ~5500 Da. At 100 amino acids or greater, the string of amino acids is considered as a protein (Weiner *et al.*, 2002)), while make up only a small percentage of pharmaceutical agents, have already been used to manipulate crucial regulatory networks in cancer cells in a few model systems (Borghouts *et al.*, 2005; Mendoza *et al.*, 2005; Nagel-Wolfrum *et al.*, 2004). In theory, peptides are likely to have the following advantages as compared to antibodies as drug candidates including: (Aina *et al.*, 2007; Graff *et al.*, 2003; Heppeler *et al.*, 2000; Ladner *et al.*, 2004): (a) lower manufacturing costs, (b) lower royalty stack than antibodies because of a simpler intellectual property landscape, (c) higher activity per mass, (d) better organ or tumor penetration, (e) less immunoreactivity, (f) greater stability, and (g) rapid blood clearance and (h) easy synthesis of conjugates with radionuclides, cytotoxic drugs or toxins. In addition, peptides are generally stable to proteolysis when they are blocked

and cyclized at the N- and C- terminal or contain D-amino acid and unnatural amino acids. However, how can specific peptides that interact with targets be isolated against valuable molecular targets in the tumor progression?

Phage display: Phage display is a simple but powerful technology that can be used to screen peptides that interact with a molecular target of interest. One can rapidly and simultaneously screen billion of clone-peptide libraries through phage display technology, leading to large numbers of "hits".

Phage display, established by George P. Smith in 1985 (Smith, 1985) is a powerful technology for selecting and engineering peptides and proteins expressed on the surface of filamentous bacteriophage (Ff). This methodology relies on a direct linkage between phenotype and genotype, which in this case is the physical link between the engineered fusion protein or peptide displayed on the phage surface and the DNA encoding them inserted in the phage gene sequence (Fig. 1) (Hartley, 2002; Kehoe *et al.*, 2005; Mersich *et al.*, 2008; Sidhu, 2000) Using simple molecular biology techniques, large and diverse phage-displayed peptide libraries can be prepared.

The most commonly used Ff is M13 phage, which consists of a single-stranded circular DNA genome packaged in a tube comprised of 2700 copies of the major coat protein pVIII and closed at the ends by 4 or 5 copies of each of four species of minor coat proteins pIII, pVI, pVII and pIX. The wild type M13 is a long (900 nm) and narrow (7 nm) filamentous particle and needs the F-pilus for infection of *Escherichia coli* host (Fig. 1) (Manoutcharian *et al.*, 2001; Rodi *et al.*, 1999).

The linkage between phenotype and genotype, along with the simplicity of *in vitro* and *in vivo* manipulations of the phage, allows rapid generation of phage-displayed peptides which bind specifically to any given molecular target-antibody, receptor, or

tumor tissue within 2-3 weeks (Nilsson *et al.*, 2000; Sidhu, 2000). The biopanning is often performed against immobilized target molecules; the library is exposed to immobilized target molecules; phage with appropriate specificity is captured, while non-binding phage is washed off. Moreover, this selection is often carried out in a "high-throughput" manner. The bound phage retains infectivity and can therefore be eluted, amplified and processed at will by infecting bacterial host cells. This amplified phage pool is greatly enriched in phage displaying peptides binding to the target and can be used in subsequent round selections. The primary sequence of the foreign peptide can be identified easily by sequencing the peptide-coding sequence in the phage DNA (Figure 2A). Affinity selection avoids analyzing clones one by one. Consequently, the number of peptides that can be screened is enormous; billionclone libraries are commonplace and much larger ones could be screened once they are available (Willats, 2002).

Conventional panning can be carried out against soluble protein coated to the solid phase. Alternatively, several new techniques have been developed for selection of phage libraries such as biopanning against live cell surface molecules, *ex vivo* phage display biopanning based on diseased tissues and *in vivo* phage display biopanning against animal model (Fig. 2B) (Hartley, 2002; Schulmann *et al.*, 2005).

In vitro, *in situ, ex vivo* and *in vivo* phage display affinity selection procedures have been employed to isolate peptides that target molecules thought to be important at different stages of cancer development and/or metastasis. Cancer-associated targets used to screen phage peptide library have included receptors, kinase proteins, carbohydrates, enzymes, and other proteins that play vital roles in cancer progression. Some of these peptides have clear prospective applications in cancer targeted-therapy.

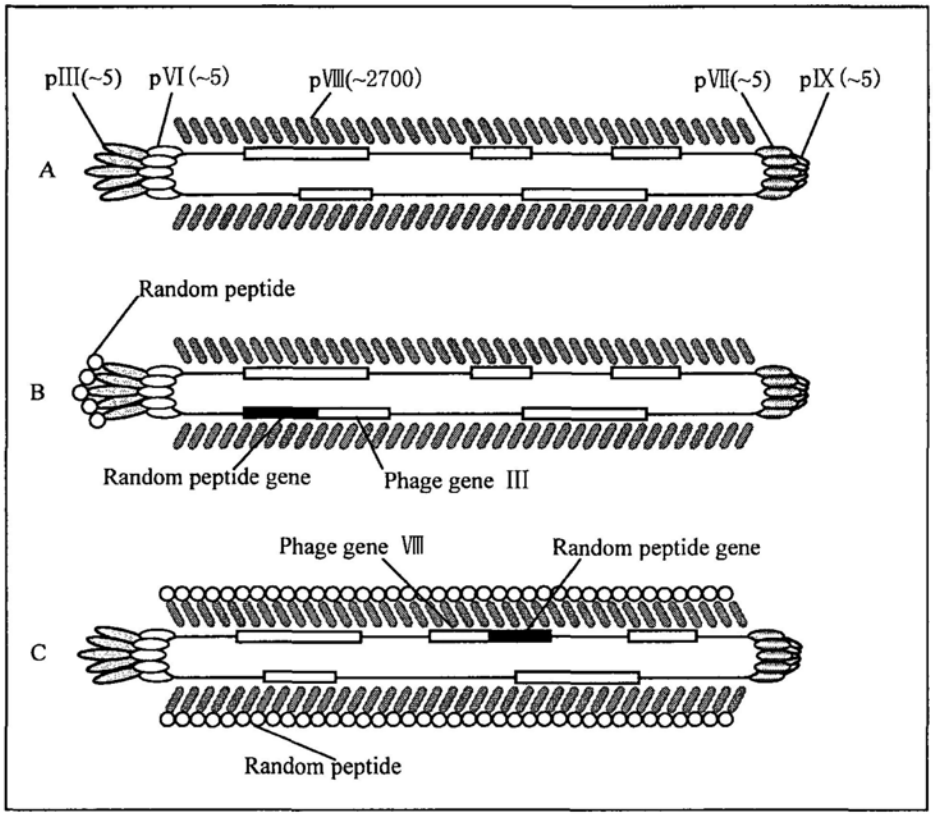

Fig. 1 Basic principle of phage display.

A, M13 phage structure. The approximate number of copies of each M13 phage capsid protein is indicated. B, Peptides are displayed on the phage capsid protein III through fusion of peptide gene to phage gene III. The pIII protein as a fusion partner displays a limited number of peptides (~5 copies). C, Peptides are displayed on the phage capsid protein VIII through fusion of peptide gene to phage gene VIII. Thousands of peptides can be displayed on the phage surface if peptide gene is fused to phage gene VIII.

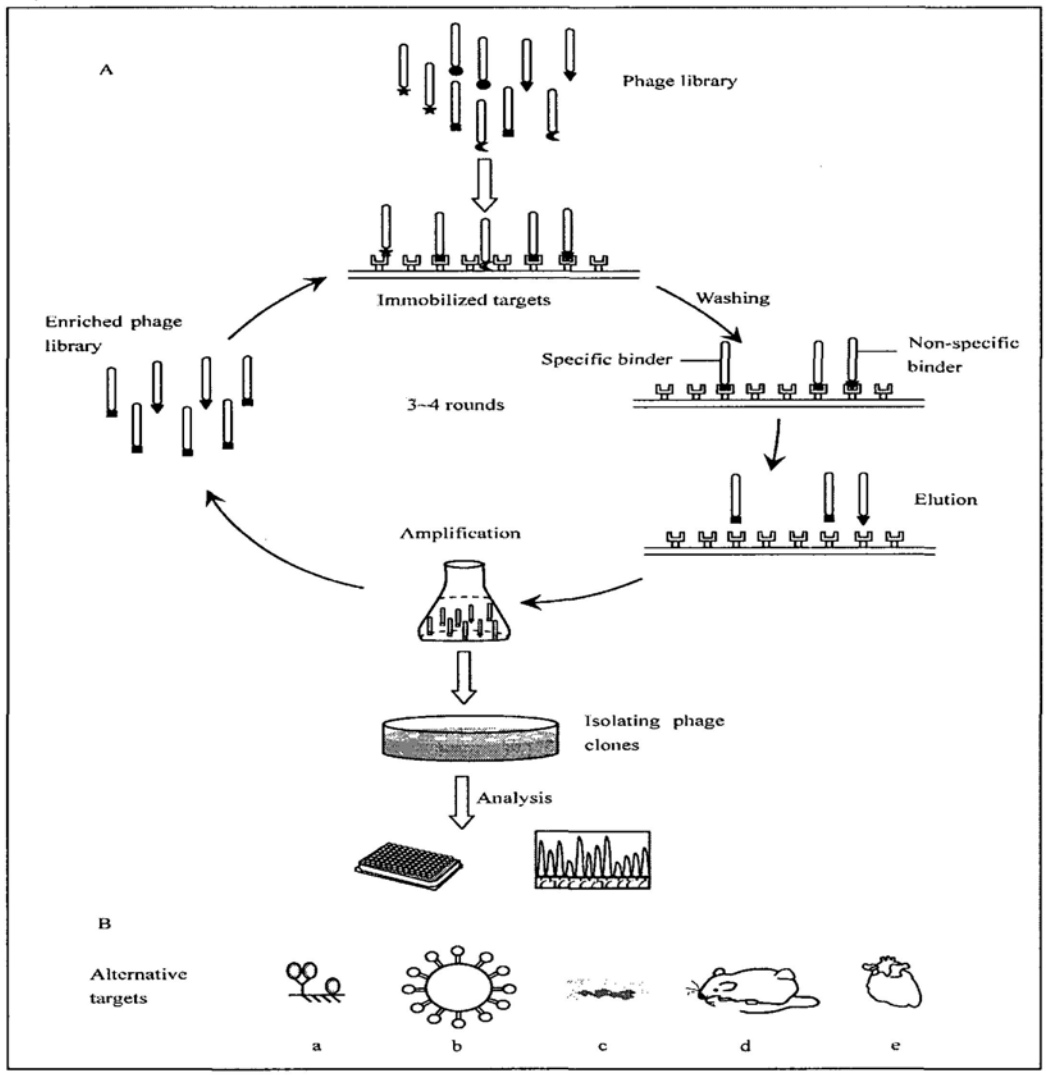

Fig. 2 The simple schema of phage display biopanning.

A, Phage display biopanning procedure. The initial phage library displaying variant peptides is incubated over immobilized target; most of the non-specific binders are washed away, specific phage and a very little non-specific phage are captured. Bound phage are eluted and amplified in host bacterial cells for subsequent biopanning. Individual phage clones may be isolated and analyzed after several-round biopanning. B, Various targets in the phage display biopanning: a, immobilized targets in microtiter plate, b, targets (protein) coated on the affinity resin, c, whole cells as targets, d, *in vivo* screening against animal model, e, *ex vivo* screening against tissues.

1.5.3 *In vivo* phage display and peptide targeting the vascular zip code of tumor

Previous studies have shown that endothelium expresses different molecules depending on which tissue or organ it is derived from. Tumor angiogenesis is essential to obtain oxygen and nutrients for tumors to grow. These new blood vessels are different from normal blood vessels structurally and functionally. Tumor neovasculature is often tortuous and leaky. Their diameter is irregular and their walls are thin (Ruoslahti, 2002). Furthermore, tumor blood vessels express a distinct set of molecules on their surface that do not exist or are expressed at much lower levels in normal resting blood vessels (Laakkonen *et al.*, 2008; Ruoslahti, 2004). These 'zip code' expressed specifically in tumor vasculature provide potential objectives for targeted therapy, such as the elevated VEGF receptors, overexpressed integrins $\alpha_v\beta_3$, $\alpha_v\beta_5$, $\alpha_5\beta_1$, MMP2/MMP-9, specific aminopeptidase N and A, etc. To search for specific molecular targets on the tumor neovasculature, '*in vivo* phage display technology' has been extensively used. Both the molecular heterogeneity of normal (Arap *et al.*, 2002b; Pasqualini *et al.*, 1996; Zhang *et al.*, 2005) and diseased (Gerlag *et al.*, 2001; Joyce *et al.*, 2003; Marchio *et al.*, 2004; Rajput *et al.*, 2008) blood vasculatures have been identified through this technology. In 1996, Rouslahti and Pasqualini pioneered a novel phage display application by performing their selections in mice to obtain organ-targeting peptides (Arap *et al.*, 1998; Pasqualini *et al.*, 1996). The relatively novel and elegant approach is named after "*in vivo* phage display" (Figure 3). This *in vivo* biopanning technology is performed by injecting a phage library into an animal and then isolating and recovering those phages that bind to a particular organ or tissue. Multiple rounds of *in vivo* selection can isolate phage displayed specific peptides targeting particular tissues (Fig. 3) (Christianson *et al.*,

2007; Hajitou *et al.*, 2006; Newton *et al.*, 2008; Trepel *et al.*, 2008). The advantage of the *in vivo* phage selection is that it does not require any previous knowledge of the molecular composition at the site of interest because of the vascular heterogeneity. The phage particle could not leave the circulation within a short circulation time (approximately 5~15 mins). Thus, only the phage clone bound to endothelium is isolated (Hajitou *et al.*, 2006). Meanwhile the phage that expresses ligands that bind to all blood vessels can be negatively selected by the rest of the target tissue (Christianson *et al.*, 2007; Enback *et al.*, 2007; Zurita *et al.*, 2003). Several dozen peptides that selectively home to tumor vasculature have been identified after introduction of *in vivo* screening of phage-displayed peptide libraries (Arap *et al.*, 1998; Hajitou *et al.*, 2006). These peptides have exhibited valuable potential in the ligand-based tumor targeted therapy and diagnosis.

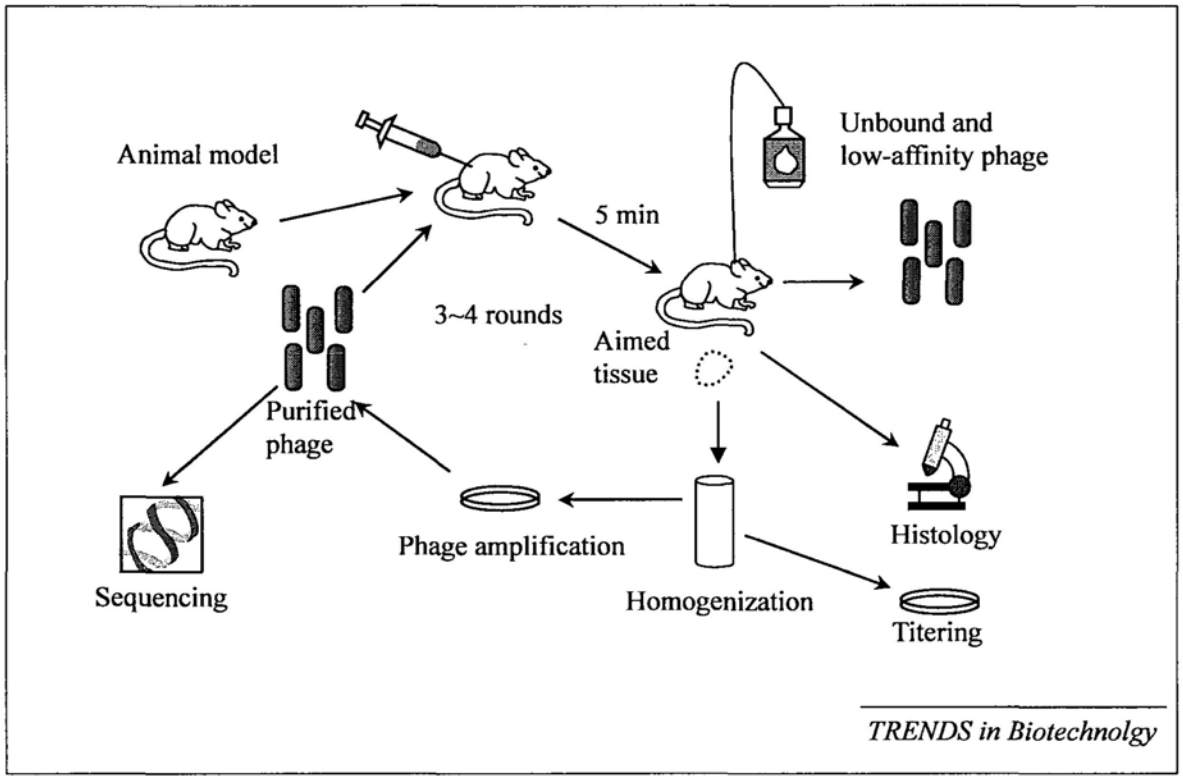

Fig. 3 A schema for *in vivo* phage display.

An animal is injected phage library through the tail vein. After 5 min of circulation, the animal is perfused to discard non-binding and low-affinity phage. The target tissue or organ is harvested, and phage bound to the tissue is rescued. This process is repeated three times and the peptide sequences of the resulting phage are determined.

1.5.4 Peptide-mediated anti-angiogenesis therapy of tumor

One potential application of peptides homing to tumor vasculature is to deliver the toxin or a pro-drug molecule as a targeted therapy agent with increasing efficacy of anti-cancer action and decreasing undesired systemic side effects in other tissues (Chang *et al.*, 2009a; Curnis *et al.*, 2004; Kolonin *et al.*, 2004). It has been estimated that 100 tumor cells are fed by a single endothelial cell. Thus anti-angiogenic therapy aiming to block the blood supply is able to constrain cancer growth for prolonged periods (Hajitou *et al.*, 2006; Kerbel, 2006). Ligand-based tumor targeting approaches can enable the ligand (drug) localized in the tumor microenvironment, with tumor-to-control organ ratios >10:1 only a few hours after intravenous administration (Hajitou *et al.*, 2006). It is possible that targeted destruction of the established tumor vasculature can shut down or at least selectively damage the blood vessel in order to lower the blood, oxygen and nutrient supplies to tumor cells without affecting normal tissues. Moreover, unlike cancer cells, tumor blood vessels serve as excellent therapeutic targets as they do not have the genetic instability that allows cancer to develop drug resistance (Ruoslahti, 2002). On the other hand, endothelial cells are directly accessible to blood-borne agents, circumventing the problem of drug delivery to tumor cells, which is a major obstacle to conventional anticancer drugs.

In vivo screening of phage-displayed peptide libraries has identified several dozen peptides that selectively home to tumor vasculature (Arap *et al.*, 1998). One of the most famous peptide motifs (RGD) discovered through phage display biopanning was previously identified as the binding motif for $\alpha_v\beta_3$ and $\alpha_v\beta_5$ integrins selectively expressed in the tumor blood vessels (Koivunen *et al.*, 1995). Peptides CNGRC (NGR) and SMSIARL were also isolated through *in vivo* screening (Pasqualini *et al.*,

2000)]. The peptides CNGRC was found to target CD13 specifically expressed in tumor vasculature. RGD and NGR peptide conjugated with doxorubicin (a DNA-interacting drug widely used in chemotherapy), could increase therapeutic efficacy of the drug against human breast cancer xenograft in nude mice and reduce its nonspecific toxicity (Arap *et al.*, 1998). The peptide SMSIARL was identified that could home to the vasculature in normal murine prostate, and also bind to vasculature in the human prostate (Arap *et al.*, 2002a). Systemic treatment of mice with the SMSIARL peptide conjugated with a pro-apoptotic peptide $_D$(KLAKLAK)$_2$ that disrupts mitochondrial membranes upon receptor-mediated cell internalization and causes programmed cell death, resulted in tissue destruction in the prostate, but not in other organs. Chimeric peptide treatment could delay the development of cancers in prostate cancer-prone transgenic mice with the (Arap *et al.*, 2002a) . Several peptides isolated by Wu's laboratory (Chang *et al.*, 2009a; Chang *et al.*, 2009b; Eichhorn *et al.*, 2007; Lo *et al.*, 2008) can target tumor vasculature originated from multiple organs. These peptides conjugated with liposomes containing doxorubicin enhance the therapeutic efficacy of the drug against human cancer xenograft in animal models. However there was no similar study reported in orthotopic colorectal cancer models. To this end, peptides specifically targeting the vasculature of CRC remain unknown. Our study focuses on the identification of peptide specifically targeting the vasculature of orthotopic CRC model established in BALB/c mice.

1.6 Orthotopic and ectopic models for colorectal cancer research

Animal models for CRC are the most informative method to obtain insight into the mechanisms that contribute to the development and pathogenesis of CRC in humans.

Orthotopic and ectopic models (mainly subcutaneous model) are two important models which have been extensively applied for colorectal cancer research. The design and use of these models depend on the specific questions that researchers are exploring. Subcutaneous models might be suitable to assay anti-tumor activity *in vivo* after administration of a cytotoxic compound, but the models might be inappropriate to isolate agents against target molecules that are only expressed when tumor is located in visceral organs and not under the skin (Killion *et al.*, 1998). Actually, the traditional subcutaneous model has obvious disadvantages for studying CRC though they are easy to be established and monitored. An important factor, tumor microenvironment, is ignored in the subcutaneous model. In fact, tumor microenvironment can produce vital influence on tumor phenotype, progression, metastasis, and even response to therapy. Tumor microenvironment is an anatomical and functional space that includes tumor cells, normal cells (parenchymal cells, epithelial cells, etc.), the extracellular matrix (ECM), stromal fibroblasts, immune cells (lymphocytes, macrophages, and mast cells), and vascular cells (endothelial cells, pericytes, and smooth muscle cells) and provides a milieu for their interactions (Ariztia *et al.*, 2006). It has become evident that the extent of angiogenic heterogeneity in malignant neoplasms is regulated by the organ microenvironment (Fidler, 2001). For example, human renal carcinoma cells implanted into the kidney of nude mice produced a high incidence of lung metastasis, whereas those implanted subcutaneously were not metastatic (Fidler, 2001; Hoffman *et al.*, 2003). Histopathologic analysis of the tissues disclosed that the tumors devolped in the subcutis of nude mice had few blood vessels, whereas the kidney tumors were highly vascularized (Ariztia *et al.*, 2006; Fidler, 2001; Hoffman *et al.*, 2003). The corresponding mechanism revealed that the expression of b-FGF (fibroblast growth

factor) from human renal carcinoma cells (HRCC) depends on the organ microenvironment. HRCC transplanted into kidneys of nude mice induced an increase of 10 to 20 times more b-FGF mRNA expression as compared to HRCC transplanted subcutaneously (Ariztia *et al.*, 2006; Hoffman *et al.*, 2003). In terms of CRC, studies found that human colon cancer cells growing in the cecum of nude mice secrete more VEGF than did those in the liver and the subcuits (Mersich *et al.*, 2008). Another study from analysis of colorectal cancer specimens also suggested that 11 of 17 patients exhibited higher VEGF levels in the primary tumor than in the liver metastasis (Mersich *et al.*, 2008). We know that VEGF as a pro-angiogenic factor, serves as important action in tumor angiogenesis. Even more orthotopic and ectopic organ environments differentially alter the sensitivity of tumor cells to chemotherapeutics. For example, colon cancers tranplanted subcutaneously were more susceptible to doxorubicin than tumors growing in the cecum of mice (Wilmanns *et al.*, 1992).

Orthotopic mouse models of CRC in colorectal lumen, which characterize tumor cells growing in the natural location, could mimic the tumor microenvironment more accurately as in human colorectal cancer with fidelity (Tseng *et al.*, 2007). In our study, orthotopic model was used to isolate the peptides against molecules specifically expressed in the vasculature of orthotopic colorectal tumor.

1.7 Our study

Targeted therapy is representing a new direction for either CRC or other solid tumors treatment. Tumor neovasculature provides a new target for targeted therapy because they can express specific markers on the surface different from normal blood vessels. Peptides bound to a specific site in the tumor neovasculature are attractive for

delivery of drug and image contrast. Homing peptide-mediating drug delivery could accumulate the drug concentration at the targeted site, increasing efficacy but decreasing adverse side effect in other tissues. Homing peptide-coupled imaging probe could enhance diagnosis specificity and reduce non-specific absorbance. Up to now, peptides targeting the neo-vasculature of CRC have not been defined. Although previous analogous studies have successfully applied the phage display technology to isolate peptides specifically targeting surface antigens on tumor cells or tumor-associated vasculature of subcutaneous xenograft model in immunodeficient mice (Chen *et al.*, 2008; Eichhorn *et al.*, 2007; Kelly *et al.*, 2003). Moreover, cancer cells are genetically unstable, easy to acquire multidrug resistance and their surface antigen expression pattern may change in response to targeted therapy. In addition, subcutaneous xenograft models cannot mimic the complexity of the internal microenvironment of the gut and the interpretation of experimental results carried out under immunocompromised conditions suffer from significant limitations. Our objectives of the study are:

(1) To biopan and identify peptides specifically targeting the vasculature of orthotopic colorectal cancer through *in vivo* phage display technology, and

(2) To develop these peptides as vectors for imaging detection and drug delivery for colorectal cancer.

Chapter 2

Materials and methods

2.1 Chemicals, animals and cell lines

2.1.1 Reagents and drugs

Name	Company	Catalog number
Agarose	Invitrogen	15510-019
Aprotinin	Sigma	A1153
Blue/Orange loading dye	Promega	G1881
Bovine serum albumin (BSA)	Sigma	A3350
Bromophenol blue	Sigma	B8026
5-Bromo-4-chloro-3-indolyl-β-D-galactosi de (X-gal)	Sigma	B4252
Dimethyl sulphoxide (DMSO)	Sigma	D8418
3-(4,5-Dimethyl-thiazol-2-yl)-2,5-diphenyl -2H-tetrazolium bromide (MTT)	Sigma	M2128
Dipotassium hydrogen orthophosphate (K_2HPO_4)	BDH	104363A
Disodium hydrogen orthophosphate (Na_2HPO_4)	BDH	102494C
Dimethyl formamide (DMF)	Merck	A3633
Dulbecco's Modified Eagle Medium (DMEM)	Invitrogen	12100046
Dextran sulphate sodium (DSS)	Advanced Techno-logy&Industrial Co. LTD	9011-18.1

Eosin Y solution	Sigma	HT110180
Ethanol	Merck	986
Ethidium bromide	Sigma	E8751
Ethylene diamine tetraacetic acid (EDTA)	Sigma	ED-2S2
Fetal bovine serum (FBS)	Invitrogen	10437-028
Glycerol	Sigma	G8773
Glycine	Bio-Rad	160-0717
Hematoxylin Solution	Sigma	GHS1128
Hydrochloride acid (HCl)	Merck	9970
Hydrogen peroxide(H_2O_2)	Sigma	H6520
Isopropanol	Merck	9634
Isopropyl-β-D-thiogalactoside (IPTG)	Sigma	I6758
Leupeptin	Sigma	L7920
LB broth base	Invitrogen	12780-052
LB/Agar	Invitrogen	22700-025
MEM	Invitrogen	41500-034
Methanol	Merck	6009
10% normal goat serum	Invitrogen	50062Z
Paraffin (Tissue Prep)	Fisher Scientific	T565
PEG 8000	Sigma	H10230
Penicillin G	Sigma	P3032
Pepstatin A	Sigma	P5318
Phenylmethylsulphonyl fluoride (PMSF)	Sigma	P7626
Potassium chloride (KCl)	BDH	295944B
Potassium dihydrogen orthophosphate	BDH	102034B

(KH_2PO_4)		
Ready-Load™ 1 kb DNA ladder	Invitrogen	12308-011
RPMI 1640	Invitrogen	23400-021
SeeBlueTM prestained standards	Invitrogen	LC5625
Sodium carbonate (Na_2CO_3)	BDH	102405Y
Sodium chloride (NaCl)	BDH	10241AP
Sodium dihydrogen orthophosphate (NaH_2PO_4)	BDH	301324Q
Sodium hydrocarbonate ($NaHCO_3$)	BDH	10247V
Sodium hydroxide (NaOH)	BDH	102524X
Streptomycin sulphate	Sigma	S9137
Sucrose	Sigma	S0389
TBE (Tis-borate-EDTA) buffer	Bio-Rad	161-0733
Tetracycline	Sigma	T8032
Tris/Glycine buffer	Bio-Rad	161-0771
Triton X-100	Sigma	T8787
Trypsin EDTA	Invitrogen	25200-056
Tween 20	Sigma	P1379
Tissue-tek O.C.T. compound	Sukura	4583
Xylene	MERCK	1.08685.9190

2.1.2 Antibodies and commercial kits

Name	Company	Catalog number
Alexa Fluor 568 goat anti-rat IgG (H+L)	Invitrogen	A11077

Alexa Fluor 568 goat anti-mouse IgG (H+L)	Invitrogen	A11031
Alexa Fluor 488 goat anti-rabbit IgG	Invitrogen	A11034
Cleaved caspase 3 antibody	Cell signaling	9661
DAB detection kit	DAKO	K3468
Goat anti-Mouse IgG-HRP conjugate	Invitrogen	62-6120
Goat anti-Rabbit IgG-HRP conjugate	Sigma	A0545
Mouse anti-human CD31 antibody	DAKO	M0823
Platinum® PCR SuperMix kit	Invitrogen	11306-016
Rabbit anti-fd bacteriophage antibody	Sigma	B7786
Ph.D.™-C7C Phage Display Peptide Library	NEB	E8121L
Rat anti-mouse CD31 antibody	BD Pharmingen	558736
In Situ Cell Death Detection Kit, Fluorescein	Roche	11 684 795 001

2.1.3 Peptide synthesis

The synthetic peptides CTPSPFSHC (TCP-1), CTPSPFSHC-GG-$_D$(KLAKLAK)$_2$ and $_D$(KLAKLAK)$_2$ were obtained commercially (AnaSpec, USA) to our specifications. For *in vivo* peptide homing validation, FITC-conjugated CTPSPFSHC (TCP-1), FITC-conjugated TPSPFSH (TP-1), CSNSDWSSC (TCP-2), FITC-conjugated CSNSDWSSC (TCP-2), and FITC-conjugated CVQTAQLLC (negative control) were also synthesized with purity≥ 95%.

2.1.4 Animals

The experimentation of this study was approved by the Laboratory Animals Ethics Committee in the Chinese University of Hong Kong. Male normal BALB/c mice at the age of 9 weeks old and 6- to 8-week-old male BALB/c nu/nu mice were used in this study. They were maintained at the Chinese University of Hong Kong Animal Facility. All animals were housed in plastic cages (four or five mice/cage) with free access to drinking water and a pelleted basal diet, under controlled conditions of humidity (50 ± 10%), light (12/12 h light/dark cycle) and temperature (23 ± 2 °C).

2.1.5 Cell lines and cell culture

The murine colorectal cancer cell colon 26, and human gastric cancer cell MKN45 were originally obtained from Health Science Research Resources Bank (Osaka, Japan). Human colon cancer cell HT-29, SW1116, and HCT116 were purchased from the American Type Culture Collection (Manassas, VA, USA). These cell lines were cultured at 37°C in a humidified atmosphere containing 5% CO_2, in RPMI-1640 medium supplemented with 2 g/L sodium bicarbonate, 100 units/ml penicillin (ICN Biomedicals, Costa Mesa, CA), 100 mg/ml streptomycin (ICN Biomedicals, Aurora, OH), pH 7.4 and 10% fetal bovine serum (FBS, Invitrogen).

2.2 Establishment of models

2.2.1 Orthotopic colorectal cancer model

The model was performed as previously published by Takahasi with some modifications (Fig. 4) (Takahashi *et al.*, 2004). Briefly, normal BALB/c mice were given the tap water containing 3% dextran sulphate sodium (DSS) for 7~9 days to induce colitis. Mice were fasted for 18 h after colitis induction, and then anesthetized with sodium pentobarbital (50 mg/kg). Colon 26 cells (3×10^6 cells/40 μl/mouse)

were infused intrarectally with a micropipette inserted 2 cm into the anus of the mice. The anus was compressed with a noncrushing microclamp immediately after instillation of tumor cells for 30 min to prevent leakage. Mice were sacrificed at 2 or 3 weeks after the implantation of cancer cells. Each colorectum was examined for the development of intraluminal tumors under a stereoscopic microscope. The tumor size was measured with a vernier caliper and tumor volume was calculated according to the following formula: Tumor volume (mm^3) = length (mm) × width^2 (mm^2) × 1/2. Mice bearing tumors were used for *in vivo* selection at 2~3 weeks after implantation of cancer cells.

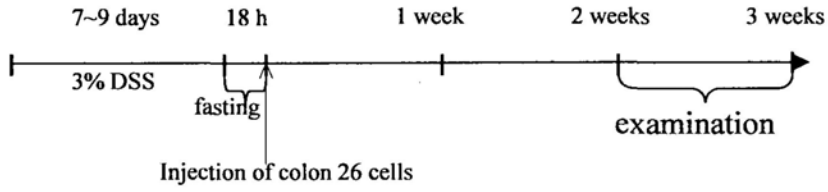

Fig. 4 Experimental protocol for establishment of orthotopic colorectal cancer model.

2.2.2 Orthotopic gastric cancer model

The model was performed as previously published with some modifications (Shin *et al.*, 2004). BALB/c nu/nu mice were implanted with MKN45 (a poorly differentiated human gastric adenocarcinoma cell line), as a human gastric cancer xenograft model for the study of the TCP-1 peptide homing ability. MNK45 cells were trypsinized, and the total cell number in the cell suspension was adjusted to 4 ×10^7 cells/ml. Mice were anesthetized, and an incision was made through the left upper abdominal paramedian line and peritoneum. The stomach wall was carefully exposed. A volume of 100 μl of this cell suspension was injected into the middle of the greater curvature of the carefully exposed stomach. The peritoneum and the skin were closed with

surgical suture. The mice were used after tumors grew for 3 weeks.

2.2.3 Subcutaneous cancer model

For subcutaneous cancer model induced by colon 26, male normal BALB/c mice at 9 weeks of age were s.c. injected with 2×10^6 colon 26 cells in 150 μl PBS. Tumors were allowed to grow for 10 days and mice were used to perform phage homing ability assay.

For subcutaneous model induced by HT-29, HCT116 and MKN 45, male nude BALB/c mice at the age of 6-8 weeks old were s.c. injected with 3×10^6 cells/150 μl PBS. Tumors were allowed to grow for 2 weeks and mice were used to perform phage homing ability assay.

2.2.4 Lung metastatic tumor model of colorectal cancer

The model was performed as previously described (Choo *et al.*, 2005; Choo *et al.*, 2006; Xiang *et al.*, 1997). Colon 26 cells were harvested with trypsin-EDTA, washed with serum-free RPMI 1640 medium and resuspended in cold PBS. The cell suspension (1×10^5/100 μl) was implanted by intravenous injection. The mice were sacrificed on day 21 after cell injection. The metastatic tumor colonies in the lungs were examined under a stereoscopic microscope. Mice at 21 days after cell injection were used to perform phage homing ability assay.

2.2.5 Acute colitis induction

Acute colitis was induced as previously published (Fukata *et al.*, 2005; Yoon *et al.*, 2008). Male 9-week-old mice were given tap water containing 3% DSS for a period of 7 days. Control mice were given regular drinking water. During the course of

DSS treatment, the body weight of animals were recorded, development of diarrhea, and rectal bleeding. Animals were killed at the end of 7 days. Colon length and weight were measured and the ratio of colon length to colon weight was calculated. The colon was prepared for Hematoxylin and Eosin (H&E) staining according to histological methods. Meanwhile, phage homing ability was tested in the mice with acute colitis.

2.2.6 Chronic colitis induction

The method for induction of chronic colitis was previously described (McCole *et al.*, 2005; Sun *et al.*, 2007). Male BALB/c mice (9 weeks old) received three cycles of DSS treatment. Each cycle consisted of 3% DSS in tap water for 7 days, followed by a 7-day interval with normal tap water. Control mice were given regular drinking water. To assess the extent of colitis, body weight and rectal bleeding were monitored. Mice were killed and colon was assessed histologically. They were also used for phage homing ability assay at the completion of the third cycle of DSS administration (Fig.5). Colon length and colon weight were measured and the ratio of colon length to weight was calculated. The colon was stained by H&E according to histological methods.

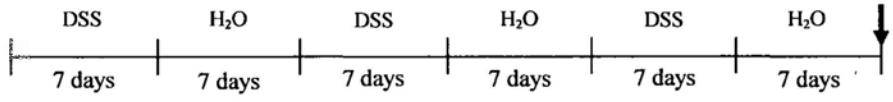

Fig. 5 Experimental protocol for establishment of chronic colitis model.

Animals were sacrificed at the end of 3-DSS cycle at the time indicated by an arrow.

2.2.7 Hematoxylin and Eosin staining

2.2.7.1 General histological procedure

Mice established from different models were killed at the end of experiments. All kinds of samples were collected and fixed in 4% buffered formalin overnight. Tissues were then immersed in a series of different percentages of ethanol for 1 h at each of the following concentrations: 75%, 95% 100% and 100% for dehydration and cleared with xylene for 45 min. Afterward, tissues were immersed in melted paraffin at 70℃ for 3 h for effective penetration of paraffin and finally embedded into a paraffin block. Sections of 5 μm in thickness were cut with a microtome (American Optical Corporation, USA), prepared on glass slides using the water floatation method at the water bath at 40℃. They were oven-dried at 40℃ overnight. The dried sections were deparaffinised with 2 changes of xylene (3 min each), and re-hydrated by successive passages of the sections, at 3-min intervals, through solutions of 100%, 100%, 95% and 70% of ethanol and finally water.

2.2.7.2 Procedures for Hematoxylin and Eosin staining

Re-hydrated sections were immersed in Harris hematoxylin solution for 10 min, following by successive washing in running tap water for 5 min. The sections were then differentiated in 1% acid alcohol (quickly dip one time) and then flushed with running tap water for 1 min. The sections were then blued in Scott's tap water for 1 min and washed in running tap water for 5 min. Finally, the sections were counterstained in eosin Y solution for 8 min. The sections were dehydrated through 95% alcohol and 2 changes of absolute alcohol, 5 min each. The sections were then cleared in 2 changes of xylene for 5 min each. The slides were finally mounted with xylene based mounting medium.

Histological assessment was performed on formalin fixed, paraffin-embedded colon tissue after H&E staining. Based on H&E staining, pathological changes such as

mucosal ulceration, and carcinoma were verified by a board-certified pathologist in a blinded manner according to the criteria previously reported.

2.3 *In vivo* phage library biopanning

2.3.1 Procedures for biopanning

The biopanning procedure was achieved as previously described (Christianson *et al.*, 2007; Joyce *et al.*, 2003; Trepel *et al.*, 2008). Briefly, mice bearing tumors were anesthetized by 50 mg/kg sodium pentobarbital and i.v. injected with a C7C phage library (New England Biolabs) in 300 μl TBS containing 5×10^{10} pfu (plaque forming unit) phage. After 8 min, mice were perfused through the heart with DMEM containing 1% BSA. For the first round of selection, 2 ml perfusion solution was used to obtain enough peptide sequences. The tumor and control organs were dissected from each mouse and the phage was rescued and titered. From the second round, the perfusion solution was increased to 5 ml to remove the unspecific binding clones. After the fourth round of biopanning, 80 phage clones were picked and suspended in 20 μl PBS. PCR was used to amplify the inserted fragments, and PCR products were sequenced. The following primer pairs were utilized for PCR: 5'-AGC AAG CTG ATA AAC CGA TAC AAT-3' (forward) and 5'-TAC CGT AAC ACT GAG TTT CGT CAC-3' (reverse). PCR condition is 94℃ 2 min, 94℃ 30 sec, 56 ℃ 30 sec, 72℃ 1 min, 35 cycles, 72℃ 2 min.

2.3.2 Phage purification

Phage purification is a necessary step for phage library biopanning. This is a universal protocol for phage purification.

1) After culture bacteria infection, centrifuged the culture at 8000 g for 10 min at 4 °C and transferred the supernatant to a new tube.
2) Added 1 ml PEG/NaCl per 6 ml of phage solution. Mixed by inversion 10 times and incubated on ice for 2–4 h, at best overnight.
3) Centrifuged the sample at 10,000 g for 15 min at 4 °C.
4) Aspirated the supernatant without disturbing the pellet and re-centrifuge at 10,000 for 5 min at 4 °C to remove the remaining PEG supernatant.
5) Re-suspended the phage in 1 ml TBS. Avoid re-suspending the phage pellet with the pipette as frothing can occur that might harm the phage or display peptides
6) Completely solubilized the pellet and then centrifuge at 10,000 g for 10 min to remove any bacteria debris.
7) Transferred the supernatant to a sterile tube and add 167 µl PEG/NaCl.
8) Left on ice for 1 h for a second phage precipitation.
9) Centrifuged at 10,000 g for 15 min at 4 °C.
10) Discarded the supernatant. Centrifuge at 10,000 g for 5 min at 4 °C.
11) Re-suspended the phage pellet in 150-200 µl of PBS.
12) Centrifuged at 10,000 g for 5 min to remove any bacterial contaminants and store at 4 °C.
13) Titered the phage
14) The amplified library was used for subsequent rounds of biopanning.

2.4 *In vivo* phage targeting assay

In vivo phage targeting assay was tested as described previously (Zhang *et al.*, 2006). Briefly mice bearing tumors were anesthetized by 50 mg/kg sodium pentobarbital and i.v. injected with 1×10^{9}~2×10^{11} pfu CTPSPFSHC phage, CSNSDWSSC phage

or control phage. After 8 min, mice were perfused through the heart with DMEM containing 1% BSA. The tumor and control organs were removed from each mouse and the phage was rescued and titered. All phage recovery data shown represent the means from triplicate plating ± SEM in one representative experiment. Every experiment was repeated in at least three mice. For histology analysis, mice were perfused with 4% paraformaldehyde (PFA) 1 h after the injection of phage. Tissues were removed, soaked in 28% sucrose in PBS overnight, and embedded in Tissue-Tek OCT (optional cut temperature, Tissue-Tek, Elkhart, IN). Ten μm sections were prepared for phage immunostaining.

2.5 Immunohistological staining (phage localization)

Frozen tissue slides were rinsed twice for 5 min with PBS. Sections were then incubated with 3%H_2O_2/methanol at room temperature for 10 min. Afterwards, samples were blocked by addition of 10% normal goat serum for 1 h. Sections were then incubated with rabbit anti-phage antibody (1:100) in 10% normal goat serum overnight at 4 ℃. Positive staining was labeled by the addition of peroxidase-conjugated goat anti-rabbit antibody followed by 3, 3'-diaminobenzidine (DAB development).

2.6 Immunofluorescent staining

Frozen tissue sections were cut, air-dried on slides, rinsed twice for 5 min with PBS and then blocked with 10% normal goat serum in PBS for 1 h. Tissue sections were incubated overnight in 10 % normal goat serum containing monoclonal rat anti-mouse CD13 (1:100) and rabbit anti-phage antibody (1:200). Slides were then rinsed three times with PBS for 5 min each and incubated for 1 h with a 0.22 μm-filtered

secondary antibody solution (10 % normal goat serum) containing Alexa Fluor 488 goat anti-rabbit IgG (1:1000) and Alexa Fluor 568 goat anti-rat IgG (1:500). Slides were rinsed three times for 5 min each with PBS, and staining of nuclei were performed with DAPI for 5 min. Finally, slides were rinsed three times for 5 min each with PBS and mounted with nail polish.

2.7 Biodistribution of fluorescein-conjugated peptides

Biodistribution of fluorescein-conjugated peptides was examined after i.v. injection of the FITC-labeled peptides (300 nM in 300 μL PBS) into the tail vein of tumor-bearing mice. The peptides were allowed to circulate for 1 h. Tumor and control tissues were collected and prepared for frozen section. Blood vessels were stained by CD31 antibody (1:100) (secondary antibody conjugated Alexa-568).

2.8 Peptide overlay of tissue sections from human cancer tissues

To determine whether the TCP-1 peptide recognizes the vasculature of human colorectal cancer samples, we used the peptide overlay assay of tissue sections (Kelly *et al.*, 2004; Kelly *et al.*, 2008; Pilch *et al.*, 2006). Multiple human biopsy samples containing both colorectal adenocarcinoma and normal colorectal tissues (approved by the Human Ethics Committee in the Chinese University of Hong Kong) were snap frozen, embedded in OCT, cut into 5 μm sections, and then arrayed on slides. The slides were incubated with 5 μmol/L FITC-CTPSPFSHC (TCP-1), FITC-CSNSDWSSC (TCP-2) or FITC- CVQTAQLLC (control peptide) for 1 h at 37°C, washed three times with PBS, fixed with 4% paraformaldehyde (PFA). Blood vessels were stained with mouse anti-human CD31 monoclonal antibody (1:100) and Alexa Fluor 568 goat anti-mouse IgG (*red*) (1:500) as above described.

2.9 Cell surface binding assay

We used the BRASIL method as described previously (Giordano *et al.*, 2001; Giordano *et al.*, 2008). Briefly, for the binding of phage to different colon cancer cell lines, 1×10^9 pfu of TCP-1 phage or control phage was respectively incubated with 1×10^6 colon 26, HT-29, SW1116 and CaCo-2 in 1% bovine serum albumin (BSA) in DMEM for 2 h on ice and centrifuged through organic phase for 10 min at 10,000 *g*. The upper aqueous phase was then discarded. The phage/cell admixture was then centrifuged through the organic phase for 10 min at 10,000 *g*. Eppendorf tubes were frozen at -80 °C for at least 10 min, and the bottom of the tube containing the cell pellet was sliced off to a new tube. Cell-bound phage was recovered by *Escherichia coli* ER 2738 bacterial infection for 30 min at room temperature, and phage recovery was determined from serial dilution on Luria-Bertani (LB) plates containing tetracycline (20 μg/ml).

2.10 Cell internalization assay

Cells were grown in specific Petri dish for confocal imaging (Corning, US), washed twice with PBS, incubated with 1×10^9 pfu of CTPSPFSHC phage (TCP-1 phage) or control phage in 1% BSA in DMEM at 37 ℃, and washed five times with PBS and two times with 150 mM NaCl, 20 mM glycine, pH 2.2, to remove cell surface binding phage. Cells were washed with PBS, fixed with 4% paraformaldehyde (PFA) in PBS for 15 min, washed with PBS, permeabilized with 0.2% Triton X-100, washed with PBS, and blocked with 10% normal goat serum for 1 h at room temperature. Cells were then incubated with a 1:100 dilution of the anti-M13 phage antibody in 10% normal goat serum at 4 ℃ overnight, washed with PBS, and

incubated with a 1:800 dilution of Alexa Fluor 488 goat anti-rabbit IgG in 10% normal goat serum for 1 h at room temperature. Finally, cells were washed with PBS, fixed with 4% PFA in PBS, mounted, and visualized under a confocal microscope.

2.11 *In vitro* cell viability assay (method of transcriptional and translational assay, MTT Assay)

Cell viability was assessed by MTT assay, which depends on the ability of viable cells to reduce the MTT to a colored formazan product. In brief, cells (10^4 cells per well) were seeded in 96-well microculture plates overnight for attachment, and then incubated for 24 h with increasing concentrations of the peptides CTPSPFSHC-GG-$_D$(KLAKLAK)2 or CTPSPFSHC or $_D$(KLAKLAK)2 in 100 µl of 1% FBS in DMEM for 6~48 hours at 37 °C. In the next step, MTT was added to each well, and the cells were further incubated for 3 h. The colored formazan product was determined photometrically at 570 nm in a multi-well plate reader (Bio-Rad).

2.12 Whole-organ imaging

For the whole-organ imaging (Pilch *et al.*, 2006), tumor-bearing mice were i.v. injected with 500 nM fluorescein-conjugated peptide (in 500µl PBS). The peptide was allowed to circulate for 20 h. Mice were killed, and various tissues were excised and examined for fluorescence. Organ imaging was done under a blue light, using the imaging system of KODAK Image Station 2000MM.

2.13 Animal treatment with TCP-1 conjuagte

Mice bearing orthotopic colorectal cancer were randomized into three groups. The therapeutic group was i.v. injected with 260 µg/dose/mouse of conjugated

CTPSPFSHC-GG-$_D$(KLAKLAK)$_2$. The control groups received an equimolar mixture of CTPSPFSHC and $_D$(KLAKLAK)$_2$, or PBS alone once every three days. Treatment was terminated 7 days after the first peptide administration (Giordano *et al.*, 2008; Kolonin *et al.*, 2004).

Tumors and control organs were dissected at the termination of the experiment. Histologic analysis was done to evaluate the apoptotic blood vessels. Apoptotic vascular endothelial cells were visualized by double staining with anticleaved caspase-3 and CD 31 antibodies (Zhang *et al.*, 2006).

2.11 TUNEL (Terminal deoxynucleotidyl transferase dUTP nick end labeling) assay with endothelial cell colocalization

Tumor sections (10 μm) were treated by *In Situ* Cell Death Detection Kit (Roche) for the detection of apoptotic cells. Co-localization for endothelial cells (CD31) was performed as described above. Staining of nuclei was performed with DAPI.

2.15 Statistical analysis

Unless otherwise specified, results were expressed as mean ± SEM. Statistical analysis was performed with either an analysis of variance (ANOVA) followed by the Turkey's t-test or unpaired Student's t-test. P values less than 0.05 were considered statistically significant.

Chapter 3

Results and Discussion

3.1 Biopanning

3.1.1 Establishment of orthotopic colorectal cancer model

To isolate phage specific for colorectal cancer, we used an orthotopic colorectal cancer mouse model to perform the *in vivo* phage library selection. Orthotopic tumors were first established. Tumor incidence and tumor volume were examined 2 or 3 weeks after orthotopic implantation of colon 26 cells in BALB/c mice. Tumor incidence was 73% and 87% respectively in 2 and 3 weeks after implantation (Figure 6A). With the extension of time, the tumor volume also gradually increased. The tumor volume was 10.99±5.79 mm^3 2 weeks after orthotopic implantation, and reached 51.49±20.42 mm^3 after 3 weeks (Figure 6B). No mice died until 4 weeks after implantation. Macroscopically, nodular tumors growing at the intraluminal side were clearly seen in the distal colon and rectum (Figure 7A). Histologically they were confirmed to be adenocarcinoma. (Figure 7B)

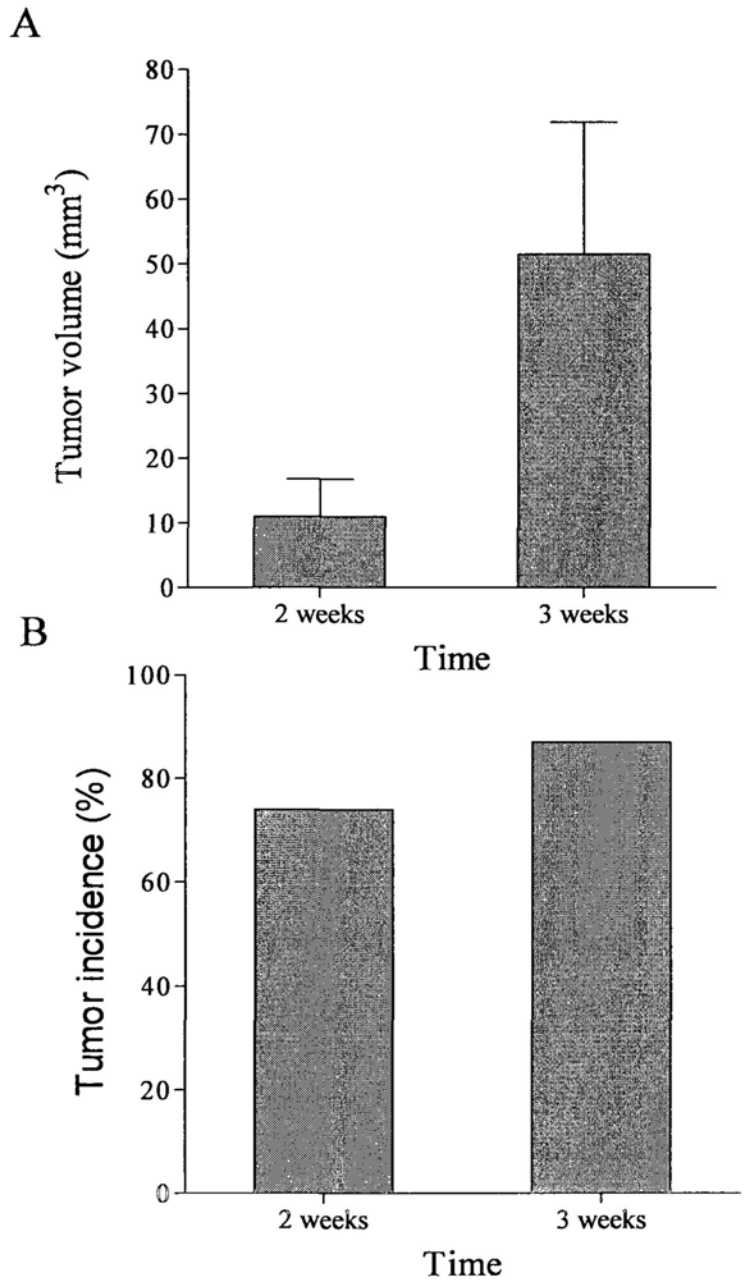

Fig.6 Tumor volume and tumor incidence at different time points after cell implantation.

Tumors were formed in the mice which were given 3% (w/w) DSS for 7 days and were then implanted colon 26 cells (4×10^6 cells/mouse) intrarectally. Mice were sacrificed at 2 (n=15) and 3 weeks (n=15) after cell instillation. Data are presented as mean ± SD. A, Tumor volume. B, Tumor incidence.

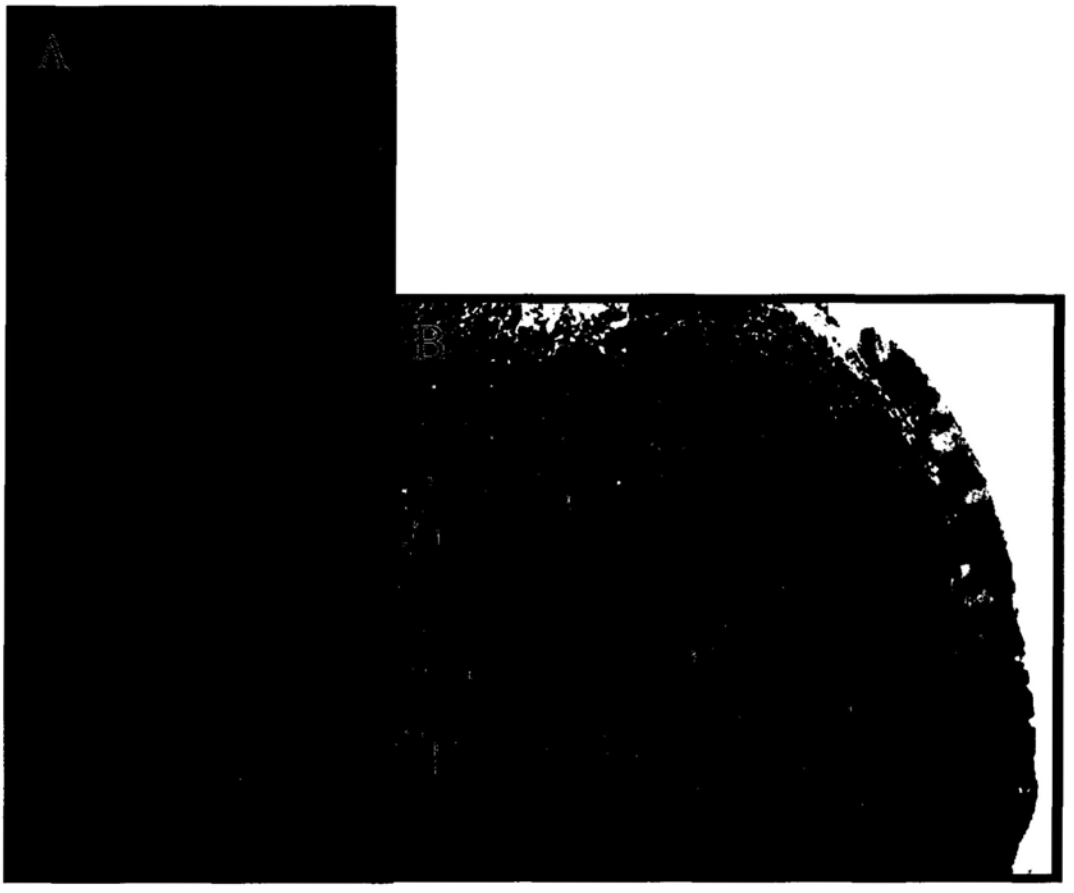

Fig.7 Macroscopic view and histopathology examination of tumors formed after intrarectal instillation of colon 26 cells.

A, Nodular tumor growing at the intraluminal side. B, The excised colon 26 tumors at 3 weeks after instillation. H&E staining. Original magnification ×100.

3.1.2 *In vivo* phage display biopanning

In order to enrich the phage that would bind to cancer tissues but not to control organs, we performed a four-round of *in vivo* phage library selection against mice bearing orthotopic colorectal cancer. Phage titering was determined through counting the phage plaques and was normalized by tissue weight (Figure 8). Four-round selection resulted in a phage pool that selectively homed to tumor tissue with 3-fold increase over the first round (Figure 9). There was no enrichment in the control organs tested, including the brain and colon (Figure 9).

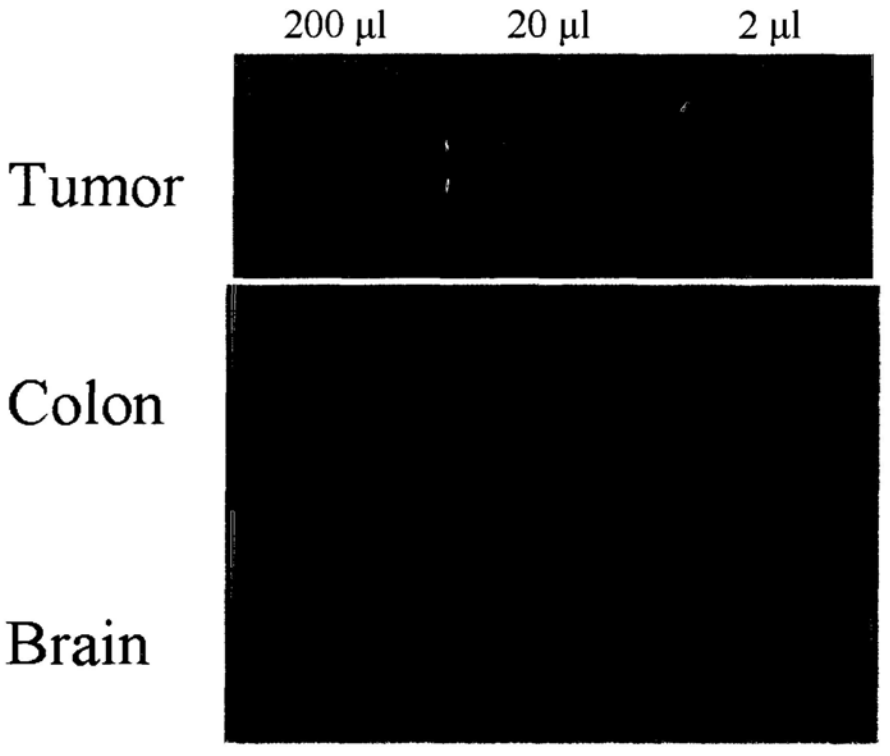

Fig.8 Phage titering and phage plaque formation from tumor and control organs.

Phage was recovered and rescued by host bacteria from tumor and control organs. Phage titering was performed through plating mixture of phage and bacteria on agar plates containing X-gal and IPTG. As the library phage are derived from the common cloning vector M13mp19, which carries the *lacZα* gene, phage plaques appear blue when plated on media containing X-gal and IPTG.

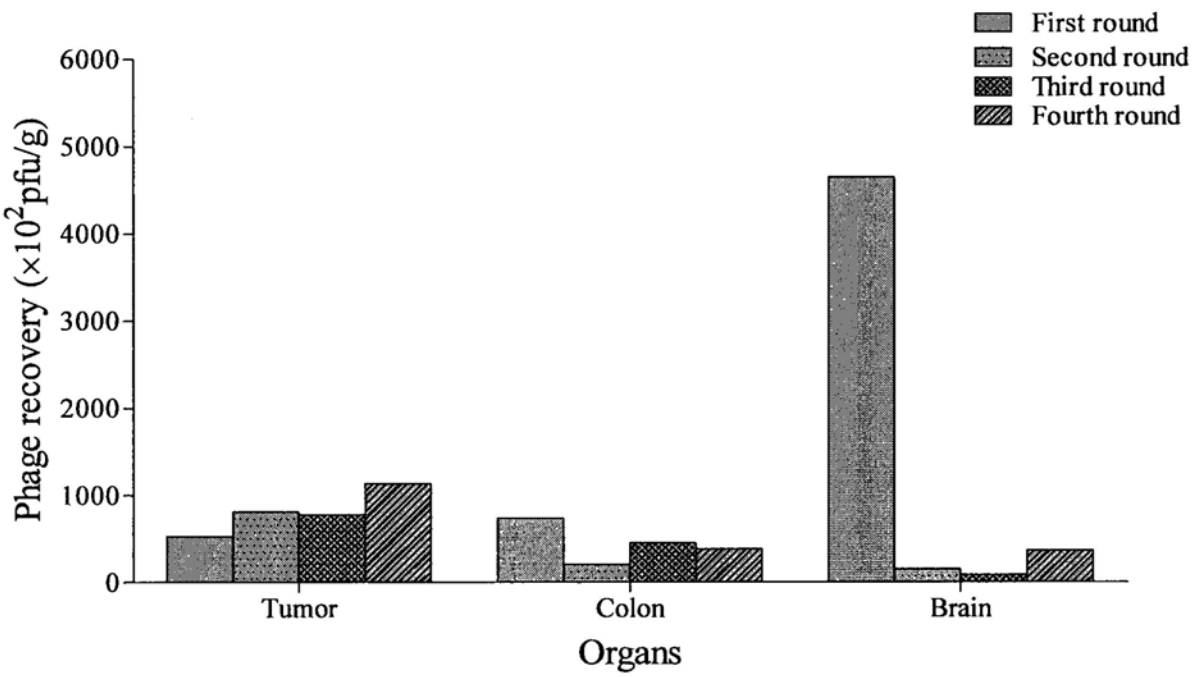

Fig. 9 *In vivo* phage library selection against mice bearing orthotopic colorectal cancer.

After the fourth round of biopanning, the phage number was enriched about three folds in tumor tissue over the first round, but control organs did not show this enrichment property.

3.1.3 Isolation of phage clones and PCR reaction

After four-round selection, 80 phage clones was isolated from the fourth-round phage pool, and PCR was used to amplify the inserted fragments encoding exogenous peptides. The product size is approximately 330 bp (Figure 10).

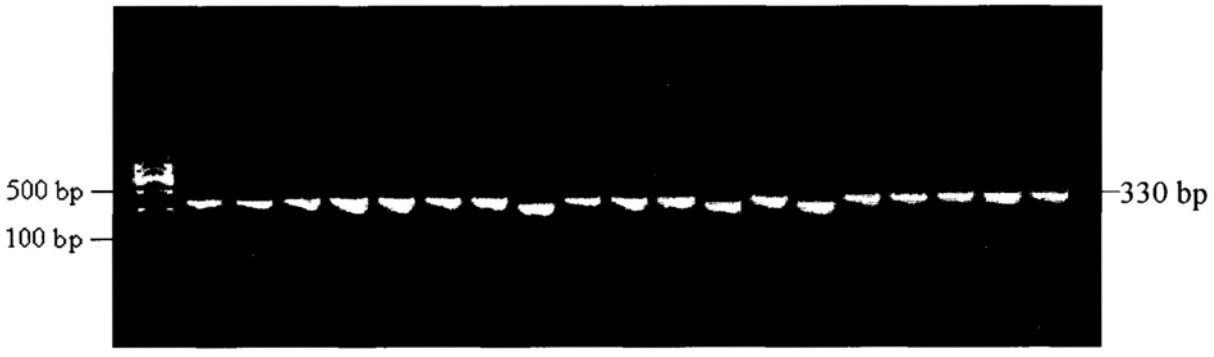

Fig. 10 The PCR results of amplifying inserted fragments.

After the fourth round of biopanning, phage clones were picked and suspended in PBS. PCR was used to amplify the inserted fragments, and PCR products were detected in agarose gel.

3.1.4 DNA sequence of inserted fragments

The PCR products were sequenced by using sequencing primer (5'-CCC TCA TAG TTA GCG TAA CG-3'). The sequence being read corresponded to the anticodon strand of the template; the complementary strand was read out and checked against the top strand sequence (Figure 11). The DNA strand was then translated into amino acid sequence using genetic code protocol provided by library manufacturer. A total of 66 inserted fragments were obtained, and 58 peptides were produced after translation. Four peptides appeared more than once among these peptides (Table 1). It is generally believed that frequently appeared peptides are highly enriched and become better candidate objectives for further analysis (Giordano *et al.*, 2008). The DNA sequencing map of the four peptides were listed (Figure 12A, B, C and D). The four peptides consisting of CTPSPFSHC, CSNSDWSSC, CNPRITPWC and CNLTSSSRC were named after TCP-1, TCP -2, TCP -3 and TCP -4

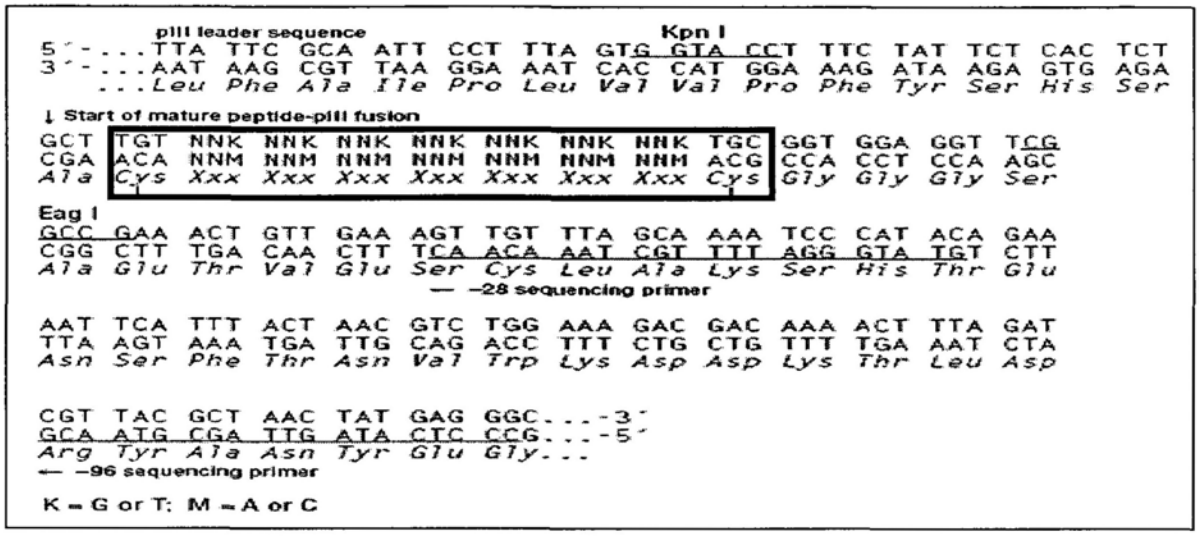

Fig.11 The fragment of phage DNA containing exogenous fusion gene.

Inserted fragment was framed by black pane.

Table 1 Phage-displayed peptide sequences selected from orthotopic colorectal cancer model.

Phage clone	Peptide	Frequency	Phage clone	Peptide	Frequency
Td1	TPSPFSH	4/66	Td29	SHSYPGG	1/66
Td30	TPSPFSH		Td33	LLDNPRT	1/66
Td46	TPSPFSH		Td34	TVPSAKL	1/66
Td73	TPSPFSH		Td35	NSPLKAS	1/66
			Td37	STRMHPD	1/66
Td4	NLTSSSR	3/66	Td39	TNQKHSQ	1/66
Td24	NLTSSSR		Td40	SPTHRAL	1/66
Td38	NLTSSSR		Td42	LPGQPST	1/66
			Td44	NQRHAAN	1/66
Td12	SNSDWSS	2/66	Td45	GLGNNSS	1/66
Td13	SNSDWSS		Td47	ETHKKFL	1/66
			Td50	RDWTHTQ	1/66
Td14	NPRITPW	3/66	Td51	NSLSNHL	1/66
Td70	NPRITPW		Td52	STAAPDL	1/66
Td79	NPRITPW		Td53	TMHESKH	1/66
			Td54	EKTKHLF	1/66
Td2	NSTRPNY	1/66	Td55	PRSPTNS	1/66
Td3	GVNNRVS	1/66	Td56	NAESPMF	1/66
Td5	APNNRHH	1/66	Td57	DKSSPSF	1/66
Td6	TNSQSRY	1/66	Td61	TKATNPV	1/66
Td8	NSPLKAS	1/66	Td62	TPTTKPK	1/66
Td9	SPIHTKQ	1/66	Td63	HPNKLQS	1/66
Td11	GPFTKLK	1/66	Td64	NNPSNLF	1/66
Td15	TTLGAKY	1/66	Td66	TNKYLPL	1/66
Td16	SFDTPAA	1/66	Td67	RESPHPG	1/66
Td17	QFTHVRN	1/66	Td68	MLSPQYK	1/66
Td18	LTTSTKS	1/66	Td69	HKYTPKL	1/66
Td19	TSQPHNQ	1/66	Td71	SNNLRPW	1/66
Td20	PLRTIHG	1/66	Td72	STQTPAV	1/66
Td21	TNKYLPL	1/66	Td74	EQPCCDE	1/66
Td22	VGAYTTT	1/66	Td75	SILSLQR	1/66
Td25	QPTGDKT	1/66	Td76	SSLQMTH	1/66
Td26	PLSFLQG	1/66	Td77	PSSNLNI	1/66
Td27	TPSLGRL	1/66	Td78	LDTLTRE	1/66
Td28	EFTSAWM	1/66	Td80	NPSHVLT	1/66

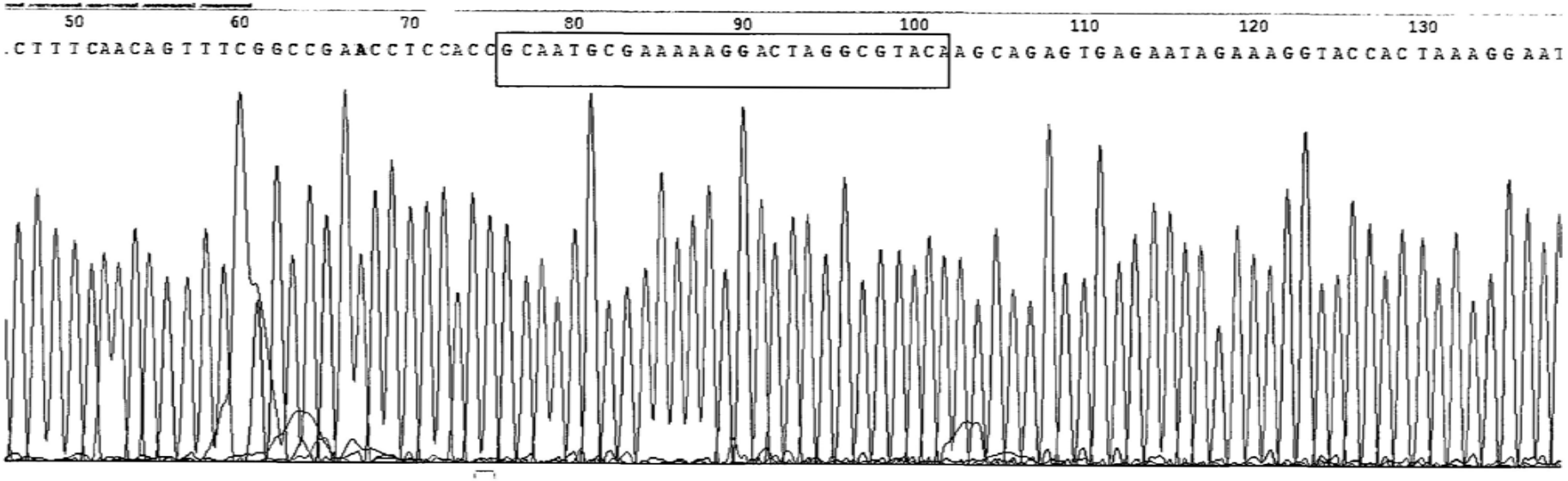

Fig. 12A DNA sequence of CTPSPFSHC phage (TCP-1 phage).

Inserted fragment was framed.

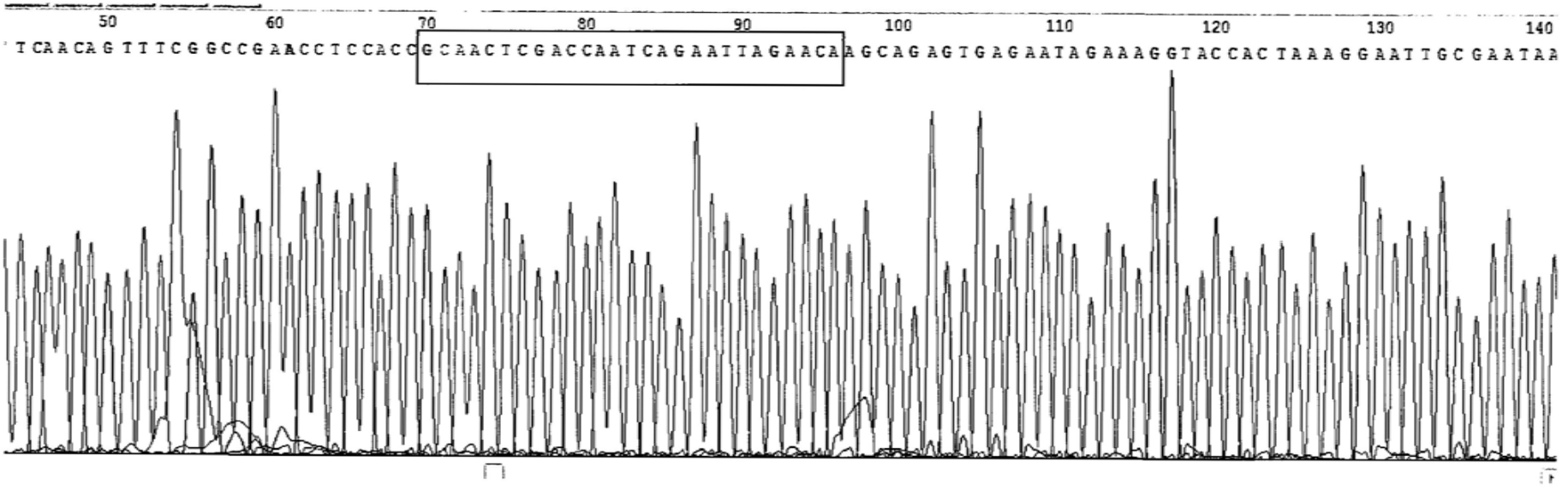

Fig. 12B DNA sequence of CSNSDWSSC phage (TCP-2 phage).

Inserted fragment was framed.

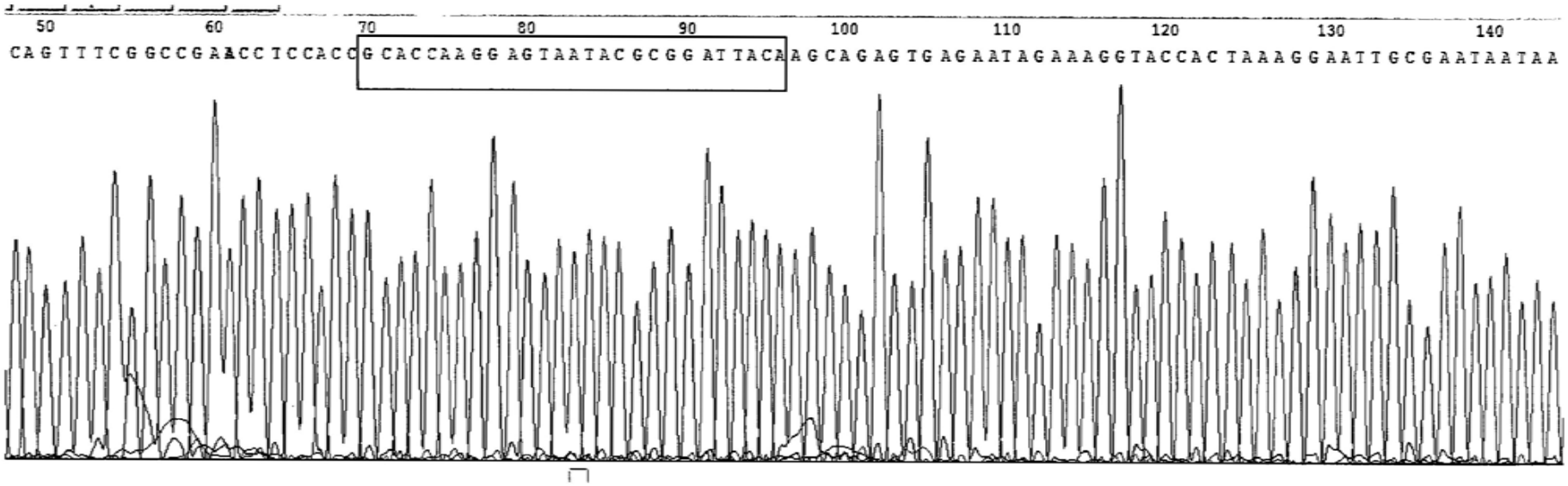

Fig.12C DNA sequence of CNPRITPWC phage (TCP-3 phage).

Inserted fragment was framed.

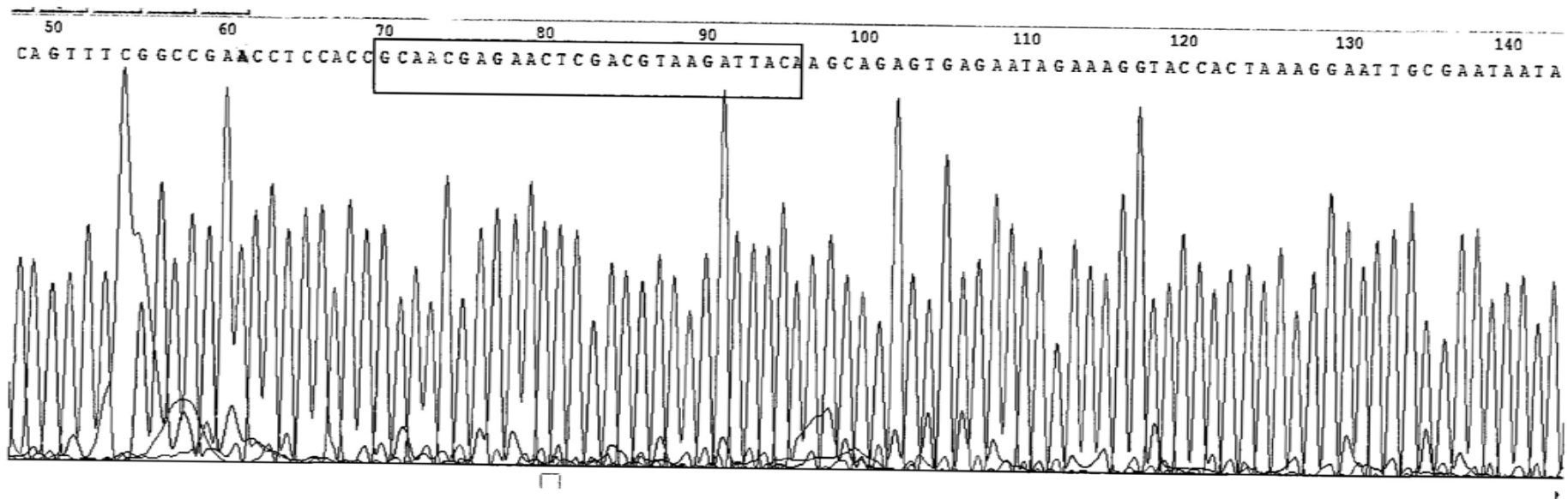

Fig. 12D DNA sequence of CNLTSSSRC phage (TCP-4 phage).

Inserted fragment was framed.

3.1.5 Primary identification of tumor homing ability of TCP-1, 2, 3, 4 phage

Since phage displaying CTPSPFSHC (TCP-1), CSNSDWSSC (TCP-2), CNPRITPWC (TCP-3) and CNLTSSSRC (TCP-4) was enriched more than once in the fourth-round phage pool, the tumor potential homing ability of these selected phage was further characterized using *in vivo* targeting assay by injecting them individually into the tumor-bearing mice. Purified phage displaying the four peptides or insertless phage (negative control) was injected respectively into mice through tail vein. After 8-minute circulation, tumor tissue and control organs (heart, brain and colon) were collected and assayed for accumulation of phage. Results suggested that the four phage but not the control phage that showed relatively higher homing ability in the tumor mass, exhibiting a concentration from 3.0- to 90-fold higher in the tumor tissues than in normal organs, including the brain, colon and heart (Figure 13A, B, C, D and E). Two phage, TCP-1 and -2, particularly showed higher tumor homing ability for further study

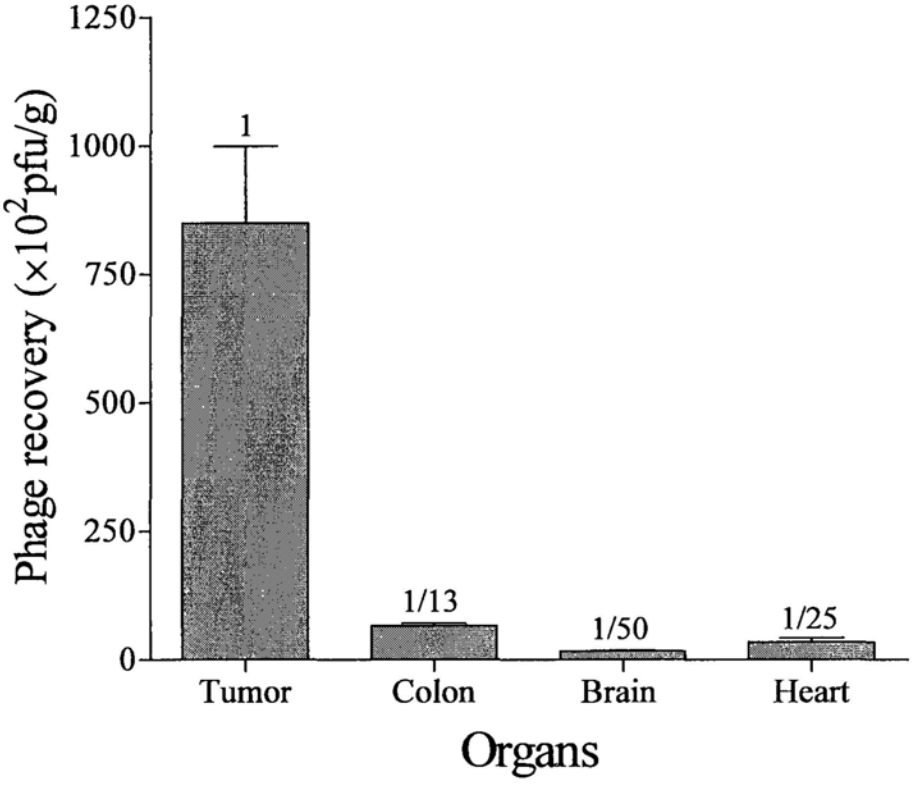

Fig. 13A CTPSPFSHC (TCP-1) phage homed strongly to tumor tissue.

1×10^{9} pfu phage was intravenously injected into tumor-bearing mice. They were sacrificed 8 min later, and the phage was recovered from tumor tissue and various control organs. Data are presented as mean ± SEM from triplicate plating in one representative experiment. The phage number from tumor tissue was considered 1, the ratios displayed in other organs were the phage numbers from other organs divided by the phage number from tumor tissue. Every experiment was repeated at least three times.

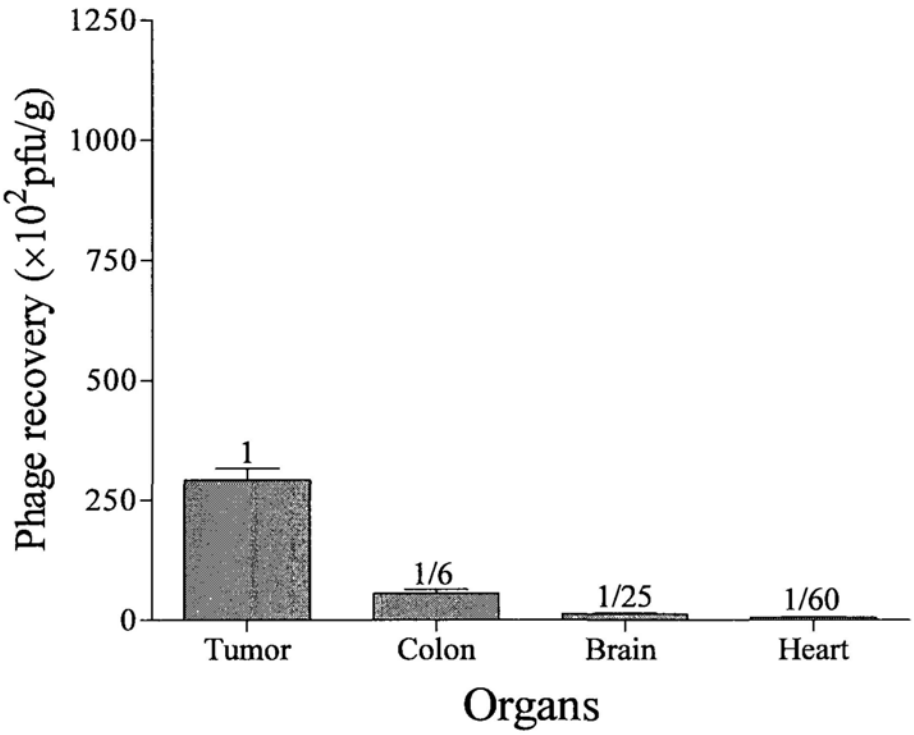

Fig. 13B CSNSDWSSC (TCP-2) phage home effectively to tumor tissue. Tumor-bearing mice were intravenously injected with 1×10^9 pfu phage. They were sacrificed 8 min later, and the phage was recovered from tumor tissue and various control organs. Data are presented as mean ± SEM from triplicate plating in one representative experiment. The phage number from tumor tissue was considered 1, the ratios displayed in other organs were the phage numbers from other organs divided by the phage number from tumor tissue. Every experiment was repeated at least three times.

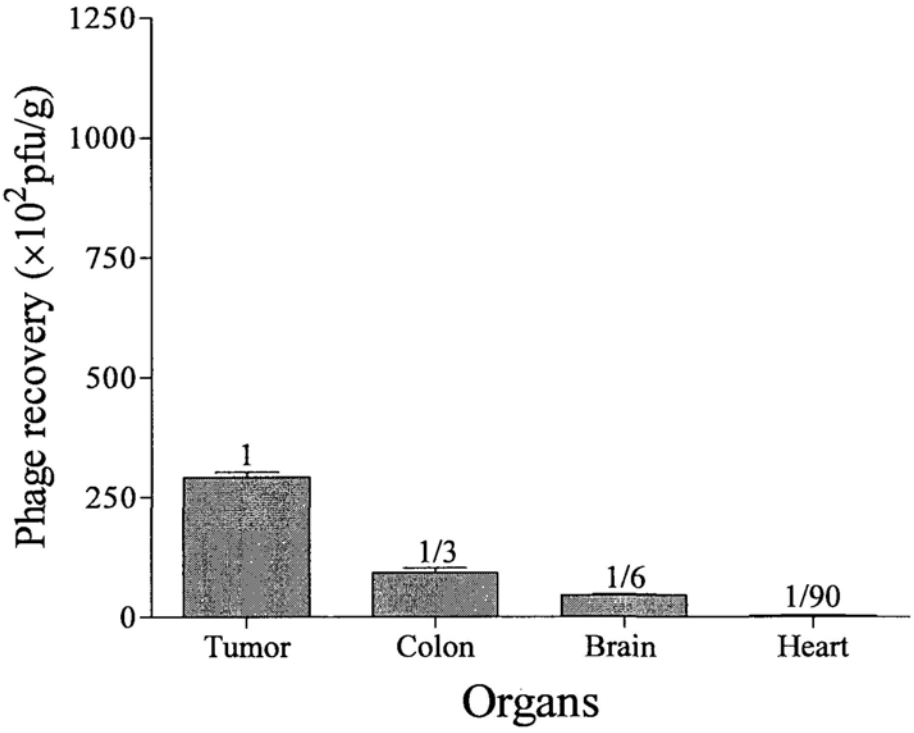

Fig. 13C CNPRITPWC (TCP-3) phage exhibited a homing ability to tumor tissue.

1×10^{9} pfu phage was intravenously injected into tumor-bearing mice. They were sacrificed 8 min later, and the phage was recovered from tumor tissue and various control organs. Data are presented as mean ± SEM from triplicate plating in one representative experiment. The phage number from tumor tissue was considered 1, the ratios displayed in other organs were the phage numbers from other organs divided by the phage number from tumor tissue. Every experiment was repeated at least three times.

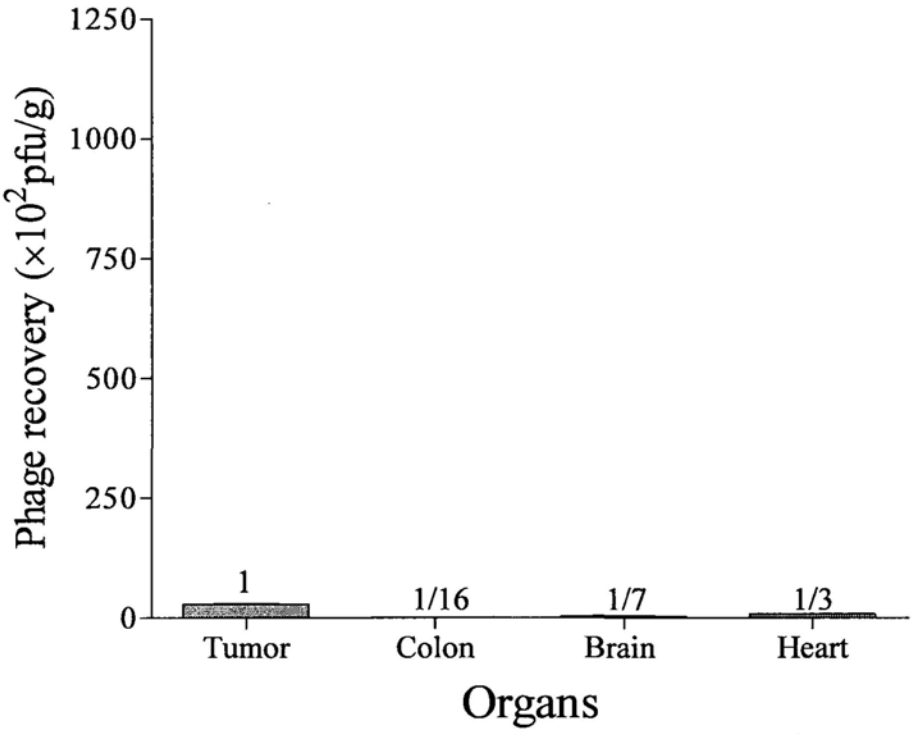

Fig. 13D CNLTSSSRC (TCP-4) phage homed to tumor tissue in a low level.

1×10^9 pfu phage was intravenously injected into tumor-bearing mice. They were sacrificed 8 min later, and the phage was recovered from tumor tissue and various control organs. Data are presented as mean ± SEM from triplicate plating in one representative experiment. The phage number from tumor tissue was considered 1, the ratios displayed in other organs were the phage numbers from other organs divided by the phage number from tumor tissue. Every experiment was repeated at least three times.

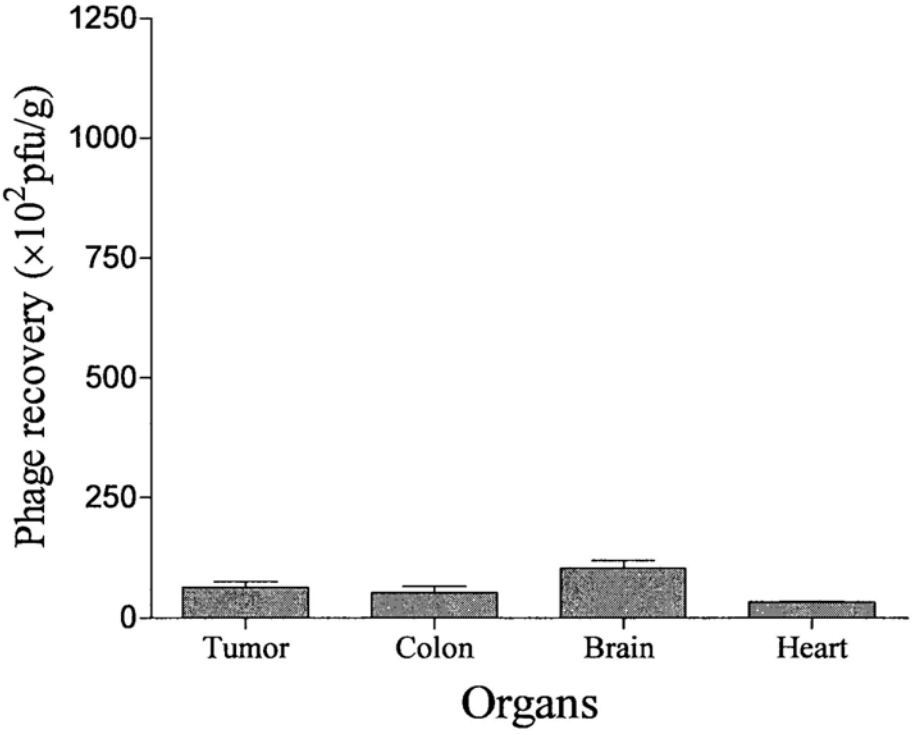

Fig. 13E Insertless phage showed no homing ability to tumor tissue.

1×10^9 pfu control phage was intravenously injected into tumor-bearing mice. They were sacrificed 8 min later, and the phage was recovered from tumor tissue and various control organs. Data are presented as mean ± SEM from triplicate plating in one representative experiment. Every experiment was repeated at least three times.

3.1.6 Preliminary Discussion

Colorectal cancer (CRC) is a leading cause of cancer and cancer deaths in the Western world and is increasing in Asian countries. Animal models of human cancer have played an important role in understanding concepts of multistage carcinogenesis, and testing novel therapeutic approaches to cancer treatment. Reliable, reproducible and clinically relevant animal models of colorectal cancer are necessary to identify the molecular events associated with disease progression and to develop efficacious strategies for tumor inhibition. It is essential that models chosen for study closely mimic the course of human colorectal tumors that are pathologically similar to those of humans (Jass *et al.*, 2002). Several models of colon cancer in rats and mice have been described and the growth and metastatic patterns of such cancers have been identified in cases of heterotopic implantation (subcutaneous, peritoneal, etc) (Garcia-Olmo *et al.*, 1998; Rajput *et al.*, 2008). Undoubtedly, all of these models contributed greatly to our understanding to colorectal cancer. However, there has been frequent use of nude animals in such models. It is noted that, on one hand, the interpretation of results from experiments carried out under these immunological conditions suffers from significant limitations and on the other hand, these animal models keep the tumors away from the complex interior environment of the gut. Therefore, in the case of colorectal cancer, orthotopic model stands a greater importance among the different colorectal cancer models. The present animal model appeared to mimic human colorectal cancer, because the site of tumor formation was found to be at the distal colon and rectum (Figure 7). The tissue tropism of tumor formation appeared to be due to instilling tumor cells in the colorectal surface with acute colitis induced by DSS treatment. Here, the injured

surface with acute colitis was necessary for cancer cells to adhere and proliferate in the lumen. Indeed this approach was highly successful and could achieve a high incidence of tumors growing *in situ* at the rectum of BALB/c mice (74% in 2 weeks, 87% in 3 weeks) (Figure 6).

Experimental evidence has indicated that the vascular beds in each individual normal organ and those involved in pathological condition are highly specialized (Enback *et al.*, 2007; Ruoslahti, 2004). In solid tumors, angiogenesis is one of the main processes by means of which tumor creates its own oxygen and nutrient supply and a route for systemic metastasis (Enback *et al.*, 2007). Angiogenic vasculature in cancer tissues displays many molecular markers at levels higher than that in normal tissues, which makes tumor vasculature become an attractive target for cancer diagnosis and targeting therapy. *In vivo* phage library selection is a powerful tool to identify peptide ligands against tissue-specific markers for the development of specific diagnosis and therapies based on targeting differential protein expression in the vasculature associated with normal or diseased tissues. In the present study, using the orthotopic colorectal cancer model, we performed an *in vivo* phage library selection to isolate peptides specifically targeting the tumor mass. A phage pool was obtained after four rounds of biopanning which exhibited 3-fold higher enrichment to tumor tissue than that of the first round (Figure 9). A total of 66 inserted DNA fragments were isolated from 80 phage clones. The 14 remaining phage clones were identified with wild-type phage without inserted fragments (wild-type phage contamination is inevitable after *in vivo* selection of several rounds as wild-type phage shows better growth advantage than recombinant phage with fused gene). Totally, 58 peptide sequences were identified and four peptides were enriched more than once in tumor

tissue. *In vivo* targeting assay primarily verified that the four phage clones displaying TCP-1, 2, 3, 4 peptides exhibited a homing ability to tumor tissue to different extents. TCP-1 and TCP-2 phage clones had relatively strong homing abilities to cancer tissue among the four phage clones and they were further examined.

3.2 Identification of TCP-1 peptide homing ability

3.2.1 *In vivo* phage targeting assay of TCP-1 phage in orthotopic colorectal cancer model

To analyze the CTPSPFSHC (TCP-1) phage specificity of tumor-homing ability *in vivo*, we intravenously injected purified TCP-1-phage or control phage (insertless phage and irrelevant phage) into tumor-bearing mice. Both tumor tissue and normal control organs were collected and titered for phage accumulation. TCP-1 phage was enriched from 11 to 94-fold higher in tumor tissue than in control organs including colon, brain and heart (Figure 14A). However, two control phages were found to be less selective for tissues from tumors and normal colon (Figure 14B).

To investigate whether the homing ability of TCP-1 phage is due to the displayed peptide sequence, we co-injected the TCP-1 phage with chemically synthetic CTPSPFSHC (TCP-1, 300μg) into the tumor-bearing mice. Phage number recovered from the tumor tissue was reduced by 95%, but control organs such as brain and colon were almost unaffected (Figure 14C).

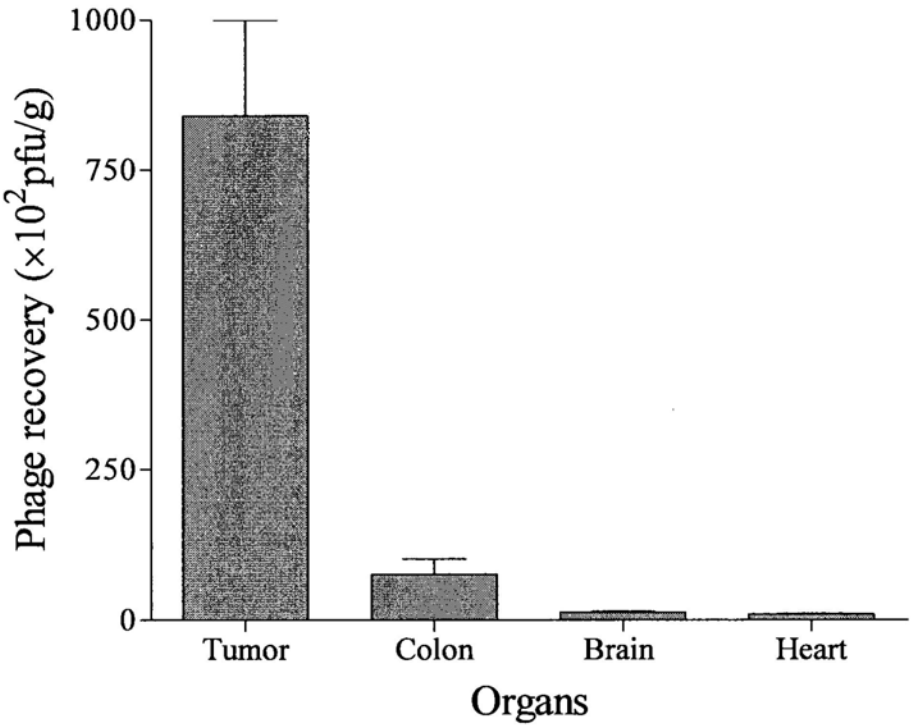

Fig. 14A Specific accumulation of TCP-1 phage to orthotopic colorectal cancer induced by colon 26 cells after phage injection.

Tumor-bearing mice were i.v. injected with purified TCP-1 phage. They were sacrificed 8 min later, and the phage was recovered from tumor tissue and various control organs. TCP-1 phage showed an obvious homing to tumor, but not to control organs. Data are presented as mean ± SEM from triplicate plating in one representative experiment. Every experiment was repeated at least three times.

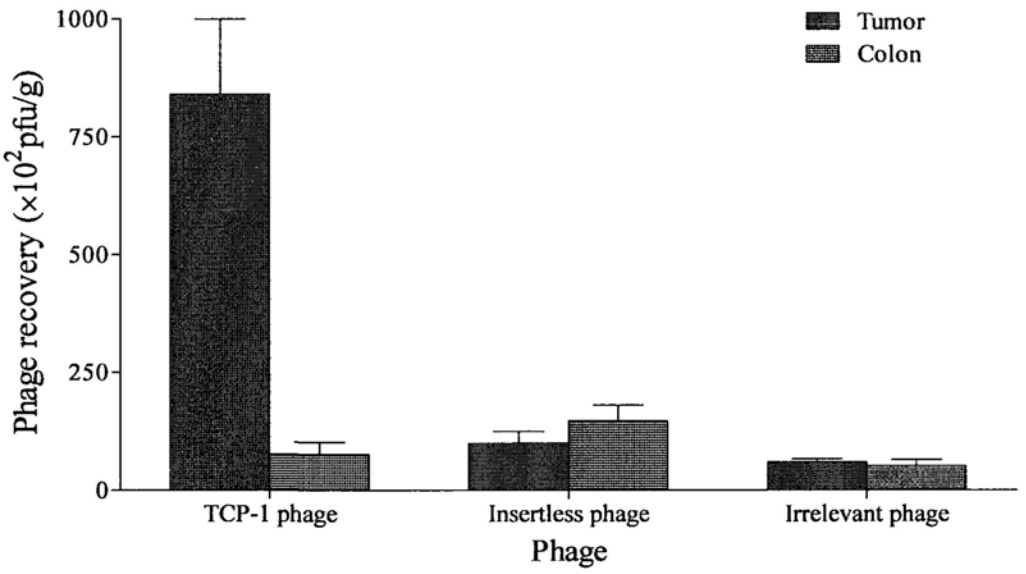

Fig. 14B Two control phage (insertless phage and irrelevant phage) did not accumulate in the tumor tissues.

Tumor-bearing mice were i.v. injected with purified control phage. They were sacrificed 8 min later, and the phage was recovered from tumor and colon tissues. These two control phage did not specifically accumulate into tumor or colon tissue. Data are presented as mean ± SEM from triplicate plating in one representative experiment. Every experiment was repeated at least three times.

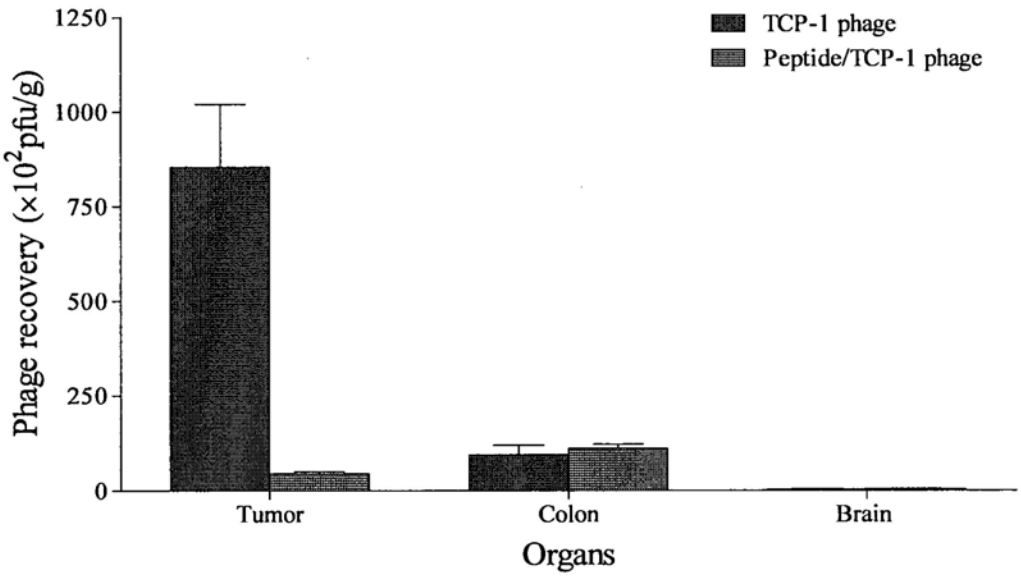

Fig. 14C The homing ability of TCP-1 to tumor was competitively inhibited by the chemically synthesized TCP-1 peptide.

TCP-1 peptide and purified TCP-1 phage were co-injected into tumor-bearing mice. After circulation of 8 min, tumor tissue and control organs were removed and phage was rescued through infecting host bacteria. TCP-1 peptide could inhibit the homing ability of TCP-1 phage to tumor. Data are presented as mean ± SEM from triplicate plating in one representative experiment. Every experiment was repeated at least three times.

3.2.2 TCP-1 phage and vasculature of subcutaneous colorectal cancer models

Next, we further investigated whether TCP-1 phage also showed a homing ability to subcutaneous colorectal cancer induced by several colon cancer cell lines: mouse colorectal cancer cell colon 26, human colorectal cancer cells HT-29 and HCT 116. Normal BALB/c mice were used for colon 26 cells because the cell line originates from the syngenic BALB/c mouse and can escape the recognition of mouse immunity system. Subcutaneous colorectal cancer models induced by HT-29 and HCT 116 were established in BALB/c nude mice.

We intravenously injected purified TCP-1 phage into mice with subcutaneous colorectal tumors. After 8-min circulation, both tumor tissue and control organs were collected and titered the accumulation of phage. TCP-1 phage differentiated poorly between the control organs and tumor tissue in these three subcutaneous colorectal cancer models (Figure 15A, B, C).

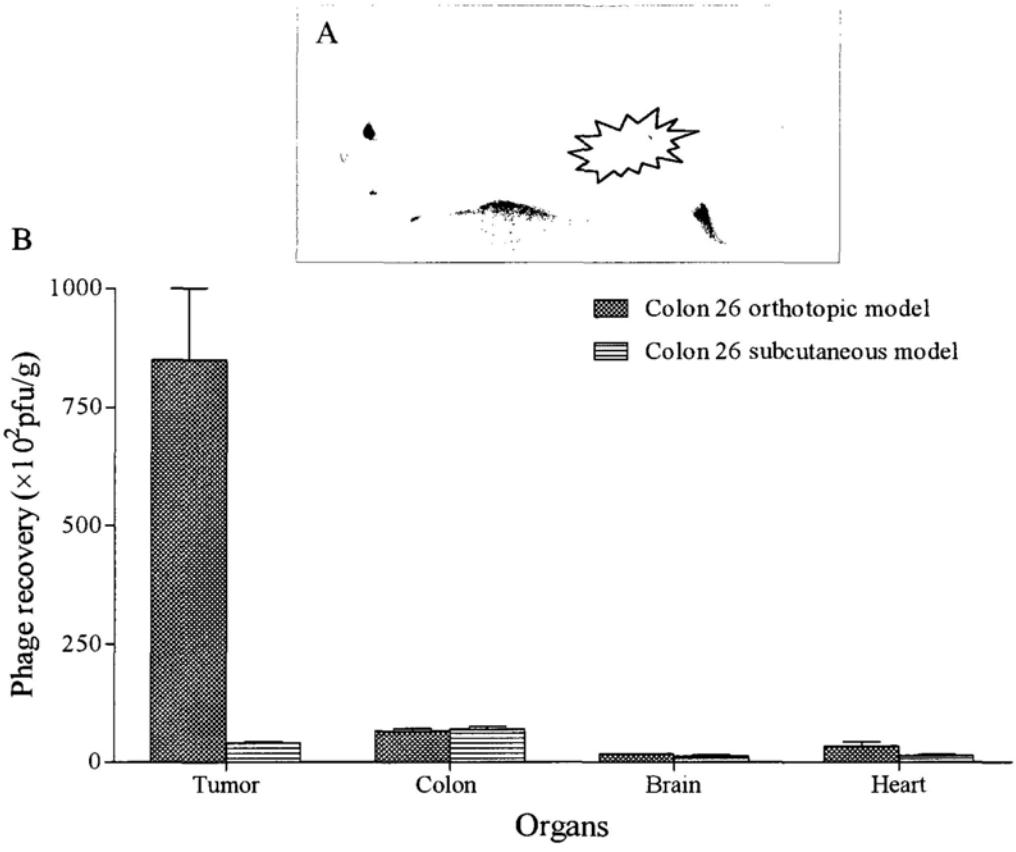

Fig. 15A No specific accumulation of TCP-1 phage into subcutaneous colorectal cancer model induced by colon 26 cells.

Purified TCP-1 phage was intravenously injected into mice bearing subcutaneous colorectal cancer. After 8 min, mice were perfused to remove unbound phage, and tumor tissue and control organs were then collected. Phage number was assayed for the accumulation for phage. Data are presented as mean ± SEM from triplicate plating in one representative experiment. Every experiment was repeated at least three times. A, Tumor view. B, Phage number recovered from various organs.

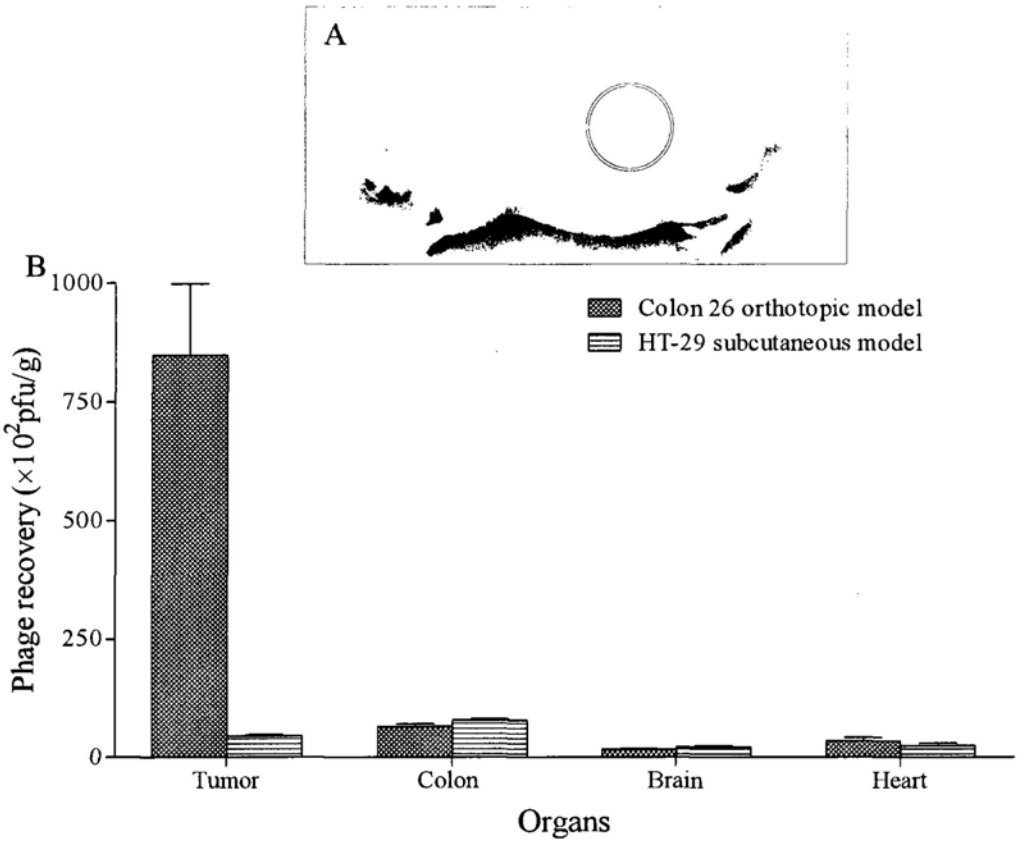

Fig. 15B No specific accumulation of TCP-1 phage into subcutaneous colorectal cancer model induced by human colorectal cancer cell HT-29.

Purified TCP-1 phage was intravenously injected into mice bearing subcutaneous colorectal cancer. After 8 min, mice were perfused to remove unbound phage, and tumor tissue and control organs were then collected. Phage number was assayed for the accumulation for phage. Data are presented as mean ± SEM from triplicate plating in one representative experiment. Every experiment was repeated at least three times. A, Tumor view. B, Phage number recovered from various organs.

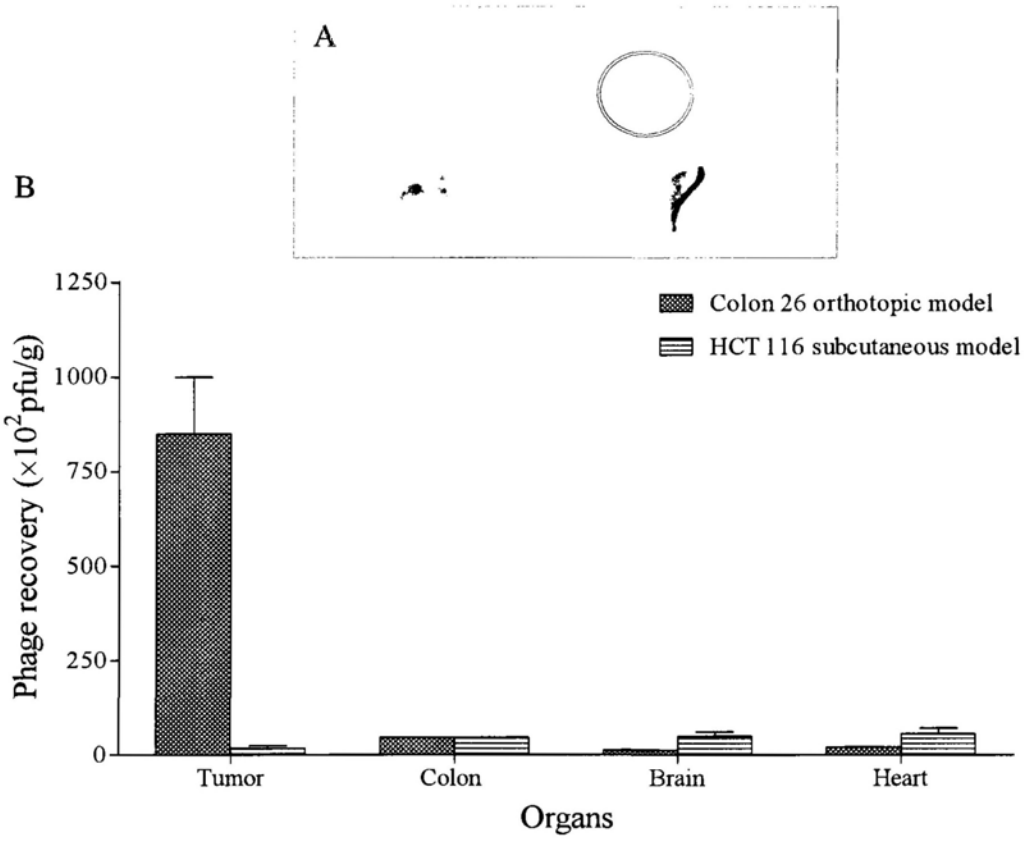

Fig. 15C No specific accumulation of TCP-1 phage into subcutaneous colorectal cancer model induced by human colorectal cancer cell HCT116.

Purified TCP-1 phage was intravenously injected into mice bearing subcutaneous colorectal cancer. After 8 min, mice were perfused to remove unbound phage, and tumor tissue and control organs were then collected. Phage number was assayed for the accumulation for phage. A, Tumor view. B, Phage number recovered from various organs. Data are presented as mean ± SEM from triplicate plating in one representative experiment. Every experiment was repeated at least three times.

3.2.3 TCP-1 phage localization

We further examined the distribution of TCP-1 phage in the orthotopic colorectal cancer model using immunohistochemistry (DAB development) with an anti-phage antibody after intravenous injection. Tumor tissue and control organs were removed and frozen sections were prepared. The TCP-1 phage was found to localize in tumor tissues, but not in control organs such as heart, brain, lung and normal colon tissues except for liver or spleen, where phage was nonspecifically phagocytized by the reticuloendothelial system (Figure 16). Insertless phage was not detectable in the tumor tissues (Figure 16).

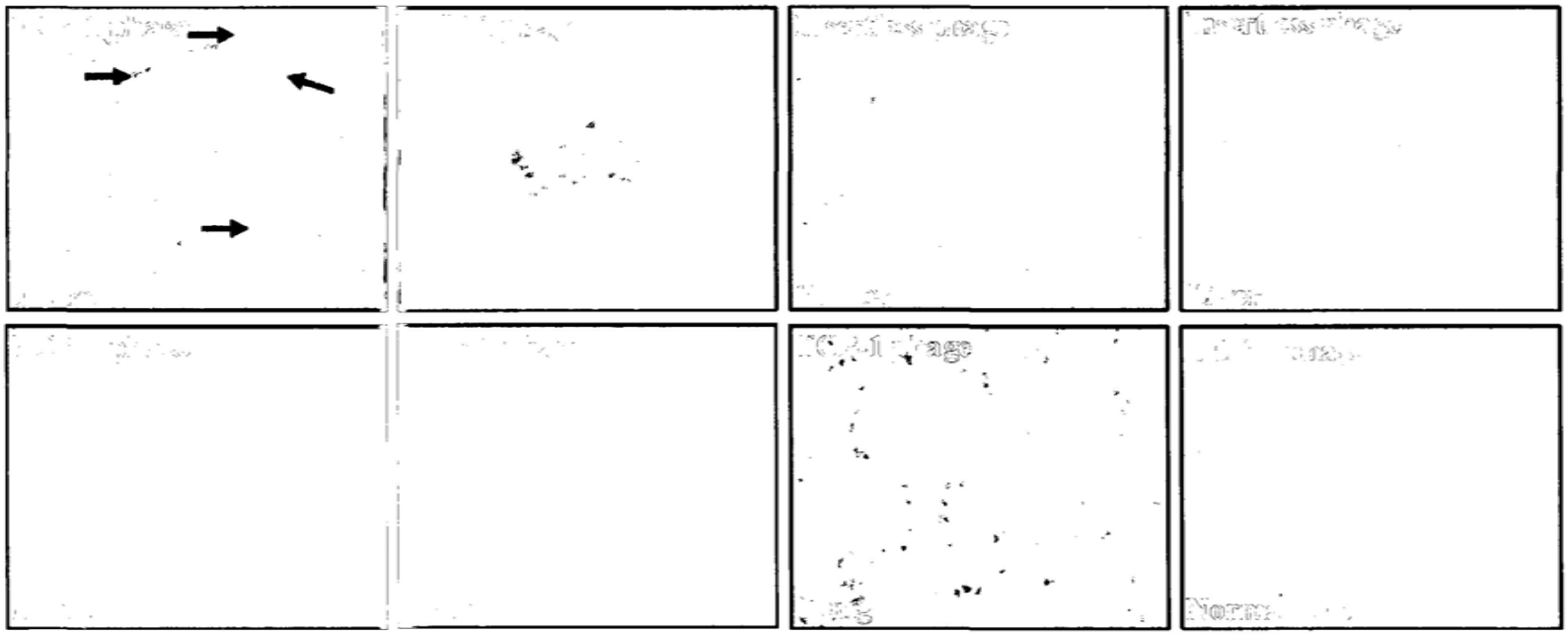

Fig. 16 *In vivo* location of TCP-1 phage by immunohistochemical analysis (DAB staining) after phage injection.

The phage was localized in the tumor tissues and no localization was observed in normal organs such as the heart, brain, lung and colon, or in the tumor tissue sections of mice injected with the insertless control phage. Liver served as positive control for TCP-1 phage and insertless phage because the reticuloendothelial system of liver can trap phage nonspecifically. Results shown are representative images. Original magnification: 400×

3.2.4 Co-localization of TCP-1 phage and tumor vasculature

Subsequently, double-label immunofluorescent staining was used to visualize the colocalization of TCP-1 phage with phage antibody (*green*) and an anti-CD31 antibody (*red*) that marked the endothelial cells of the vasculature. TCP-1 phage colocalized with CD-31-positive endothelial cells in the tumor tissue but not with the vessels in the control organs (Figure 17). Insertless phage did not react with the vasculature of tumor tissues (Figure 17 bottom).

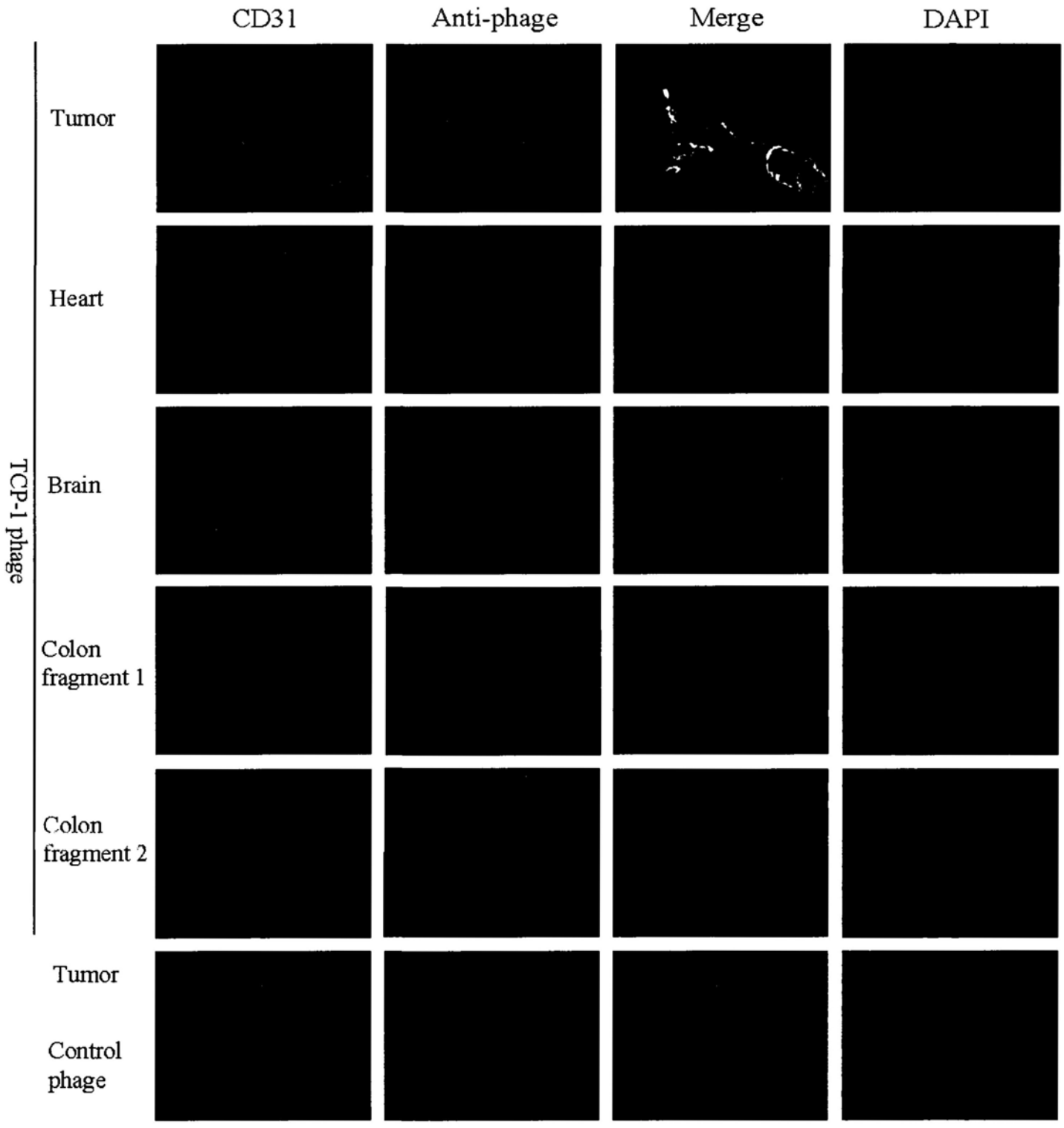
CD31
Anti-phage
Merge
DAPI
TCP-1 phage
Tumor
Heart
Brain
Colon fragment 1
Colon fragment 2
Tumor
Control phage

Fig.17 Vascular localization of TCP-1 phage in tumor tissue.

Tumor-bearing mice were i.v. injected with purified individual TCP-1 phage. They were sacrificed 1 h later, and the phage was stained in frozen sections with rabbit anti-phage antibody (*green*; Alexa 488). Vasculature was detected with rat anti-mouse CD31 antibody (*red*; Alexa 568). TCP-1 phage colocalized with CD31 in the tumor tissues, but not in control organs including heart, brain and normal colon tissue. Insertless control phage was not detectable in tumor tissue. Results shown are representative images. Original magnification: 400×.

3.2.5 Co-localization of FITC-labeled TCP-1 peptide and vasculature of colorectal cancer

To further confirm whether the selective phage homing was due to the TCP-1 peptide, synthetic FITC-conjugated TCP-1 or control peptide was intravenously injected into tumor-bearing mice to study the location of the peptide in which it was targeting at. Various tissues were collected and prepared for frozen sections. Blood vessels were stained by CD31 antibody (*red*). The FITC-labeled TCP-1 colocalized with CD31 in the tumor tissues (Figure 18). It was not detectable in control organs (Figure 18). FITC-labeled control peptide was not found in the tumor tissues (Figure 18). Taken together with the immunolocalization analyses of TCP-1 phage homing, the peptide localization data suggested that TCP-1 peptide homed specifically to blood vessels in tumor tissues but not to the vasculature of control organs.

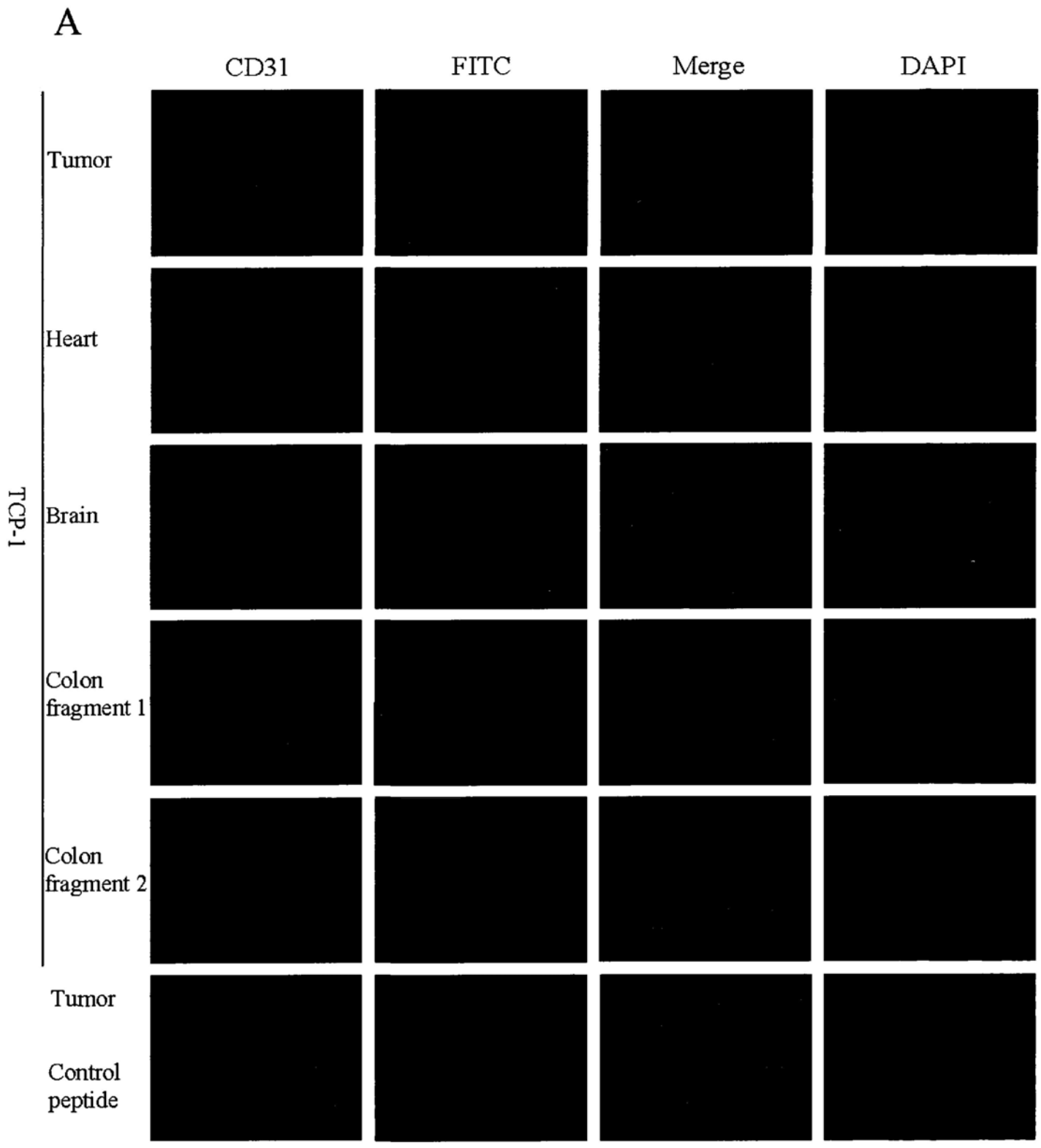
A
CD31
FITC
Merge
DAPI
TCP-1
Tumor
Heart
Brain
Colon fragment 1
Colon fragment 2
Tumor
Control peptide

Fig. 18 Colocalization of FITC-labeled TCP-1 with vascular marker in mouse tumor tissue.

FITC-labeled peptides were i.v. injected into mice bearing tumors. They were sacrificed 1 h later, and the peptide localization was detected in the various tissue sections. FITC-labeled TCP-1 (*green*) colocalizes with CD31 (*red*) in the vasculature of tumor tissue but not in control organs including heart, brain and normal colon tissues. FTIC-labeled irrelevant peptide did not recognize the blood vessels of tumor tissue. Results shown are representative images. Original magnification: 400×.

3.2.6 Binding of TCP-1 peptide and human colorectal cancer specimens

Next, we determined whether the TCP-1 peptide recognizes the vasculature of human colorectal cancer samples by using peptide overlay assay of tissue sections. Vasculature from both colorectal cancer tissues and normal colorectal tissues were stained by an anti-human CD31 antibody (*red*). Overlay assay showed that FITC-labeled TCP-1 peptide (*green*) bound to blood vessels of cancer tissues but not to the vasculature of normal colorectal tissues (Figure 19). FITC-labeled control peptide did not interact with the blood vessels of either cancer or normal colon tissues (Figure 20). Fifty percent (5/10) of colon adenocarcinomas and fifty-five percent of rectal adenocarcinomas (6/11) from a total of 21 patients were found to be recognized by the peptide.

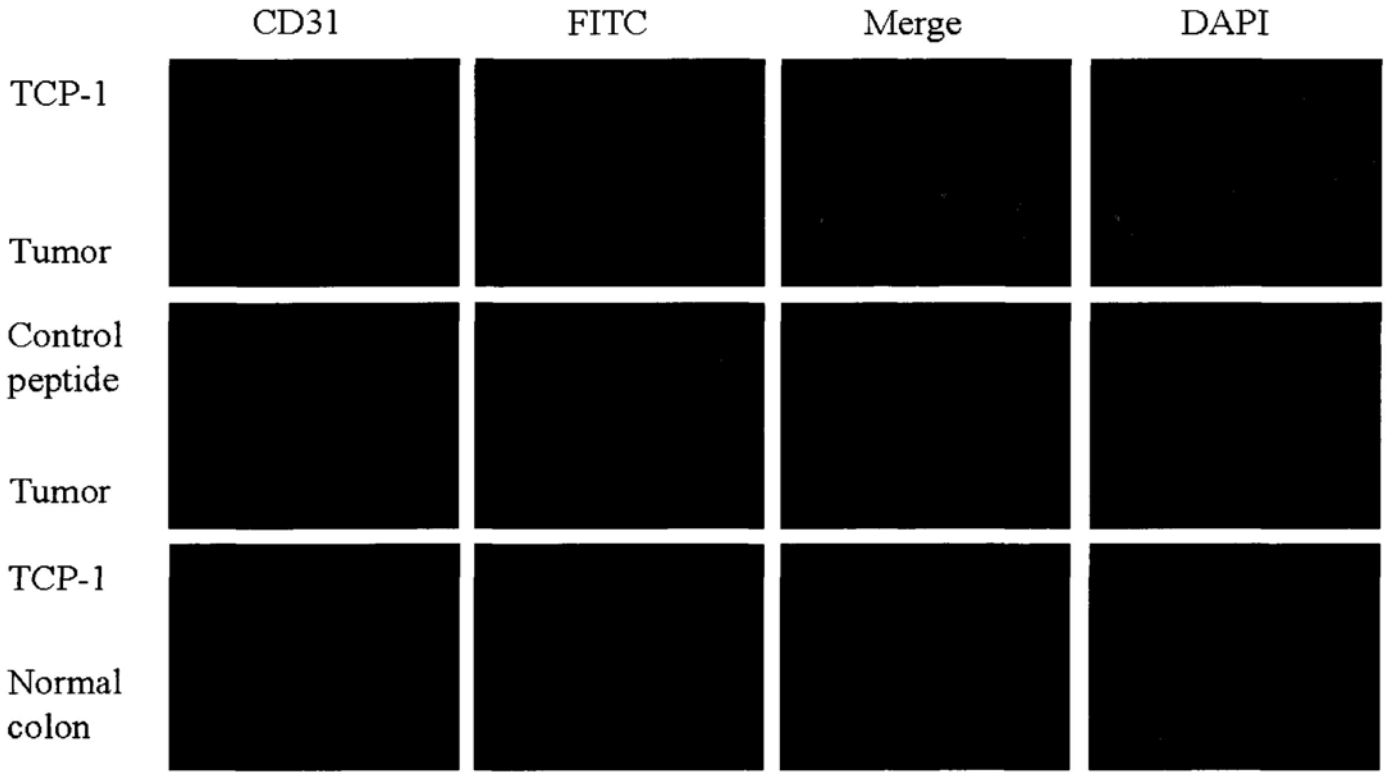

Fig. 19 Colocalization of FITC-labeled TCP-1 with vascular marker in human colorectal cancer.

Peptide overlay of tissue sections from human cancer samples. FITC-labeled TCP-1 (*green*) or irrelevant peptide was incubated with tissue sections of colorectal cancer specimen with normal colon control. Mouse anti-human CD31 antibody was used as a marker for tissue blood vessels (*red*). The targeting peptide specifically bound to the vasculature of cancer tissues but not to normal colon tissues. Results shown are representative images. Original magnification: 400×.

3.2.7 TCP-1 phage and vasculature of acute colitis tissues

It is well known that inflammation causes changes in the endothelium of adjacent vessels. The expression of adhesion molecules that bind leukocytes from blood is increased, and the production of cytokines that attract and activate leukocytes is turned on. Colitis is highly associated with an increased risk for developing CRC. Therefore, we investigated whether TCP-1 phage could also recognize the blood vessels of acute and chronic colitis induced by DSS in BALB/c mice.

Firstly, the acute colitis model was induced by giving 3% DSS in tap water for 7 days. Body weight was recorded for each day, and compared with the water control group. There was no significant decrease in the DSS-treated group (Figure 20). The colon length and the ratio of colon weight to colon length were assessed as two markers of inflammation. After 7 days of DSS treatment, the colon length shortened remarkably and the ratio of colon weight to colon length increased significantly in DSS-treated mice when compared with the water control group (Figure 21A, B, C). The histological analysis of colon disclosed that there was an obvious shortening and loss of crypt, and the lamina propria and submucosa showed an inflammatory infiltrate as compared to the normal colon (Figure 22).

Next, we performed the *in vivo* phage targeting assay of TCP-1 phage in the animals with acute colitis or normal mice. Phage was intravenously injected into the animals and allowed circulation for 8 min. Colon tissue and control organs were collected and assayed for accumulation of phage. The TCP-1 phage showed no marked preference for colon tissue with acute colitis compared with other organs or normal colon (Figure 23).

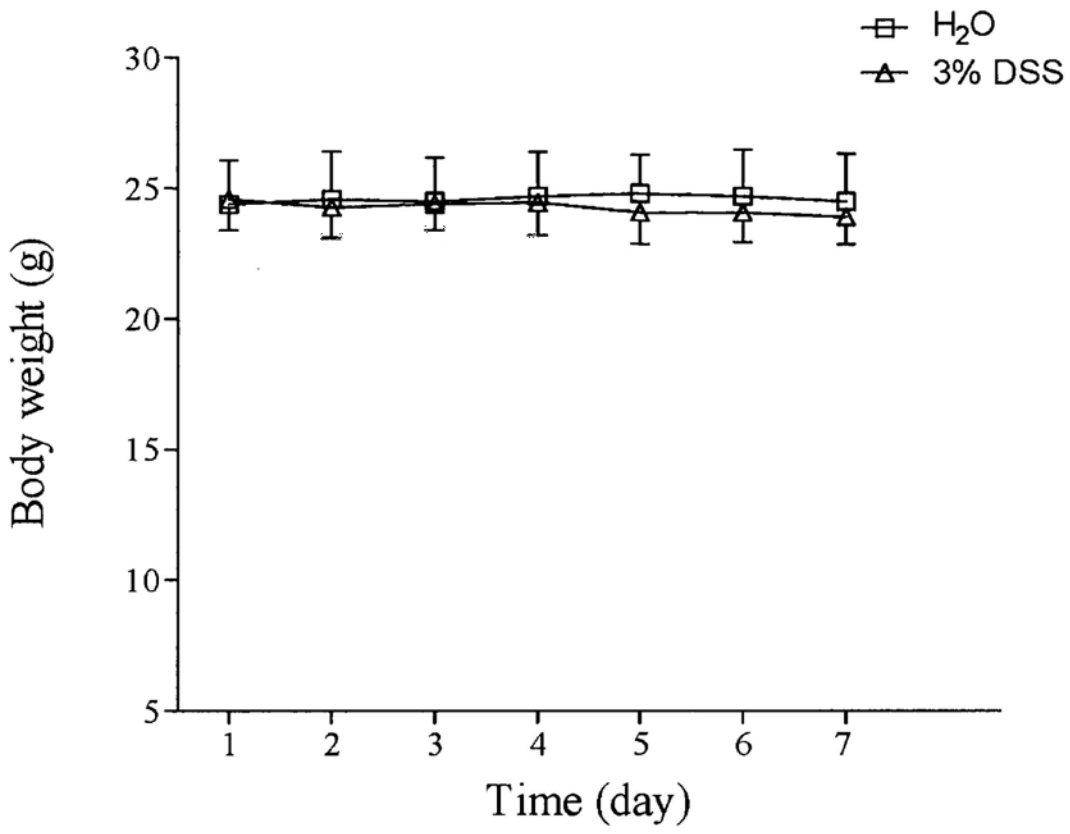

Fig. 20 Changes of body weight in BALB/c mice with acute colitis induced by DSS.

Male BALB/c mice (n=6) were given 3% DSS in drinking water for 7 days. Body weight was measured daily. Data are presented as mean ± SD. Body weight was not significantly different between DSS-treated and H_2O-treated groups.

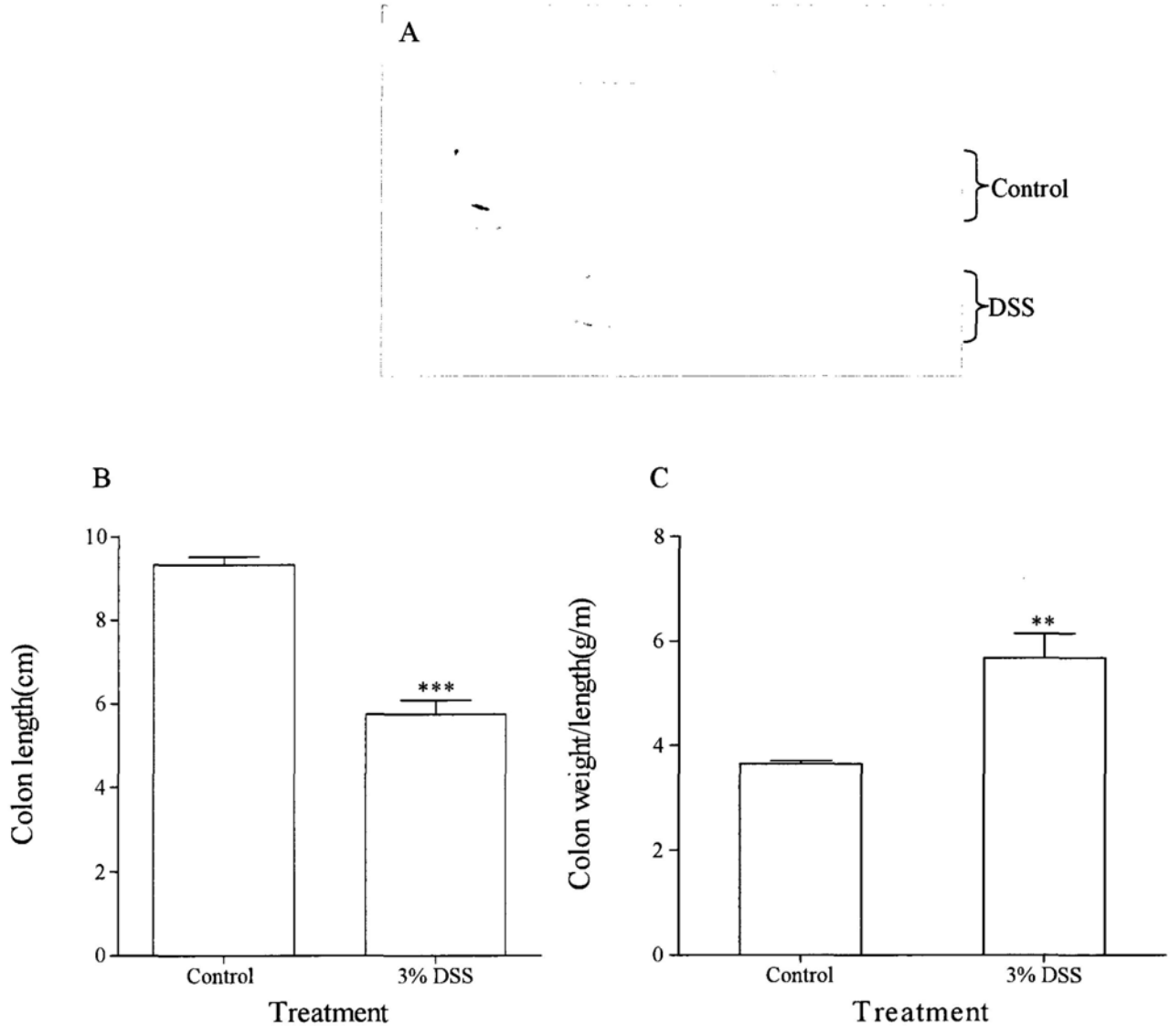

Fig. 21 Changes of colon tissues in BALB/c mice with acute colitis induced by DSS.

Mice were sacrificed after 7-day DSS treatment. Colon tissues were collected and length and weight were measured. A, Representative gross appearance of colon tissues. B, Colon length (n=6). C, The ratio of colon weight to colon length (n=6). Data are presented as mean ± SEM. (** $P<0.01$, *** $P<0.001$).

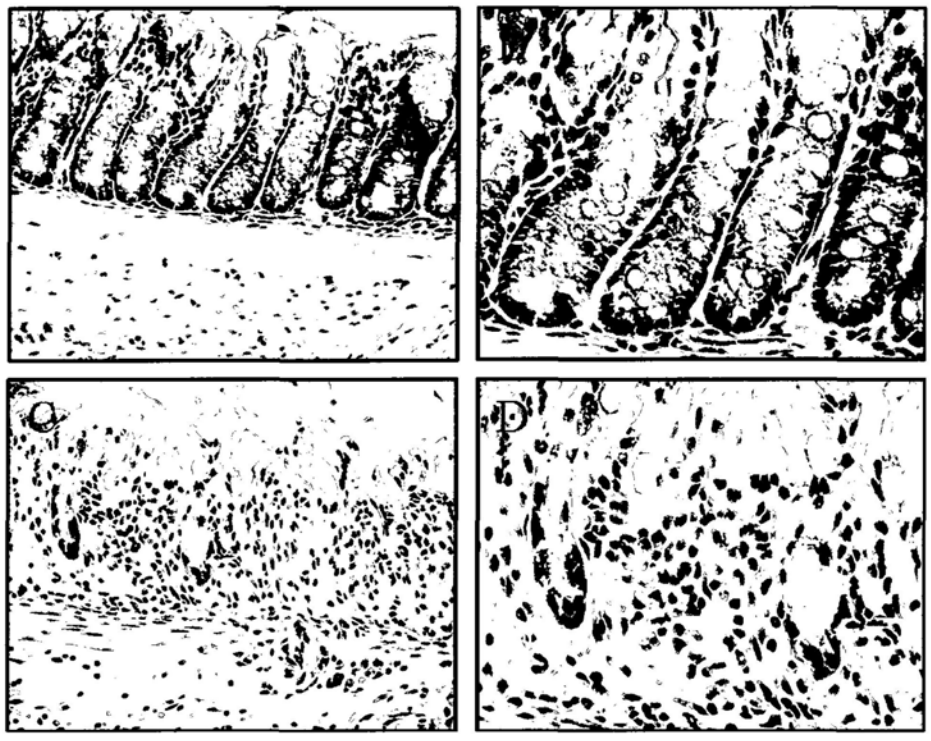

Fig. 22 Histological changes of colon tissues with acute colitis.

A and B, Control colon. The crypts sit straightly on the base of muscularis mucosae. C and D, Colon tissues with acute colitis. There were shortening, distortion or part loss of crypts. The base of crypts failed to sit on the muscularis mucosae, and indigenous lamina propria cells appear prominent due to loss of crypts. H&E staining, left panel, 200×, right panel, 400×.

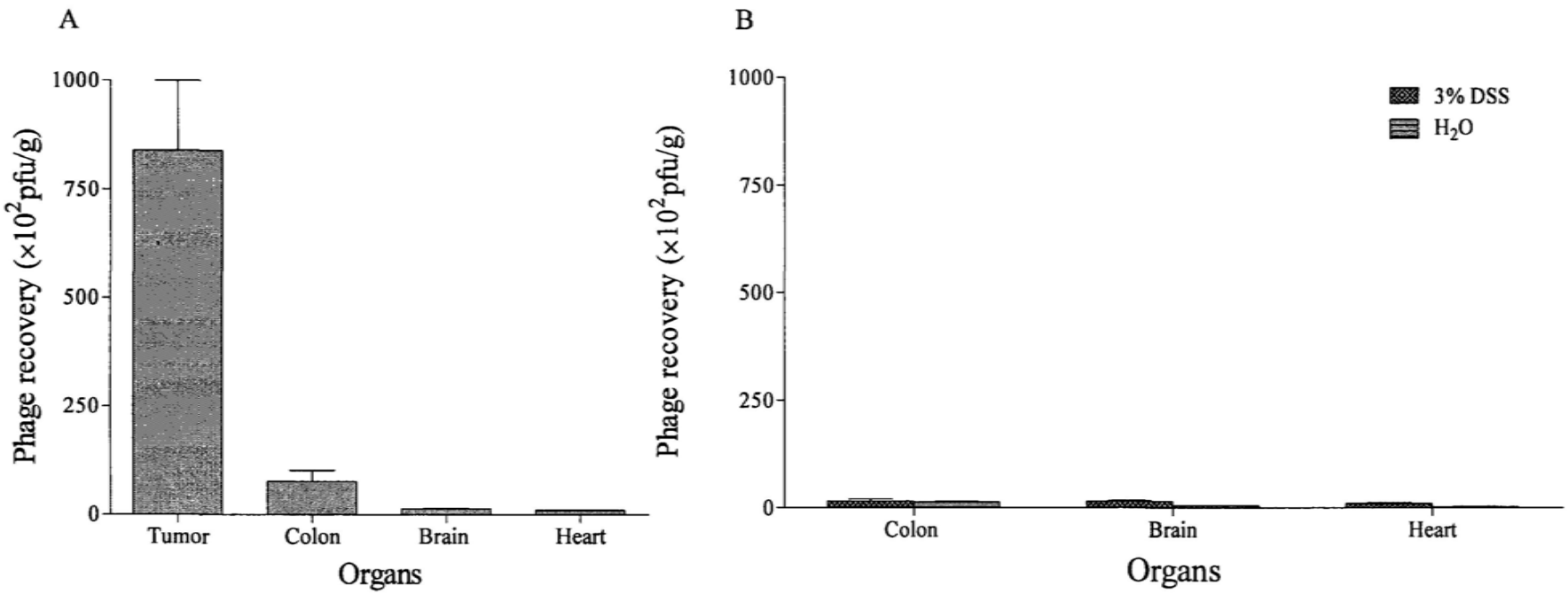

Fig. 23 TCP-1 phage did not specifically accumulate in the colon tissue with acute colitis.

A, TCP-1 phage specifically homed to orthotopic colorectal cancer tissue. B, TCP-1 phage did not exhibit specific homing ability to colon tissue with acute colitis as compared to control organ or normal colon tissue. Purified TCP-1 phage was intravenously injected into mice. After 8 min, mice were perfused and various organs were then collected. Phage number was assayed for the accumulation for phage. Data are presented as mean ± SEM from triplicate plating in one representative experiment. Every experiment was repeated three times.

3.2.8 TCP-1 phage and vasculature of chronic colitis tissues

Subsequently, we investigated whether TCP-1 phage could target the vasculature of chronic colitis tissues. The chronic colitis model was firstly established through given 3 cycles of DSS (7 days) and water (7 days). During the treatment, the body weight of DSS group had no obvious decrease compared with that of water control group (Figure 24). The colon length shortened remarkably and the ratio of colon weight to colon length increased significantly in the DSS-treated mice when compared with the water control group (Figure 25A, B, C). The histological analysis still found prominent crypt distortion or loss in colon tissues of DSS-treated group (Figure 26). Microscopic erosion was still present (Figure 26).

Next, *in vivo* phage targeting assay was performed by phage injection into chronic colitis model. TCP-1 phage was intravenously injected into the animals and allowed circulation for 8 min. Colon tissue and control organs were collected and phage was rescued by infecting host bacteria for phage number. The TCP-1 phage showed no marked homing ability to colon tissue with chronic colitis when compared to other organs or normal colon (Figure 27).

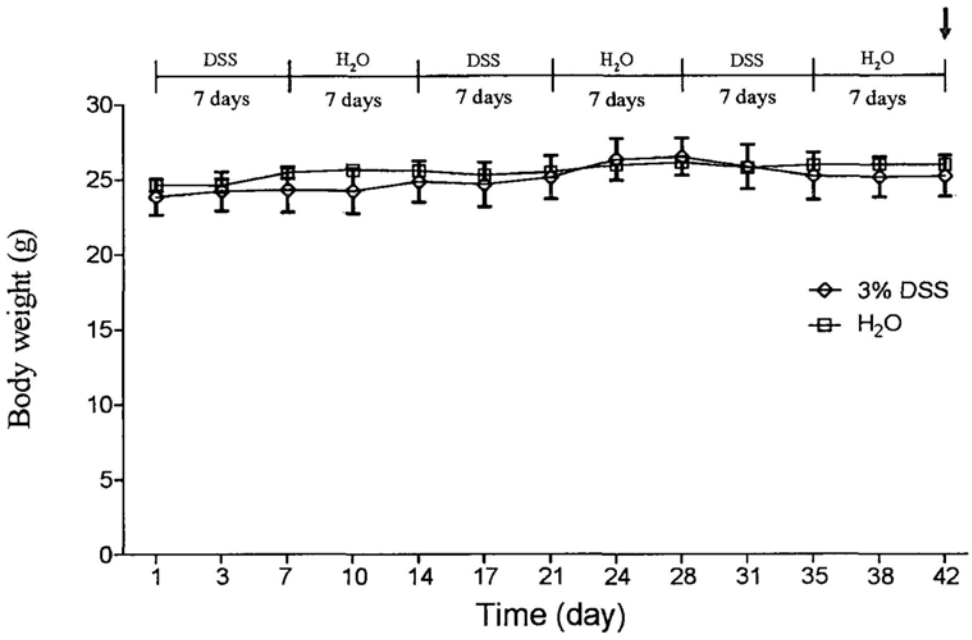

Fig. 24 Changes of body weight in BALB/c mice with chronic colitis induced by DSS.

Male BALB/c mice (n=6) were given 3 cycles of 7-day DSS followed by 7-day water. Body weight was measured three times every week. Data are presented as mean ± SD. Body weight was not significantly different between DSS-treated and H_2O-treated groups.

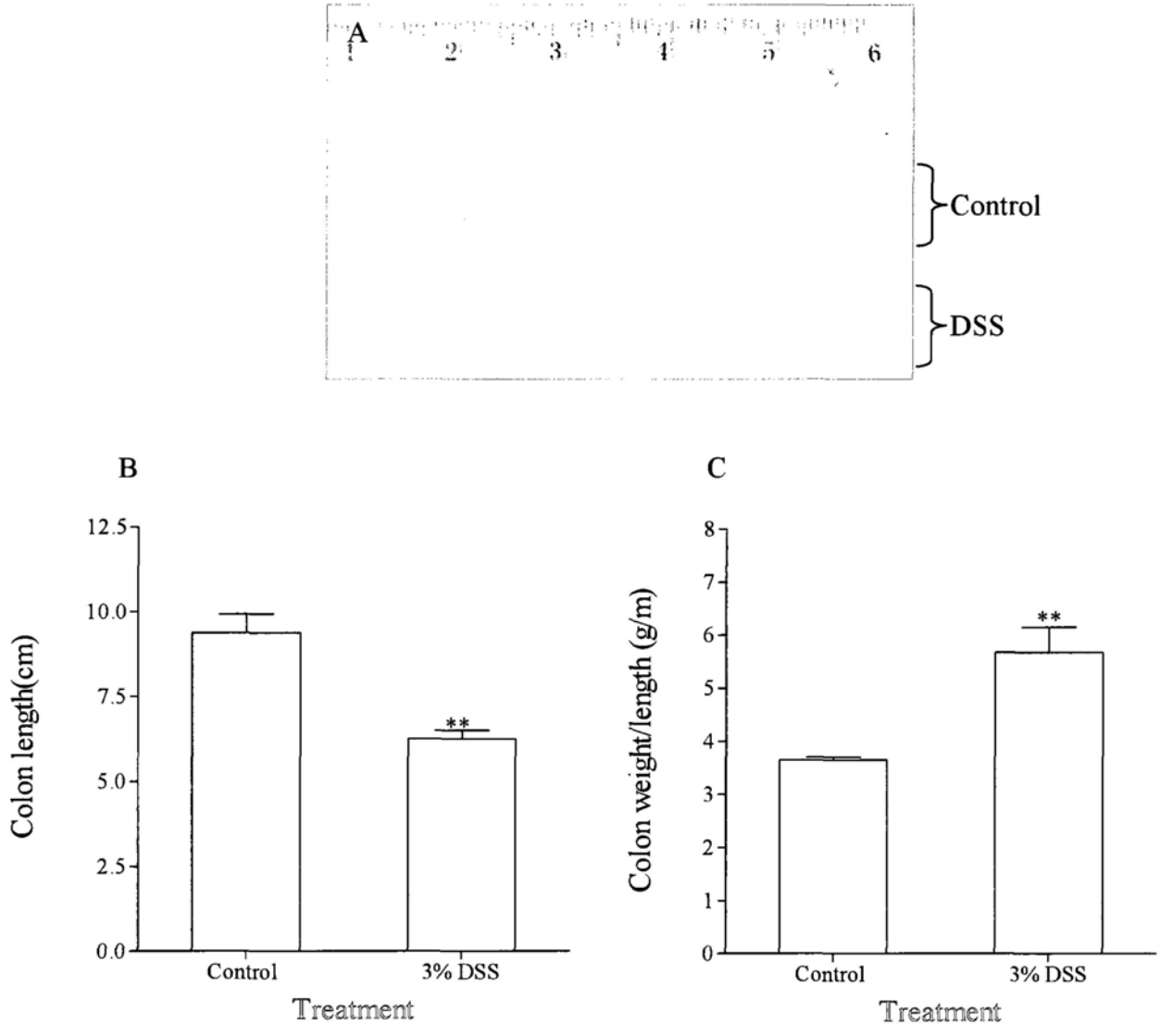

Fig. 25 Changes of colon tissues in BALB/c mice with chronic colitis induced by DSS.

Mice were sacrificed after the end of third cycle, colon tissues were collected and length and weight were measured. A, Representative gross appearance of colon tissues. B, Colon length (n=6). C, The ratio of colon weight to colon length (n=6). Data are presented as mean ± SEM. (** $P<0.01$).

Fig. 26 Histological changes of colon tissues with chronic colitis.

A, Control colon. The crypts sit straightly on the base of muscularis mucosae. B and C, Colon tissues with chronic colitis. Crypt distortion and loss was still prominent; microscopic erosions were detectable. H&E staining, original magnification , 200×.

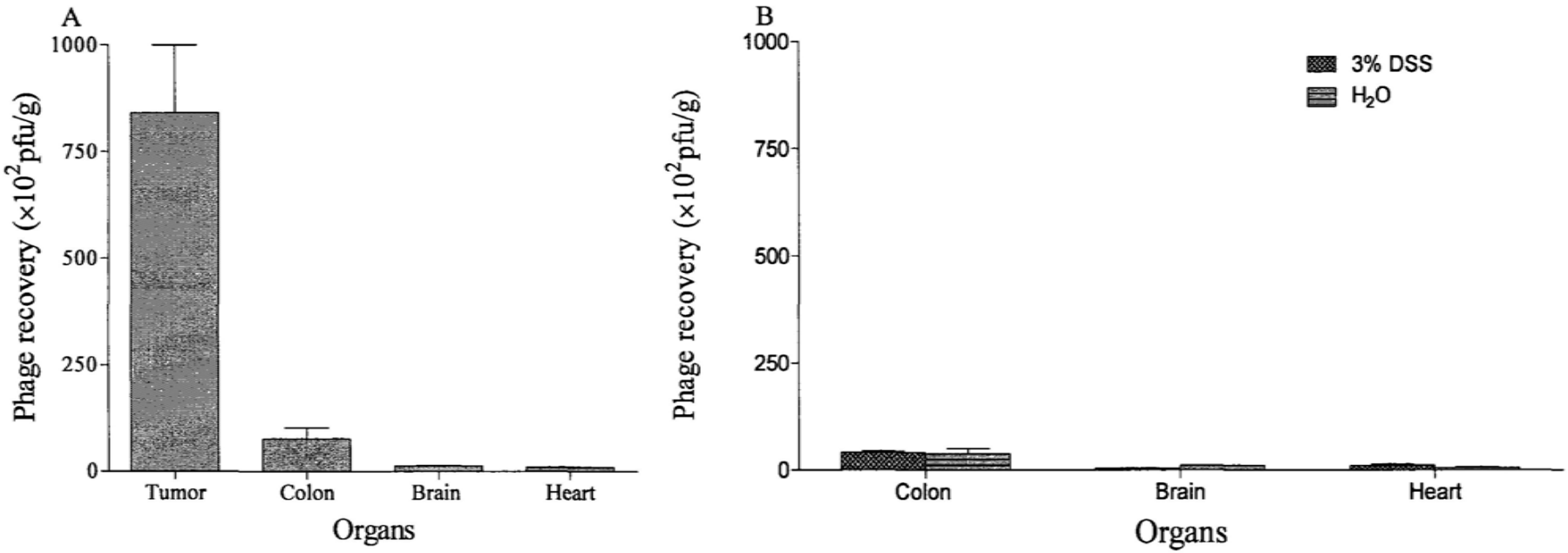

Fig. 27 TCP-1 phage did not specifically accumulate in the colon tissue with chronic colitis.

A, TCP-1 phage specifically homed to orthotopic colorectal cancer tissue. B, TCP-1 phage did not show specific homing ability to colon tissue with chronic colitis as compared to control organ or normal colon tissue. Purified TCP-1 phage was intravenously injected into mice. After 8 min, mice were perfused and various organs were then collected. Phage number was assayed for the accumulation for phage. Data are presented as mean ± SEM from triplicate plating in one representative experiment. Every experiment was repeated three times.

3.2.9 TCP-1 phage and the vasculature of lung matastatic tumor of colorectal cancer

Approximately half of all patients with CRC will develop local recurrence or distant metastasis during the course of their illness (Xiong *et al.*, 2004). The most common recurrence sites are liver and/or lung. About 10% of patients with colorectal cancer have lung metastasis (Lin *et al.*, 2009). Therefore, we further investigated whether TCP-1 phage can target the vasculature of lung matastatic tumor of colorectal cancer induced by colon 26 in normal BALB/c mice.

Lung metastatic model was firstly established through injection of colon 26 cells. Animals were sacrificed and examined for metastases 21 days after tumor cell inoculation. Results suggested that lung surface was covered by a number of visible metastatic foci (Figure 28A). Histological analysis confirmed tumor formation in the lung (Figure 28B).

Next, TCP-1 phage homing ability was tested in the model. Lung with metastatic tumor and control organs were collected and assayed for accumulation of phage after phage injection. Results showed that TCP-1 phage did not home to the vasculature of lung with metastatic tumor as compared to other control organs (Figure 28C).

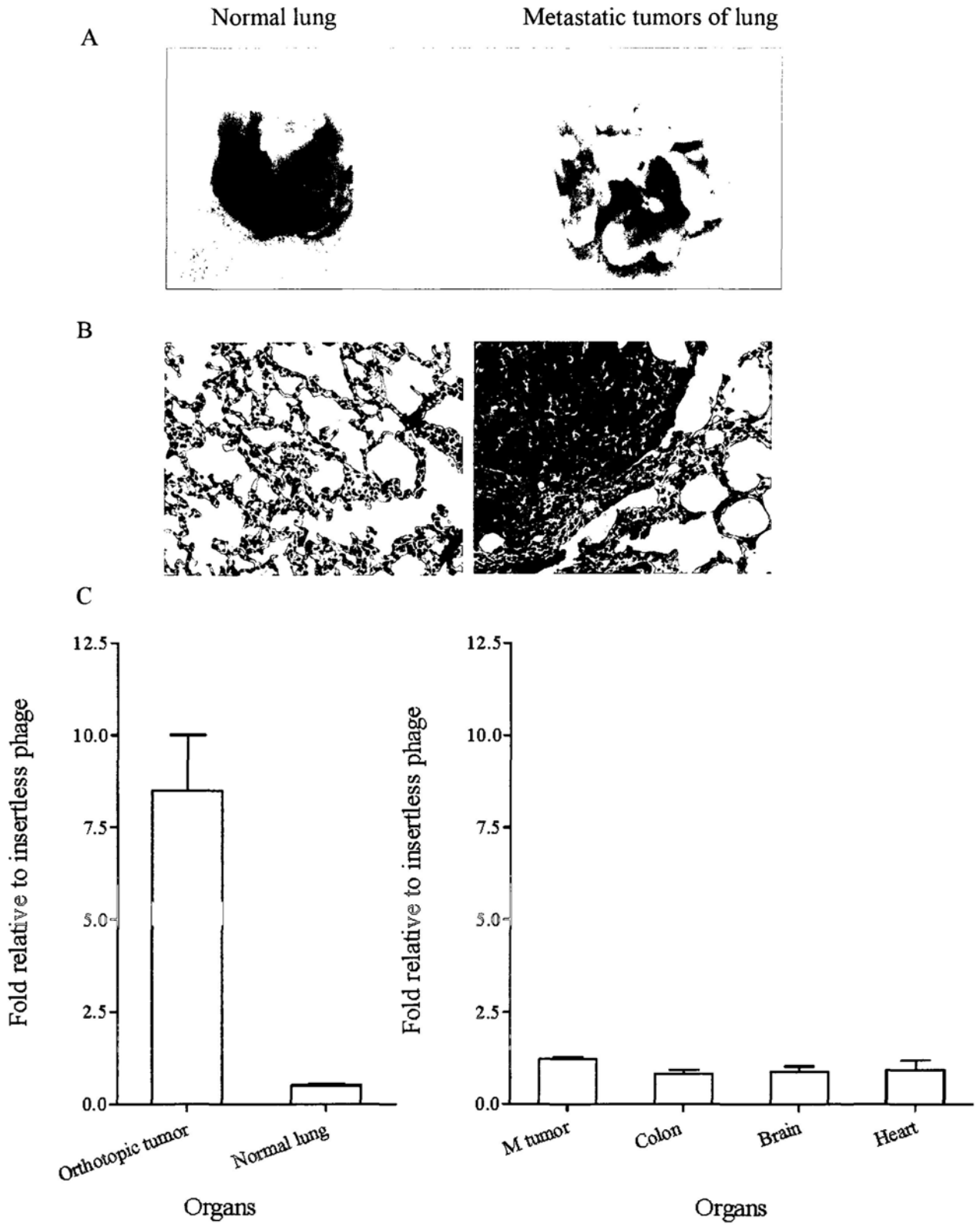
A
Normal lung
Metastatic tumors of lung
B
C
Fold relative to insertless phage
12.5
10.0
7.5
5.0
2.5
0.0
Orthotopic tumor
Normal lung
Organs
Fold relative to insertless phage
12.5
10.0
7.5
5.0
2.5
0.0
M tumor
Colon
Brain
Heart
Organs

Fig. 28 Lung metastatic model of colon cancer induced by colon 26 and TCP-1 homing ability.

A, Formation of Lung metastatic tumor. Colon 26 cells were harvested with trypsin-EDTA. The cell suspension (1 $\times 10^5$/100 μl) were injected slowly into the lateral tail vein. The mice were sacrificed on day 21 after injection. Grossly visible metastases were detectable on the surface of the organs 21 days after tumor cell injection. B, H&E staining confirmed the presence of metastasis. Original magnification: 200×. C, TCP-1 phage could not target the tumor tissues from lung metastasis of colorectal cancer. TCP-1 phage homed to the tumor tissues, not the normal lung tissue from the orthotopic models (left); but it did not show any homing ability to tumor tissues from lung metastasis induced by colon 26 when compared with other control organs (right). M tumor=lung tissue with metastatic tumors. Data are presented as mean ± SEM from triplicate plating in one representative experiment. Every experiment was repeated three times.

3.2.10 TCP-1 phage targets the vasculature of orthotopic gastric cancer

To examine whether TCP-1 phage also homed to the gastric cancer, an orthotopic gastric cancer model was used to perform the *in vivo* phage targeting assay. Orthotopic gastric cancer formed at 3 weeks after cell implantation. H&E staining for the tumor tissue confirmed the tumor formation (Figure 29A, B). TCP-1 phage or insertless control phage was intravenously injected into gastric cancer-bearing mice. Both tumor tissue and normal control organs were collected and assayed for phage accumulation. TCP-1 phage was enriched from 14 to 115-fold higher in tumor tissue than in control organs including normal stomach, heart and brain (Figure 29C). Insertless control phage hardly showed selectivity to tumor tissue and normal control organ (Figure 29D). Meanwhile we also found that the TCP-1 phage homed less efficiently to subcutaneous tumor of MKN45 cell than to orthotopic tumor in nude mice of the same cell line (Figure 29E).

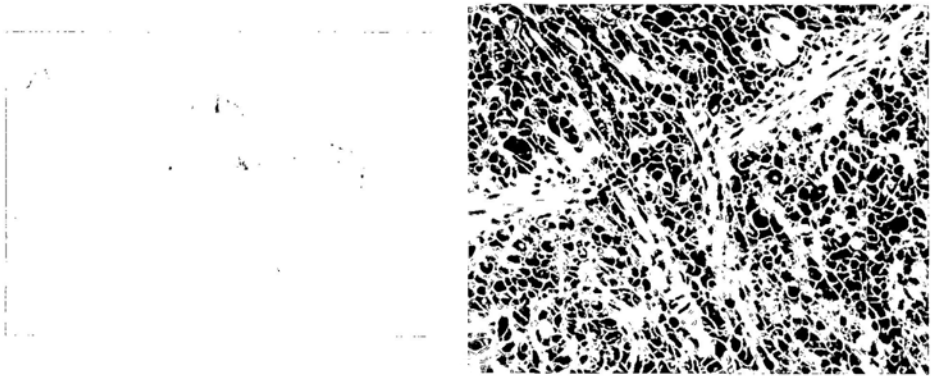

C

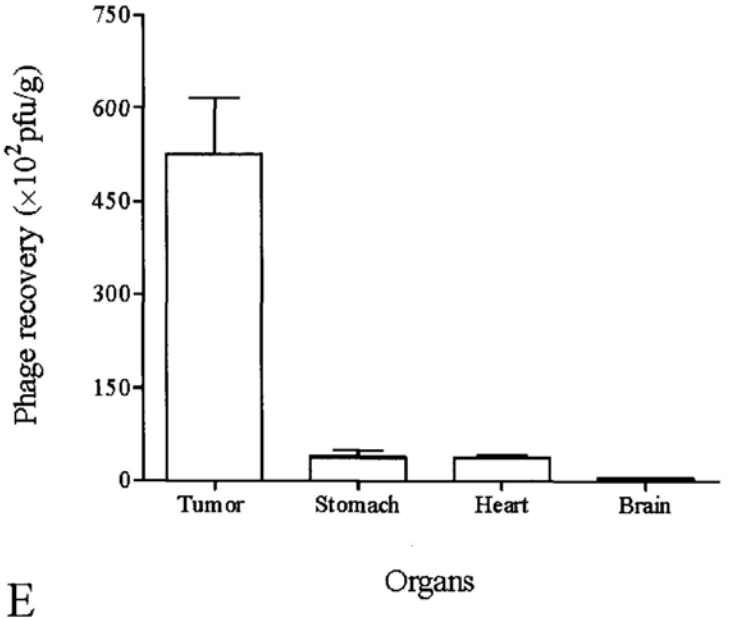
750
600
450
300
150
0
Phage recovery (×10²pfu/g)
Tumor
Stomach
Heart
Brain
Organs

D

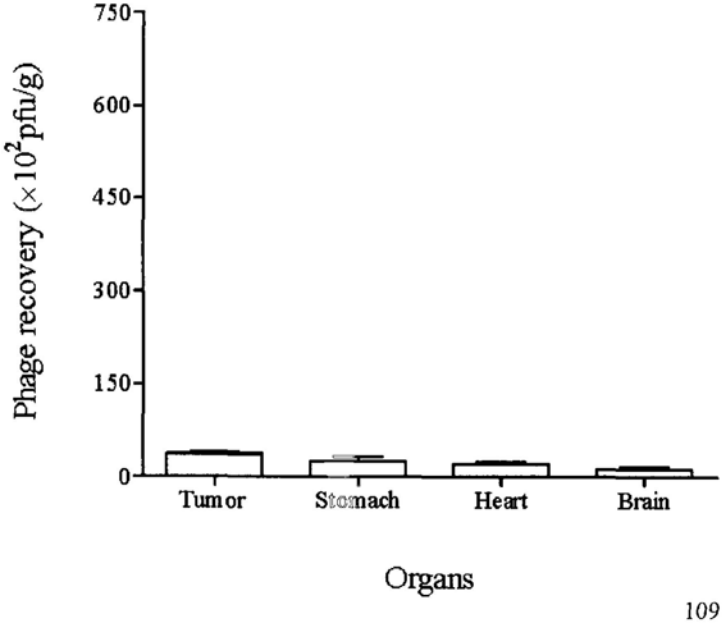
750
600
450
300
150
0
Phage recovery (×10²pfu/g)
Tumor
Stomach
Heart
Brain
Organs

E

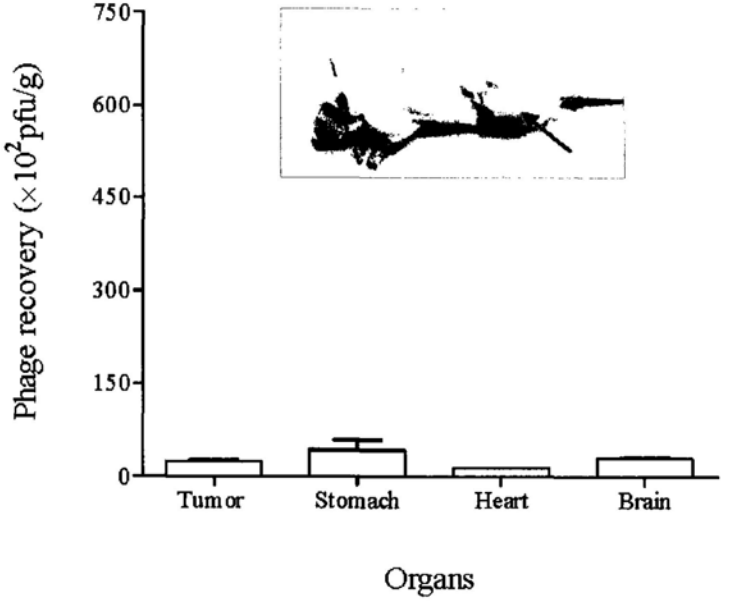
750
600
450
300
150
0
Phage recovery (×10²pfu/g)
Tumor
Stomach
Heart
Brain
Organs

Fig. 29 TCP-1 phage targeted the orthotopic gastric cancer.

A, Gross appearance of orthotopic gastric cancer. B, H&E staining for tumor tissue. C. TCP-1 phage exhibited strong homing ability to orthotopic gastric cancer after phage injection. D. Insertless phage had no selectivity to orthotopic gastric cancer tissue or control organs. E, TCP-1 phage did not home to subcutaneous gastric cancer tissue.

All of the in vivo phage targeting assays were performed 8 min after phage injection. Tumor tissue and control organs were collected and phage number was determined by counting phage plaques. Data are presented as mean ± SEM from triplicate plating in one representative experiment. Every experiment was repeated at least three times.

3.3.11 TCP-1 phage location in orthotopic gastric cancer model

To investigate the location of TCP-1 phage in the mice bearing orthotopic gastric cancer, we first performed the immunohistochemistry (DAB development) with the anti-phage antibody after intravenous injection. Tumor tissue and control organs were removed and frozen sections were prepared. The TCP-1 phage was found to localize in gastric cancer tissues, but not control organs such as heart, brain and normal stomach tissues, etc (Figure 30). Insertless phage was not detectable in the gastric cancer tissue (Figure 30).

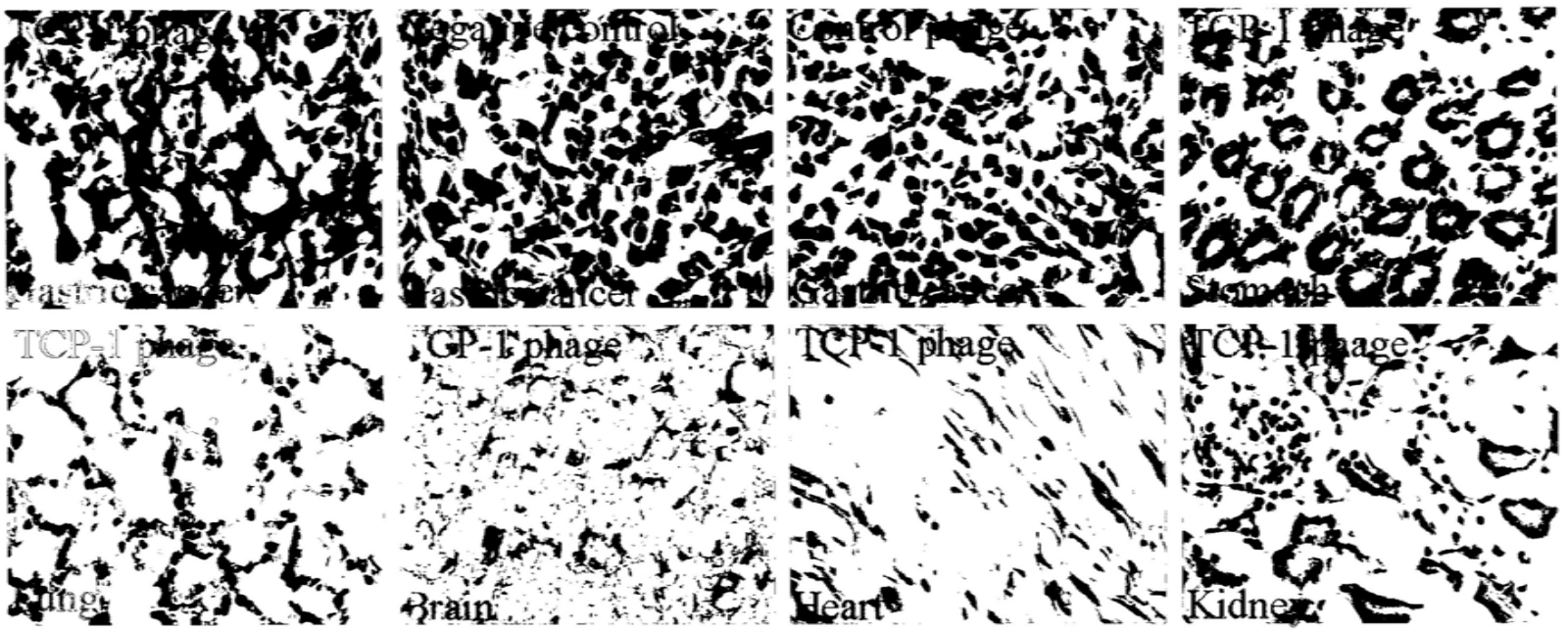

Fig. 30 *In vivo* of location TCP-1 phage in the orthotopic gastric cancer model.

Tumor-bearing mice were i.v. injected with purified individual TCP-1 phage or control phage. They were sacrificed 1 h later, and the phage was stained in frozen sections with rabbit anti-phage. The TCP-1 phage was localized in the tumor tissues and no localization was observed in normal organs such as the heart, brain, lung and stomach after phage injection. Insertless control phage was not detectable in the tumor tissue sections after phage injection. Negative control means that sections were incubated only with secondary antibody. Results shown are representative images. Original magnification: 400×.

3.2.12 Co-localization of TCP-1 phage and the vasculature of gastric cancer

Subsequently, double-label immunofluorescent staining was used to visualize the colocalization of phage (*green*, anti-phage antibody) and vasculature (*red*, CD31 antibody). TCP-1 phage colocalized with CD-31 positive endothelial cells in gastric cancer tissues but not with the blood vessels in control organs (Figure 31). Insertless phage was not detectable in the vasculature of tumor tissues (Figure 31 bottom).

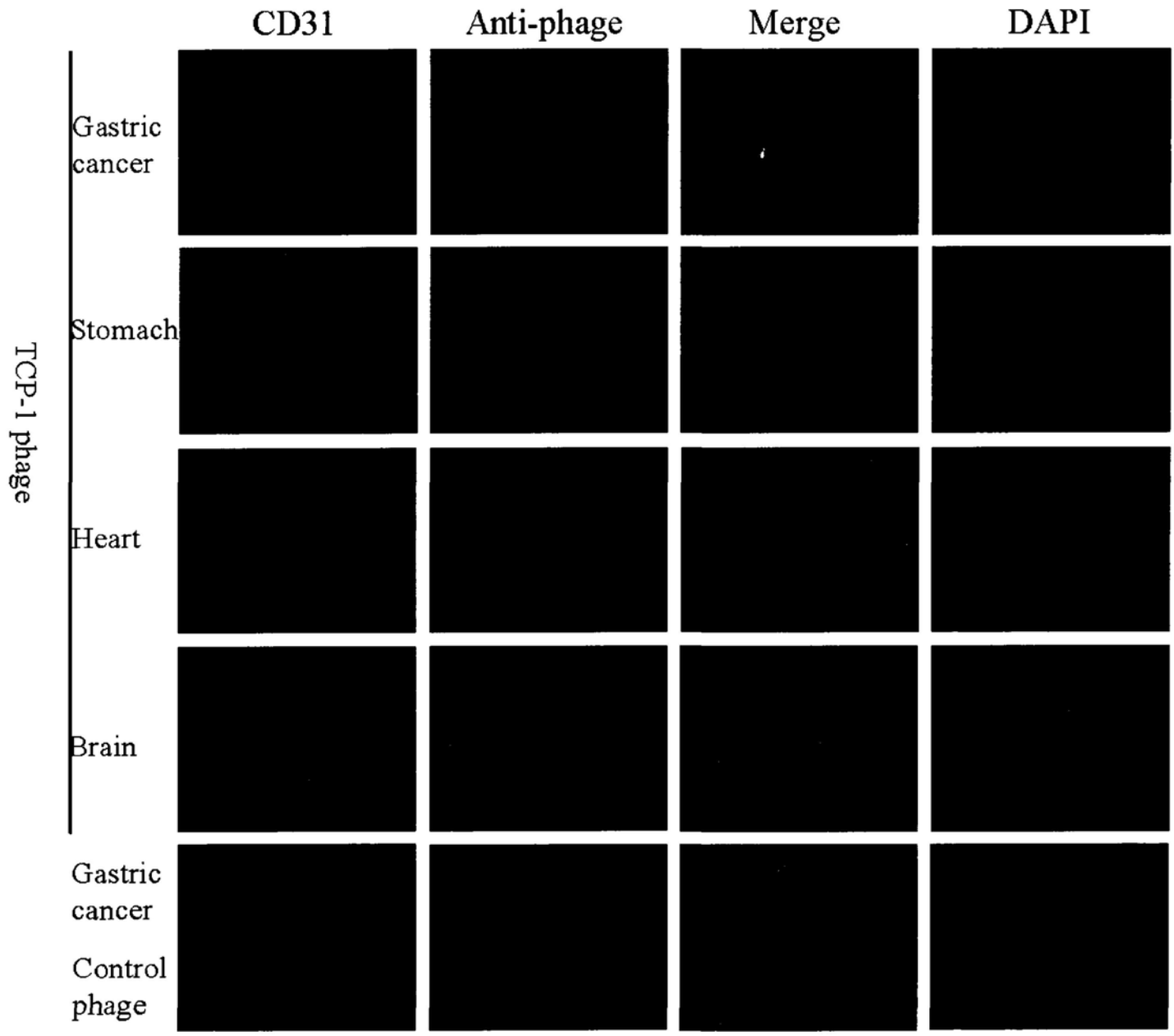
CD31
Anti-phage
Merge
DAPI
TCP-1 phage
Gastric cancer
Stomach
Heart
Brain
Gastric cancer
Control phage

Fig. 31 Vascular localization of TCP-1 phage in orthotopic gastric tissue.

Tumor-bearing mice were i.v. injected with purified individual TCP-1 phage. Mice were sacrificed 1 h later, and the phage was stained in frozen sections with rabbit anti-phage (*green*; Alexa 488). Vasculature was detected with rat anti-mouse CD31 (*red*; Alexa 568). TCP-1 phage colocalized with CD31 in the tumor tissue, but not in control organs including heart, brain and normal stomach tissue. Insertless control phage was not detectable in tumor tissue. Results shown are representative images. Original magnification: 400×.

3.2.13 Co-localization of FITC-labeled TCP-1 peptide and the vasculature of gastric cancer

To further confirm whether the selective phage homing was due to the TCP-1 peptide, chemically synthetic FITC-conjugated TCP-1 or control peptide was intravenously injected into gastric cancer-bearing mice to study the location of the peptide. Biodistribution of fluorescein-conjugated peptides was examined after i.v. injection of the peptide (300 nmol in 300 μl PBS) into the tail vein of a gastric cancer-bearing mouse. The peptide was allowed to circulate for 1 hour.

Tumor and control tissues were collected and frozen sections were prepared as described above. Blood vessels were stained by CD31 antibody (secondary antibody conjugated Alexa-568, *red*). The FITC-labeled TCP-1 colocalized with CD31 in the tumor tissues (Figure 32). But it was not detectable in control organs (Figure 32). FITC-labeled control peptide was not found in the tumor tissues (Figure 32 bottom). Taken together with the immunolocalization analyses of TCP-1 phage homing, the peptide localization data confirmed that TCP-1 peptide also homed specifically to blood vessels in gastric cancer tissues but not to the vasculature of control organs.

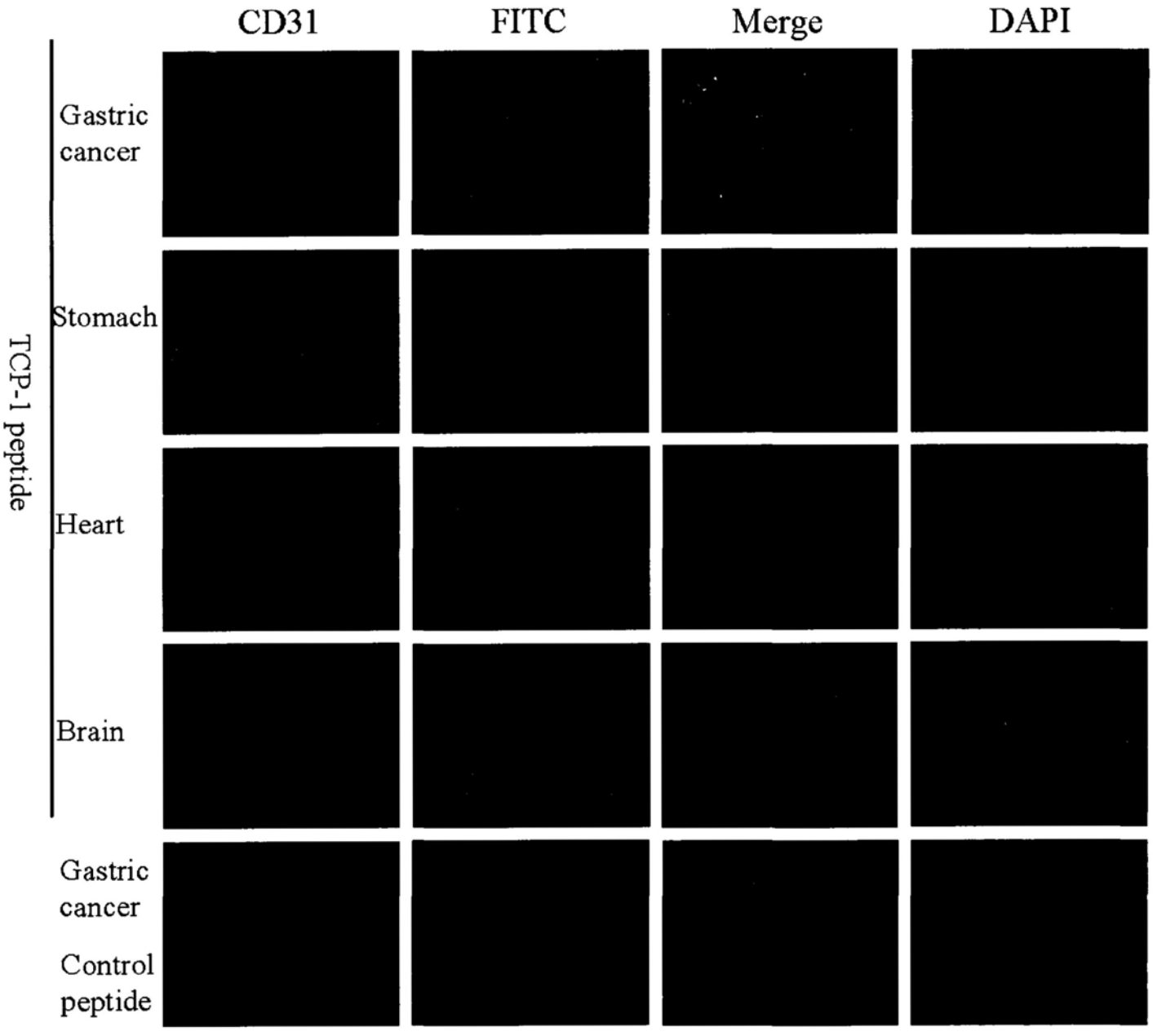
CD31
FITC
Merge
DAPI
TCP-1 peptide
Gastric cancer
Stomach
Heart
Brain
Gastric cancer
Control peptide

Fig. 32 Colocalization of FITC-labeled TCP-1 with vascular marker in tumor tissue.

FITC-labeled peptides were i.v. injected into mice bearing orthotopic gastric cancer. Mice were sacrificed 1 h later, and the peptide localization was detected in the various tissue sections. FITC-labeled TCP-1 colocalized with CD31 in the vasculature of tumor tissues but not in control organs including heart, brain and normal stomach tissues. FTIC-labeled irrelevant peptide did not recognize the blood vessels of tumor tissues. Results shown are representative images. Original magnification: 400×.

3.2.14 TCP-1 peptide without two flanking cysteines and vasculature of orthotopic colorectal cancer

TCP-1 peptide consists of seven amino acids (TPSPFSH) with two flanking cysteines (C, C) at the both ends of the peptide. The two cysteines can form a disulfide bond through cyclization reaction, which enables TPSPFSH peptide (termed TP-1) to acquire a cyclic secondary structure. We investigated whether a linear peptide (TPSPFSH, termed TP-1) without secondary structure also recognized the vasculature of orthotopic colorectal cancer tissues.

We chemically synthesized FITC-labeled TP-1 peptide. Mice bearing orthotopic colorectal cancer were injected FITC-labeled TP-1 peptide or control peptide. After one-hour circulation, various tissues were removed and frozen sections were prepared. Blood vessels were stained by CD31 antibody (*red*). The FITC-labeled TP-1 (*green*) was detected in CD31-positive vasculature of the tumor tissues (Figure 33). It was not detectable in control organs (Figure 33). FITC-labeled control peptide was not found in the tumor tissues (Figure 33). The result indicated that secondary structure via the disulfide bond is not absolutely required for targeting *in vivo*.

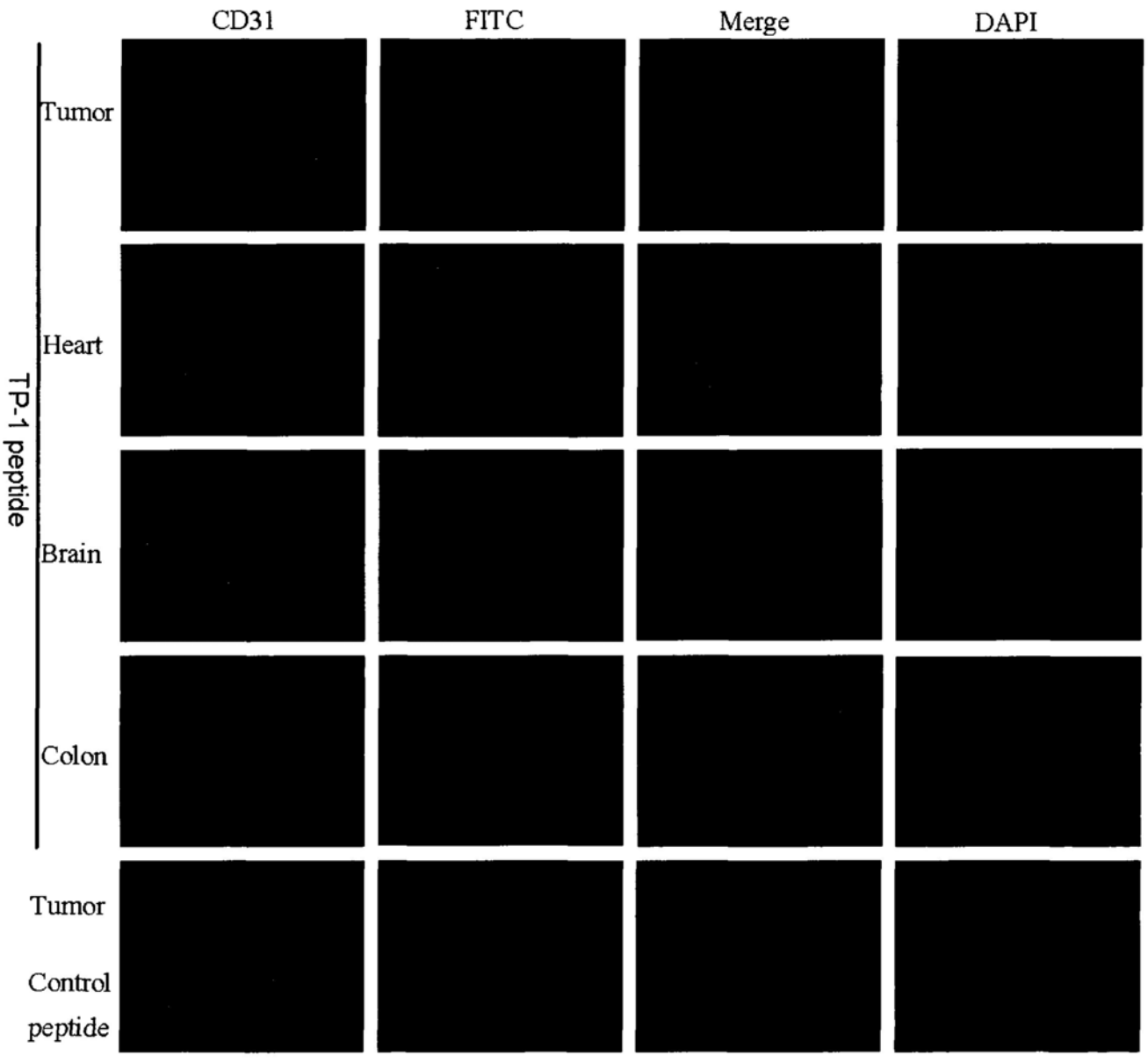

Fig. 33 TP-1 peptide without cysteines specifically recognized the vasculature of orthotopic colorectal cancer.

FITC-labeled TP-1 or control peptide was i.v. injected into mice bearing tumors. The peptide localization was detected in the various tissue sections 1 hour after peptide injection. FITC-labeled TP-1 colocalizes with CD31 in the vasculature of tumor tissue but not in control organs including heart, brain and normal colon tissues. FITC-labeled irrelevant peptide did not recognize the blood vessels of tumor tissue. Results shown are representative images. Original magnification: 400×.

3.2.15 Did TCP-1 phage translocate from gut to blood?

Oral administration is one of the most convenient and acceptable ways for internal use of drug. Therefore, we examined whether TCP-1 peptide displayed on the surface of phage particle can transport phage particles across the intestinal barrier to blood so that TCP-1 phage could target orthotopic colorectal cancer tissue by this manner. 1×10^{12} pfu TCP-1 phage in 500μl PBS was orally administered into mice bearing orthotopic colorectal cancer. After 1 hour or 4 hours retention, mice were sacrificed and blood was first collected. Tumor tissue and control organs (heart, brain, colon and spleen) were then removed. Phage from each organs and blood was quantified by plaque assay. Results suggested that no phage was recovered from all of the organs at 1 hour after oral administration of TCP-1 phage or insertless phage. Several hundred phage particles were detected from blood and spleen at 4 hours after oral administration of TCP-1 phage or insertless phage. The phage number recovered accounted for a very small part of the oral administrated dose. No phage was recovered in the tumor tissue. The results demonstrated that it is difficult for TCP-1 phage to translocate from gut to blood within the first 4 hours after oral administration.

Table 2 Oral administration of TCP-1 phage to colorectal cancer-bearing mice (1 hour)

Tissues	TCP-1	Insertless control
Blood	NR*	NR
Heart	NR	NR
Brain	NR	NR
Spleen	NR	NR
Colon	NR	NR
Tumor	NR	NR

* NR = No phage recovery. Data are presented as mean ± SEM from triplicate plating in one representative experiment. Every experiment was repeated three times.

Table 3 Oral administration of TCP-1 phage to colorectal cancer-bearing mice (4 hours)

Tissues	TCP-1	Insertless control
Blood	740±145 pfu/ml	830±95 pfu/ml
Heart	NR	NR
Brain	NR	NR
Spleen	1030±136 pfu/g	976±78 pfu/g
Colon	NR	NR
Tumor	NR	NR

* NR = No phage recovery. Data are presented as mean ± SEM from triplicate plating in one representative experiment. Every experiment was repeated three times.

3.2.16 Binding of TCP-1 phage and colorectal cancer cells

Several peptides targeting tumor vasculature could interact with tumor cells. Therefore, we tested whether TCP-1 phage could bind to colorectal cancer cell lines through BRASIL method. We performed phage-binding experiments with TCP-1 phage or insertless control phage on murine colon 26, SW1116, HT-29 and CaCo-2 cells. It was found that there was a marked increase in binding of TCP-1 phage to colon 26 and SW1116 cells in comparison to the control phage (Figure 34). However, the binding of TCP-1 phage to HT-29 and CaCo2 cells were detected only at background levels as compared to the control phage (Figure 34).

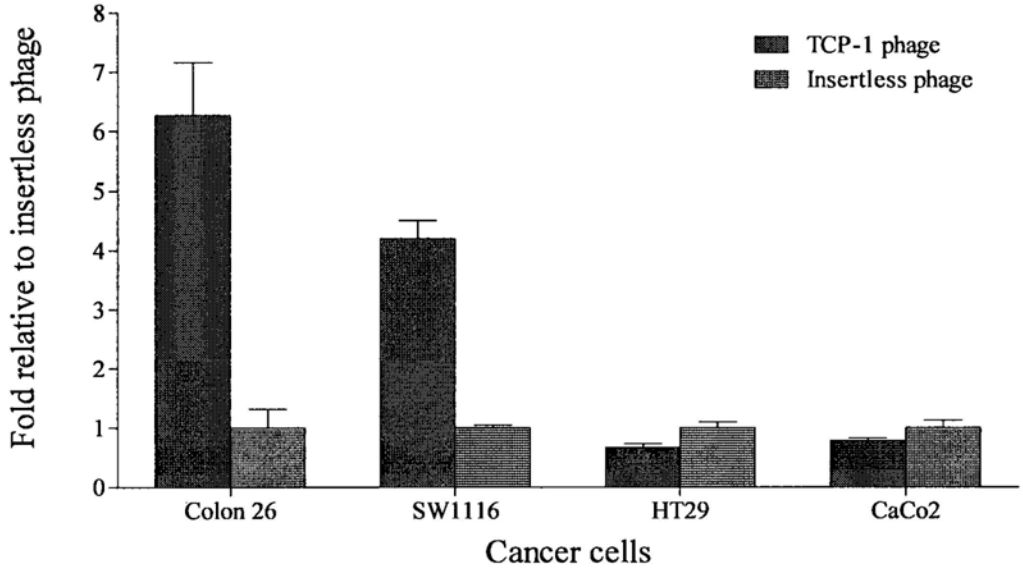

Fig. 34 TCP-1 phage binds to colorectal cancer cell lines.

TCP-1 phage or control phage was incubated with different cancer cells for 2 h on ice. Cells was then collected and assayed for phage binding. TCP-1 phage bound to colon 26 and SW1116 cells, but not to HT-29 and CaCo-2 cells. * NR = No phage recovery. Data are presented as mean ± SEM from triplicate plating in one representative experiment. Every experiment was repeated three times.

3.2.17 Internalization of TCP-1 phage in the colon 26 and SW1116

Next, we evaluated whether the TCP-1 peptide displayed on the phage surface could mediate phage internalization into cancer cells. TCP-1 phage or control phage was incubated with colon 26 and SW1116 cells for 4 h at 37 ℃. Cells were then removed with unbound phage, permeabilized and stained with anti-phage antibody. An Alexa 488-conjugated secondary antibody (*green*) was used to detect the localization of phage particles. We found that TCP-1 phage particles were internalized into colon 26 and SW1116 cells (Figure 35). Control phage particles were not detectable except for background staining (Figure 35).

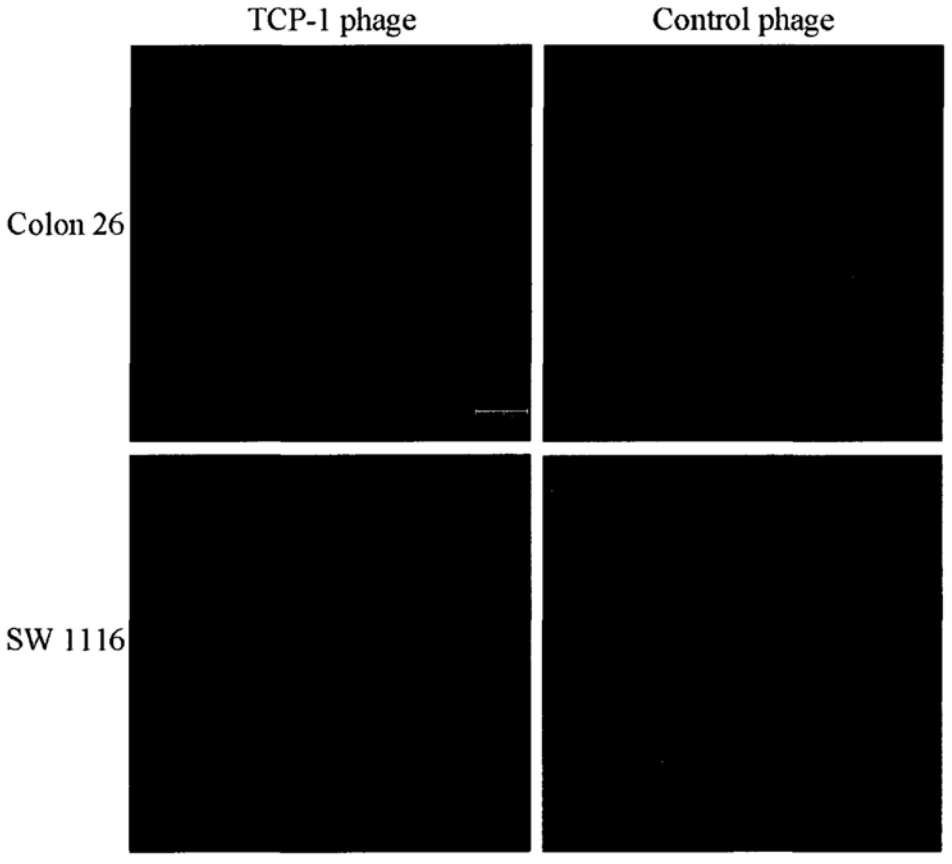

Fig. 35 TCP-1 peptide mediated internalization of phage particles into cancer cells.

TCP-1 phage and control phage was incubated with colon 26 and SW 1116 cells at 37 ℃. Cells were stained with anti-phage antibody after removal of membrane-bound phage. The results showed that TCP-1 phage was internalized by colon 26 and SW 1116 cells. *Bar*, 10 μm.

3.2.18 TCP-1 conjugate and induction of apoptosis in colorectal cancer cells

Next, in order to examine whether the TCP-1 peptide could serve as a drug carrier into cancer cells, we synthesized a chimeric peptide of TCP-1 peptide to a proapoptotic peptide $_D$(KLAKLAK)$_2$, which disrupts mitochondrial membranes upon receptor-mediated cell internalization and causes programmed cell death (Ellerby *et al.*, 1999). Increasing concentrations of TCP-1 conjugate (TCP-GG-$_D$(KLAKLAK)$_2$), equimolar TCP-1 or $_D$(KLAKLAK)$_2$ were incubated with colon 26 or SW1116 cells at 37℃. Cell viability was assessed after 6 h (colon 26) and 48 h (SW1116). The effect of TCP-1 conjugate on the cell viability was determined and compared respectively with TCP-1 or $_D$(KLAKLAK)$_2$ alone. TCP-1 conjugate inhibited the proliferation of colon 26 and SW1116 cells more efficiently than $_D$(KLAKLAK)$_2$ alone, whereas no significant effect on cell viability was observed for TCP-1 alone in concentration-dependent manner (Figures 36 and 37). The non-conjugated peptide TCP-1 revealed no detectable toxic effects on the two cell lines, but non-conjugated peptide $_D$(KLAKLAK)$_2$ has a much weaker toxic effects on these two cell lines when compared with TCP-1 conjugate, which might be due to non-specific uptake of $_D$(KLAKLAK)$_2$ by colorectal cancer cells.

A

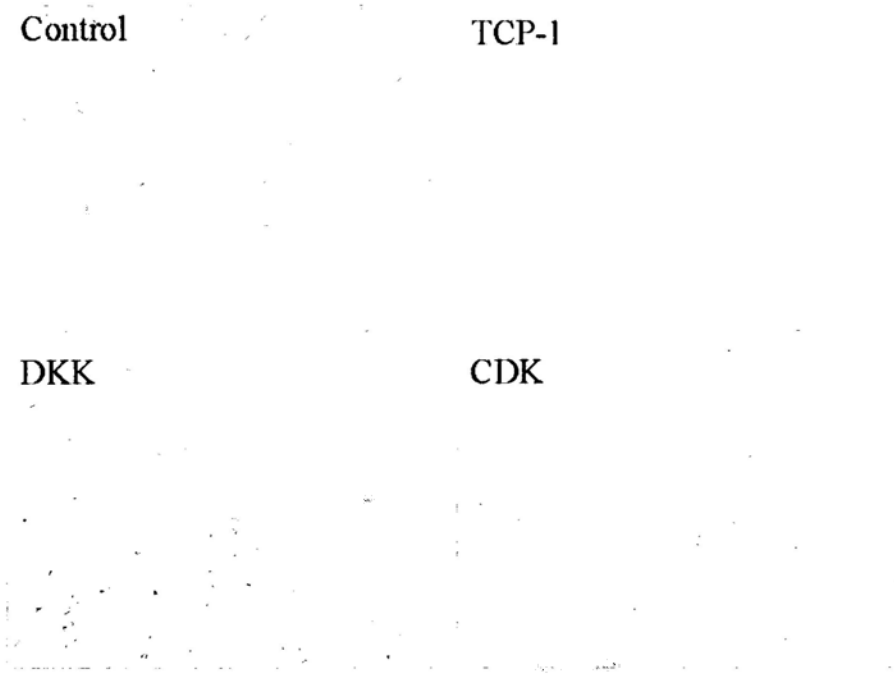
Control
TCP-1
DKK
CDK

B

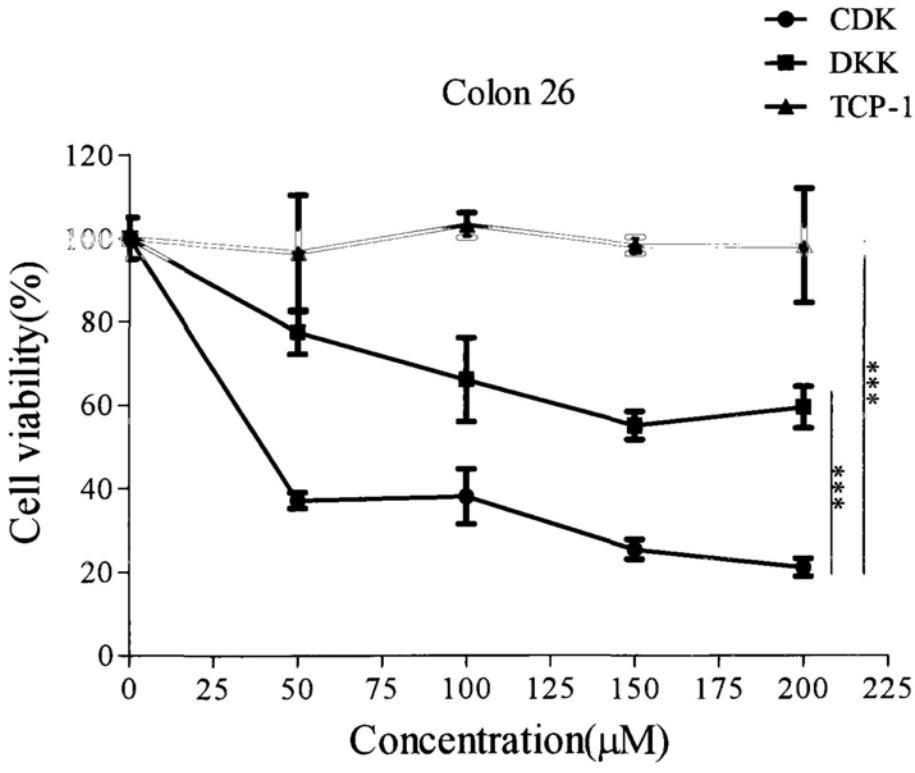
CDK
DKK
TCP-1
Colon 26
Cell viability(%)
120
100
80
60
40
20
0
0
25
50
75
100
125
150
175
200
225
Concentration(μM)
***
***

Fig. 36 Cell viability of colon 26 cell was inhibited by TCP-1 conjugate.

A, Morphological changes associated with cell death after exposure to TCP-1 conjugate. The colon 26 cells were incubated with 200 μM TCP-1 conjugate, $_D$(KLAKLAK)$_2$, or TCP-1 for 6 h. Morphological changes were recorded. CDK: TCP-1 conjugate, DKK: $_D$(KLAKLAK)$_2$, original magnification: 200 ×. B, Cytotoxic effects of TCP-1 conjugate on colon 26 cells. The tumor cells were incubated with various concentration of CDK, DKK or TCP-1 for 6 h. Cell viability was determined by MTT assay. All experiments were performed in triplicate, and data are presented as mean ± SEM. ***, $P < 0.001$.

A

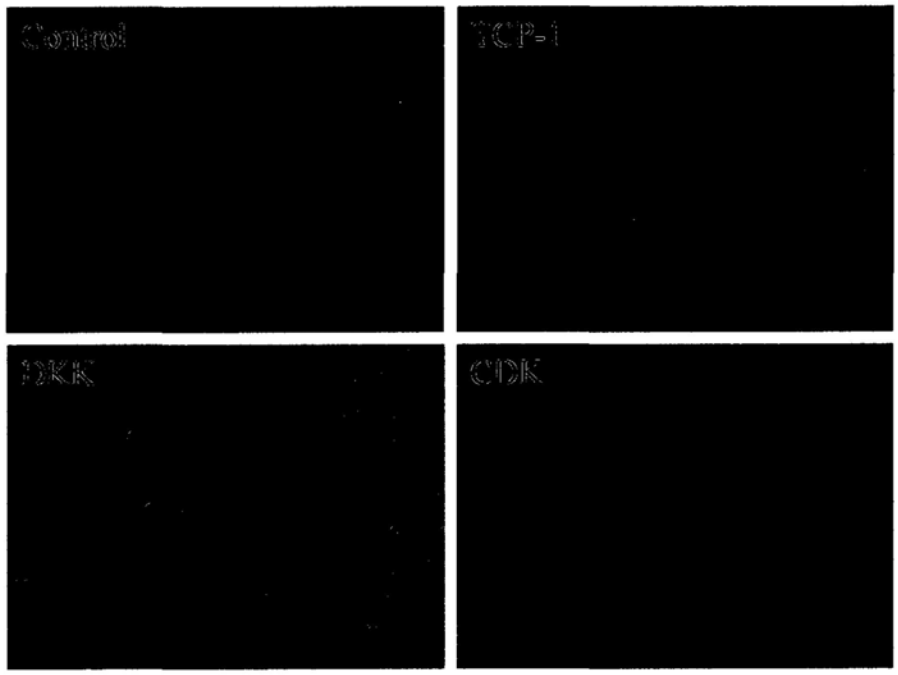
Control
TCP-1
DKK
CDK

B

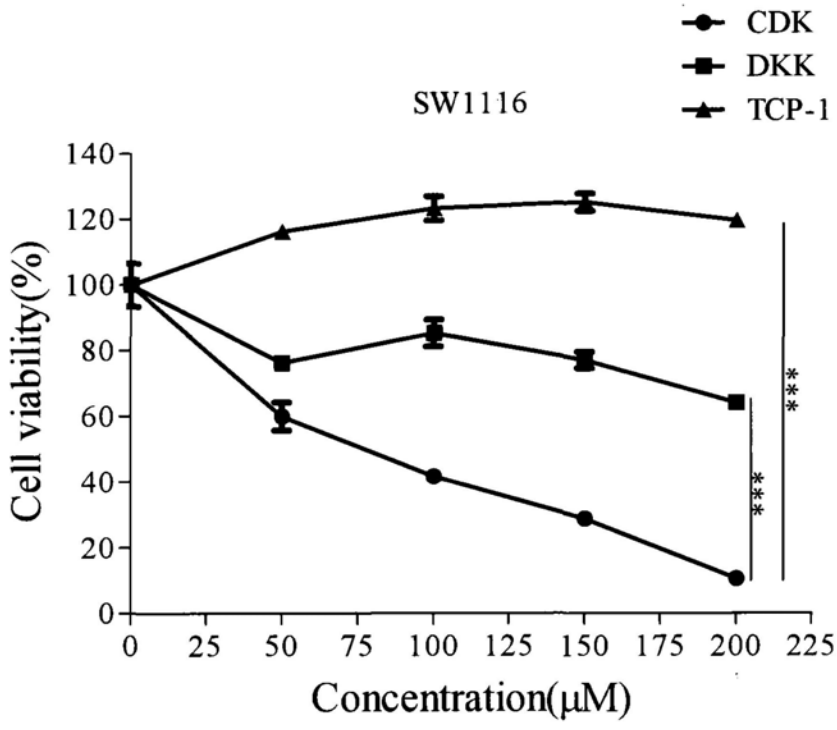
CDK
DKK
TCP-1
SW1116
Cell viability(%)
140
120
100
80
60
40
20
0
0
25
50
75
100
125
150
175
200
225
Concentration(μM)
***
***

Fig. 37 Cell viability of SW1116 cell was inhibited by TCP-1 conjugate.

A, Morphological changes associated with cell death after exposure to TCP-1 conjugate. The SW1116 cells were incubated with 200 μM TCP-1 conjugate, $_{D}$(KLAKLAK)$_{2,}$ or TCP-1 for 48 h. Morphological changes were recorded. CDK: TCP-1 conjugate, DKK: $_{D}$(KLAKLAK)$_{2}$, original magnification: 200 ×. B, Cytotoxic effects of TCP-1 conjugate on SW1116 cells. The tumor cells were incubated with various concentration of CDK, DKK or TCP-1 for 48 h. Cell viability was determined by MTT assay. All experiments were performed in triplicate, and data are presented as mean ± SEM. ***, $P < 0.001$.

3.2.19 Recognition of TCP-1 phage in colorectal cancer tissues of the subcutaneous cancer model

TCP-1 peptide can bind to colorectal cancer cells and mediate internalization of phage particles *in vitro*. Next, we assessed whether TCP-1 peptide can target cancer tissue *in vivo*. Here, subcutaneous colorectal cancer model induced by colon 26 in normal BALB/c mice was used rather than the orthotopic cancer model, since our previous data have verified that TCP-1 peptide did not bind to the vasculature of subcutaneous colorectal cancer in a short circulation time and thereby could prevent trapping of TCP-1 at the tumor vasculature. We further allowed phage to circulate for 24 h after phage injection to provide enough time for the interaction between TCP-1 phage and cancer cells *in vivo*. Subsequently, tumor tissue and control organs were collected after perfusion and frozen sections were prepared for immnuostaining. First, phage localization was determined by DAB development with anti-phage antibody. After 24 h of circulation, TCP-1 phage was localized in the tumor tissue but not in control organs including heart, brain and colon (Figure 38 A). Control phage was not detectable in the tumor tissue after injection. Similarly, immunofluorescent staining of phage confirmed the homing of TCP-1 phage to tumor tissue. Strong phage-positive staining was observed in tumor tissue outside the vasculature but not in control organ sections. In contrast, insertless control phage was not stained in tumor tissue (Figure 38B).

A

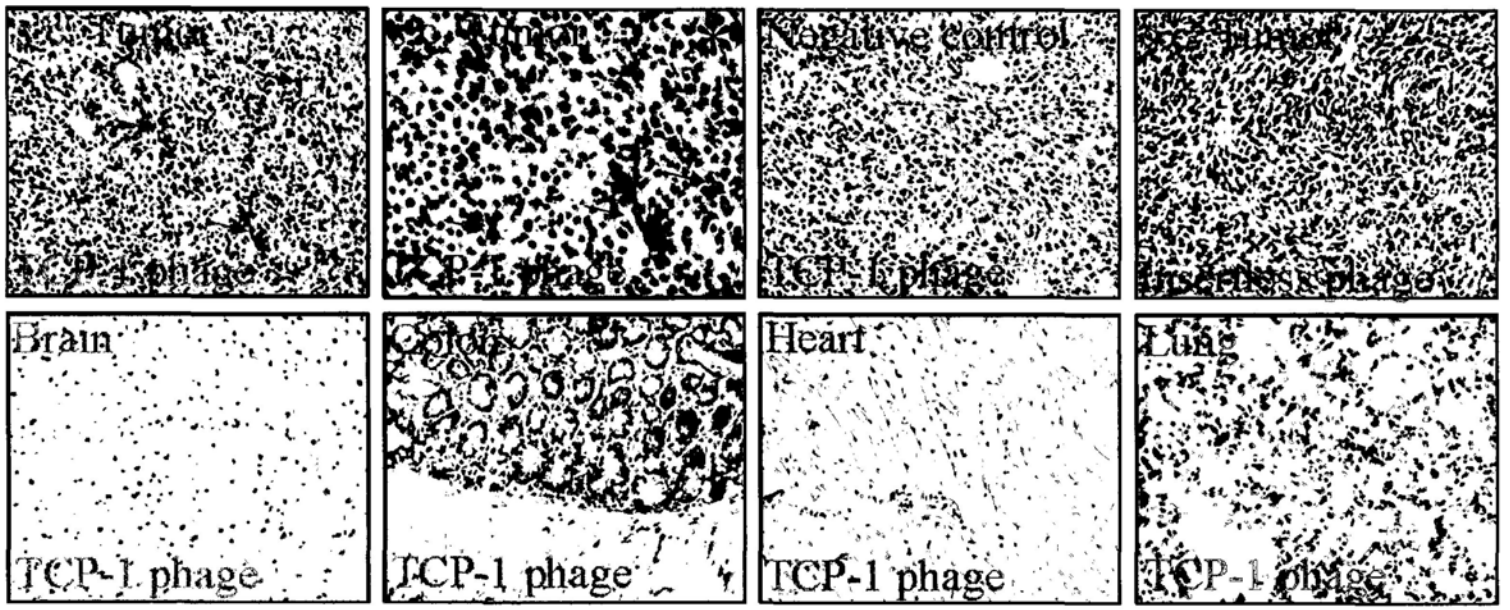
Tumor
TCP-1 phage
Tumor
TCP-1 phage
Negative control
TCP-1 phage
Tumor
Insertless phage
Brain
TCP-1 phage
Colon
TCP-1 phage
Heart
TCP-1 phage
Lung
TCP-1 phage

B

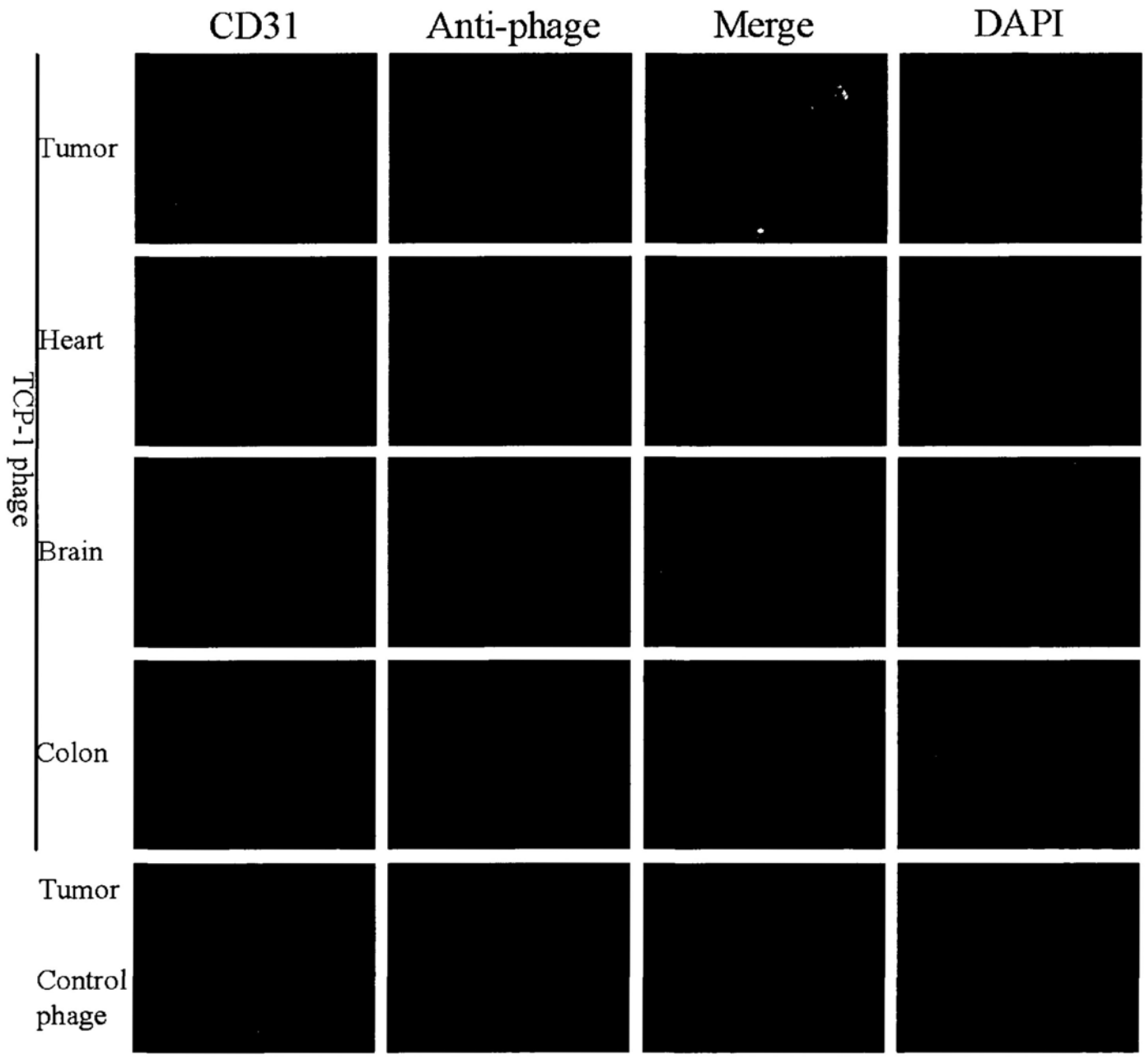
CD31
Anti-phage
Merge
DAPI
TCP-1 phage
Tumor
Heart
Brain
Colon
Tumor
Control phage

Fig. 38 TCP-1 phage targeted tumor tissue of subcutaneous cancer model *in vivo*.

A, Phage staining was performed by DAB development with an anti-phage antibody and a HRP-labeled secondary antibody. Negative control means only secondary antibody used. Original magnification: 200× except for *: 400×. B, Immunofluorescent staining was performed for phage (*green*) and vasculature marker CD31 (*red*) with fluorescence labeling secondary antibodies. Original magnification: 400×.

2×10^{10} pfu TCP-1 phage or control phage were administered intravenously into mice bearing subcutaneous tumor. Tumor tissue and control organs were recovered 24 h after the phage injections. An anti-phage antibody was used for staining. Representative results are shown.

3.2.20 Preliminary Discussion

In this study, a phage (TCP-1 phage) displaying CTPSPFSHC peptide was identified by *in vivo* phage library selection in an orthotopic colorectal cancer model induced by a mouse colon 26 cell line in mice with normal immunity. After four rounds of biopanning, TCP-1 phage displaying CTPSPFSHC peptide appeared most frequently and showed strong tumor homing ability (Table 1 and Figure 14A). The binding activity of TCP-1 phage was inhibited by synthetic peptide TCP-1 (Figure 14C), indicating that the homing ability was mediated by the TCP-1 peptide but not the phage particle. Furthermore, TCP-1 phage was only observed in the tumor tissue but not other normal control organs as revealed by immunohistochemical staining (Figure 16); TCP-1 phage and synthetic FITC-labeled TCP-1 also colocalized with CD31 in the tumor vascular endothelia but were hardly detected in normal control organs (Figures 17 and 18). At the same time, TP-1 peptide without two flanking cysteines still recognized the vasculature of colorectal cancer tissue (Figure 33). Moreover, TCP-1 peptide could specifically recognize the blood vessels of human colorectal cancer samples (Figure 19). Thus, the data demonstrate that TCP-1 may be useful as an imaging or drug delivery agent for colorectal cancer.

Interestingly, we found that the tumor-specific peptide TCP-1 did not home to subcutaneously transplanted tumors and lung metastatic tumors induced by colon 26 cells, the same cell line used in the orthotopic tumor model (Figures 15A and 28). Moreover, TCP-1 also did not exhibit any targeting ability to subcutaneous tumors induced by human colorectal cancer cells HT-29, HCT116 (Figures 15B and C). We speculate that the difference between the microenvironments of these models might

account for the differential homing capabilities by the peptide. Angiogenesis and functions of resultant vessels differ significantly between the same tumors grown in different host organs (Fukumura *et al.*, 2007). Microenvironment could influence endothelial cell phenotype by the site-specific expression of angiogenic factors. Site-specific microenvironment regulation of tumor angiogenesis is one of the most important determinants of the organ preference of metastases (Mersich *et al.*, 2008). A similar study performed by Joyce *et al.* (2003) found that five peptides selectively homed to neoplastic lesions in the pancreas but not to islet β-cell tumors growing subcutaneously, xenotransplant tumors from a human cancer cell line, or an endogenously arising squamous cell tumor of the skin (Joyce *et al.*, 2003). Similar results have also been obtained in the study by Hoffman *et al.*(2003), in which they found that among the three peptides homed to transplant tumors, none accumulated in the angiogenic islet dysplasias or solid tumors in the RIPI-Tag model of pancreatic islet carcinogenesis (Hoffman *et al.*, 2003). These data implicate that distinctive vascular markers are induced by tumorigenesis in different organ microenvironments. Our study also found that TCP-1 can target the orthotopic gastric cancer tissue induced by human gastric cancer cell MNK45, but homed less efficiently to subcutaneous tumor of MKN45 cell (Figures 29, 30 and 31). These data indicate that TCP-1 only homed to vasculature of orthotopic cancers in the gastrointestinal (GI) tract. It is well known that the GI tract has a complex interior environment. It is proposed that colon cancer may be caused by carcinogens in food or generated by interaction of constituents of luminal contents together with the intestinal microflora (Wu *et al.*, 2005), and gastric cancer is also associated directly with *Helicobacter pylori* infection and gastroesophageal reflux disease (Yin et al., 2009). Therefore, in the case of GI cancer, orthotopic tumor model in the mouse could mimic the tumor

microenvironment more accurately as in human GI cancer. The binding site(s) for TCP-1 peptide, which could be regulated under GI microenvironment, may only be expressed in the vasculature of orthotopic GI cancers.

On the other hand, it is well known that IBD has an increased risk for the development of CRC. Studies about the links between cancer and inflammation also verified that tumors often arose at the sites of chronic inflammation (Mantovani *et al.*, 2008; Wang *et al.*, 2009). The hallmarks of inflammation associated with cancer include the presence of inflammatory cells and inflammatory factors in tumor tissues, tissue remodeling and angiogenesis similar to that seen in chronic inflammatory response (Mantovani *et al.*, 2008). And one found that angiogenesis related to inflammation often shares the same marker on the surface of endothelial cells with tumor vessels (Lahdenranta *et al.*, 2007). Angiogenic vasculature in hypoxia-induced retinopathies also overexpresses the α_v integrins and aminopeptidase N and A that specifically express in the tumor vasculature. Phage targeting the integrins and aminopeptidase N and A can also home to angiogenic retina. In our study, we also extensively tested the homing ability of TCP-1 phage in acute colitis and chronic colitis model induced by DSS. Our results showed that the TCP-1 phage homed less efficiently to tissues from the acute or chronic colitis (Figures 23 and 27), which implies that the binding sites of TCP-1 peptide might not be expressed on the vasculature of colitis tissues.

In addition, many homing motifs isolated by *in vivo* phage display are expressed not only in the endothelial cells but also in the tumor cells, such as aminopeptidase N and A, MMP-2, MMP-9 and αv integrins (Decuzzi *et al.*, 2009; Hajitou *et al.*, 2006).

Phage targeting these molecules can home not only to the endothelial cells but also to the tumor cells. We also found that TCP-1 phage not only targeted to the vasculature of colorectal cancer tissues but also recognized the colorectal cancer cells (Figures 34 and 35). The data implicate that the homing motif of TCP-1 peptide is simultaneously expressed in the blood vessels and tumor cells. Moreover if this motif is highly expressed at the vasculature of tumors, TCP-1 would be trapped at this juncture and could not internalize further into the cancer cells. However, if the tumor does not or lowly express this binding motif at the blood vessels, TCP-1 could have great chances to penetrate into the tumor cells. All these unique properties would make the peptide very useful as a carrier for anticancer drugs either targeting the vasculature or cancer cells depending on the nature and the site of this homing motif in the tumor.

Finally, we also tested whether TCP-1 peptide can translocate the phage particles across the intestinal mucosal barrier. Transcytosis is a physiological course for transporting macromolecular therapeutics across endothelial and epithelial cells, which belongs to receptor-mediated endocytosis (Kang *et al.*, 2008). Large molecules are internalized into one plasma membrane domain of a polarized cell and transported to the opposite side of plasma membrane via vesicular intermediates (Kang *et al.*, 2008; Okamoto, 1998). Immunoglobulin G (Ig G), lactoferrin, transferrin or folic acid, etc. serve as molecular carriers for large molecular drugs. Several peptide sequences have been identified that can transport phage particles from intestinal lumen to systemic circulation (Duerr *et al.*, 2004; Kang *et al.*, 2008). But our data showed that phage particles cannot be easily transported across the intestinal mucosa together with TCP-1 peptide when compared with the control

insertless phage (Tables 2 and 3). It seems that parenteral injection would be the appropriate route of administration for TCP-1. However, it is unknown whether the TCP-1 peptide by itself can translocate through the intestinal mucosa and then to the targeted tumor tissues.

3.3 Application of TCP-1 peptide in imaging detection and drug delivery

3.3.1 Whole-organ imaging of FITC-labeled TCP-1 in orthotopic colorecrtal cancer

To determine whether FITC-labeled TCP-1 peptide accumulated in the tumor tissues can be visualized at the organ level, tumor-bearing mice were injected intravenously with FITC-labeled TCP-1, FITC-labeled control peptide or PBS alone. Examination of whole tissues from these mice under blue light 20 h after injection disclosed strong fluorescent signal in tumors from the mice injected with TCP-1 (Figure 39), whereas no fluorescent signal was detectable in the tumors from the FITC-labeled control peptide- or PBS-injected mice (Figure 39). We also detected no specific fluorescent signal in other control tissues either with the peptide or PBS alone (Figure 39).

Histological analysis for these tissues suggested that TCP-1 peptide fluorescence remained in the vasculature of tumor tissues but not in the control organs for at least 20 h after administration (Figure 40). FITC-labeled control peptide was not detectable in the tumor tissues (Figure 40, bottom).

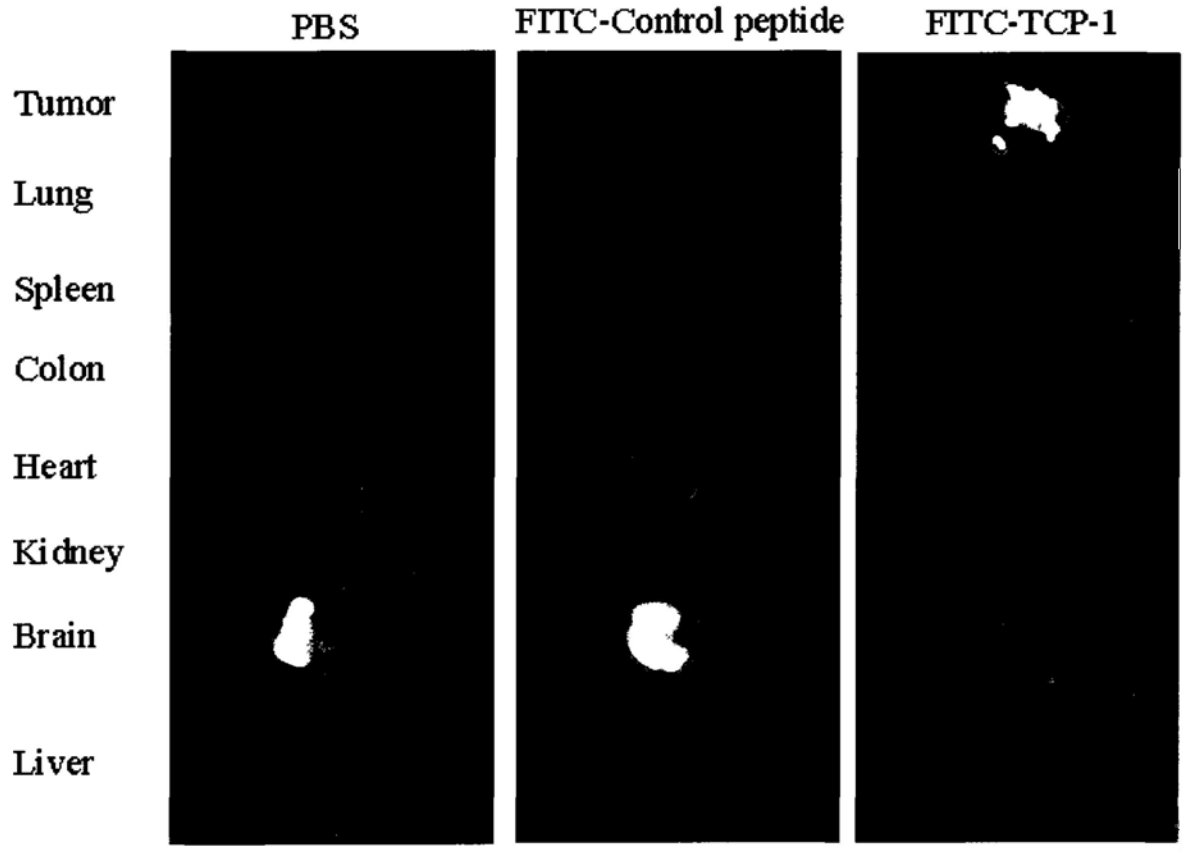

Fig. 39 Specific imaging detection of colorectal cancer tissues with FITC-labeled TCP-1.

Mice bearing orthotopic colorectal cancer were intravenously injected with 500 nmol of FITC-labeled TCP-1, control peptide or PBS. After 20 h, they were perfused with PBS. The tumors and various organs were macroscopically examined for fluorescence under blue light. FITC-labeled TCP-1 produced strong fluorescence in excised tumor but not in control organs. FITC-labeled control peptide or PBS conveyed no fluorescence to the tumors. Representative images are shown.

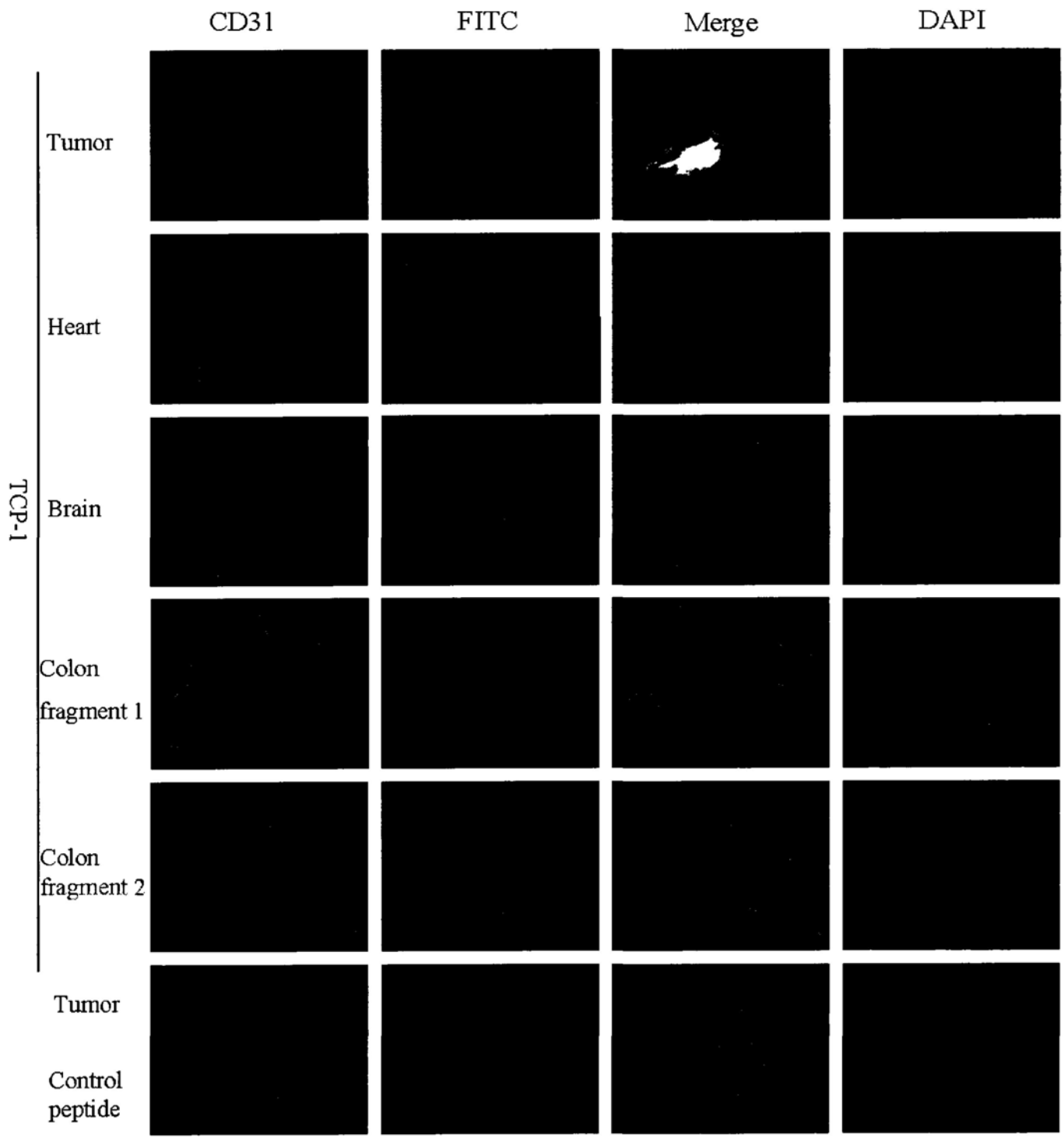
CD31
FITC
Merge
DAPI
TCP-1
Tumor
Heart
Brain
Colon fragment 1
Colon fragment 2
Tumor
Control peptide

Fig. 40 Histological examination of various tissues 20 h after FITC-labeled TCP-2 injection.

Mice bearing orthotopic colorectal cancer were intravenously injected with 500 nmol of FITC-labeled CTPSPFSHC or control peptide as in Fig 39. Frozen sections from tumors and various control tissues were prepared and examined microscopically. Strong fluorescent signal is observed in the vasculature of tumor tissues of mice injected intravenously with FITC-labeled TCP-1 but not in the control organs such as heart, brain and normal colon tissues. FITC-labeled control peptide was not detected in vasculature of tumor tissues after peptide injection. Representative tissue fluorescence results are shown. Original magnification: 400×.

3.3.2 Accumulation of FITC-labeled TCP-1 in tumor tissues with various sizes

Furthermore, we found that FITC-labeled TCP-1 could specifically accumulate in the tumor tissues with various sizes as small as 2 mm to 6 mm and 8 mm in diameters (Figure 41).

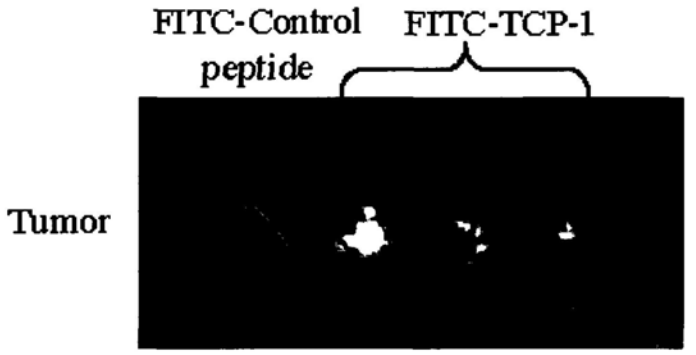

Fig. 41 FITC-labeled TCP-1 also specifically accumulates in tumors of different size.

Mice bearing orthotopic colorectal cancer were intravenously injected with 500 nmol of FITC-labeled TCP-1, control peptide or PBS. After 20 h, the mice were perfused with PBS. The tumors with various volumes were macroscopically examined for fluorescence under blue light.

3.3.3 Did FITC-labeled TCP-1 display in subcutaneous colorectal cancer?

Our data have shown that TCP-1 exhibited a binding ability to colorectal cancer cells such as colon 26 and SW1116. Next, we evaluated whether FITC-labeled TCP-1 accumulated in the subcutaneous tumor tissues can also be visualized at the organ level. S.C. tumor-bearing mice were injected intravenously with FITC-labeled TCP-1, FITC-labeled control peptide or PBS alone. Examination of whole tissues from these mice under blue light 20 h after injection disclosed that no fluorescent signal was detectable in the subcutaneous tumor tissues or control organs tested from the groups injected with FITC-labeled TCP-1, FITC-labeled control peptide or PBS (Figure 42).

The result indicated that FITC-TCP-1 did not produce signal strong enough for imaging detection through the internalization of labeled peptide into the subcutaneous colon 26 cancer tissues (Figure 42)

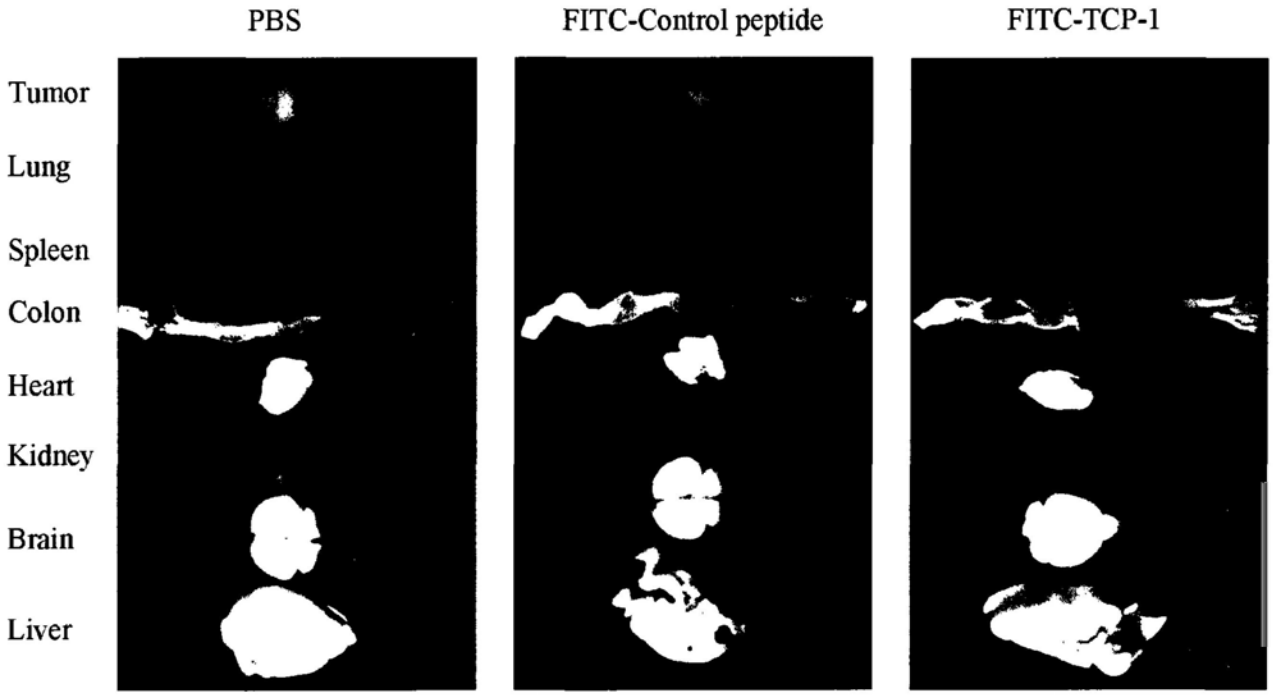

Fig. 42 Imaging detection of subcutaneous colorectal cancer tissues from tumor-bearing mice with FITC-labeled TCP-1.

Mice bearing subcutaneous colorectal cancer were intravenously injected with 500 nmol of FITC-labeled TCP-1 or control peptide. After 20 h, the mice were perfused with PBS. The tumors and various organs were macroscopically examined for fluorescence under blue light. No fluorescence signal was detectable in excised tumor or control organs from the three groups (PBS, FITC-labeled control peptide and FITC-labeled TCP-1).

3.3.4 TCP-1 conjugate and expression of cleaved caspase 3 in the tumor vasculature

To assess whether TCP-1 peptide can be used to deliver toxic payloads to the vasculature of tumors, mice bearing orthotopic colorectal cancer were treated with TCP-1 conjugate (TCP-1-GG-$_D$(KLAKLAK)$_2$), the equimolar mixture of TCP-1 and $_D$(KLAKLAK)$_2$, or PBS alone. Tumors and control organs were dissected and analyzed at the termination of the experiment. Apoptotic vascular endothelial cells were assessed by double staining with anti-cleaved caspase-3 and CD 31 antibodies. We examined the frequency of apoptosis in the vasculature by staining cleaved caspase 3 and vasculature marker CD31. Tumors of mice injected with TCP-GG-$_D$(KLAKLAK)$_2$ had an obvious increase in vasculature endothelial cells (*red*) expressing active caspase 3 (*green*) compared with tumors of mice treated with PBS or a uncoupled mixture of TCP-1 and $_D$(KLAKLAK)$_2$ (Figure 43A). Accordingly, quantification of active caspase 3 revealed a remarkable increase in the number of apoptotic cells in the tumor vasculature of TCP-1 conjugate-treated mice when compared with the other two groups (Figure 43B). In contrast, examination of apoptotic vasculature in the normal colon and brain tissues rarely showed caspase-3 positive cells among all three groups (Figure 44).

A

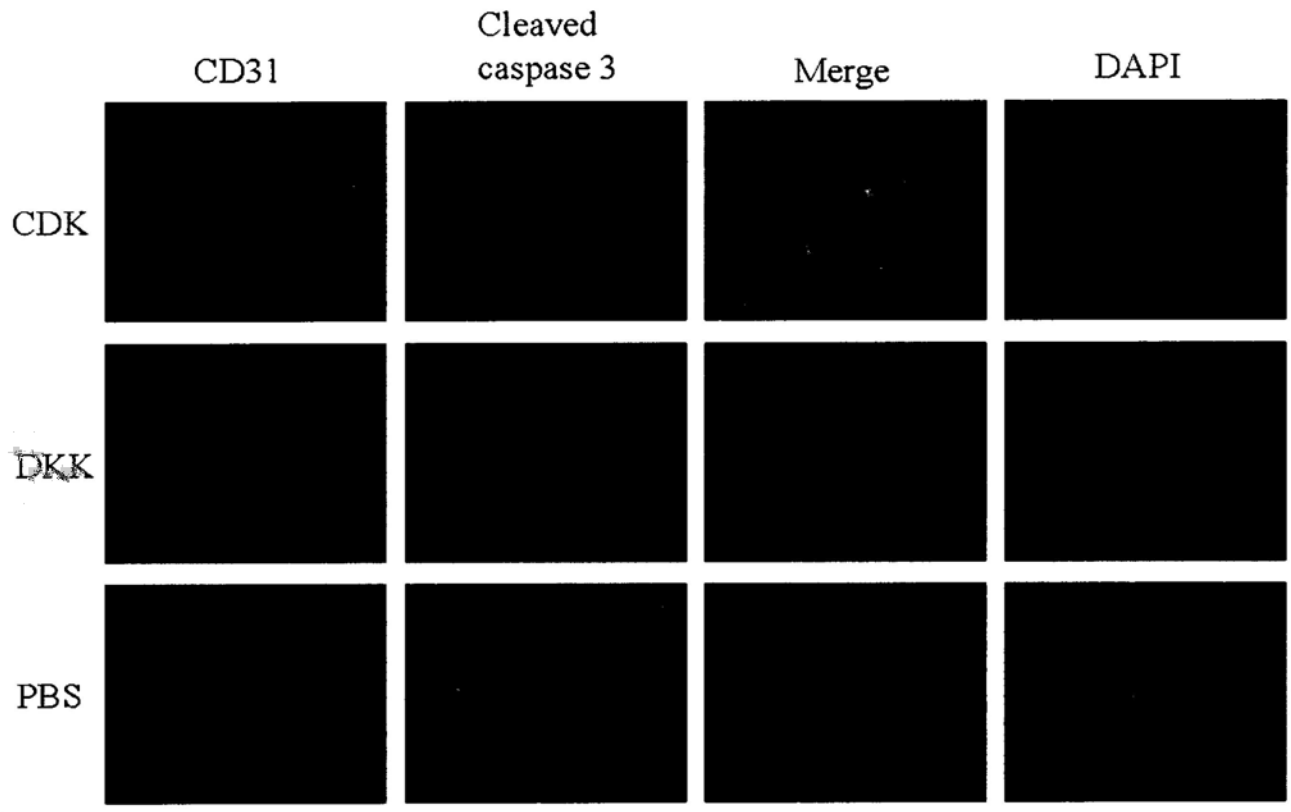
CD31
Cleaved caspase 3
Merge
DAPI
CDK
DKK
PBS

B

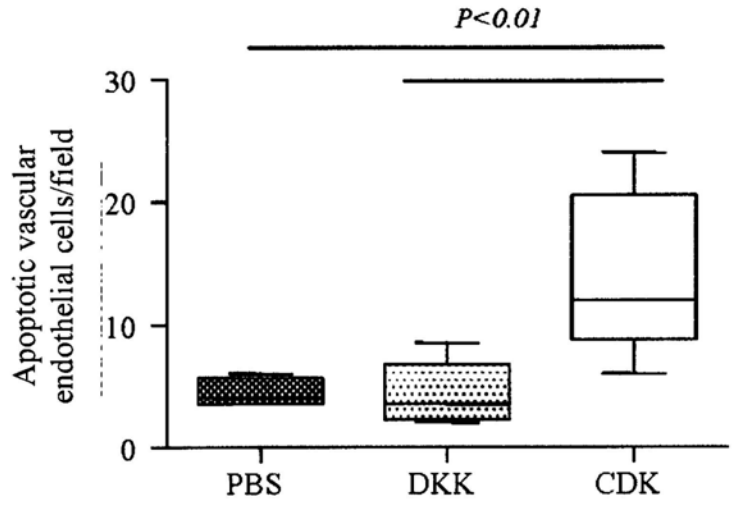
P<0.01
Apoptotic vascular endothelial cells/field
30
20
10
0
PBS
DKK
CDK

Fig. 43 Targeting the tumor vasculature with TCP-1 linked to $_D$(KLAKLAK)$_2$. Tumor-bearing mice (5 mice per group) were systemically treated with TCP-GG-$_D$(KLAKLAK)$_2$, equimolar amounts of the uncoupled peptides, or with the vehicle (PBS). At termination, frozen sections of tumor tissues and various control organs were prepared for immunofluorescent staining. A, Detection of active caspase-3 expression in the vasculature of tumor tissues after treatment by double staining with anti-active caspase-3 (*green*; Alexa 488) and anti-CD31 antibodies (*red*; Alexa 568). TCP-GG-$_D$(KLAKLAK)$_2$ peptide-treated tumor tissues showed abundant active caspase-3 positive endothelial cells in contrast to control-treated tumor tissues. Results shown are representative images. Original magnification: 200×, CDK: TCP-GG-$_D$(KLAKLAK)$_2$ conjugate, DKK: TCP-1 and $_D$(KLAKLAK)$_2$ mixture. B, Quantification of number of endothelial cells positive for caspase-3 showed a significant increase in apoptosis of endothelial cells in the tumor tissues of mice treated with TCP-GG-$_D$(KLAKLAK)$_2$ conjugate when compared with the control. Data are presented as mean ± SEM, (P<0.01).

A

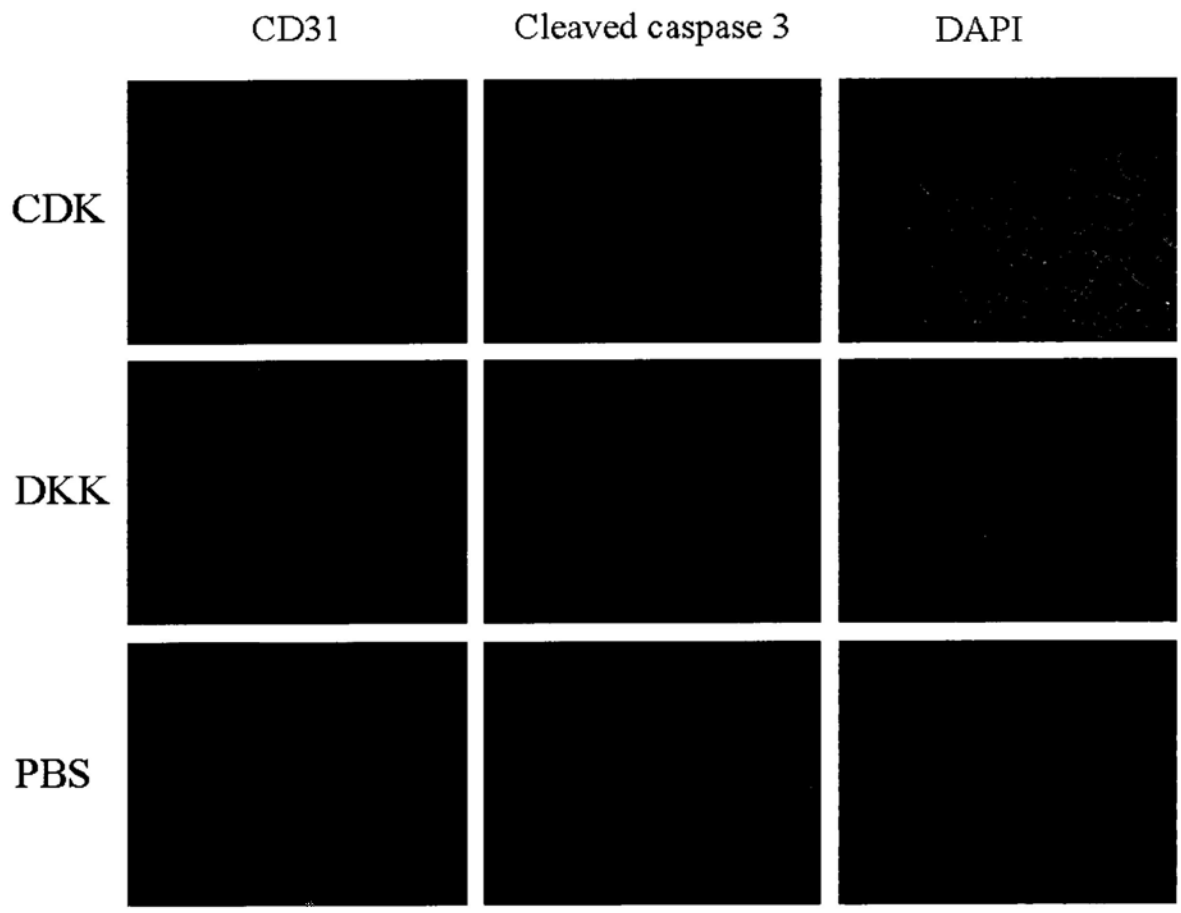

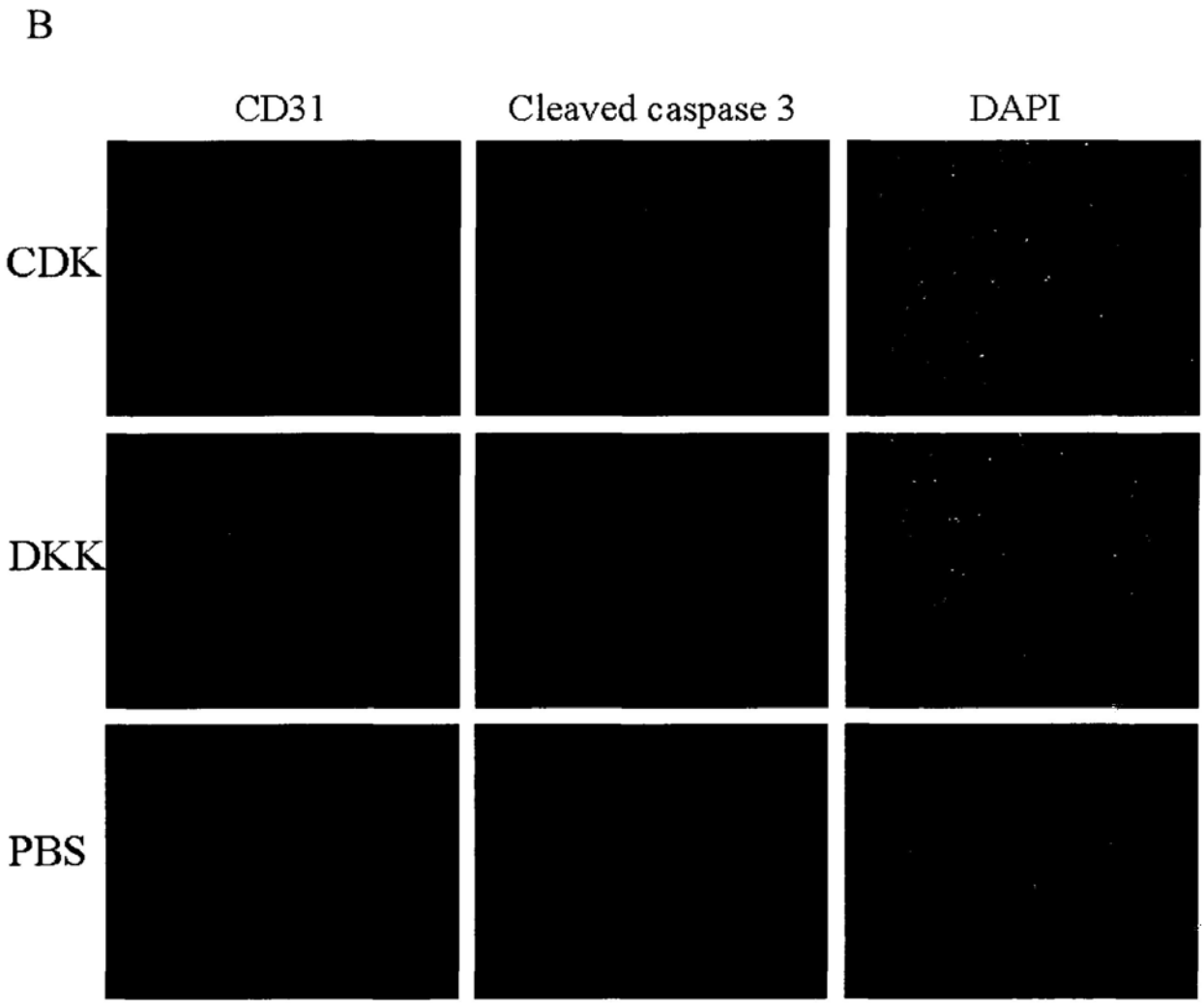

Fig. 44 Examination of active caspase-3 expression in the vasculature of control organs after treatment through double staining with anti-active caspase-3 and anti-CD31 antibodies.

A, Colon tissues. B, Brain tissues. No obvious differences were observed among the three groups. Original magnification: 200×, CDK: TCP-GG-$_D$(KLAKLAK)$_2$, DKK: the mixture of TCP-1 and $_D$(KLAKLAK)$_2$.

3.3.5 TCP-1 conjugate and apoptotic cells in the tumor vasculature (TUNEL assay)

In addition, the TUNEL assay also used to assess the apoptosis in endothelial cells and tumor cells. The result disclosed an increased number of apoptotic cells (*green*) in the tumor vasculature (CD31-positive) treated with TCP-1 conjugate but not with the control peptide or PBS (Figure 45).

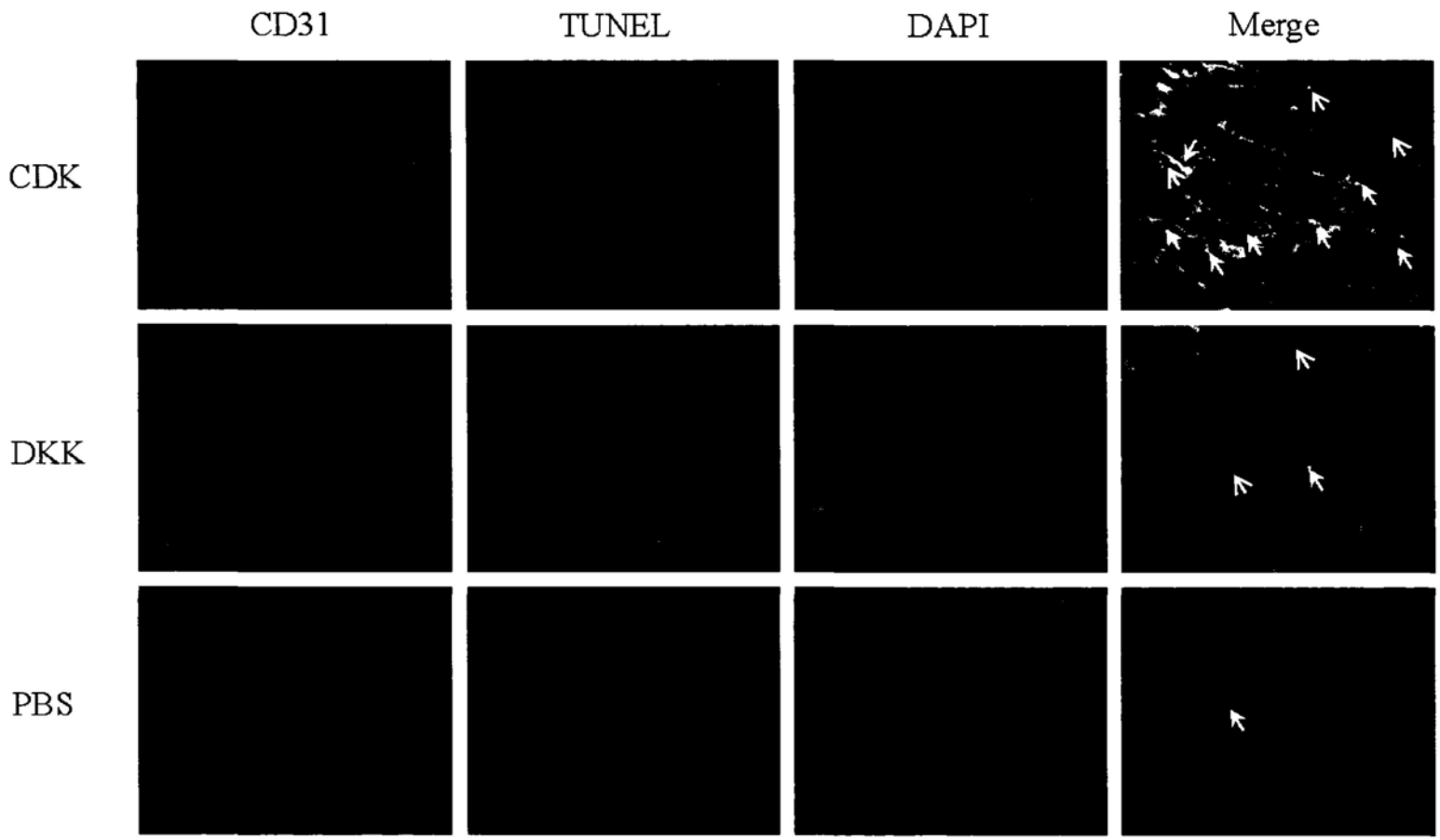
CD31
TUNEL
DAPI
Merge
CDK
DKK
PBS

Fig. 45 TUNEL assay detected the apoptotic endothelial cells and tumor cells in the tumor tissues after treatment of TCP-1 conjugate, control peptide and PBS. Apoptotic cells were detected by TUNEL assay (*green*), endothelial cells were marked by anti-CD31 antibody (*red*), and cell nuclei were stained with DAPI (*blue*). TUNEL-positive cells in CD31-positive cells were marked with yellow arrows. TUNEL-positive cells in tumor cells were labeled with white arrows. Pictures shown are representative images. Original magnification: 200×.

3.3.6 Preliminary Discussion

It is generally agreed that precise and early detection of cancer can ultimately result in an improved cure rate. Compared with conventional anatomic imaging techniques, molecular imaging detection of cancer is considered to be a more sensitive and specific monitoring of key molecular targets associated with early events in carcinogenesis (Kelly *et al.*, 2008; Weissleder, 2006). Peptides homing to tumor vasculature or lymphatics have been used successfully in tumor imaging by systemic delivery of the peptide conjugated with radiotracers (Haubner *et al.*, 2001; Liu *et al.*, 2009) or fluorescein (Laakkonen *et al.*, 2004) to tumor-bearing mice. In our study, we also assessed whether TCP-1 peptide had a potential to detect colorectal cancers. FITC-labeled TCP-1 was found to have a strong accumulation in the tumor mass at microscopic and whole-organ levels after intravenous injection (Figure 39). The efficacy and specificity of this peptide were sufficient to visualize the orthotopic colorectal tumor in the colorectal lumen. Histology analysis showed that the peptide could stay in the tumor vessels for at least 20 h after intravenous injection (Figure 40). Conventional anatomic imaging techniques typically detect cancers when they are bigger than a centimeter in diameter (Weissleder, 2006). Here we found that TCP-1 showed an excellent specificity to tumors with different diameters, as small as 2 mm (Figure 41). If this technological approach can be reproduced in clinical setting, targeted TCP-1 peptide probe together with endoscopic confocal microscopy may greatly improve the diagnosis of patients with colorectal cancer. In addition, we also found that TCP-1 showed a binding ability to colorectal cancer cells such as colon 26 and SW1116 (Figures 34, 35, 36). However, FITC-TCP-1 did not produce signal strong enough for imaging detection through internalization into the tumor cells as

demonstrated by the analysis of subcutaneous colon 26 cancer tissues (Figure 42). FITC labeled methodology may not be a good method in this experimental setting. Other methods are under investigation to improve the sensitivity of this tumor imaging.

One potential application of peptides homing to tumor vasculature is to deliver toxins or pro-drug molecules as targeted therapeutic agents to increase the efficacy of anti-cancer therapy and decrease the undesired systemic side-effects in other tissues (Curnis *et al.*, 2004; Kolonin *et al.*, 2004; Lin *et al.*, 2009). It has been estimated that 100 tumor cells are fed by a single endothelial cell, thus antiangiogenic therapy aiming at blocking the blood supply is able to constrain cancer growth for prolonged periods (Hajitou *et al.*, 2006; Kerbel, 2006). Results of recent clinical trials indicated that antiangiogenic drug could render cancer cells more sensitive to cytotoxic chemotherapy without substantially increasing toxicity to normal cells (Hurwitz *et al.*, 2004; Kerbel, 2006). Three distinct mechanisms might be involved in the chemosensitizing activity of antiangiogenic drugs including normalizing tumor vasculature, preventing rapid tumor cell repopulation, and augmenting the antivascular effects of chemotherapy (Fukumura *et al.*, 2007; Jain, 2005; Kerbel, 2006; Langenkamp *et al.*, 2009). In the present study, we harnessed vascular homing peptide TCP-1 to deliver $_{D}$(KLAKLAK)$_2$, a proapototic peptide, to the tumor. These targeted TCP-1 conjugate could significantly increase the apoptosis of tumor-associated vasculature but had negligible effects on control organs (Figures 43, 45). These data further demonstrate that the TCP-1 peptide specifically recognizes the endothelial cells of tumor blood vessel, thus giving it a great potential as a drug carrier in the treatment of colorectal cancer.

3.4 TCP-2 phage and peptide

3.4.1 *In vivo* phage targeting assay of TCP-2 phage in orthotopic colorectal cancer model

TCP-2 phage displaying CSNSDWSSC peptide is the second phage clone that might target the vasculature of orthotopic colorectal cancer. To confirm the result, the *in vivo* phage targeting assay was repeated in other three mice bearing orthotopic tumors. The phage was allowed to circulate for 8 min after injection. The tumor tissues and control organs were collected and assayed for phage accumulation. The TCP-2 phage exhibited stronger homing ability to tumor tissue than to control organs including colon, brain and heart after phage injection (Figure 46A). Insertless control phage was negative for homing ability to any organs (Figure 46B) after phage injection.

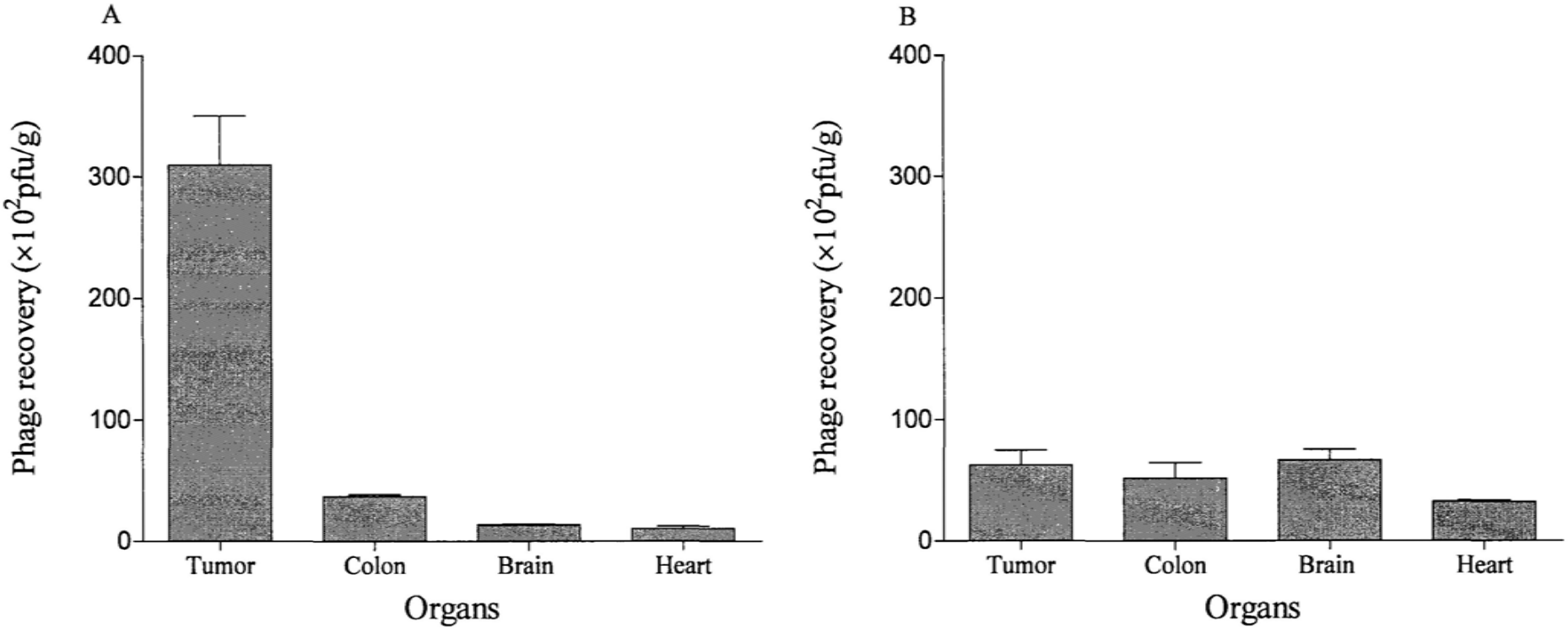

Fig. 46 TCP-2 phage accumulated into the orthotopic colorectal cancer tissue.

A, The homing ability of TCP-2 phage to orthotopic colorectal cancer model. B, Phage titers of insertelss phage from various organs. 1×10^9 pfu TCP-2 phage or control phage was injected i.v. into mice bearing tumors and allowed circulation for 8 min. Phage was rescued from various organs and phage titers were shown. TCP-2 phage accumulation in tumor tissue was remarkably higher than that in the normal control. Control phage did not exhibit any homing ability to any tissues. Data are presented as mean ± SEM from triplicate plating in one representative experiment. Every experiment was repeated three times.

3.4.2 TCP-2 phage and vasculature of subcutaneous colorectal cancer model

Next, we further examined the homing ability of TCP-2 phage to subcutaneous colorectal cancer model induced by colon 26 in normal BALB/c mice. I.v. injected TCP-2 phage did not appreciably home to subcutaneous colorectal cancer tissues. The data also showed that TCP-2 phage like TCP-1 phage selectively homed to the orthotopic colorectal cancer tissue.

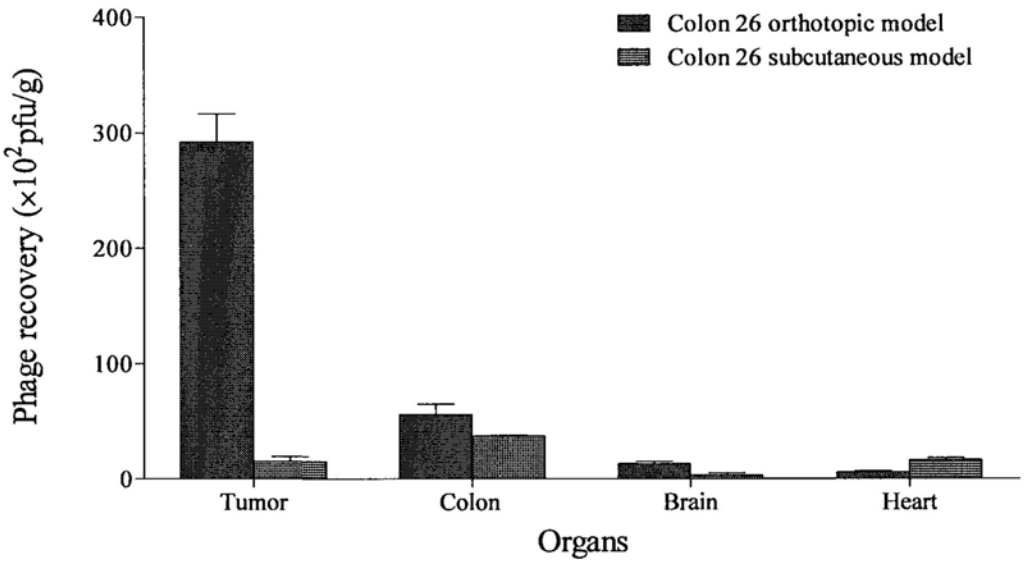

Fig. 47 No homing ability of TCP-2 phage to subcutaneous colorectal cancer tumors.

TCP-2 phage was injected i.v. into mice bearing subcutaneous colorectal cancer. After 8 min, tumor tissue and control organs were removed and phage accumulation was tested. Unlike the orthotopic model, subcutaneous colorectal cancer tissue did not bind the TCP-2 phage. Data are presented as mean ± SEM from triplicate plating in one representative experiment. Every experiment was repeated three times.

3.4.3 TCP-2 phage and vasculature of lung metastatic tumor of colorectal cancer

Next, we further investigated whether TCP-2 phage can target the lung metastatic tumor of colorectal cancer induced by colon 26 in normal BALB/c mice.

Lung metatatic model was established as described above. Histological analysis confirmed that lung tumor was formed 21 days after cancer cell inoculation.

TCP-2 phage homing ability was then examined in this model. TCP-2 phage or control phage was allowed to circulate 8 min after phage injection. Lung with metastatic tumors and control organs were collected and phage accumulation was examined. Again results showed that there was no detectable homing ability of TCP-2 phage to the tumors as compared to other control organs (Figure 48).

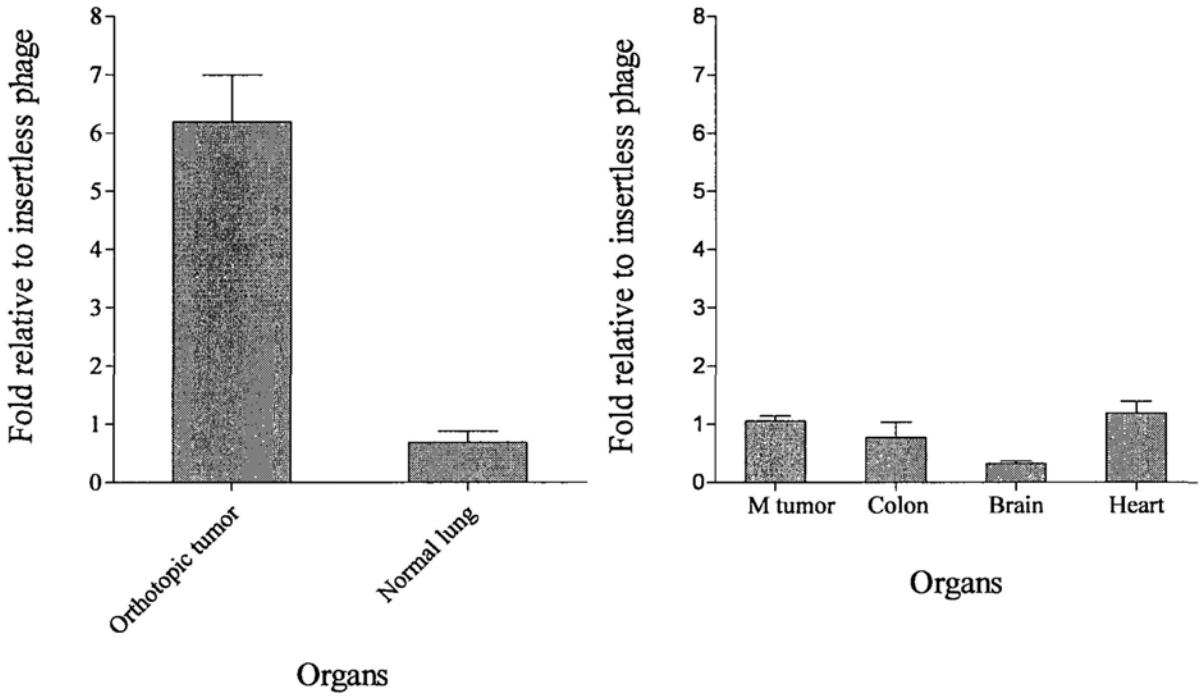

Fig. 48 No homing ability of TCP-2 phage to lung metastatic tumors.

TCP-2 phage homed to the tumor tissue not the normal lung from the orthotopic tumor model (left); also it did not appreciably home to the tissues from the lung metastatic tumors induced by colon 26 when compared with other control organs (right). M tumor: lung tissue with Metastatic tumors. Data are presented as mean ± SEM from triplicate plating in one representative experiment. Every experiment was repeated three times.

3.4.4 TCP-2 phage localization

Next, we investigated the distribution of TCP-2 phage using DAB staining with an anti-phage antibody after phage injection. TCP-2 phage and control phage was injected i.v. into mice bearing orthotopic colorectal cancer and allowed circulation for 1 h. Tumor tissue and control organs were collected and frozen sections were prepared. The TCP-2 phage was found to localize in tumor tissue, but not in control organs such as heart, brain, lung and normal colon tissues. Insertelss control phage did not react with the tumor tissue (Figure 49)

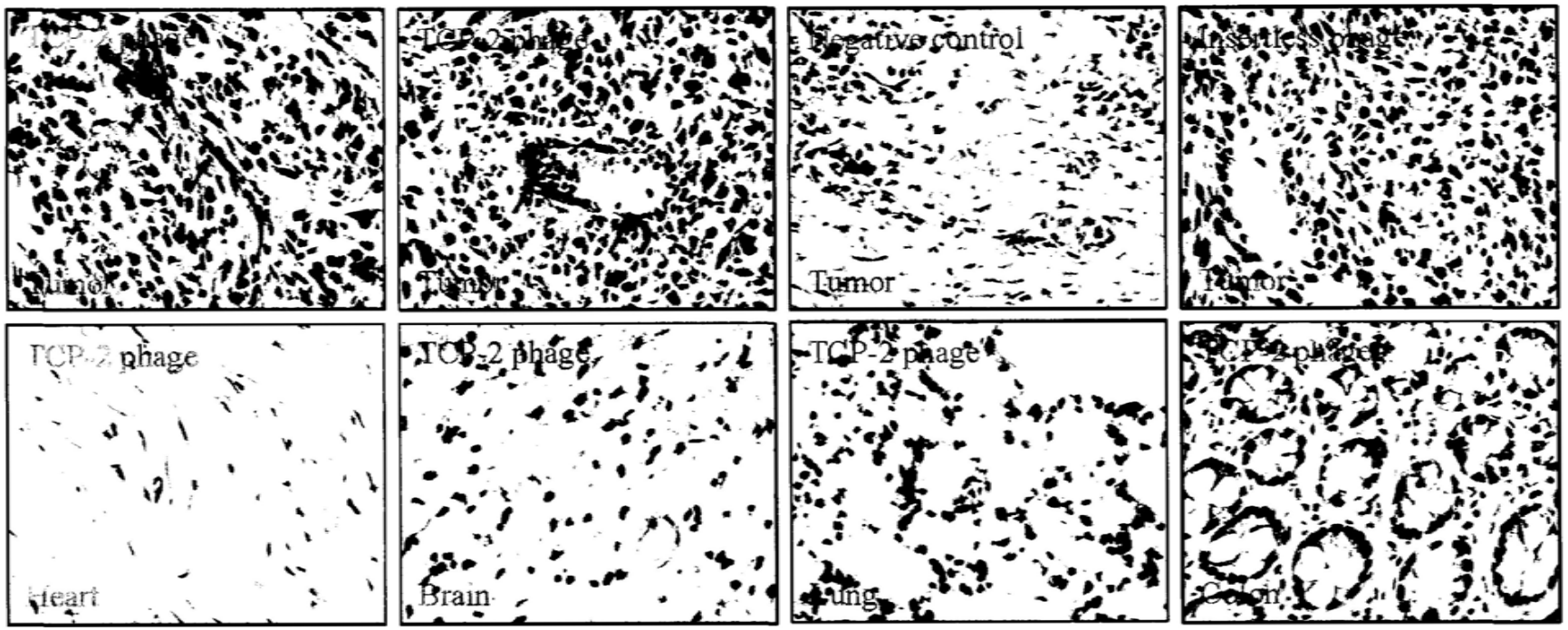

Fig. 49 *In vivo* localization of TCP-2 phage by immunohistochemical analysis after phage injection.

Tumor-bearing mice were injected i.v. with TCP-2 phage or control phage. The phage location was studied by immunohistochemistry with anti-phage antibody in frozen sections. The TCP-2 phage was localized in the tumor tissue but not in normal organs such as heart, brain, lung and colon. Insertless phage was not detectable in the tumor tissue after phage injection. Negative control means that sections were incubated only with secondary antibody after TCP-2 phage injection. Representative images are shown. Original magnification: 400×

3.4.5 Synthetic TCP-2 peptide inhibited the accumulation of TCP-2 phage in cancer tissue

To prove the homing ability of TCP-2 phage is due to its displayed TCP-2 peptide sequence CSNSDWSSC. Chemically synthesized TCP-2 peptide (300 nmol) was co-injected i.v.with the TCP-2 phage. After 1 h of circulation, tumor tissues were collected and frozen sections were prepared. Tissue sections with anti-phage antibody showed that TCP-2 peptide could competitively inhibit the localization of TCP-2 phage in tumor tissue. Again control phage was not observed in the tumor tissue. These data implied that TCP-2 peptide not the phage particle could interact and bind with the tumor tissue.

Fig. 50 TCP-2 peptide inhibited the localization of TCP-2 phage in the orthotopic tumor tissue.

TCP-2 peptide and TCP-2 phage were co-injected i.v. into the tumor-bearing mice. After 1 h of circulation, tumor tissues were collected and phage was stained in frozen sections of tumor tissues with anti-phage antibody. Phage was positively stained in the tumor tissue only after TCP-2 phage injection. Phage was not observed in the tumor tissue after co-injection with TCP-2 phage and TCP-2 peptide. Negative control means only secondary antibody was added to the tissues from the TCP-2 phage injection group. Representative images are shown. Original magnification: 400×

3.4.6 Synthetic TCP-1 peptide did not inhibit the accumulation of TCP-2 phage in cancer tissues

Because both TCP-1 and TCP-2 phage can bind to the vasculature in the orthotopic colorectal cancer tissues, we further investigated whether they share the same binding site expressed in the tumor blood vessles. We co-injected TCP-1 peptide together with TCP-2 phage into mice bearing orthotopic colorectal cancer. After 1 h of circulation, tumor tissues were removed and frozen sections were prepared. TCP-2 phage was stained by anti-phage antibody in tumor tissue sections. We found that TCP-1 peptide could not inhibit the localization of TCP-2 phage in the tumor tissues (Figure 51).

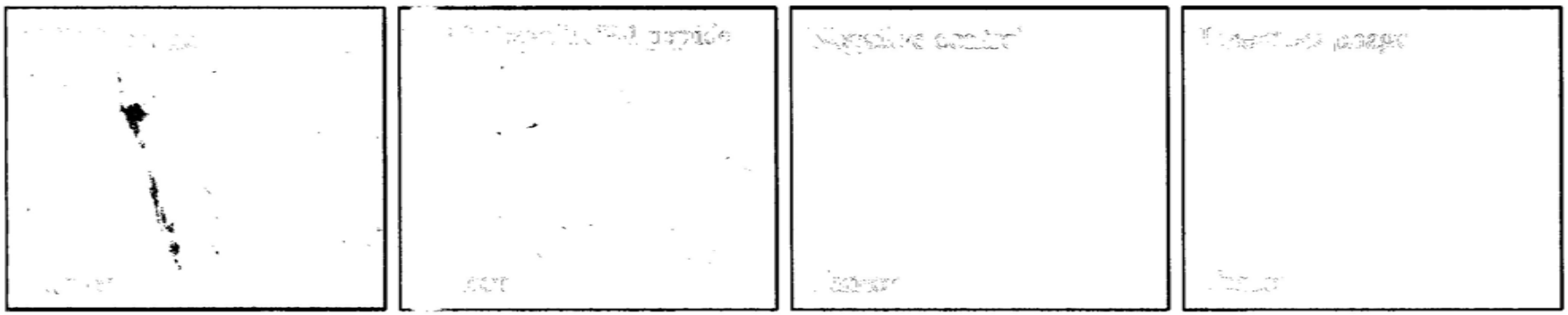

Fig. 51 TCP-1 peptide did not inhibit the localization of TCP-2 phage in the orthotopic colon tumor tissue.

TCP-1 peptide and TCP-2 phage were co-injected i.v. into the tumor-bearing mice. After 1 h of circulation, tumor tissues were collected and phage was stained in frozen sections of tumor tissues with anti-phage antibody. Positive-phage staining was observed in tumor tissues after either TCP-2 phage injection or co-injection of TCP-1 peptide and TCP-2 phage. Negative control means that sections were detected only in the presence of secondary antibody after TCP-2 phage injection. Representative images are shown. Original magnification: 400×

3.4.7 Co-localization of TCP-2 phage and the vasculature of colorectal cancer

Subsequently, we investigated whether TCP-2 phage could also target the vasculature of orthotopic colorectal cancer. Double-labeled immunofluorescent staining was used to visualize the co-localization of TCP-2 phage with phage antibody (*green*) and vasculature marker CD31 with anti-CD31 antibody (*red*). TCP-2 phage and control phage was separately injected i.v. into mice bearing orthotopic colorectal cancer and allowed to circulate for 1 h. Tumor tissues and control organs were collected and frozen sections were prepared. Co-localized staining was observed in tumor tissue sections of mice injected with TCP-2 phage when stained with phage antibody (*green*) and CD31-positive endothelial cells (*red*), but not in normal organs including heart, brain and colon (Figure 52). Control phage failed to bind to the vasculature of tumor tissues (Figure 52, bottom). This finding indicated that TCP-2 could also bind to the endothelial cells of blood vessels.

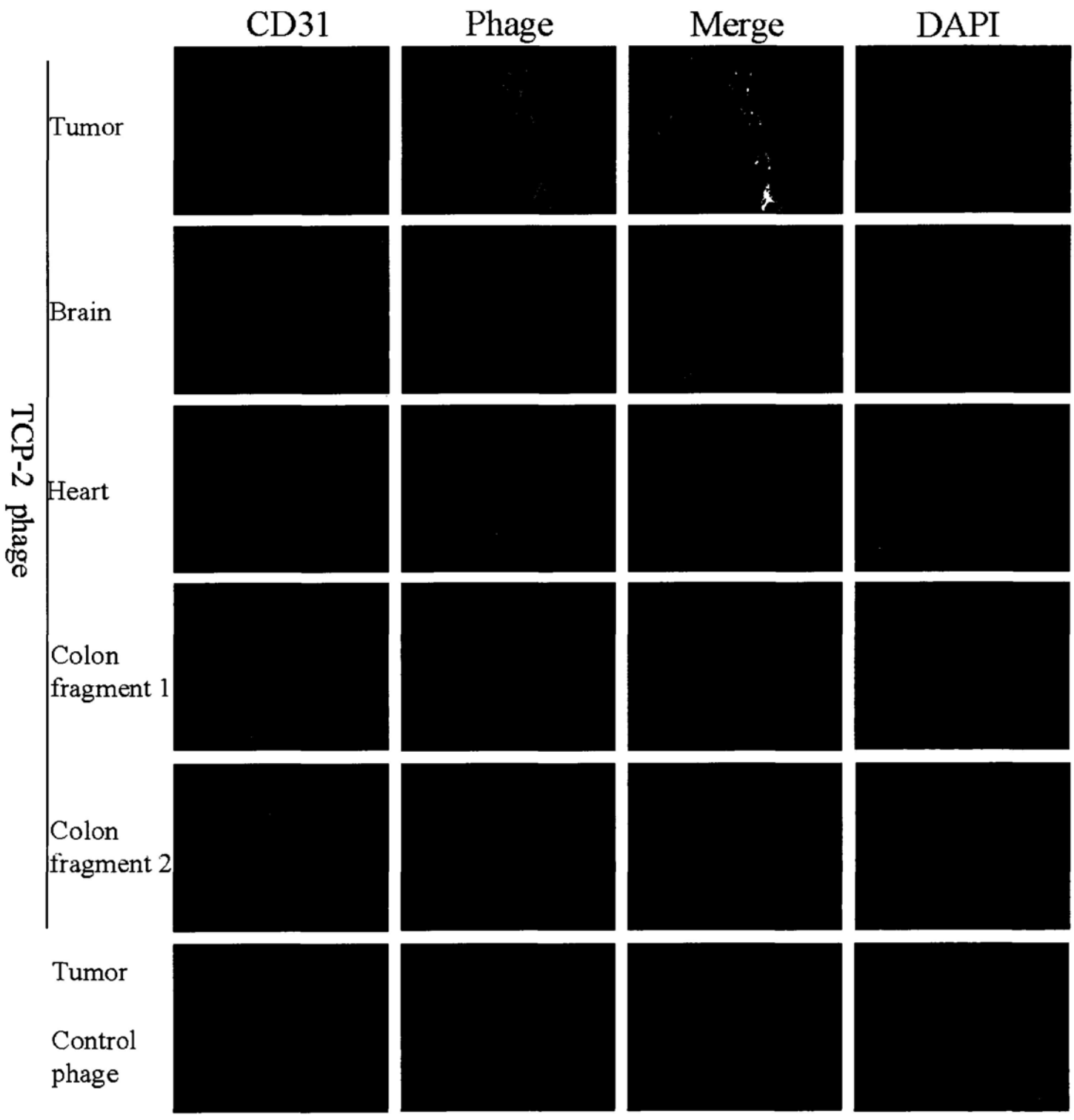
CD31
Phage
Merge
DAPI
TCP-2 phage
Tumor
Brain
Heart
Colon fragment 1
Colon fragment 2
Tumor
Control phage

Fig. 52 Co-localization of TCP-2 phage with the vasculature marker CD31 in colon cancer tissues.

Tumor-bearing mice were i.v. injected with purified TCP-2 phage. The tumor tissue and various control organs were collected for staining 1 h after the injection. The phage was stained in frozen sections with rabbit anti-phage antibody (*green*; Alexa 488). Vasculature was detected with rat anti-mouse CD31 antibody (*red*; Alexa 568). TCP-2 phage co-localized with CD31 in the tumor tissue, but not in control organs including heart, brain and normal colon tissue. Insertless control phage was not detectable in tumor tissue. Results shown are representative images. Original magnification: 400×.

3.4.8 Co-localization of synthetic FITC-labeled TCP-2 peptide and the vasculature of colorectal cancer

To confirm that the homing ability of TCP-2 phage is due to the TCP-2 peptide, we chemically synthesized the peptide conjugated with FITC and i.v. injected the conjugate into mice bearing orthotopic colorectal cancer. After 1 h of circulation, various tissues were removed and prepared for frozen sections. Blood vessels were stained by CD31 antibody (*red*). FITC-labeled TCP-2 peptide also accumulated in the tumor tissues. It was found to co-localize with CD31-positive endothelial cells (Figure 53). It was not detectable in control organs (Figure 53). FITC-labeled control peptide was not observed in the tumor tissues after injection (Figure 53).

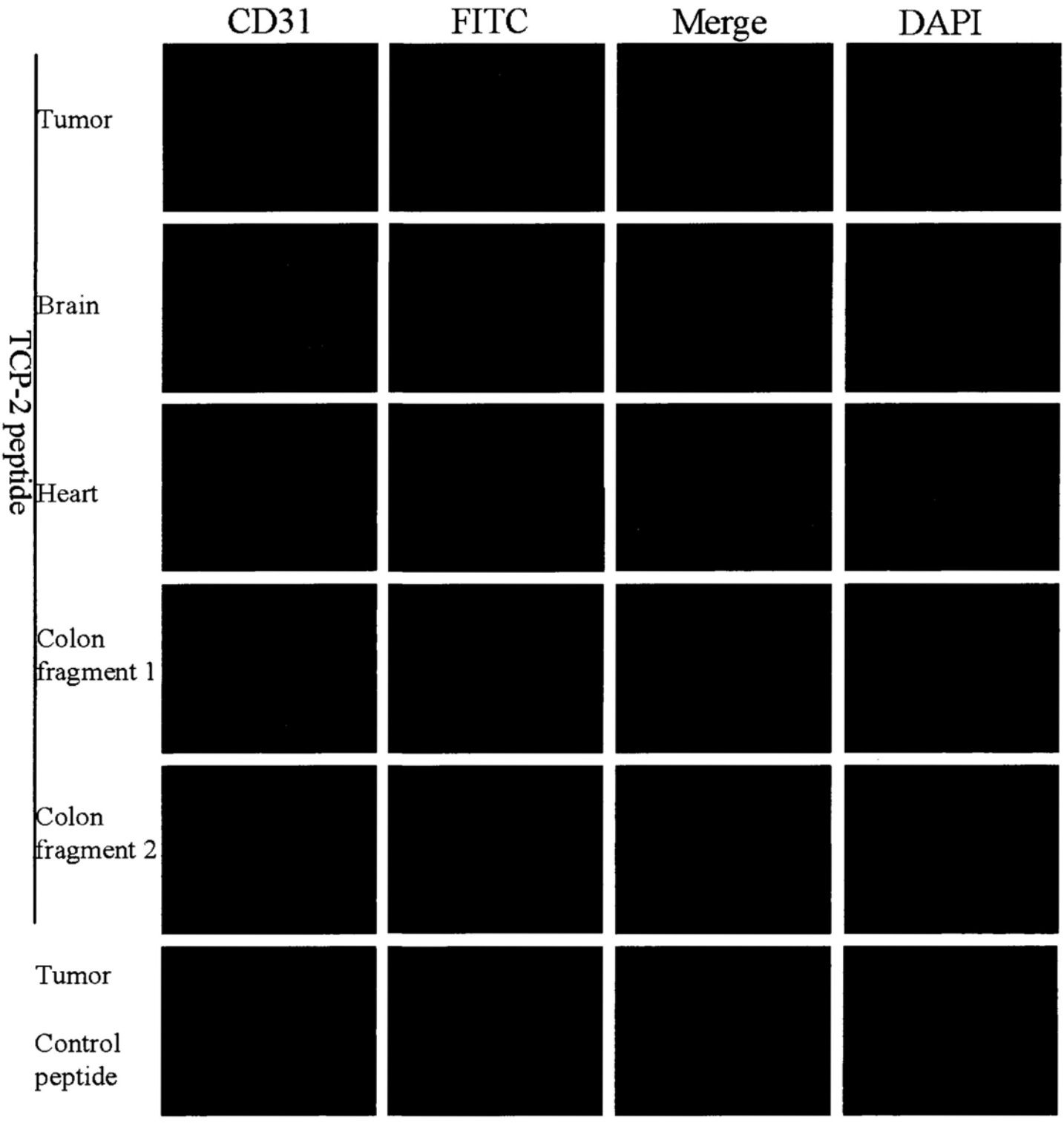
CD31
FITC
Merge
DAPI
TCP-2 peptide
Tumor
Brain
Heart
Colon fragment 1
Colon fragment 2
Tumor
Control peptide

Fig. 53 Co-localization of FITC-labeled TCP-2 with the vascular marker in the tumor tissues.

FITC-labeled peptides were i.v. injected into mice bearing tumors, the mice were sacrificed 1 h later, and the peptide localization was detected in the various tissue sections. FITC-labeled TCP-2 co-localized with CD31 in the vasculature of tumor tissues but not in control organs including heart, brain and normal colon tissues. FTIC-labeled irrelevant peptide did not recognize the blood vessels of tumor tissue. Results shown are representative images. Original magnification: 400×.

3.4.9 Binding of TCP-2 in human colorectal cancer specimens

Next, we investigated whether the TCP-2 peptide also recognizes the vasculature of human colorectal cancer samples by using peptide overlay assay of tissue sections. Sections from both colorectal cancer tissues and normal colorectal tissues were incubated with an anti-human CD31 antibody (*red*) for staining blood vessels. Overlay assay showed that FITC-labeled TCP-2 peptide interacted with blood vessels of cancer tissues but not to the vasculature of normal colorectal tissues (Figure 54). FITC-labeled control peptide did not recognize the blood vessels of either cancer or normal colon tissues (Figure 54). Two of the five patients with colorectal adenocarcinomas showed obviously positive staining by the TCP-2 peptide.

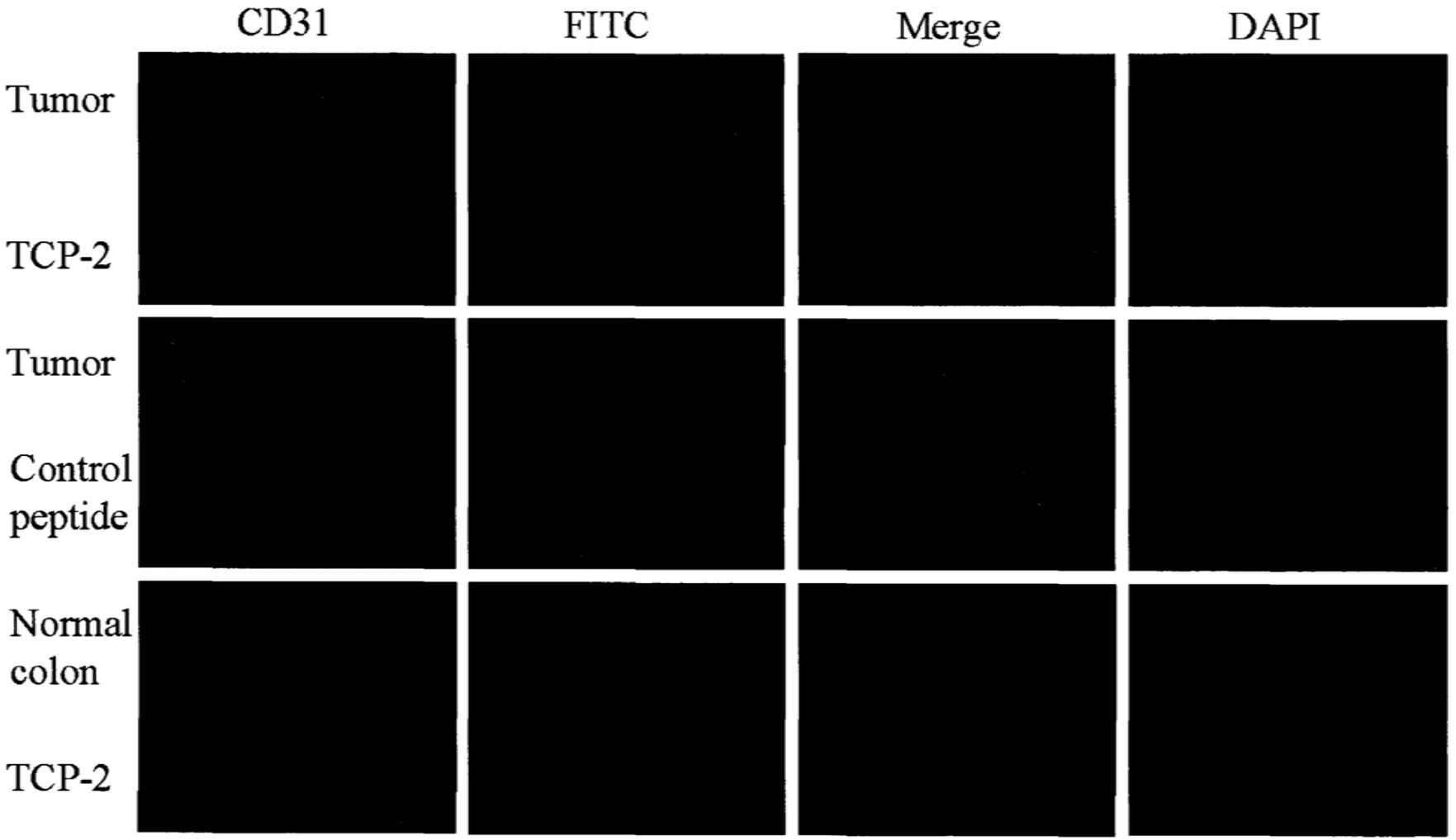
CD31
FITC
Merge
DAPI
Tumor
TCP-2
Tumor
Control peptide
Normal colon
TCP-2

Fig. 54 FITC-labeled TCP-2 recognized blood vessels of human colorectal cancer.

FITC-labeled TCP-2 or irrelevant peptide was incubated with tissue sections of colorectal cancer specimens and normal colon control. Mouse anti-human CD31 antibody was used as a marker for tissue blood vessels. The targeting peptide specifically bound to the vasculature of cancer tissues but not to normal colon tissues. Results shown are representative images. Original magnification: 400×.

3.4.10 Application of FITC-labeled TCP-2 in imaging detection

To examine whether FITC-labeled TCP-2 accumulated in the tumor tissues could be visualized at the organ level, tumor-bearing mice were injected i.v. with FITC-labeled TCP-2, FITC-labeled control peptide or PBS alone. Whole tissues from these mice were examined under blue light 20 h after injection. Results disclosed relatively strong fluorescent signal in tumors from the mice injected with TCP-2 (Figure 55), whereas no signal was observed in the tumors from the FITC-labeled control peptide- or PBS-injected mice (Figure 55). We also detected no specific fluorescent signal in other control tissues either with the peptide or PBS alone (Figure 55).

Histological analysis for these tissues revealed that TCP-2 peptide fluorescence remained in the vasculature of tumor tissues but not in the control organs (Figure 56). FITC-labeled control peptide was not detectable in the tumor tissues (Figure 56, bottom).

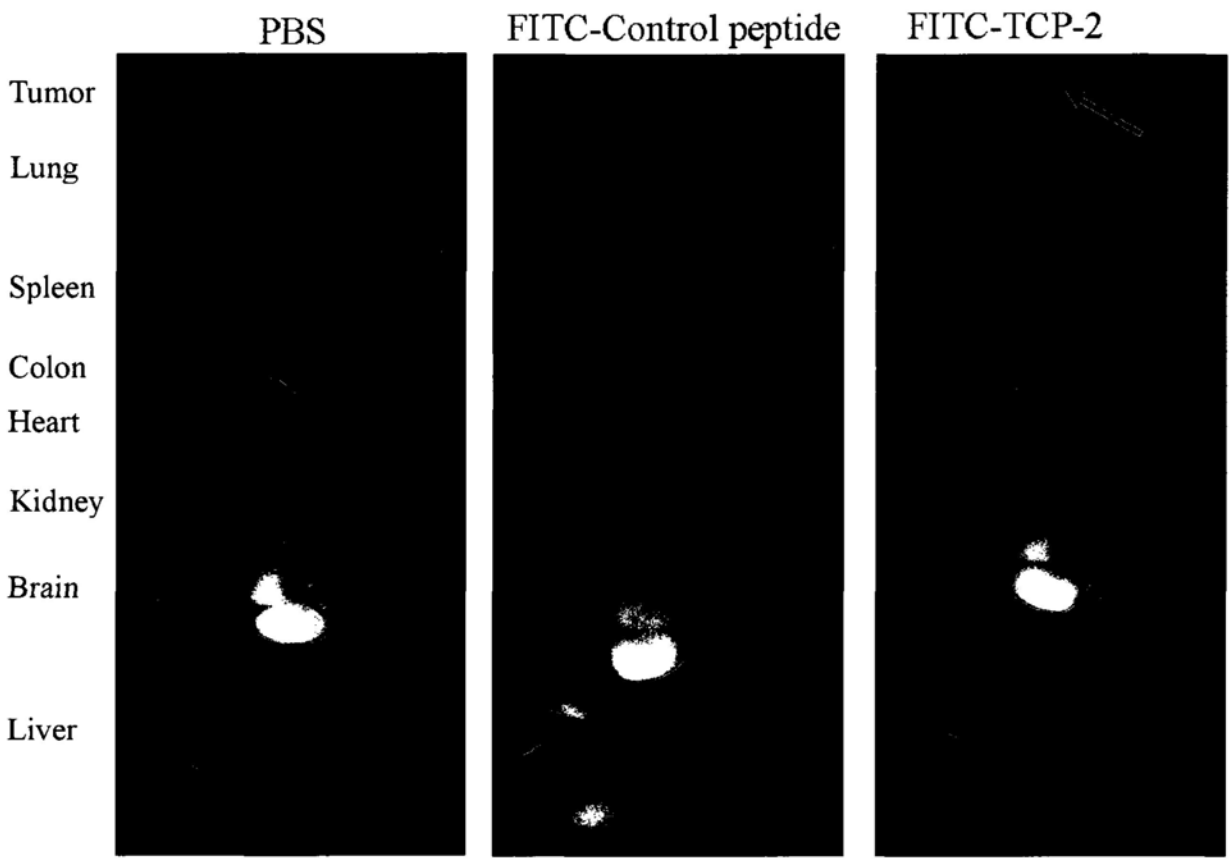

Fig. 55 Imaging detection of colorectal cancer tissues with FITC-labeled TCP-2. Mice bearing orthotopic colorectal cancer were i.v. injected with 500 nmol of FITC-labeled TCP-2, control peptide or PBS. After 20 h, the mice were perfused with PBS. The tumors and various organs were macroscopically examined for fluorescence under blue light. FITC-labeled TCP-2 produced fluorescence in the excised tumors (shown by a arrow) but not in control organs. FITC-labeled control peptide or PBS conveyed no fluorescence to the tumors. Pictures shown are representative images. Original magnification: 400×.

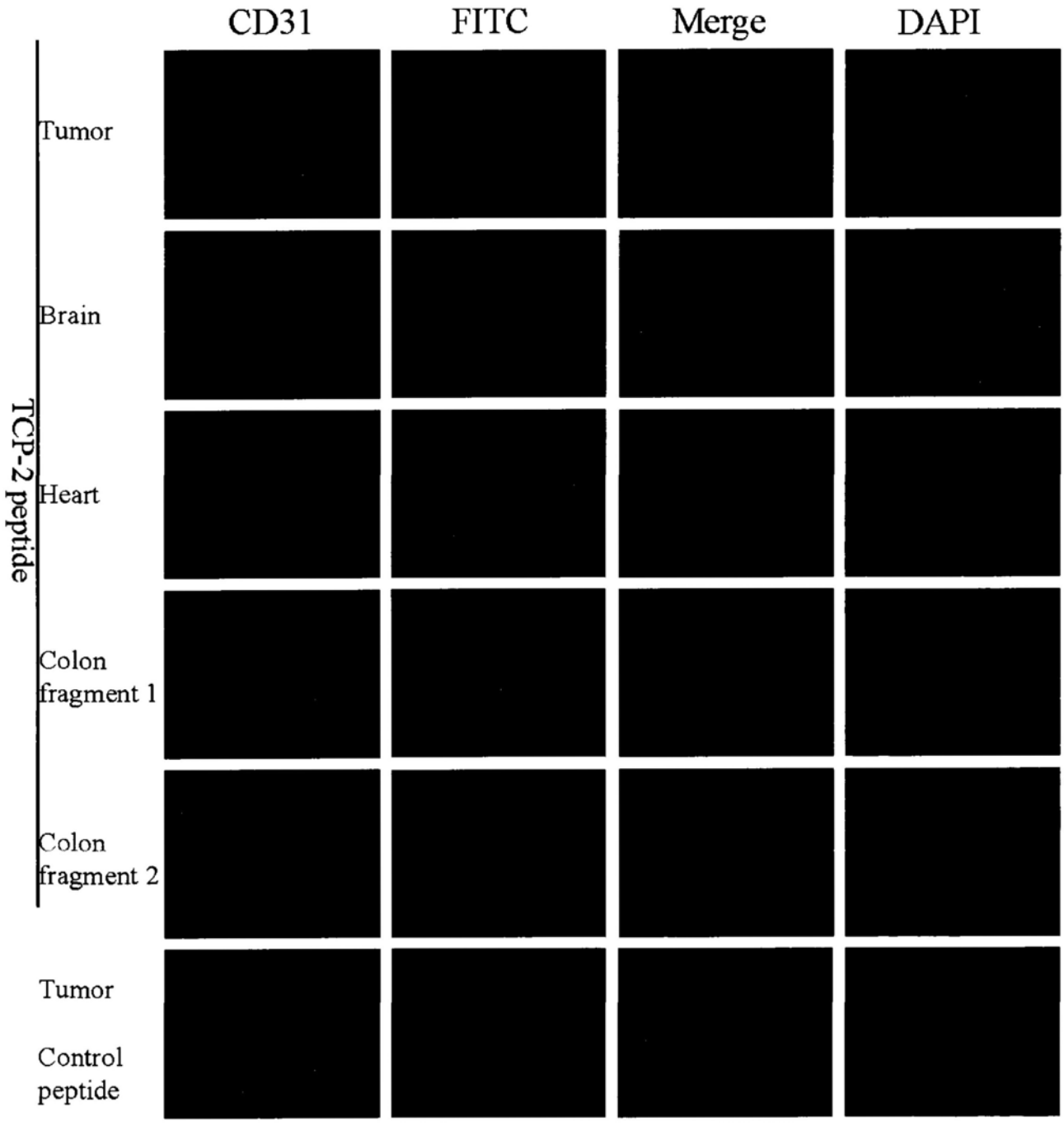
CD31
FITC
Merge
DAPI
TCP-2 peptide
Tumor
Brain
Heart
Colon fragment 1
Colon fragment 2
Tumor
Control peptide

Fig. 56 Histological examination of various tissues 20 h after FITC-labeled TCP-2 injection.

Mice bearing orthotopic colorectal cancer were i.v. injected with 500 nmol of FITC-labeled TCP-2 or control peptide as shown in Fig. 55. After 20 h of circulation, various tissues were removed, and frozen sections were prepared and examined microscopically. FITC signal could be observed in the vasculature of tumor tissues of mice injected i.v. with FITC-labeled TCP-2 but not in the control organs such as heart, brain and normal colon tissues. FITC-labeled control peptide was not detectable in the vasculature of tumor tissues after peptide injection. Representative results are shown. Original magnification: 400×.

3.4.11 Preliminary Discussion

In this study, we identified the second peptide TCP-2 that could specifically bind to both tumor blood vessels in the orthotopic colon cancer model and the blood vessels of human colorectal cancer tissues (Figures 46, 49, 52, 53 and 54). Further, we found that TCP-2 exhibited the homing ability only to the vasculature of orthotopic colorectal cancer, but not to the blood vessels of subcutaneous colorectal cancer or lung metastatic tumors of colorectal cancer (Figures 47 and 48), suggesting the binding site of TCP-2 also is only expressed in the blood vessels of orthotopic colorectal cancer in a site-specific manner. It is suggested that the tumor microenvironment might be an important factor which could influence the expression of the binding site at the tumor blood vessels.

On the other hand, our findings also indicated that both TCP-1 and TCP-2 phages are able to precisely home to orthotopic tumor tissue blood vessels but at different binding sites. In our study, we found that TCP-1 peptide could not inhibit the localization and distribution of TCP-2 phage when they were co-injected into tumor-bearing mice (Figure 51), which implies that these two peptides target the different molecular markers on tumor blood vessels. Several papers from different laboratories reported that more than one peptide was isolated and identified in their *in vivo* phage biopanning against other tumor models, and further showed that these peptides bound to different target molecules on tumor vasculature (Chang *et al.*, 2009a; Joyce *et al.*, 2003; Rajput *et al.*, 2008). These data suggest that multiple markers discriminated from the vasculature of normal organs are specifically expressed on the blood vessels of tumor tissues.

Peptides specifically targeting tumor vasculature provide new opportunities for targeted delivery of therapeutics and imaging agents. We found that tumor tissues of mice injected FITC-labeled TCP-2 peptide produced detectable fluorescent signal under blue light, but no signal was detected from either the control organs or organs from the control groups (Figure 55). Histological analysis revealed that FITC-labeled TCP-2 peptide was still identified in the vasculature of tumor tissues but not the control organs after 20 h of injection (Figure 56). This would greatly prolong the anti-cancer action of any chemotherapeutic agents if TCP-2 is used as a drug carrier targeting the tumor blood vessels in colorectal cancer. All these data indicate that TCP-2 has a potential to be used as a carrier for delivery of imaging agents and anti-cancer drugs in the diagnosis and therapy for colorectal cancer.

Chapter 4

Conclusions and Perspectives

Phage display technology provides a rapid, simple, even high-throughput method to isolate peptides bind specifically to predetermined molecular targets. Phage display has become an important platform in molecular biology and is extensively applied in multiple research fields including prediction of protein-protein interactions as well as protein-binding domain, and mapping antibody functional epitopes, etc (Sidhu, 2000). *In vivo* phage display is considered as one of important landmarks in the phage display development. Molecular differences in the vasculature of individual normal and diseased tissues have been disclosed by *in vivo* phage display library biopanning to a great extent, which suggests that endothelial cells express a set of distinct molecular markers depending on which tissue it has been derived from (George *et al.*, 2003; Ruoslahti, 2004). Neovasculature formation is essential for the continued growth of solid tumors. The endothelial cells in this neovasculature often express some molecular markers that do not exist or are lowly expressed in normal blood vessels (Ruoslahti, 2004). The vasculature is becoming an attractive target because these markers are specific for tumor blood vessels, and targeted vascular agents also provide new opportunities for drug design and targeted therapy. *In vivo* phage display has been widely used to isolate peptides targeting tumor vasculature and these peptides are becoming good drug candidates as carriers of therapeutic and diagnostic agents (Hajitou *et al.*, 2006; Ruoslahti, 2004). In our study, our aims are to isolate specific peptides targeting the vasculature of colorectal cancer tissues and to couple these peptides with fluorescein or pro-apoptotic peptide for imaging detection or targeted therapy of colorectal cancer in an orthotopic cancer model.

We established an orthotopic colorectal cancer model in normal BALB/c mice

through DSS treatment to induce ulcerative colitis (to facilitate cancer cell growth in the colon) and colon cancer cells (colon 26 cells) implantation. This orthotopic tumor model mimics the developmental characters of corresponding human tumors in the colon to some extent because the tumor microenvironment would highly influence tumor progression. Interactions between tumor microenvironment and tumor mass affect tumor cell expression profiles. These include the levels of different growth factors and cytokines, secretion of some factors related to tumor angiogenesis and metastatic behavior (Vignjevic *et al.*, 2007). In our study, orthotopic tumor mass formed within 2-3 weeks after cancer cell implantation. It grew in the distal colonic and rectal lumen similar to human colorectal cancer. We believe that the molecular markers expressed on the surface of tumor endothelial cells in the current model might greatly reflect and mimic the development of markers found on the blood vessels of human colorectal cancer. Therefore, we subsequently screened the phage library against the current orthotopic tumor model to isolate specific peptides homing to tumor blood vessels.

After four-round biopanning selections, a phage pool was obtained which showed a 3-fold enrichment in the tumor tissues than that in the first round of screening. Eighty phage clones were randomly picked and inserted fragments of these clones were sequenced. We totally obtained 58 peptides after translation of these inserted DNA. Four peptides termed TCP-1, -2, -3, -4 were enriched more than once which were more than the other peptide sequences. These four peptides were further analyzed. *In vivo* targeting assay suggested that the four phage displayed TCP-1, -2, -3, -4 peptides exhibited a homing ability to orthotopic colorectal cancer tissues to different extents. It was noted that the homing ability of TCP-1 and TCP-2 phage to the tumor

tissues was obviously highest among the four phage clones and they were chosen for further evaluation in our study.

The data described above demonstrate that *in vivo* phage display is an effective technology to biopan and isolate the peptides specifically targeting tumor tissues. Multiple peptides were shown to be enriched after several rounds of selections. The whole process was performed in a relatively short period of time for about 1-2 weeks. *In vivo* phage display also provides us an excellent opportunity and possibility to rapidly isolate and identify peptides targeting various tissues, in particular tumor blood vessels.

We further investigated the homing ability of TCP-1 phage in various animal models. First, TCP-1 phage markedly targeted the orthotopic colorectal cancer tissues, and the homing property could be inhibited competitively by TCP-1 peptide. However we found that TCP-1 phage did not bind to subcutaneous colorectal cancer tissues induced by the same cancer cell line (colon 26) as in the orthotopic cancer model. Moreover, the homing ability of TCP-1 phage was also not observed in lung metastatic tumors induced by colon 26. At the same time, immunohistochemistry staining disclosed that TCP-1 phage or synthetic TCP-1 peptide was co-localized with the tumor endothelial cells expressing CD31. Taken together, these data implicate that TCP-1 peptide seems to only bind to the vasculature of *in situ* colorectal cancer tissues. Moreover the tumor microenvironment might be an important factor that affects the expression profile of surface markers on the endothelial cells of blood vessels more than that by cancer cells themselves. This conclusion is verified by our findings that TCP-1 was selectively bound to the

orthotopic tumors in the colon but not to the distant organs grown in the skin and lung tissues.

Furthermore we found that TCP-1 peptide could also home to the vasculature of orthotopic gastric cancer but not to the subcutaneous gastric cancer induced by the same poorly differentiated gastric cancer cell line MKN 45. All these findings indicate that TCP-1 peptide seems to specifically bind the vasculature of orthotopic GI cancers to a great extent although this needs to be further examined in other orthotopic tumor animal models induced by different GI cancer cell lines. The data also suggest that the binding site(s) of TCP-1 peptide might be expressed universally and specifically on the endothelial cells of orthotopic GI cancers. All of these hypotheses described above need further investigation. They are indeed our future directions in research.

Similarly, the homing ability of TCP-2 phage was also observed in the orthotopic colorectal cancer but not in the subcutaneous colorectal cancer and lung metastatic tumor of colorectal cancer induced by colon 26. Although both TCP-1 and TCP-2 peptides were co-localized in the vasculature of tumor tissues, it seems that they do not share the same binding site at the vasculature of colon cancer. It was evidenced by the fact that the binding ability of either peptide at the tumor blood vessels was not mutually affected when co-injected with both TCP-1 and TCP-2. This result suggests that there might be two separate binding sites with different molecular make-up expressed on the tumor blood vessels for these peptides.

It is estimated that inflammatory responses, especially during chronic inflammation

are associated with the pathogenesis of approximately 15% to 20% of human tumors, including colorectal, gastric, liver and bladder cancers (Srikrishna *et al.*, 2009). The association between chronic inflammatory bowel diseases (IBD) and the increased risk of colorectal cancer has been elucidated by a substantial body of experimental and epidemiological evidences (Kraus *et al.*, 2009). Therefore, we investigated whether TCP-1 peptide was able to bind to the vasculature of acute and chronic colitis tissues, in order to demonstrate any evolutional changes in colon tissues during the process of cancer development. The data disclosed that the homing ability of TCP-1 peptide was negative in the tissues of two colitis models, which demonstrate that the binding site of TCP-1 peptide might not be expressed on the surface of endothelial cells of colitis tissues. This TCP-1 binding site would only be expressed during malignant changes in the colon tissues. This unique property may be useful for the diagnosis of colorectal cancer but not for colitis.

Indeed a potential application of peptides targeting tumor vasculature is used to deliver contrast probes and toxic payloads to tumor tissues for specific diagnosis and targeted therapy. Therefore, we firstly investigated whether TCP-1 and TCP-2 peptides conjugated with FITC can be employed to specifically detect the tumor tissue in the whole organ level. Results showed that FITC-labeled TCP-1 or TCP-2 peptides can produce relatively strong fluorescent signal in tumor tissues as compared to control organs or control tissues injected with FITC-labeled control peptide or PBS alone. On the other hand, we also found that these two peptides can specifically recognize the vasculature of human colorectal cancer tissues. Taken together, these findings reveal that TCP-1 and TCP-2 peptides are potentially useful in the imaging detection of human colorectal cancer if these results can be

reproduced in preclinical or clinical settings. In this regard, live *in vivo* imaging mediated by the two peptides is the ultimate objective of our study. Under these circumstances, more sensitive agents and special instruments are needed, for example a more suitable *in vivo* tumor imaging detection is to label the peptides with radioactive agents or nanoparticle. At the same time, positron emission tomography (PET) or fluorescence confocal microendocopy is also necessary for *in vivo* imaging in live animal models.

Likewise, another question attracted our attention is whether colorectal cancer cell lines also express the binding site of TCP-1 peptide like tumor blood vessels because several markers found firstly in tumor endothelial cells had subsequently been verified their existence in the tumor cells. Therefore, we performed the binding assay between TCP-1 phage and four colorectal cancer cell lines (Colon 26, SW1116, HT-29, CaCo-2). The data indicate that TCP-1 phage exhibit a binding activity to Colon 26 and SW1116 but not to HT-29 and CaCo2. Further study also found that TCP-1 peptide can mediate the internalization of phage particles into Colon 26 and SW1116. Moreover, TCP-1 peptide could also carry a pro-apoptotic peptide $_{D}(KLAKLAK)_2$ into these two cell lines and highly enhance its pro-apoptotic effect. Collectively, all these results imply that the binding site of TCP-1 is also expressed in the colorectal cancer cells such as colon 26 and SW1116. Identifying the binding site of TCP-1 peptide in these cancer cells is becoming an attractive approach for further development of the peptide in cancer therapy and diagnosis in view of the difficulty in identifying the binding site at the tumor blood vessels. We expect that the molecular makeup for the binding site in the tumor blood vessels and cancer cells would be the same.

Finally, we verified that TCP-1 peptide could deliver a pro-apoptotic peptide $_{D}$(KLAKLAK)2 to tumor blood vessels and significantly increase the number of apoptotic endothelial cells when compared to the control groups. Control organs such as colon and brain hardly found any apoptotic endothelial cells. Thus, it is reasonable to believe that TCP-1 peptide is a good vector for drug delivery in the treatment of colorectal cancer. Subsequent work will be focusing on whether TCP-1 peptide can also carry other anti-cancer compounds to the tumor vasculature of colorectal or gastric cancers. In addition, the real-time monitoring of tumor growth is can be used to assess the efficacy of anti-cancer chemotherapy. Unlike the subcutaneous cancer model, it is difficult to monitor tumor growth in the orthotopic cancer models, as the tumors are growing inside the primary organ. *In vivo* bioluminescent imaging (BLI) system provides a new opportunity to monitor tumor growth, metastasis, and therapeutic responses *in vivo* through a longitudinal and real-time manner (Klerk *et al.*, 2007; Sato *et al.*, 2004). This sensitive and advanced system is based on detection of light emission from cells or tissues stably expressing luciferase reporter gene (Klerk *et al.*, 2007; Sato *et al.*, 2004). It is required for BLI system to firstly establish a cell line with a stable expression cassette composed of a bioluminescent reporter gene (such as luciferases gene) under the control of a selected gene promoter constitutively inducing the light reporter through genetic engineering method. Various tumor cell lines that stably express luciferase have been constructed and widely employed to detect multiple tumor responses through *in vivo* BLI system (Jenkins *et al.*, 2005; Klerk *et al.*, 2007; Sato *et al.*, 2004). Other ongoing work in our laboratory is to develop a new colon 26 cell line capable of constitutively expressing luciferase through a lentiviral expression system. In this regard the growth of the

orthotopic colorectal cancer can be monitored longitudinally in different time points through an *in vivo* BLI system after treatment by TCP-1 conjugates (other anti-cancer drugs).

In summary, in the present study, we isolated two peptides (TCP-1 and TCP-2) through an *in vivo* phage library biopanning against an orthotopic colorectal cancer model. The homing abilities of the two peptides were extensively tested in various models associated with colorectal cancer. Both TCP-1 and TCP-2 peptides can home to the vasculature of orthotpopic colorectal cancer tissues. Moreover, TCP-1 peptide was also verified to target the blood vessels of orthotopic gastric and colorectal cancers and also colon cancer cells. Further study disclosed that both TCP-1 and TCP-2 peptides coupled with fluorescein can specifically accumulate into tumor tissues for imaging detection. TCP-1 peptide conjugated with a pro-apoptotic peptide can remarkably increase the number of apoptotic endothelial cells in tumor tissues and colon cancer cells. They also bind to the vasculature of human colorectal cancer tissues. All these findings suggest that TCP-1 and TCP-2 peptides have a great potential as good carriers of anti-cancer drugs and imaging probes for targeted therapy and diagnosis of human colorectal cancer. Figure 57 summarizes collectively the main findings in the present study. It provides significant insights regarding the functions and applications of TCP-1 and TCP-2 peptides in cancer therapy and diagnosis. Furthermore, it also opens up several new windows for future explorations, including:

1 Identifying the binding sites of TCP-1/2 peptides,

2 Testing the homing abilities of TCP-1 peptide to other GI cancers,

3 Analyzing the binding activities between TCP-1 peptide and other GI cancer cell

lines,

4 Evaluating the interaction between TCP-1 peptide and human colorectal cancer tissues in addition to blood vessels,

5 Investigating *in vivo* tumor imaging mediated by TCP-1/2 peptides coupled with radioactive agents or nanoparticles,

6 Exploring the therapeutic potentials of TCP-1/2 peptides conjugated with other anti-cancer drugs.

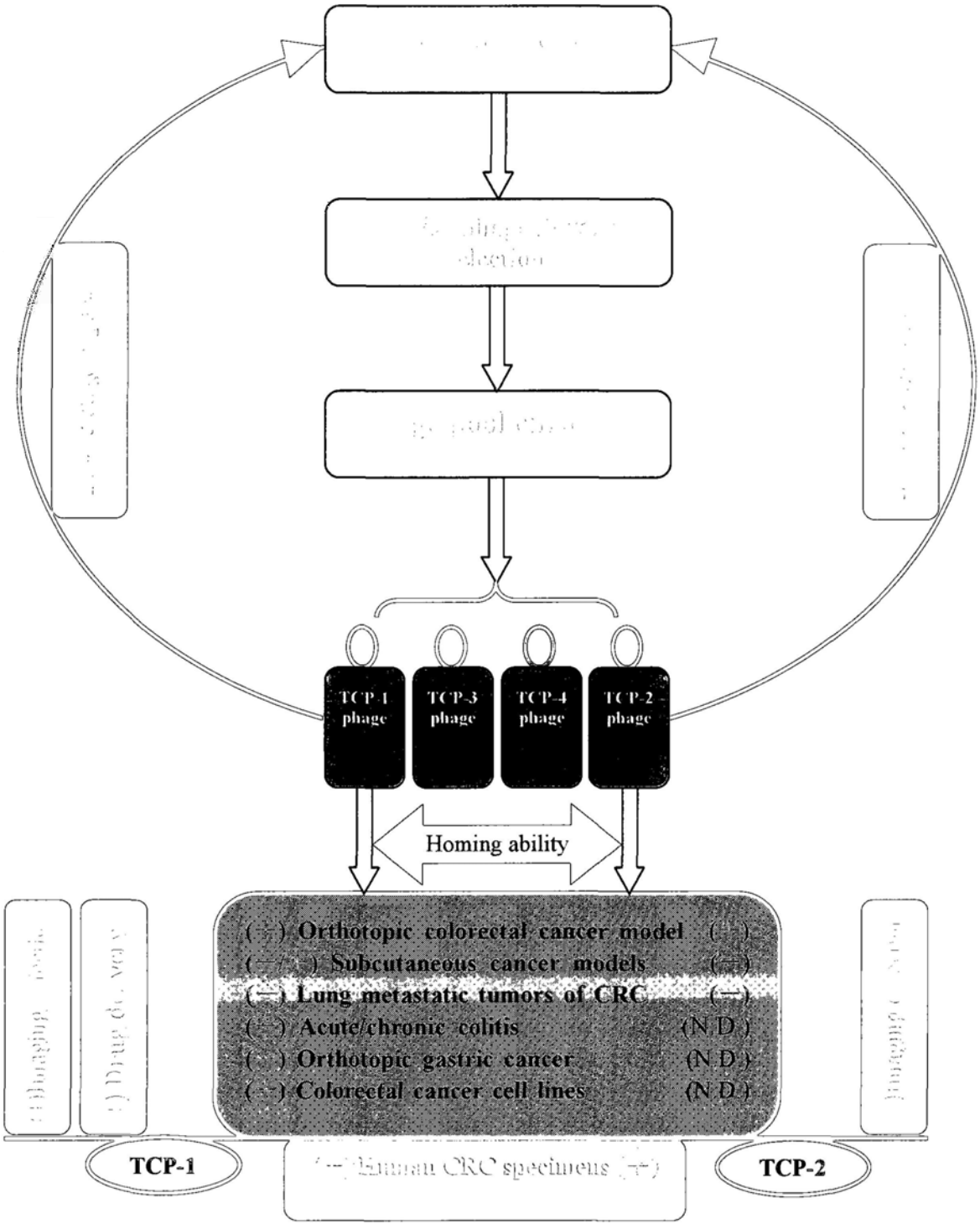

Fig. 57 Experimental procedures and main findings in the present study.

(+) positive results; (−) negative results; (N.D.): not determined. (−/+): TCP-1 peptide cannot recognize the blood vessels of various subcutaneous tumors but can bind to subcutaneous cancer tissue induced by colon 26 cells.

References

Ahlskog, J., Paganelli, G. & Neri, D. (2006). Vascular tumor targeting. Q J Nucl Med Mol Imaging, 50, 296-309.

Ahmadi, A., Polyak, S. & Draganov, P.V. (2009). Colorectal cancer surveillance in inflammatory bowel disease: the search continues. World J Gastroenterol, 15, 61-6.

Ahmed, F.E. (2004). Effect of diet, life style, and other environmental/chemopreventive factors on colorectal cancer development, and assessment of the risks. J Environ Sci Health C Environ Carcinog Ecotoxicol Rev, 22, 91-147.

Aina, O.H., Liu, R., Sutcliffe, J.L., Marik, J., Pan, C.X. & Lam, K.S. (2007). From combinatorial chemistry to cancer-targeting peptides. Mol Pharm, 4, 631-51.

Al-Sukhni, W., Aronson, M. & Gallinger, S. (2008). Hereditary colorectal cancer syndromes: familial adenomatous polyposis and lynch syndrome. Surg Clin North Am, 88, 819-44, vii.

Allegra, C. & Sargent, D.J. (2005). Adjuvant therapy for colon cancer--the pace quickens. N Engl J Med, 352, 2746-8.

Andre, T., Boni, C., Mounedji-Boudiaf, L., Navarro, M., Tabernero, J., Hickish, T., Topham, C., Zaninelli, M., Clingan, P., Bridgewater, J., Tabah-Fisch, I. & de Gramont, A. (2004). Oxaliplatin, fluorouracil, and leucovorin as adjuvant treatment for colon cancer. N Engl J Med, 350, 2343-51.

Arap, W., Haedicke, W., Bernasconi, M., Kain, R., Rajotte, D., Krajewski, S.,

Ellerby, H.M., Bredesen, D.E., Pasqualini, R. & Ruoslahti, E. (2002a). Targeting the prostate for destruction through a vascular address. Proc Natl Acad Sci U S A, 99, 1527-31.

Arap, W., Kolonin, M.G., Trepel, M., Lahdenranta, J., Cardo-Vila, M., Giordano, R.J., Mintz, P.J., Ardelt, P.U., Yao, V.J., Vidal, C.I., Chen, L., Flamm, A., Valtanen, H., Weavind, L.M., Hicks, M.E., Pollock, R.E., Botz, G.H., Bucana, C.D., Koivunen, E., Cahill, D., Troncoso, P., Baggerly, K.A., Pentz, R.D., Do, K.A., Logothetis, C.J. & Pasqualini, R. (2002b). Steps toward mapping the human vasculature by phage display. Nat Med, 8, 121-7.

Arap, W., Pasqualini, R. & Ruoslahti, E. (1998). Cancer treatment by targeted drug delivery to tumor vasculature in a mouse model. Science, 279, 377-80.

Ariztia, E.V., Lee, C.J., Gogoi, R. & Fishman, D.A. (2006). The tumor microenvironment: key to early detection. Crit Rev Clin Lab Sci, 43, 393-425.

Armstrong, B. & Doll, R. (1975). Environmental factors and cancer incidence and mortality in different countries, with special reference to dietary practices. Int J Cancer, 15, 617-31.

Aust, D.E., Terdiman, J.P., Willenbucher, R.F., Chang, C.G., Molinaro-Clark, A., Baretton, G.B., Loehrs, U. & Waldman, F.M. (2002). The APC/beta-catenin pathway in ulcerative colitis-related colorectal carcinomas: a mutational analysis. Cancer, 94, 1421-7.

Bapat, B.V., Madlensky, L., Temple, L.K., Hiruki, T., Redston, M., Baron, D.L., Xia, L., Marcus, V.A., Soravia, C., Mitri, A., Shen, W., Gryfe, R., Berk, T., Chodirker, B.N., Cohen, Z. & Gallinger, S. (1999). Family history characteristics, tumor

microsatellite instability and germline MSH2 and MLH1 mutations in hereditary colorectal cancer. Hum Genet, 104, 167-76.

Boland, C.R., Koi, M., Chang, D.K. & Carethers, J.M. (2008). The biochemical basis of microsatellite instability and abnormal immunohistochemistry and clinical behavior in Lynch syndrome: from bench to bedside. Fam Cancer, 7, 41-52.

Boocock, C.A., Charnock-Jones, D.S., Sharkey, A.M., McLaren, J., Barker, P.J., Wright, K.A., Twentyman, P.R. & Smith, S.K. (1995). Expression of vascular endothelial growth factor and its receptors flt and KDR in ovarian carcinoma. J Natl Cancer Inst, 87, 506-16.

Borghouts, C., Kunz, C. & Groner, B. (2005). Current strategies for the development of peptide-based anti-cancer therapeutics. J Pept Sci, 11, 713-26.

Boyle, P. & Langman, J.S. (2000). ABC of colorectal cancer: Epidemiology. Bmj, 321, 805-8.

Carmeliet, P. (2003). Angiogenesis in health and disease. Nat Med, 9, 653-60.

Carmichael, J., Popiela, T., Radstone, D., Falk, S., Borner, M., Oza, A., Skovsgaard, T., Munier, S. & Martin, C. (2002). Randomized comparative study of tegafur/uracil and oral leucovorin versus parenteral fluorouracil and leucovorin in patients with previously untreated metastatic colorectal cancer. J Clin Oncol, 20, 3617-27.

Carter, M.J., Lobo, A.J. & Travis, S.P. (2004). Guidelines for the management of inflammatory bowel disease in adults. Gut, 53 Suppl 5, V1-16.

Cassidy, J., Twelves, C., Van Cutsem, E., Hoff, P., Bajetta, E., Boyer, M., Bugat, R., Burger, U., Garin, A., Graeven, U., McKendric, J., Maroun, J., Marshall, J.,

Osterwalder, B., Perez-Manga, G., Rosso, R., Rougier, P. & Schilsky, R.L. (2002). First-line oral capecitabine therapy in metastatic colorectal cancer: a favorable safety profile compared with intravenous 5-fluorouracil/leucovorin. Ann Oncol, 13, 566-75.

Chang, D.K., Chiu, C.Y., Kuo, S.Y., Lin, W.C., Lo, A., Wang, Y.P., Li, P.C. & Wu, H.C. (2009a). Antiangiogenic targeting liposomes increase therapeutic efficacy for solid tumors. J Biol Chem, 284, 12905-16.

Chang, D.K., Lin, C.T., Wu, C.H. & Wu, H.C. (2009b). A novel peptide enhances therapeutic efficacy of liposomal anti-cancer drugs in mice models of human lung cancer. PLoS One, 4, e4171.

Chao, A., Thun, M.J., Jacobs, E.J., Henley, S.J., Rodriguez, C. & Calle, E.E. (2000). Cigarette smoking and colorectal cancer mortality in the cancer prevention study II. J Natl Cancer Inst, 92, 1888-96.

Chen, L., Wang, Y., Liu, X., Dou, S., Liu, G., Hnatowich, D.J. & Rusckowski, M. (2008). A new TAG-72 cancer marker peptide identified by phage display. Cancer Lett, 272, 122-32.

Choo, M.K., Sakurai, H., Koizumi, K. & Saiki, I. (2005). Stimulation of cultured colon 26 cells with TNF-alpha promotes lung metastasis through the extracellular signal-regulated kinase pathway. Cancer Lett, 230, 47-56.

Choo, M.K., Sakurai, H., Koizumi, K. & Saiki, I. (2006). TAK1-mediated stress signaling pathways are essential for TNF-alpha-promoted pulmonary metastasis of murine colon cancer cells. Int J Cancer, 118, 2758-64.

Christianson, D.R., Ozawa, M.G., Pasqualini, R. & Arap, W. (2007). Techniques to

decipher molecular diversity by phage display. Methods Mol Biol, 357, 385-406.

Chung, K.Y., Shia, J., Kemeny, N.E., Shah, M., Schwartz, G.K., Tse, A., Hamilton, A., Pan, D., Schrag, D., Schwartz, L., Klimstra, D.S., Fridman, D., Kelsen, D.P. & Saltz, L.B. (2005). Cetuximab shows activity in colorectal cancer patients with tumors that do not express the epidermal growth factor receptor by immunohistochemistry. J Clin Oncol, 23, 1803-10.

Ciardiello, F. & Tortora, G. (2001). A novel approach in the treatment of cancer: targeting the epidermal growth factor receptor. Clin Cancer Res, 7, 2958-70.

Cummings, J.H. & Bingham, S.A. (1998). Diet and the prevention of cancer. Bmj, 317, 1636-40.

Cunningham, D., Humblet, Y., Siena, S., Khayat, D., Bleiberg, H., Santoro, A., Bets, D., Mueser, M., Harstrick, A., Verslype, C., Chau, I. & Van Cutsem, E. (2004). Cetuximab monotherapy and cetuximab plus irinotecan in irinotecan-refractory metastatic colorectal cancer. N Engl J Med, 351, 337-45.

Curnis, F., Gasparri, A., Sacchi, A., Longhi, R. & Corti, A. (2004). Coupling tumor necrosis factor-alpha with alphaV integrin ligands improves its antineoplastic activity. Cancer Res, 64, 565-71.

Dai, Z., Xu, Y.C. & Niu, L. (2007). Obesity and colorectal cancer risk: a meta-analysis of cohort studies. World J Gastroenterol, 13, 4199-206.

de Gramont, A., Bosset, J.F., Milan, C., Rougier, P., Bouche, O., Etienne, P.L., Morvan, F., Louvet, C., Guillot, T., Francois, E. & Bedenne, L. (1997). Randomized trial comparing monthly low-dose leucovorin and fluorouracil bolus with bimonthly

high-dose leucovorin and fluorouracil bolus plus continuous infusion for advanced colorectal cancer: a French intergroup study. J Clin Oncol, 15, 808-15.

de Gramont, A., Figer, A., Seymour, M., Homerin, M., Hmissi, A., Cassidy, J., Boni, C., Cortes-Funes, H., Cervantes, A., Freyer, G., Papamichael, D., Le Bail, N., Louvet, C., Hendler, D., de Braud, F., Wilson, C., Morvan, F. & Bonetti, A. (2000). Leucovorin and fluorouracil with or without oxaliplatin as first-line treatment in advanced colorectal cancer. J Clin Oncol, 18, 2938-47.

Decuzzi, P., Pasqualini, R., Arap, W. & Ferrari, M. (2009). Intravascular delivery of particulate systems: does geometry really matter? Pharm Res, 26, 235-43.

Desai, T.K. & Barkel, D. (2008). Syndromic colon cancer: lynch syndrome and familial adenomatous polyposis. Gastroenterol Clin North Am, 37, 47-72, vi.

Douillard, J.Y., Hoff, P.M., Skillings, J.R., Eisenberg, P., Davidson, N., Harper, P., Vincent, M.D., Lembersky, B.C., Thompson, S., Maniero, A. & Benner, S.E. (2002). Multicenter phase III study of uracil/tegafur and oral leucovorin versus fluorouracil and leucovorin in patients with previously untreated metastatic colorectal cancer. J Clin Oncol, 20, 3605-16.

Duerr, D.M., White, S.J. & Schluesener, H.J. (2004). Identification of peptide sequences that induce the transport of phage across the gastrointestinal mucosal barrier. J Virol Methods, 116, 177-80.

Eaden, J.A., Abrams, K.R. & Mayberry, J.F. (2001). The risk of colorectal cancer in ulcerative colitis: a meta-analysis. Gut, 48, 526-35.

Eichhorn, M.E., Kleespies, A., Angele, M.K., Jauch, K.W. & Bruns, C.J. (2007).

Angiogenesis in cancer: molecular mechanisms, clinical impact. Langenbecks Arch Surg, 392, 371-9.

Ellerby, H.M., Arap, W., Ellerby, L.M., Kain, R., Andrusiak, R., Rio, G.D., Krajewski, S., Lombardo, C.R., Rao, R., Ruoslahti, E., Bredesen, D.E. & Pasqualini, R. (1999). Anti-cancer activity of targeted pro-apoptotic peptides. Nat Med, 5, 1032-8.

Enback, J. & Laakkonen, P. (2007). Tumour-homing peptides: tools for targeting, imaging and destruction. Biochem Soc Trans, 35, 780-3.

Fernando, N.H. & Hurwitz, H.I. (2004). Targeted therapy of colorectal cancer: clinical experience with bevacizumab. Oncologist, 9 Suppl 1, 11-8.

Ferrara, N. (2002). Role of vascular endothelial growth factor in physiologic and pathologic angiogenesis: therapeutic implications. Semin Oncol, 29, 10-4.

Fidler, I.J. (2001). Angiogenic heterogeneity: regulation of neoplastic angiogenesis by the organ microenvironment. J Natl Cancer Inst, 93, 1040-1.

Fukata, M., Michelsen, K.S., Eri, R., Thomas, L.S., Hu, B., Lukasek, K., Nast, C.C., Lechago, J., Xu, R., Naiki, Y., Soliman, A., Arditi, M. & Abreu, M.T. (2005). Toll-like receptor-4 is required for intestinal response to epithelial injury and limiting bacterial translocation in a murine model of acute colitis. Am J Physiol Gastrointest Liver Physiol, 288, G1055-65.

Fukumura, D. & Jain, R.K. (2007). Tumor microvasculature and microenvironment: targets for anti-angiogenesis and normalization. Microvasc Res, 74, 72-84.

Galizia, G., Lieto, E., Ferraraccio, F., Orditura, M., De Vita, F., Castellano, P.,

Imperatore, V., Romano, C., Ciardiello, F., Agostini, B. & Pignatelli, C. (2004). Determination of molecular marker expression can predict clinical outcome in colon carcinomas. Clin Cancer Res, 10, 3490-9.

Garcia-Olmo, D., Garcia-Rivas, M., Garcia-Olmo, D.C. & Atienzar, M. (1998). Orthotopic implantation of colon carcinoma cells provides an experimental model in the rat that replicates the regional spreading pattern of human colorectal cancer. Cancer Lett, 132, 127-33.

George, A.J., Lee, L. & Pitzalis, C. (2003). Isolating ligands specific for human vasculature using in vivo phage selection. Trends Biotechnol, 21, 199-203.

Gerlag, D.M., Borges, E., Tak, P.P., Ellerby, H.M., Bredesen, D.E., Pasqualini, R., Ruoslahti, E. & Firestein, G.S. (2001). Suppression of murine collagen-induced arthritis by targeted apoptosis of synovial neovasculature. Arthritis Res, 3, 357-61.

Giordano, R.J., Cardo-Vila, M., Lahdenranta, J., Pasqualini, R. & Arap, W. (2001). Biopanning and rapid analysis of selective interactive ligands. Nat Med, 7, 1249-53.

Giordano, R.J., Lahdenranta, J., Zhen, L., Chukwueke, U., Petrache, I., Langley, R.R., Fidler, I.J., Pasqualini, R., Tuder, R.M. & Arap, W. (2008). Targeted induction of lung endothelial cell apoptosis causes emphysema-like changes in the mouse. J Biol Chem, 283, 29447-60.

Goldenberg, D.M. (2003). Advancing role of radiolabeled antibodies in the therapy of cancer. Cancer Immunol Immunother, 52, 281-96.

Goyle, S. & Maraveyas, A. (2005). Chemotherapy for colorectal cancer. Dig Surg, 22, 401-14.

Grady, W.M. & Markowitz, S.D. (2002). Genetic and epigenetic alterations in colon cancer. Annu Rev Genomics Hum Genet, 3, 101-28.

Graff, C.P. & Wittrup, K.D. (2003). Theoretical analysis of antibody targeting of tumor spheroids: importance of dosage for penetration, and affinity for retention. Cancer Res, 63, 1288-96.

Grothey, A. & Sargent, D. (2005). Overall survival of patients with advanced colorectal cancer correlates with availability of fluorouracil, irinotecan, and oxaliplatin regardless of whether doublet or single-agent therapy is used first line. J Clin Oncol, 23, 9441-2.

Grothey, A., Sargent, D., Goldberg, R.M. & Schmoll, H.J. (2004). Survival of patients with advanced colorectal cancer improves with the availability of fluorouracil-leucovorin, irinotecan, and oxaliplatin in the course of treatment. J Clin Oncol, 22, 1209-14.

Hajitou, A., Pasqualini, R. & Arap, W. (2006). Vascular targeting: recent advances and therapeutic perspectives. Trends Cardiovasc Med, 16, 80-8.

Hampel, H., Frankel, W.L., Martin, E., Arnold, M., Khanduja, K., Kuebler, P., Nakagawa, H., Sotamaa, K., Prior, T.W., Westman, J., Panescu, J., Fix, D., Lockman, J., Comeras, I. & de la Chapelle, A. (2005). Screening for the Lynch syndrome (hereditary nonpolyposis colorectal cancer). N Engl J Med, 352, 1851-60.

Hanahan, D. & Folkman, J. (1996). Patterns and emerging mechanisms of the angiogenic switch during tumorigenesis. Cell, 86, 353-64.

Hanahan, D. & Weinberg, R.A. (2000). The hallmarks of cancer. Cell, 100, 57-70.

Hannan, L.M., Jacobs, E.J. & Thun, M.J. (2009). The association between cigarette smoking and risk of colorectal cancer in a large prospective cohort from the United States. Cancer Epidemiol Biomarkers Prev, 18, 3362-7.

Harriss, D.J., Atkinson, G., Batterham, A., George, K., Cable, N.T., Reilly, T., Haboubi, N. & Renehan, A.G. (2009). Lifestyle factors and colorectal cancer risk (2): a systematic review and meta-analysis of associations with leisure-time physical activity. Colorectal Dis, 11, 689-701.

Harriss, D.J., Cable, N.T., George, K., Reilly, T., Renehan, A.G. & Haboubi, N. (2007). Physical activity before and after diagnosis of colorectal cancer: disease risk, clinical outcomes, response pathways and biomarkers. Sports Med, 37, 947-60.

Hartley, O. (2002). The use of phage display in the study of receptors and their ligands. J Recept Signal Transduct Res, 22, 373-92.

Haubner, R., Wester, H.J., Burkhart, F., Senekowitsch-Schmidtke, R., Weber, W., Goodman, S.L., Kessler, H. & Schwaiger, M. (2001). Glycosylated RGD-containing peptides: tracer for tumor targeting and angiogenesis imaging with improved biokinetics. J Nucl Med, 42, 326-36.

Hayat, M.J., Howlader, N., Reichman, M.E. & Edwards, B.K. (2007). Cancer statistics, trends, and multiple primary cancer analyses from the Surveillance, Epidemiology, and End Results (SEER) Program. Oncologist, 12, 20-37.

Heppeler, A., Froidevaux, S., Eberle, A.N. & Maecke, H.R. (2000). Receptor targeting for tumor localisation and therapy with radiopeptides. Curr Med Chem, 7, 971-94.

Hernegger, G.S., Moore, H.G. & Guillem, J.G. (2002). Attenuated familial adenomatous polyposis: an evolving and poorly understood entity. Dis Colon Rectum, 45, 127-34; discussion 134-6.

Herszenyi, L., Miheller, P. & Tulassay, Z. (2007). Carcinogenesis in inflammatory bowel disease. Dig Dis, 25, 267-9.

Hoffman, J.A., Giraudo, E., Singh, M., Zhang, L., Inoue, M., Porkka, K., Hanahan, D. & Ruoslahti, E. (2003). Progressive vascular changes in a transgenic mouse model of squamous cell carcinoma. Cancer Cell, 4, 383-91.

Hurwitz, H., Fehrenbacher, L., Novotny, W., Cartwright, T., Hainsworth, J., Heim, W., Berlin, J., Baron, A., Griffing, S., Holmgren, E., Ferrara, N., Fyfe, G., Rogers, B., Ross, R. & Kabbinavar, F. (2004). Bevacizumab plus irinotecan, fluorouracil, and leucovorin for metastatic colorectal cancer. N Engl J Med, 350, 2335-42.

Huxley, R. (2007). The role of lifestyle risk factors on mortality from colorectal cancer in populations of the Asia-Pacific region. Asian Pac J Cancer Prev, 8, 191-8.

Huxley, R.R., Ansary-Moghaddam, A., Clifton, P., Czernichow, S., Parr, C.L. & Woodward, M. (2009). The impact of dietary and lifestyle risk factors on risk of colorectal cancer: a quantitative overview of the epidemiological evidence. Int J Cancer, 125, 171-80.

Itzkowitz, S.H. & Yio, X. (2004). Inflammation and cancer IV. Colorectal cancer in inflammatory bowel disease: the role of inflammation. Am J Physiol Gastrointest Liver Physiol, 287, G7-17.

Iyer, L., Das, S., Janisch, L., Wen, M., Ramirez, J., Karrison, T., Fleming, G.F.,

Vokes, E.E., Schilsky, R.L. & Ratain, M.J. (2002). UGT1A1*28 polymorphism as a determinant of irinotecan disposition and toxicity. Pharmacogenomics J, 2, 43-7.

Jain, R.K. (2005). Normalization of tumor vasculature: an emerging concept in antiangiogenic therapy. Science, 307, 58-62.

Jass, J.R., Young, J. & Leggett, B.A. (2002). Evolution of colorectal cancer: change of pace and change of direction. J Gastroenterol Hepatol, 17, 17-26.

Jemal, A., Siegel, R., Ward, E., Hao, Y., Xu, J. & Thun, M.J. (2009). Cancer statistics, 2009. CA Cancer J Clin, 59, 225-49.

Jenkins, D.E., Hornig, Y.S., Oei, Y., Dusich, J. & Purchio, T. (2005). Bioluminescent human breast cancer cell lines that permit rapid and sensitive in vivo detection of mammary tumors and multiple metastases in immune deficient mice. Breast Cancer Res, 7, R444-54.

Joyce, J.A., Laakkonen, P., Bernasconi, M., Bergers, G., Ruoslahti, E. & Hanahan, D. (2003). Stage-specific vascular markers revealed by phage display in a mouse model of pancreatic islet tumorigenesis. Cancer Cell, 4, 393-403.

Kang, S.K., Woo, J.H., Kim, M.K., Woo, S.S., Choi, J.H., Lee, H.G., Lee, N.K. & Choi, Y.J. (2008). Identification of a peptide sequence that improves transport of macromolecules across the intestinal mucosal barrier targeting goblet cells. J Biotechnol, 135, 210-6.

Kehoe, J.W. & Kay, B.K. (2005). Filamentous phage display in the new millennium. Chem Rev, 105, 4056-72.

Kelly, K., Alencar, H., Funovics, M., Mahmood, U. & Weissleder, R. (2004).

Detection of invasive colon cancer using a novel, targeted, library-derived fluorescent peptide. Cancer Res, 64, 6247-51.

Kelly, K.A., Bardeesy, N., Anbazhagan, R., Gurumurthy, S., Berger, J., Alencar, H., Depinho, R.A., Mahmood, U. & Weissleder, R. (2008). Targeted nanoparticles for imaging incipient pancreatic ductal adenocarcinoma. PLoS Med, 5, e85.

Kelly, K.A. & Jones, D.A. (2003). Isolation of a colon tumor specific binding peptide using phage display selection. Neoplasia, 5, 437-44.

Kerbel, R.S. (2006). Antiangiogenic therapy: a universal chemosensitization strategy for cancer? Science, 312, 1171-5.

Killion, J.J., Radinsky, R. & Fidler, I.J. (1998). Orthotopic models are necessary to predict therapy of transplantable tumors in mice. Cancer Metastasis Rev, 17, 279-84.

Kim, K.J., Li, B., Houck, K., Winer, J. & Ferrara, N. (1992). The vascular endothelial growth factor proteins: identification of biologically relevant regions by neutralizing monoclonal antibodies. Growth Factors, 7, 53-64.

Klein, C.E., Gupta, E., Reid, J.M., Atherton, P.J., Sloan, J.A., Pitot, H.C., Ratain, M.J. & Kastrissios, H. (2002). Population pharmacokinetic model for irinotecan and two of its metabolites, SN-38 and SN-38 glucuronide. Clin Pharmacol Ther, 72, 638-47.

Klerk, C.P., Overmeer, R.M., Niers, T.M., Versteeg, H.H., Richel, D.J., Buckle, T., Van Noorden, C.J. & van Tellingen, O. (2007). Validity of bioluminescence measurements for noninvasive in vivo imaging of tumor load in small animals. Biotechniques, 43, 7-13, 30.

Koivunen, E., Wang, B. & Ruoslahti, E. (1995). Phage libraries displaying cyclic peptides with different ring sizes: ligand specificities of the RGD-directed integrins. Biotechnology (N Y), 13, 265-70.

Kolonin, M.G., Saha, P.K., Chan, L., Pasqualini, R. & Arap, W. (2004). Reversal of obesity by targeted ablation of adipose tissue. Nat Med, 10, 625-32.

Kraus, S. & Arber, N. (2009). Inflammation and colorectal cancer. Curr Opin Pharmacol, 9, 405-10.

Kuebler, J.P., Wieand, H.S., O'Connell, M.J., Smith, R.E., Colangelo, L.H., Yothers, G., Petrelli, N.J., Findlay, M.P., Seay, T.E., Atkins, J.N., Zapas, J.L., Goodwin, J.W., Fehrenbacher, L., Ramanathan, R.K., Conley, B.A., Flynn, P.J., Soori, G., Colman, L.K., Levine, E.A., Lanier, K.S. & Wolmark, N. (2007). Oxaliplatin combined with weekly bolus fluorouracil and leucovorin as surgical adjuvant chemotherapy for stage II and III colon cancer: results from NSABP C-07. J Clin Oncol, 25, 2198-204.

Laakkonen, P., Akerman, M.E., Biliran, H., Yang, M., Ferrer, F., Karpanen, T., Hoffman, R.M. & Ruoslahti, E. (2004). Antitumor activity of a homing peptide that targets tumor lymphatics and tumor cells. Proc Natl Acad Sci U S A, 101, 9381-6.

Laakkonen, P., Zhang, L. & Ruoslahti, E. (2008). Peptide targeting of tumor lymph vessels. Ann N Y Acad Sci, 1131, 37-43.

Ladner, R.C., Sato, A.K., Gorzelany, J. & de Souza, M. (2004). Phage display-derived peptides as therapeutic alternatives to antibodies. Drug Discov Today, 9, 525-9.

Lahdenranta, J., Sidman, R.L., Pasqualini, R. & Arap, W. (2007). Treatment of

hypoxia-induced retinopathy with targeted proapoptotic peptidomimetic in a mouse model of disease. Faseb J, 21, 3272-8.

Langenkamp, E. & Molema, G. (2009). Microvascular endothelial cell heterogeneity: general concepts and pharmacological consequences for anti-angiogenic therapy of cancer. Cell Tissue Res, 335, 205-22.

Larsson, S.C. & Wolk, A. (2007). Obesity and colon and rectal cancer risk: a meta-analysis of prospective studies. Am J Clin Nutr, 86, 556-65.

Lee, J.C., Chow, N.H., Wang, S.T. & Huang, S.M. (2000). Prognostic value of vascular endothelial growth factor expression in colorectal cancer patients. Eur J Cancer, 36, 748-53.

Liang, P.S., Chen, T.Y. & Giovannucci, E. (2009). Cigarette smoking and colorectal cancer incidence and mortality: systematic review and meta-analysis. Int J Cancer, 124, 2406-15.

Limsui, D. & Limburg, P.J. (2008). Cigarette smoking and colorectal cancer risk: a burning issue. Gastroenterology, 135, 704-5.

Lin, B.R., Chang, T.C., Lee, Y.C., Lee, P.H., Chang, K.J. & Liang, J.T. (2009). Pulmonary resection for colorectal cancer metastases: duration between cancer onset and lung metastasis as an important prognostic factor. Ann Surg Oncol, 16, 1026-32.

Lindor, N.M., Petersen, G.M., Hadley, D.W., Kinney, A.Y., Miesfeldt, S., Lu, K.H., Lynch, P., Burke, W. & Press, N. (2006). Recommendations for the care of individuals with an inherited predisposition to Lynch syndrome: a systematic review. Jama, 296, 1507-17.

Liu, Z., Liu, S., Wang, F., Liu, S. & Chen, X. (2009). Noninvasive imaging of tumor integrin expression using (18)F-labeled RGD dimer peptide with PEG (4) linkers. Eur J Nucl Med Mol Imaging, 36, 1296-307.

Lo, A., Lin, C.T. & Wu, H.C. (2008). Hepatocellular carcinoma cell-specific peptide ligand for targeted drug delivery. Mol Cancer Ther, 7, 579-89.

Maeda, O., Ando, T., Watanabe, O., Ishiguro, K., Ohmiya, N., Niwa, Y. & Goto, H. (2006). DNA hypermethylation in colorectal neoplasms and inflammatory bowel disease: a mini review. Inflammopharmacology, 14, 204-6.

Mancuso, A. & Sternberg, C.N. (2005). Colorectal cancer and antiangiogenic therapy: what can be expected in clinical practice? Crit Rev Oncol Hematol, 55, 67-81.

Manoutcharian, K., Gevorkian, G., Cano, A. & Almagro, J.C. (2001). Phage displayed biomolecules as preventive and therapeutic agents. Curr Pharm Biotechnol, 2, 217-23.

Mantovani, A., Allavena, P., Sica, A. & Balkwill, F. (2008). Cancer-related inflammation. Nature, 454, 436-44.

Marchio, S., Lahdenranta, J., Schlingemann, R.O., Valdembri, D., Wesseling, P., Arap, M.A., Hajitou, A., Ozawa, M.G., Trepel, M., Giordano, R.J., Nanus, D.M., Dijkman, H.B., Oosterwijk, E., Sidman, R.L., Cooper, M.D., Bussolino, F., Pasqualini, R. & Arap, W. (2004). Aminopeptidase A is a functional target in angiogenic blood vessels. Cancer Cell, 5, 151-62.

Mayer, R.J. (2009). Targeted therapy for advanced colorectal cancer--more is not always better. N Engl J Med, 360, 623-5.

McCole, D.F., Rogler, G., Varki, N. & Barrett, K.E. (2005). Epidermal growth factor partially restores colonic ion transport responses in mouse models of chronic colitis. Gastroenterology, 129, 591-608.

Mendelsohn, J. & Baselga, J. (2000). The EGF receptor family as targets for cancer therapy. Oncogene, 19, 6550-65.

Mendoza, F.J., Espino, P.S., Cann, K.L., Bristow, N., McCrea, K. & Los, M. (2005). Anti-tumor chemotherapy utilizing peptide-based approaches--apoptotic pathways, kinases, and proteasome as targets. Arch Immunol Ther Exp (Warsz), 53, 47-60.

Merg, A., Lynch, H.T., Lynch, J.F. & Howe, J.R. (2005a). Hereditary colon cancer--part I. Curr Probl Surg, 42, 195-256.

Merg, A., Lynch, H.T., Lynch, J.F. & Howe, J.R. (2005b). Hereditary colorectal cancer-part II. Curr Probl Surg, 42, 267-333.

Mersich, C. & Jungbauer, A. (2008). Generation of bioactive peptides by biological libraries. J Chromatogr B Analyt Technol Biomed Life Sci, 861, 160-70.

Meyerhardt, J.A. & Mayer, R.J. (2005). Systemic therapy for colorectal cancer. N Engl J Med, 352, 476-87.

Mocellin, S., Lise, M. & Nitti, D. (2005). Targeted therapy for colorectal cancer: mapping the way. Trends Mol Med, 11, 327-35.

Moghaddam, A.A., Woodward, M. & Huxley, R. (2007). Obesity and risk of colorectal cancer: a meta-analysis of 31 studies with 70,000 events. Cancer Epidemiol Biomarkers Prev, 16, 2533-47.

Nagel-Wolfrum, K., Buerger, C., Wittig, I., Butz, K., Hoppe-Seyler, F. & Groner, B. (2004). The interaction of specific peptide aptamers with the DNA binding domain and the dimerization domain of the transcription factor Stat3 inhibits transactivation and induces apoptosis in tumor cells. Mol Cancer Res, 2, 170-82.

Newton, R.U. & Galvao, D.A. (2008). Exercise in prevention and management of cancer. Curr Treat Options Oncol, 9, 135-46.

Nilsson, F., Tarli, L., Viti, F. & Neri, D. (2000). The use of phage display for the development of tumour targeting agents. Adv Drug Deliv Rev, 43, 165-96.

Okamoto, C.T. (1998). Endocytosis and transcytosis. Adv Drug Deliv Rev, 29, 215-228.

Pang, R.W. & Poon, R.T. (2006). Clinical implications of angiogenesis in cancers. Vasc Health Risk Manag, 2, 97-108.

Pasqualini, R., Koivunen, E., Kain, R., Lahdenranta, J., Sakamoto, M., Stryhn, A., Ashmun, R.A., Shapiro, L.H., Arap, W. & Ruoslahti, E. (2000). Aminopeptidase N is a receptor for tumor-homing peptides and a target for inhibiting angiogenesis. Cancer Res, 60, 722-7.

Pasqualini, R. & Ruoslahti, E. (1996). Organ targeting in vivo using phage display peptide libraries. Nature, 380, 364-6.

Pearson, J.R., Gill, C.I. & Rowland, I.R. (2009). Diet, fecal water, and colon cancer--development of a biomarker. Nutr Rev, 67, 509-26.

Penna, C. & Nordlinger, B. (2002). Colorectal metastasis (liver and lung). Surg Clin North Am, 82, 1075-90, x-xi.

Pentheroudakis, G. & Twelves, C. (2002). The rational development of capecitabine from the laboratory to the clinic. Anticancer Res, 22, 3589-96.

Perez-Soler, R. & Saltz, L. (2005). Cutaneous adverse effects with HER1/EGFR-targeted agents: is there a silver lining? J Clin Oncol, 23, 5235-46.

Perrotte, P., Matsumoto, T., Inoue, K., Kuniyasu, H., Eve, B.Y., Hicklin, D.J., Radinsky, R. & Dinney, C.P. (1999). Anti-epidermal growth factor receptor antibody C225 inhibits angiogenesis in human transitional cell carcinoma growing orthotopically in nude mice. Clin Cancer Res, 5, 257-65.

Pilch, J., Brown, D.M., Komatsu, M., Jarvinen, T.A., Yang, M., Peters, D., Hoffman, R.M. & Ruoslahti, E. (2006). Peptides selected for binding to clotted plasma accumulate in tumor stroma and wounds. Proc Natl Acad Sci U S A, 103, 2800-4.

Poon, R.T., Fan, S.T. & Wong, J. (2003). Clinical significance of angiogenesis in gastrointestinal cancers: a target for novel prognostic and therapeutic approaches. Ann Surg, 238, 9-28.

Powell, S.M., Zilz, N., Beazer-Barclay, Y., Bryan, T.M., Hamilton, S.R., Thibodeau, S.N., Vogelstein, B. & Kinzler, K.W. (1992). APC mutations occur early during colorectal tumorigenesis. Nature, 359, 235-7.

Prat, A., Casado, E. & Cortes, J. (2007). New approaches in angiogenic targeting for colorectal cancer. World J Gastroenterol, 13, 5857-66.

Rajpal, S. & Venook, A.P. (2006). Targeted therapy in colorectal cancer. Clin Adv Hematol Oncol, 4, 124-32.

Rajput, A., Dominguez San Martin, I., Rose, R., Beko, A., Levea, C., Sharratt, E.,

Mazurchuk, R., Hoffman, R.M., Brattain, M.G. & Wang, J. (2008). Characterization of HCT116 human colon cancer cells in an orthotopic model. J Surg Res, 147, 276-81.

Raymond, E., Buquet-Fagot, C., Djelloul, S., Mester, J., Cvitkovic, E., Allain, P., Louvet, C. & Gespach, C. (1997). Antitumor activity of oxaliplatin in combination with 5-fluorouracil and the thymidylate synthase inhibitor AG337 in human colon, breast and ovarian cancers. Anticancer Drugs, 8, 876-85.

Raymond, E., Faivre, S., Chaney, S., Woynarowski, J. & Cvitkovic, E. (2002). Cellular and molecular pharmacology of oxaliplatin. Mol Cancer Ther, 1, 227-35.

Raymond, E., Faivre, S., Woynarowski, J.M. & Chaney, S.G. (1998). Oxaliplatin: mechanism of action and antineoplastic activity. Semin Oncol, 25, 4-12.

Reddy, B.S. (1999). Role of dietary fiber in colon cancer: an overview. Am J Med, 106, 16S-19S; discussion 50S-51S.

Reilly, R.M., Sandhu, J., Alvarez-Diez, T.M., Gallinger, S., Kirsh, J. & Stern, H. (1995). Problems of delivery of monoclonal antibodies. Pharmaceutical and pharmacokinetic solutions. Clin Pharmacokinet, 28, 126-42.

Reinacher-Schick, A., Pohl, M. & Schmiegel, W. (2008). Drug Insight: antiangiogenic therapies for gastrointestinal cancers-focus on monoclonal antibodies. Nat Clin Pract Gastroenterol Hepatol.

Rodi, D.J. & Makowski, L. (1999). Phage-display technology--finding a needle in a vast molecular haystack. Curr Opin Biotechnol, 10, 87-93.

Ruoslahti, E. (2002). Specialization of tumour vasculature. Nat Rev Cancer, 2,

83-90.

Ruoslahti, E. (2004). Vascular zip codes in angiogenesis and metastasis. Biochem Soc Trans, 32, 397-402.

Rutter, M., Saunders, B., Wilkinson, K., Rumbles, S., Schofield, G., Kamm, M., Williams, C., Price, A., Talbot, I. & Forbes, A. (2004). Severity of inflammation is a risk factor for colorectal neoplasia in ulcerative colitis. Gastroenterology, 126, 451-9.

Saltz, L.B., Meropol, N.J., Loehrer, P.J., Sr., Needle, M.N., Kopit, J. & Mayer, R.J. (2004). Phase II trial of cetuximab in patients with refractory colorectal cancer that expresses the epidermal growth factor receptor. J Clin Oncol, 22, 1201-8.

Sandler, R.S. (1996). Epidemiology and risk factors for colorectal cancer. Gastroenterol Clin North Am, 25, 717-35.

Sato, A., Klaunberg, B. & Tolwani, R. (2004). In vivo bioluminescence imaging. Comp Med, 54, 631-4.

Schaedel, O. & Reiter, Y. (2006). Antibodies and their fragments as anti-cancer agents. Curr Pharm Des, 12, 363-78.

Schulmann, K., Mori, Y., Croog, V., Yin, J., Olaru, A., Sterian, A., Sato, F., Wang, S., Xu, Y., Deacu, E., Berki, A.T., Hamilton, J.P., Kan, T., Abraham, J.M., Schmiegel, W., Harpaz, N. & Meltzer, S.J. (2005). Molecular phenotype of inflammatory bowel disease-associated neoplasms with microsatellite instability. Gastroenterology, 129, 74-85.

Shin, V.Y., Wu, W.K., Ye, Y.N., So, W.H., Koo, M.W., Liu, E.S., Luo, J.C. & Cho, C.H. (2004). Nicotine promotes gastric tumor growth and neovascularization by

activating extracellular signal-regulated kinase and cyclooxygenase-2. Carcinogenesis, 25, 2487-95.

Sidhu, S.S. (2000). Phage display in pharmaceutical biotechnology. Curr Opin Biotechnol, 11, 610-6.

Smith, G.P. (1985). Filamentous fusion phage: novel expression vectors that display cloned antigens on the virion surface. Science, 228, 1315-7.

Srikrishna, G. & Freeze, H.H. (2009). Endogenous damage-associated molecular pattern molecules at the crossroads of inflammation and cancer. Neoplasia, 11, 615-28.

Strate, L.L. & Syngal, S. (2005). Hereditary colorectal cancer syndromes. Cancer Causes Control, 16, 201-13.

Sulkes, A., Benner, S.E. & Canetta, R.M. (1998). Uracil-ftorafur: an oral fluoropyrimidine active in colorectal cancer. J Clin Oncol, 16, 3461-75.

Sun, X., Yamada, H., Yoshihara, K., Awaya, A. & Yoshikai, Y. (2007). In vivo treatment with a nonapeptide thymic hormone, facteur thymique serique (FTS), ameliorates chronic colitis induced by dextran sulphate sodium in mice. Int Immunopharmacol, 7, 928-36.

Tabernero, J., Salazar, R., Casado, E., Martinelli, E., Gomez, P. & Baselga, J. (2004). Targeted therapy in advanced colon cancer: the role of new therapies. Ann Oncol, 15 Suppl 4, iv55-62.

Takahashi, T., Morotomi, M. & Nomoto, K. (2004). A novel mouse model of rectal cancer established by orthotopic implantation of colon cancer cells. Cancer Sci, 95,

514-9.

Takayama, T., Miyanishi, K., Hayashi, T., Sato, Y. & Niitsu, Y. (2006). Colorectal cancer: genetics of development and metastasis. J Gastroenterol, 41, 185-92.

Tarmin, L., Yin, J., Harpaz, N., Kozam, M., Noordzij, J., Antonio, L.B., Jiang, H.Y., Chan, O., Cymes, K. & Meltzer, S.J. (1995). Adenomatous polyposis coli gene mutations in ulcerative colitis-associated dysplasias and cancers versus sporadic colon neoplasms. Cancer Res, 55, 2035-8.

Thirion, P., Michiels, S., Pignon, J.P., Buyse, M., Braud, A.C., Carlson, R.W., O'Connell, M., Sargent, P. & Piedbois, P. (2004). Modulation of fluorouracil by leucovorin in patients with advanced colorectal cancer: an updated meta-analysis. J Clin Oncol, 22, 3766-75.

Thomas, T., Nair, P., Dronfield, M.W. & Mayberry, J.F. (2005). Management of low and high-grade dysplasia in inflammatory bowel disease: the gastroenterologists' perspective and current practice in the United Kingdom. Eur J Gastroenterol Hepatol, 17, 1317-24.

Trail, P.A., King, H.D. & Dubowchik, G.M. (2003). Monoclonal antibody drug immunoconjugates for targeted treatment of cancer. Cancer Immunol Immunother, 52, 328-37.

Trepel, M., Pasqualini, R. & Arap, W. (2008). Chapter 4. Screening phage-display Peptide libraries for vascular targeted peptides. Methods Enzymol, 445, 83-106.

Triantafillidis, J.K., Nasioulas, G. & Kosmidis, P.A. (2009). Colorectal cancer and inflammatory bowel disease: epidemiology, risk factors, mechanisms of

carcinogenesis and prevention strategies. Anticancer Res, 29, 2727-37.

Tseng, W., Leong, X. & Engleman, E. (2007). Orthotopic mouse model of colorectal cancer. J Vis Exp, 484.

Uneda, S., Toi, H., Tsujie, T., Tsujie, M., Harada, N., Tsai, H. & Seon, B.K. (2009). Anti-endoglin monoclonal antibodies are effective for suppressing metastasis and the primary tumors by targeting tumor vasculature. Int J Cancer, 125, 1446-53.

van Dieren, J.M., Wink, J.C., Vissers, K.J., van Marion, R., Hoogmans, M.M., Dinjens, W.N., Schouten, W.R., Tanke, H.J., Szuhai, K., Kuipers, E.J., van der Woude, C.J. & van Dekken, H. (2006). Chromosomal and microsatellite instability of adenocarcinomas and dysplastic lesions (DALM) in ulcerative colitis. Diagn Mol Pathol, 15, 216-22.

van Duijnhoven, F.J., Bueno-De-Mesquita, H.B., Ferrari, P., Jenab, M., Boshuizen, H.C., Ros, M.M., Casagrande, C., Tjonneland, A., Olsen, A., Overvad, K., Thorlacius-Ussing, O., Clavel-Chapelon, F., Boutron-Ruault, M.C., Morois, S., Kaaks, R., Linseisen, J., Boeing, H., Nothlings, U., Trichopoulou, A., Trichopoulos, D., Misirli, G., Palli, D., Sieri, S., Panico, S., Tumino, R., Vineis, P., Peeters, P.H., van Gils, C.H., Ocke, M.C., Lund, E., Engeset, D., Skeie, G., Suarez, L.R., Gonzalez, C.A., Sanchez, M.J., Dorronsoro, M., Navarro, C., Barricarte, A., Berglund, G., Manjer, J., Hallmans, G., Palmqvist, R., Bingham, S.A., Khaw, K.T., Key, T.J., Allen, N.E., Boffetta, P., Slimani, N., Rinaldi, S., Gallo, V., Norat, T. & Riboli, E. (2009). Fruit, vegetables, and colorectal cancer risk: the European Prospective Investigation into Cancer and Nutrition. Am J Clin Nutr, 89, 1441-52.

Varesco, L. (2004). Familial adenomatous polyposis: genetics and epidemiology.

Tech Coloproctol, 8 Suppl 2, s305-8.

Vasen, H.F. (2007). Review article: The Lynch syndrome (hereditary nonpolyposis colorectal cancer). Aliment Pharmacol Ther, 26 Suppl 2, 113-26.

Vignjevic, D., Fre, S., Louvard, D. & Robine, S. (2007). Conditional mouse models of cancer. Handb Exp Pharmacol, 263-87.

Wang, F., Arun, P., Friedman, J., Chen, Z. & Van Waes, C. (2009). Current and potential inflammation targeted therapies in head and neck cancer. Curr Opin Pharmacol, 9, 389-95.

Warren, R.S., Yuan, H., Matli, M.R., Gillett, N.A. & Ferrara, N. (1995). Regulation by vascular endothelial growth factor of human colon cancer tumorigenesis in a mouse model of experimental liver metastasis. J Clin Invest, 95, 1789-97.

Weber, G.F. (2008). Molecular mechanisms of metastasis. Cancer Lett, 270, 181-90.

Weiner, R.E. & Thakur, M.L. (2002). Radiolabeled peptides in the diagnosis and therapy of oncological diseases. Appl Radiat Isot, 57, 749-63.

Weissleder, R. (2006). Molecular imaging in cancer. Science, 312, 1168-71.

Whisenant, J. & Bergsland, E. (2005). Anti-angiogenic strategies in gastrointestinal malignancies. Curr Treat Options Oncol, 6, 411-21.

Widel, M.S. & Widel, M. (2006). [Mechanisms of metastasis and molecular markers of malignant tumor progression. I. Colorectal cancer]. Postepy Hig Med Dosw (Online), 60, 453-70.

Willats, W.G. (2002). Phage display: practicalities and prospects. Plant Mol Biol, 50,

837-54.

Willett, W. (1989). The search for the causes of breast and colon cancer. Nature, 338, 389-94.

Willett, W.C., Stampfer, M.J., Colditz, G.A., Rosner, B.A. & Speizer, F.E. (1990). Relation of meat, fat, and fiber intake to the risk of colon cancer in a prospective study among women. N Engl J Med, 323, 1664-72.

Wilmanns, C., Fan, D., O'Brian, C.A., Bucana, C.D. & Fidler, I.J. (1992). Orthotopic and ectopic organ environments differentially influence the sensitivity of murine colon carcinoma cells to doxorubicin and 5-fluorouracil. Int J Cancer, 52, 98-104.

Wong, H.P., Li, Z.J., Shin, V.Y., Tai, E.K., Wu, W.K., Yu, L. & Cho, C.H. (2009). Effects of cigarette smoking and restraint stress on human colon tumor growth in mice. Digestion, 80, 209-14.

Wong, H.P., Yu, L., Lam, E.K., Tai, E.K., Wu, W.K. & Cho, C.H. (2007a). Nicotine promotes cell proliferation via alpha7-nicotinic acetylcholine receptor and catecholamine-synthesizing enzymes-mediated pathway in human colon adenocarcinoma HT-29 cells. Toxicol Appl Pharmacol, 221, 261-7.

Wong, H.P., Yu, L., Lam, E.K., Tai, E.K., Wu, W.K. & Cho, C.H. (2007b). Nicotine promotes colon tumor growth and angiogenesis through beta-adrenergic activation. Toxicol Sci, 97, 279-87.

Woodhouse, E.C., Chuaqui, R.F. & Liotta, L.A. (1997). General mechanisms of metastasis. Cancer, 80, 1529-37.

Wu, W.K., Wong, H.P., Luo, S.W., Chan, K., Huang, F.Y., Hui, M.K., Lam, E.K.,

Shin, V.Y., Ye, Y.N., Yang, Y.H. & Cho, C.H. (2005). 4-(Methylnitrosamino)-1-(3-pyridyl)-1-butanone from cigarette smoke stimulates colon cancer growth via beta-adrenoceptors. Cancer Res, 65, 5272-7.

Xiang, R., Lode, H.N., Dolman, C.S., Dreier, T., Varki, N.M., Qian, X., Lo, K.M., Lan, Y., Super, M., Gillies, S.D. & Reisfeld, R.A. (1997). Elimination of established murine colon carcinoma metastases by antibody-interleukin 2 fusion protein therapy. Cancer Res, 57, 4948-55.

Xie, J. & Itzkowitz, S.H. (2008). Cancer in inflammatory bowel disease. World J Gastroenterol, 14, 378-89.

Xiong, H.Q. & Ajani, J.A. (2004). Treatment of colorectal cancer metastasis: the role of chemotherapy. Cancer Metastasis Rev, 23, 145-63.

Yin, M., Hu, Z., Tan, D., Ajani, J.A. & Wei, Q. (2009). Molecular epidemiology of genetic susceptibility to gastric cancer: focus on single nucleotide polymorphisms in gastric carcinogenesis. Am J Transl Res, 1, 44-54.

Yoon, S.W., Lee, C.H., Kim, J.Y., Kim, J.Y., Sung, M.H. & Poo, H. (2008). Lactobacillus casei secreting alpha-MSH induces the therapeutic effect on DSS-induced acute colitis in Balb/c Mice. J Microbiol Biotechnol, 18, 1975-83.

Zhang, L., Giraudo, E., Hoffman, J.A., Hanahan, D. & Ruoslahti, E. (2006). Lymphatic zip codes in premalignant lesions and tumors. Cancer Res, 66, 5696-706.

Zhang, L., Hoffman, J.A. & Ruoslahti, E. (2005). Molecular profiling of heart endothelial cells. Circulation, 112, 1601-11.

Zucker, S. & Vacirca, J. (2004). Role of matrix metalloproteinases (MMPs) in

colorectal cancer. Cancer Metastasis Rev, 23, 101-17.

Zurita, A.J., Arap, W. & Pasqualini, R. (2003). Mapping tumor vascular diversity by screening phage display libraries. J Control Release, 91, 183-6.